Scottish Rhodolith Bed Blue Carbon in a Changing World

Kelly Margaret James

Submitted in fulfilment of the requirements for the degree of Doctor of Philosophy

School of Geographical and Earth Sciences

College of Science and Engineering

University of Glasgow

Abstract

The current climate crisis, caused by elevated atmospheric CO_2 and Greenhouse Gases, has the potential to cause ecological, social and economic impacts. Marine systems can act as a natural-based solution to help mitigate climate change, with systems drawing down CO_2 by sequestering and storing carbon (termed blue carbon (BC)).

Rhodolith beds are globally ubiquitous systems and are formed from non-geniculate red coralline algae. There is recent evidence that their 3D structure facilitates the burial of allochthonous and autochthonous organic carbon (OC), thus rhodolith beds can act as BC repositories. Currently, little is known about how rhodolith bed blue carbon varies with structure and health status, with beds existing in a variety of sheltered and exposed environments, ranging from 100% live to 100% dead coralline algae on the surface of the beds. Furthermore, with increasing evidence that climate change (such as warming and ocean acidification (OA)) can reduce the capacity of BC systems to sequester and store carbon, research is needed to determine if rhodolith beds will continue to operate as BC repositories under future climate scenarios.

Using Scotland as a model system, this thesis aimed to contribute to these knowledge gaps by investigating 1) spatial and temporal trends in rhodolith bed blue carbon, 2) how autochthonous carbon production is affected by elevated temperature and OA, and 3) how carbon burial and the current sedimentary OC (SOC) stock is affected by elevated temperature and OA.

Rhodolith beds were characterised by having low decomposition rates which facilitated the burial of SOC. The rhodolith bed SOC stock was found to vary 10-fold between sheltered and exposed sites, with sheltered fjordic sites storing a higher amount of BC. There was also evidence that the SOC was “locked away” after a certain depth, meaning that BC may be preserved in rhodolith beds for centuries. Dead rhodolith beds continued to store SOC, with OC preserved when the dead bed was undisturbed. Under future conditions, rhodolith bed communities experienced increased carbonate dissolution, suggesting that both live and dead rhodolith bed distribution may decrease over the coming century. The effects of climate change on OC burial and storage depended on carbon type, with labile carbon (more biodegradable) vulnerable to warming and ocean acidification. On the other hand, refractory carbon (less biodegradable) was not affected by future conditions, suggesting that the current SOC stock will remain preserved if undisturbed.

This thesis provided evidence that rhodolith beds can act as BC repositories, with their global distribution meaning that they may contribute to both national and global carbon inventories. Not acknowledging the ability of both live and dead beds to store carbon could result in beds being damaged. This could result in carbon that has accumulated over thousands of years being exposed to O_2 and released back into the environment further exasperating the climate crisis.

Table of Contents

List of Tables

List of Figures

Acknowledgements

I would like to express my thanks to my supervisors, Nick Kamenos, Heidi Burdett, John MacDonald, Karen Cameron, Ian Davies and John Baxter, for their expertise and support throughout the last 4 years. There were many highs and lows throughout my PhD and their continued support and guidance throughout the process were greatly appreciated.

Thanks also to the technicians at GES – particularly to Charlotte Slaymark, Kenny Roberts and Mark Wildman. In terms of technical support, I wouldn't have managed the experiments without Charlotte who provided constant help over 12 months of running experiments in the lab. In particular, I'd like to thank her help to analyse 414 samples of water for DIC analysis – an analysis that took many months but provided some critical results. I'd also like to say thanks to Kenny Roberts and Thomas Prentice for helping acidify and analyse water samples (828!). In terms of emotional support, thanks again to Charlotte Slaymark for being a personal cheerleader over the last 4 years. My experiments were run during Covid, a time when there were few people in the building. This was in many ways an incredibly lonely time and at points, I wasn't sure I would finish my PhD. Socially distanced lunch and tea breaks with Charlotte and Mark was a lifeline during these times so thanks for helping me get to the end!

I'd also like to thank several PGR friends and colleagues from the University of Glasgow. A big shout out to my office mates – Marli De Jongh and Octria Prasojo – who also submitted their PhD's in 2022 and provided both advice and support throughout the writing-up period. A big shout out to Beth Langley also who joined the lab group in September 2021. Beth provided such a fresh breath of air at a time when I had been running experiments for 6 months and was also a massive help running experiments, including stepping in during March 2022 to collect some TOU data when I had Covid! Beth made the last year of my PhD so much more enjoyable and helped reignite my passion for my PhD again which helped when writing up. Also, a big thanks to (now Dr!) Ellen Macdonald whose advice throughout the PhD process has been paramount to getting to the end - I'm glad we both got there! A massive thanks to everyone not yet mentioned in the Global Change Research Group (both past and present!): Irene Olivé, Jinhua Mao, Sophie Plant, Seb Leveque, and Heather Baxter. I've learnt so much being part of this research group and hope we all keep in touch in the future. Thanks also to my other GES friends including Aine O'Brian, Sammy Griffins, and Cameron Floyd.

Outside of the University of Glasgow, I'd like to thank several people. In particular, thanks to Beau Marsh and Sofie Voerman whose physical height was a massive help during core extraction! Diving with Beau and Sofie throughout September 2019 was so much fun and I'll always remember the diving antics, the lemur café, end of day pints at various locations around Scotland. Also thanks to Connie Simon-Nutbrown who also carried out work during the September 2019 field trip. Connie has provided so much advice on all things coralline algae throughout my PhD and I can't wait to see her findings from her research! Thanks to Craig Smeaton for introducing me to TGA analysis and providing me with technical support to obtain my CRI data. A massive thanks to Rona McGill at SUERC also for analysing many samples for stable isotope analysis. I really enjoyed the day I spent at SUERC learning about stable isotope analysis – it was so nice to meet after 2 years of working virtually during the pandemic. I'd also like to say thanks to the members of the Blue Carbon Forum for all the good times during the many conferences we attended together – MASTs and the Scottish Blue Carbon Conferences were such a highlight during my PhD. I can't wait to see where Scottish blue carbon research goes. It is definitely an exciting time for science in this field.

A big shout out to all my friends and family for their support till the end. In particular, thanks to my girls Isobel, Jenny, Freya, Beth, Shannon and Gemma for providing much-needed laughter throughout the process. In terms of family, thanks to my Auntie Elaine, who provided an ear whenever I needed it. Thanks to my Mum (Kathy), Dad (Ian) and Brother (Peter) for the constant encouragement. I'm not sure any of you are wiser about why I have used teabags during my PhD but I appreciate you listening!! I'd also like to mention my Grandad (Charlie), who got me interested in the natural world from a young age.

Finally, the biggest shout out of all to my partner Charlie. From helping collect seawater during the pandemic at Largs to listening to me ramble on about my results he's supported me throughout the process. Thanks for always listening and for helping me to be more than just PhD Kelly. I've definitely learnt how consuming PhDs can be and Charlie helped me get out of my head whether that be by bagging Munros, going to gigs, or discovering Glasgow together. I can't wait for the next step!

Author’s Declaration

I declare that, except where explicit reference is made to the contribution of others, this dissertation is the result of my own work and has not been submitted for any other degree at the University of Glasgow or any other institution.

Kelly James

December 2022

Abbreviations

A_T	Total alkalinity
BC	BC
Ca	Calcium
CMIP	Coupled model intercomparison project
CO_2	Carbon dioxide
CO_3^{2-}	Carbonate ion
C_T	Dissolved inorganic carbon
DIC	Dissolved inorganic carbon
DO	Dissolved oxygen
GHG	Greenhouse gases
GPP	Gross primary productivity
H^+	Hydrogen ion
H_2O	Water
H_2CO_3	Carbonic acid
HCl	Hydrochloric acid
HCO_3^-	Bicarbonate ion
IC	Inorganic carbon
IPCC	Intergovernmental panel on climate change
Ksp	Solubility product at equilibrium
NBS	Nature-based solution
NCS	Nature climate solution
NCM	Net community metabolism
NDP	Net daytime production
NEM	Net ecosystem metabolism
O_2	Oxygen (compound)
OA	Ocean acidification
OC	Organic carbon
pCO_2	Atmospheric CO_2
pH_{NBS}	pH
POC	Particulate organic carbon
R	Respiration
RCP	Reasons for concern
REDD	Reducing Emissions from Deforestation and Forest Degradation
SNH	Scottish Natural Heritage
SOC	Sedimentary organic carbon
SSP	Shared socioeconomic pathways
TOC	Total organic carbon
Ω	Saturation state
Ω_{Arg}	Aragonite saturation state
Ω_{Ca}	Calcite saturation state

Chapter 1 Introduction

1.1 Global climate change

Since the Industrial Revolution, anthropogenic activities including, the burning of fossil fuels, deforestation and cement production, have significantly increased the concentration of atmospheric CO_2 (pCO_2) and other Greenhouse Gases (GHG; including methane and nitric oxide; Friedlingstein *et al.*, 2022; Intergovernmental Panel on Climate Change (IPCC) 2022). With regards to pCO_2, current concentrations have increased by 48% from 280 ppm in 1750 to 412.5 ppm in 2021 (Friedlingstein *et al.*, 2022). During this century, pCO_2 concentrations are expected to continue to rise, with peak pCO_2 concentrations dependent on future climate scenarios (IPCC 2022). GHG increases have, and will, cause significant changes to the world's climate, with gasses absorbing and re-emitting outgoing energy (IPCC 2022). As GHG concentrations continue to rise, their effect on the climate will grow, increasing global temperatures, causing more frequent and intense extreme weather events, and acidifying the oceans (IPCC 2022; Figure 1.1).

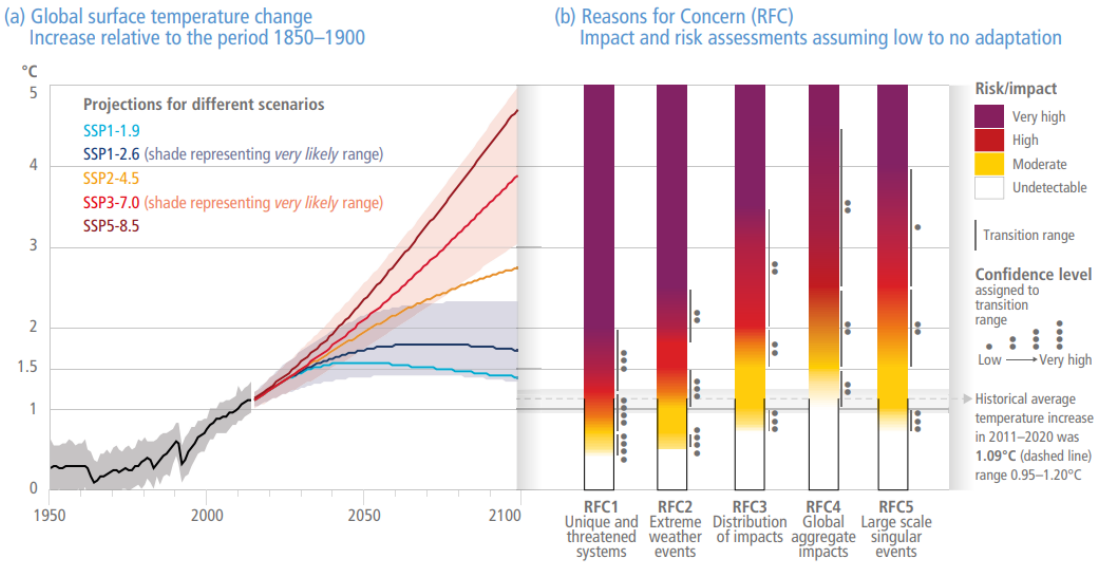

Figure 1.1: a) showing projected global surface temperature change (°C) since the baseline (1850-1900) for each future scenario. SSP1-1.9 (Shared Socioeconomic Pathways) represents the most optimistic scenario, with global CO_2 emissions cut to zero by 2050, whereas SSP5-8.5 represents the worst-case scenario, where CO_2 emissions continue to rise throughout the 21st century. b) Showing risk/impact for 5 Reasons for Concern (RFC) against global temperature rise. Taken from IPCC (2022).

1.1.1 Climate change in the ocean

The ocean plays a substantial role in climate regulation. Since 1970 an estimated 93% of excess thermal energy has been absorbed by the ocean resulting in an increase in oceanic temperatures (Rhein *et al.*, 2013; IPCC 2022), and thermal expansion resulting in sea-level rise (Wigley and Raper 1987; Church *et al.*, 2013; IPCC 2022). The ocean also plays a large role in the absorption of atmospheric CO_2 and has absorbed approximately 20-35% of anthropogenic CO_2 emissions released since the Industrial Revolution (Sabine *et al.*, 2004; Canadell *et al.*, 2007; IPCC 2022). Absorbing excess thermal energy and CO_2 has caused significant changes to the ocean's physical and chemical state including increased temperature, ocean acidification and decreased O_2 concentrations, with the changes anticipated to exasperate as GHG continue to be emitted (IPCC 2022; Figure 1.2). Globally, the ocean provides a multitude of services and functions (Costanza *et al.*, 1997; Moberg and Folke 1999; Barbier *et al.*, 2011), including food resources (Smith *et al.*, 2010; Barange *et al.*, 2014), coastal protection (Costanza *et al.*, 2008; Spalding *et al.*, 2014; Sutton-Grier *et al.*, 2015), carbon sequestration (McLeod *et al.*, 2011; Howard *et al.*, 2017), and water purification (Higgins *et al.*, 2011). Therefore, any changes to the ocean's climate can result in natural, ecological, social and economic impacts globally (Hoegh-Guldberg and Bruno 2010; Armstrong McKay *et al.*, 2022; IPCC 2022).

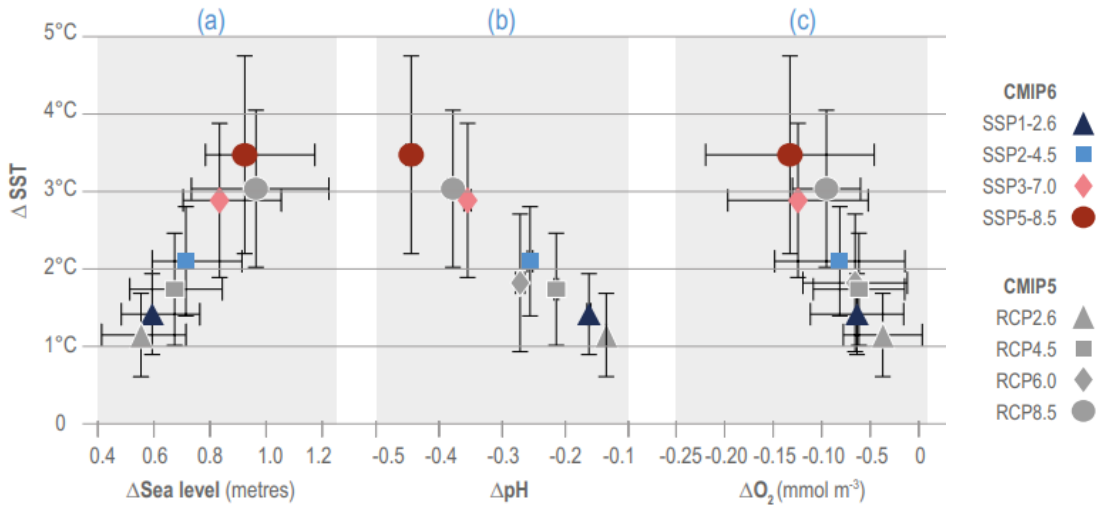

Figure 1.2: Projected trends in a) global sea level; b) average surface pH; c) subsurface (100-600m) dissolved organic concentration against anomalies in sea surface temperatures for the Coupled Model Intercomparison Project 5 (CMIP5) RCPs and the Coupled Model Intercomparison Project 6 (CMIP6) SSPs. Anomalies show projected averages over 2080-2099 in relation to the 1870-1899 baseline, with sea-level showing projected sea level at 2100 compared to 1901. Taken from IPCC (2022).

1.1.1.1 Temperature

Absorbing excess thermal energy has caused changes to the physical state of the oceans. For example, oceanic temperatures have risen with global mean sea surface temperature increasing by 0.88°C since the start of the 20th century. Marine heatwaves have also become more prominent, with the probability of occurrence of marine heatwaves increasing by 20-fold in the last 30 years. Absorbing excess heat has also resulted in thermal expansion, with global mean sea level increased by 0.2m since 1901. As GHG continue to increase, so will changes to the ocean, with global average temperature projected to rise by 0.43-4.07°C and sea level by 0.28-1.02m, and changes in some places much greater. (Figure 1.2; IPCC 2022)

Global warming causes significant changes to marine ecosystems. The distribution of marine species is, in part, driven by physiological thermal optimums (Sunday *et al.,* 2012; Hastings *et al.,* 2020). Whilst mobile species can move to avoid adverse conditions (Hastings *et al.*, 2020), the process for benthic species is much slower (Brodie *et al.*, 2014; Cornwall *et al.,* 2019), with relocation dependant on the movement of planktonic larvae. Instead, benthic species must either adapt or tolerate warming to survive (Brodie *et al.,* 2014; Hughes *et al.,* 2017; Cornwall *et al.,* 2019). Global warming and extreme warming events (referred to as marine heatwaves) can have devastating impacts on marine ecosystems, for example, resulting in mass coral bleaching (Hughes *et al.,* 2017) and reducing the distribution of globally important marine ecosystems (rhodolith beds, seagrass meadows, kelp forests; Koch *et al.,* 2013; Simon-Nutbrown *et al.,* 2020).

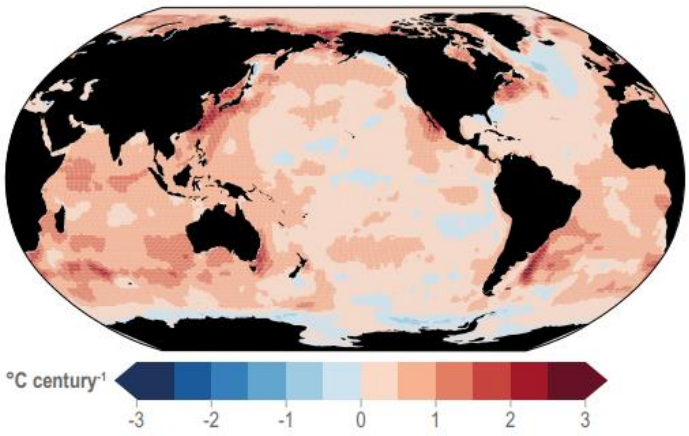

Figure 1.3: Showing observed surface ocean warming (in °C) over the last 100 years. Taken from IPCC (2022).

1.1.1.2 Ocean acidification

Ocean acidification (OA) is a further consequence of increased CO_2 emissions, with OA defined as the decrease in oceanic pH. Naturally, seawater carbonate chemistry is controlled by an equilibrium between different carbonate ions (Eq. 1).

Eq. 1 $$CO_2(aq) + H_2O \rightleftharpoons H_2CO_3 \rightleftharpoons HCO_3^- + H^+ \rightleftharpoons CO_3^{2-} + 2H^+$$

When CO_2 dissolves into the ocean, it quickly reacts with water to form carbonic acid (H_2CO_3), which can then turn into bicarbonate (HCO_3^-) by losing an H^+ ion. Bicarbonate can then turn into a carbonate ion (CO_3^{2-}), however, this change is controlled by pH, with a decreasing pH reducing the carbonate ion concentration. As the ocean has absorbed excess CO_2, the concentration of bicarbonate ions has increased and carbonate ions decrease by 2% since the industrial revolution (Fabry *et al.*, 2008; Doney *et al.*, 2009).

The decrease in carbonate ions negatively affects calcifying organisms, favouring the dissolution of calcium carbonate ($CaCO_3$) skeletons (Eq. 2). Furthermore, the process of calcification controlled by the carbonate saturation state (Ω; Eq. 3), with calcification less energetically costly at high Ω. As the amount of carbonate ions decreases, so does the Ω, making calcification more energetically costly to calcifying organisms (Gattuso *et al.*, 1999; Doney *et al.*, 2009; Kamenos *et al.*, 2013; Feely *et al.*, 2014; Figuerola *et al.*, 2021). The effects of OA on marine ecosystems have been documented by natural CO_2 vents, which have more acidic surrounding water (Hall-Spencer *et al.*, 2008; Porzio *et al.*, 2013; Fabricius et al., 2015). In these systems, OA results in a decrease in the abundance of calcifying algae and fauna, and an increase in invasive species tolerant to OA and fleshy algae, which can harness the excess CO_2 for photosynthesis (Hall-Spencer *et al.*, 2008; Porzio *et al.*, 2013). Oceanic pH is projected to continue to decrease over the century, with pH decreasing by 0.08-0.37 units by the end of the century depending on the projected climate scenario (IPCC 2022; Figure 1.2).

Eq. 2 $$CaCO_3 \leftrightarrow Ca^{2+} + CO_3^{2-}$$

Eq. 3 $$\Omega = \frac{[Ca^{2+}][CO_3^{2-}]}{K_{sp}\ (solubility\ product)}$$

1.1.1.3 Deoxygenation

GHG emissions have also resulted in a reduction in oceanic O_2 concentrations (deoxygenation) resulting in hypoxia. Hypoxia occurs when dissolved oxygen (DO) concentrations of the water column fall below 2ml O_2 L^{-1}, causing organisms to become physiologically stressed (Diaz and Rosenberg 1995). Once DO decreases below 0.5 O_2 L^{-1}, organisms can undergo mass mortality, resulting in extreme changes within the ecosystem (Diaz and Rosenberg 1995; Rabalais *et al.,* 2002; Keeling *et al.,* 2010).

Hypoxia can be caused by several factors including nutrient enrichment, increased water temperature, and altered ocean circulation. Both natural (i.e. coastal upwelling) and anthropogenic (i.e. fertiliser run-off) nutrient enrichment can result in hypoxia, with excess nutrients, such as nitrogen and phosphorus, causing phytoplankton blooms which deplete DO within the water column (Valiela *et al.,* 1997; Camargo and Alonso 2006). Hypoxia is also a direct and indirect consequence of global warming (Keeling *et al.,* 2010). Directly, hypoxia is caused by the decreasing solubility of oxygen with increased water temperature (Keeling *et al.,* 2010). Indirectly, hypoxia is caused by ocean stratification, which increases with temperature and altered ocean circulation (Keeling *et al.,* 2010).

Hypoxia is a current and growing problem, with extensive "dead zones" found worldwide (Rabalais *et al.,* 2002; Diaz and Rosenberg 2008). As ocean models predict that the world's O_2 inventory may decline by 4.1-11.2% by 2100 (IPCC 2022), increased hypoxia will continue to have an affect within the marine environment (Keeling *et al.,* 2010).

As GHG emissions, including CO_2, can cause significant changes to the world's climate, there have been calls from both the scientific community and international governments to respond to the climate crisis and reduce greenhouse gas (GHG) emissions. This can be achieved through a three-pronged approach to adopt an energy transition to reduce GHG emissions, and increase GHG uptake via negative emissions technologies and natural climate solutions (Griscom *et al.,* 2017, 2019; Anderson *et al.,* 2019; Baldocchi and Penuelas 2019).

1.2 Carbon storage in natural systems

1.2.1 CO_2 absorption via natural solutions and geoengineering

Whilst climate change is caused by many different GHG, CO_2 emissions are a major driver (IPCC 2022). CO_2 absorption can be achieved via natural solutions and geoengineering. Natural climate solutions (NCS) are recognised internationally as a nature-based solution (NBS) to climate change, with such solutions acknowledging the importance of ecosystem conservation and restoration for the mitigation of climate change. On the other hand, geoengineering can be used to remove CO_2 from the atmosphere. There is an ongoing debate regarding the amount of CO_2 that can be removed via NCS (Griscom *et al.,* 2017, 2019; Anderson *et al.,* 2019; Baldocchi and Penuelas 2019; Seddon *et al.,* 2021), with carbon sequestration and storage by natural systems argued not to be fast enough to make a large difference to GHG (Baldocchi and Penuelas 2019). However, whilst absorption by geoengineering can be faster, a lot of technological options discussed are still under development and are not yet ready to be deployed at a large scale (McLaren 2012; Anderson and Peters 2016; Pires 2019).

With regards to NCS, many schemes, including the Reducing Emissions from Deforestation and Forest Degradation (REDD) programme (Ahmed and Glaser 2016; Howard *et al.,* 2017), have been mainly focused on carbon storage in terrestrial systems. With increasing evidence that marine ecosystems can be more efficient carbon stores than terrestrial systems, with carbon sequestration rates 10-1000x larger (Duarte *et al.,* 2005; McLeod *et al.,* 2011; Pan *et al.,* 2011), the capacity for NCS to absorb CO_2 is likely much larger than previous estimates. Along with geoengineering, NCS is anticipated to play a role in carbon dioxide absorption over the coming century (Griscom *et al.,* 2017, 2019).

1.2.2 Blue carbon

Carbon sequestered by the marine environment is referred to as blue carbon (BC). Traditionally, BC is defined as the amount of organic carbon (OC) stored and sequestered by vegetated marine systems (McLeod *et al.,* 2011; Howard *et al.,* 2017). However, there is debate over this definition, with some arguing that inorganic carbon (IC) represents a long-term geological store of carbon in the marine environment and that it should be included under the term BC (i.e. Burrows *et al.,* 2017). As the production of biological IC can produce CO_2 (e.g. via calcification; Frankignoulle and Canon 1994; Gattuso *et al.,* 1998; Howard *et al.,* 2017), there has been discussion about whether it is appropriate to include IC under the term BC. However, whilst theoretically, the process of calcification results in the net release of CO_2, the amount of CO_2 released vs IC stored (Ψ) varies on a species and ecosystem basis, with calcifying phototrophs able to recycle some of the calcification-derived CO_2 via photosynthesis (Ware *et al.,* 1992; Frankignoulle *et al.,* 1994; Mao 2019). There has been further discussions about whether dissolved inorganic carbon (DIC) could also be included under the term BC, with DIC increasing with atmospheric CO_2 concentrations (Hilmi *et al.,* 2021). However, little is understood about where the DIC ends up, with the potential for DIC to be expelled back into the atmosphere. As there is current uncertainty surrounding the inclusion of IC (both calcified derived and DIC) under the term BC when considering its role as an NBS, this thesis will use the traditional definition of BC, with BC defined as the storage and sequestration of OC in the marine environment. Furthermore, for OC to quantify as BC, it should be sequestered over a long period of time (>100 years), with annual growth of macroalgae and phytoplankton not counting as BC unless it is sequestered and stored in other BC systems (Macleod *et al.,* 2011).

BC has received increasing interest from scientists over the last decade, and the significant role of marine systems in sequestering and storing carbon has been highlighted (Nellemann *et al.,* 2009; McLeod *et al.,* 2011; Howard *et al.,* 2017; Macreadie *et al.,* 2019a). It is now known that BC stores are comparable - if not more efficient - carbon reserves with more carbon sequestered per unit area by seagrass, mangroves and saltmarsh compared to tropical, boreal and temperate forests (Figure 1.4; Duarte *et al.,* 2005; McLeod *et al.,* 2011; Pan *et al.,* 2011). Furthermore, unlike land sinks, BC does not come into direct conflict with agriculture (Wolf *et al.,* 2019); meaning that marine systems will continue to provide a viable sink for centuries assuming they are not directly impacted by extraction activities such as trawling, sediment extraction and deep

sea mining (IPCC 2013). Once sequestered, BC ecosystems can store carbon for centuries to millennia making BC a long-term store of atmospheric CO_2 (McLeod *et al.*, 2011).

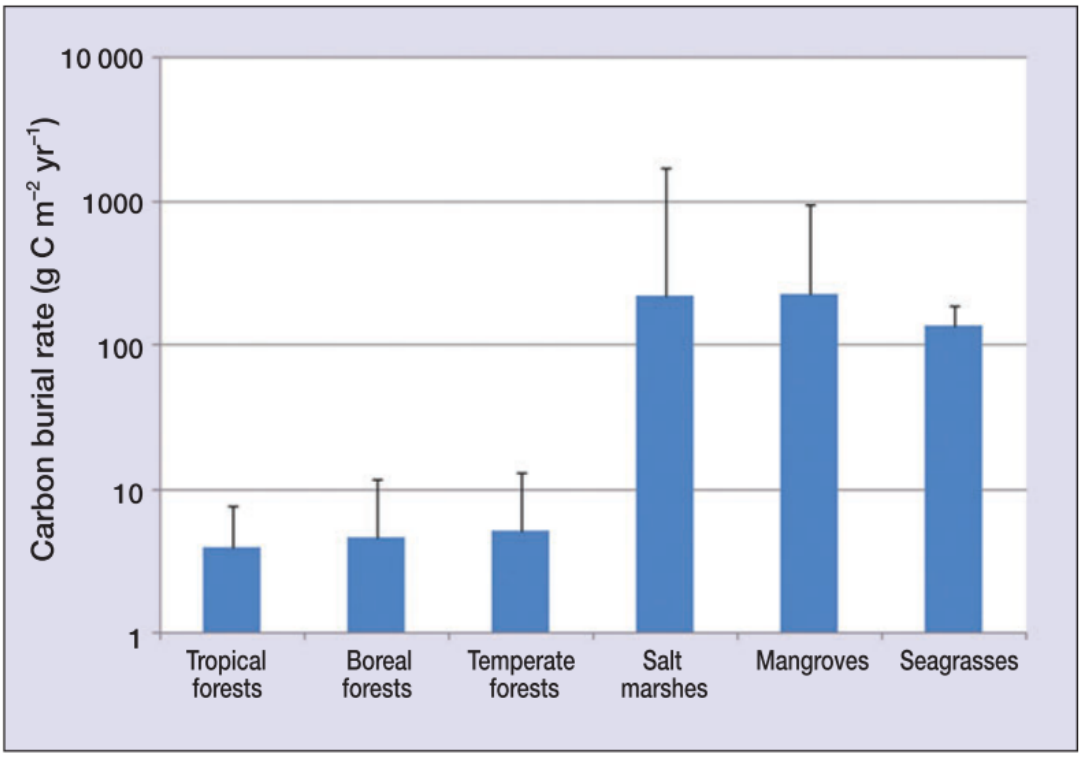

Figure 1.4: Comparing the mean long-term rates of C burial (g C m^{-2} yr^{-1}) in soils in terrestrial forests and sediments in coastal ecosystems. Taken from Macleod *et al.,* (2011).

Classical BC systems are vegetated systems that have been considered to sequester and store BC stores since the start of BC research over a decade ago (Macleod *et al.*, 2011). Such systems include seagrass meadows (Duarte *et al.*, 2005; Kennedy *et al.*, 2010; Marbà *et al.*, 2018), saltmarshes (Kirwan and Mudd 2012; Chmura *et al.*, 2003), and mangroves (Bouillon *et al.*, 2008; Donato *et al.*, 2011; Alongi 2012, 2014). The role of such systems in NCS is well understood, and it has been estimated that globally seagrass meadows, salt marshes, and mangroves sequester between 27-112 Tg C yr^{-1} (Kennedy *et al.*, 2010; Fourqurean *et al.*, 2012), 5-87 Tg C yr^{-1} (Chmura *et al.*, 2003; Duarte *et al.*, 2005; McLeod *et al.*, 2011), and 31-34 Tg C yr^{-1} respectively (McLeod *et al.*, 2011). In classical systems, OC can be sequestered both by the habitat (referred to as autochthonous carbon) and through the deposition of allochthonous carbon from external sources (Lavery *et al.*, 2013; Pérez *et al.*, 2018). The ratio of autochthonous and allochthonous stored by a system can vary. For example, in seagrass meadows, the amount of autochthonous stored within the sediment can range from 50-88% (Kennedy *et al.*, 2010; Reef *et al.*, 2017). Classical BC habitats play a global role in climate

mitigation and store a significant amount of carbon permanently stored within the oceans (Nellemann *et al.,* 2009).

Much less is understood about non-classical BC systems (including calcifying organisms, macroalgae, and sediments; Lovelock and Duarte 2019; Macreadie *et al.,* 2019a). Non-classical BC systems are those that were initially discounted as BC stores (Howard *et al.,* 2017; Lovelock and Duarte 2019), however recent research has suggested that they may be able to act as BC systems (i.e. Fodrie *et al.,* 2017; Mao *et al.,* 2020). Such systems were discounted for a variety of reasons. In calcifying ecosystems, for every 1 mol of IC precipitated, theoretically 0.6 mol of CO_2 is released which releases of CO_2 (Ware *et al.,* 1992). Along with respiration, this can result in the net release of CO_2 at a organism level (Ware *et al.,*1992; Frankignoulle and Canon 1994). Furthermore, as the precipitation of 1 mol of $CaCO_3$ reduces total alkalinity (TA) by 2 mol, this reduces the ability of the ocean to buffer against H^+ ions, further facilitating the return of CO_2 to the atmosphere (Frankignoulle and Canon 1994; Macreadie *et al.,*2017). Due to this many have argued that calcifying ecosystems (such as rhodolith beds, coral reefs, and bivalve beds) act as carbon sources unless the habitat is severely degraded or dominated by the growth of fleshy macroalgae which produce OC (Gattuso *et al.,* 1993; Gattuso *et al.,* 1998; Howard *et al.,* 2017; Macreadie *et al.,* 2017; Lovelock and Duarte 2019). The ability of fleshy macroalgae to sequester BC has also been questioned, with fleshy macroalgae instead considered an important BC donor for storage in other habitats (Duarte *et al.,* 2013a; Howard *et al.,* 2017; Lovelock and Duarte 2019; Macreadie *et al.,* 2019a). Finally, the role of coastal and offshore sediments in BC storage has previously been discounted, with research arguing that per area a small amount of carbon is sequestered (Howard *et al.,* 2017; Lovelock and Duarte 2019).

However, recent research has shown that non-classical systems (including rhodolith beds, bivalve beds, and sediment) can store BC, with some systems able to play a comparable role in carbon storage compared to classical habitats (Krause-Jensen *et al.,* 2018; Mao *et al.,* 2020). For example, rhodolith beds (also known as maerl or coralline algae beds) have been found to store and sequester large quantities of carbon, with the amount of carbon stored comparable to temperate Australian seagrass beds (Mao *et al.,* 2020). Furthermore, oyster reefs have been found to act as BC sinks, storing OC in some depositional environments (Fodrie *et al.,* 2017; Lee et al., 2020). Fjordic sediments have also been found to store vast quantities of carbon due to high depositional rates and area, with estimates that 11% of marine carbon is stored in the

top 10cm of fjordic sediments (Smeaton *et al.,* 2016; Smith *et al.*, 2015). Furthermore, whilst macroalgae may not be large BC stores, they are important donors, with deep-sea sediments burying an estimated 14 Tg C of macroalgae-derived particulate OC (POC) annually (Krause-Jensen *et al.*, 2018).

Whilst there is increasing evidence of the ability of non-classical systems to store BC, there is still a paucity of information regarding how much BC is stored and the rate of BC sequestration, with evidence for some systems only coming from a few study sites (i.e. Fodrie *et al.,* 2017; Mao *et al.,* 2020). With regards to rhodolith beds, current knowledge regarding their capacity to act as BC repositories comes from one site (Mao *et al.,* 2020), and it is not known if this capacity will change with climate change. As BC systems can draw down CO_2 from the atmosphere, thus as an NBS to climate change, this represents a crucial knowledge gap.

1.3 Blue carbon storage in rhodolith beds

1.3.1 Rhodolith beds

Red coralline algae are globally distributed ecosystem engineers that can bury both OC and IC (van der Heijden and Kamenos 2015; Mao 2019; Schubert *et al.,* 2020). Coralline algae are calcifying organisms and can take several forms; geniculate (articulate forms) and non-geniculate (crustose (CCA) and rhodolith forms; Foster 2001). Rhodolith beds (also known as maerl beds and coralline algae beds) form when free-living non-geniculate red coralline algae aggregate (Figure 1.5), accreting over centuries to millennia to form complex 3D beds which can extend several meters below the contemporary sea bed (Foster 2001; Riosmena-Rodríguez *et al.,* 2017; Mao *et al.,* 2020). Rhodolith beds occur globally (Figure 1.6; Foster 2001; van der Heijden and Kamenos 2015), and may be one of the most abundant macrophyte benthic habitats, along with kelp forests, and seagrass meadows (Foster 2001). Coralline algae first appear in the fossil record during the Early Cretaceous (Aguirre *et al.,* 2000), and some rhodolith beds have grown for over 8000 years (Birkett *et al.,* 1998).

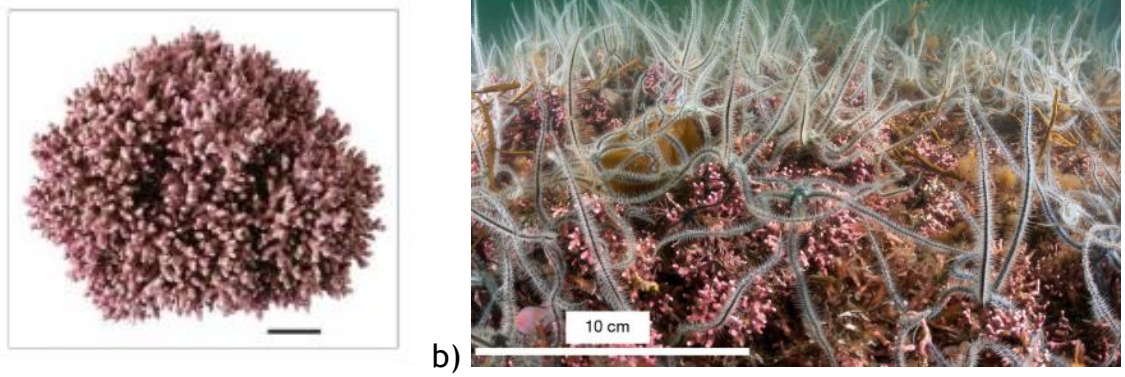

Figure 1.5: a) showing a non-geniculate individual from Loch Sween (scale bar = 1cm). Photo credit: Nick Kamenos, image taken from McCoy and Kamenos (2015); b) a rhodolith bed (Loch Sween) formed of multiple individuals of coralline algae. Photo credit: Rob Cook (Heriot-Watt University), image taken from Attard *et al.,* (2015).

Rhodolith beds are important global habitats, providing a multitude of functions and services (Figure 1.3; van der Heijden and Kamenos 2015). Rhodolith beds harbour high biodiversity at multiple trophic levels, with their rugged 3D structure providing shelter for juveniles of commercially important fish and shellfish (Kamenos *et al.,* 2004b, 2004a).

Scotland has a high abundance of rhodolith beds, being home to 30% of the beds in northwest Europe (Tyler-Walters *et al.,* 2016). Within Scotland, rhodolith beds are predominantly found

in the West Coast, Orkney and Shetland (Figure 1.7; Baxter *et al.*, 2011; Tyler-Walters *et al.*, 2016) with the most common rhodolith bed forming coralline algae species are *Phymatolithon calcareum* and *Lithothamnion glaciale* (Simon-Nutbrown *et al.*, 2020). Within Scotland, the role of rhodolith beds in promoting biodiversity and providing shelter to juveniles of fish and shellfish is recognised (Baxter *et al.*, 2011), with rhodolith beds protected in Scotland as a Priority Marine Feature (Tyler-Walters *et al.*, 2016), and in Europe under the EU habitat red list and OSPAR Commission in the North Atlantic (under "OSPAR List of Threatened and/or Declining habitats"; Hall-Spencer *et al.*, 2010). Rhodolith beds are recognised by the Scottish Government as a BC system (Burrows *et al.*, 2014) with recent research finding that rhodolith beds can store large quantities of BC (Mao *et al.*, 2020).

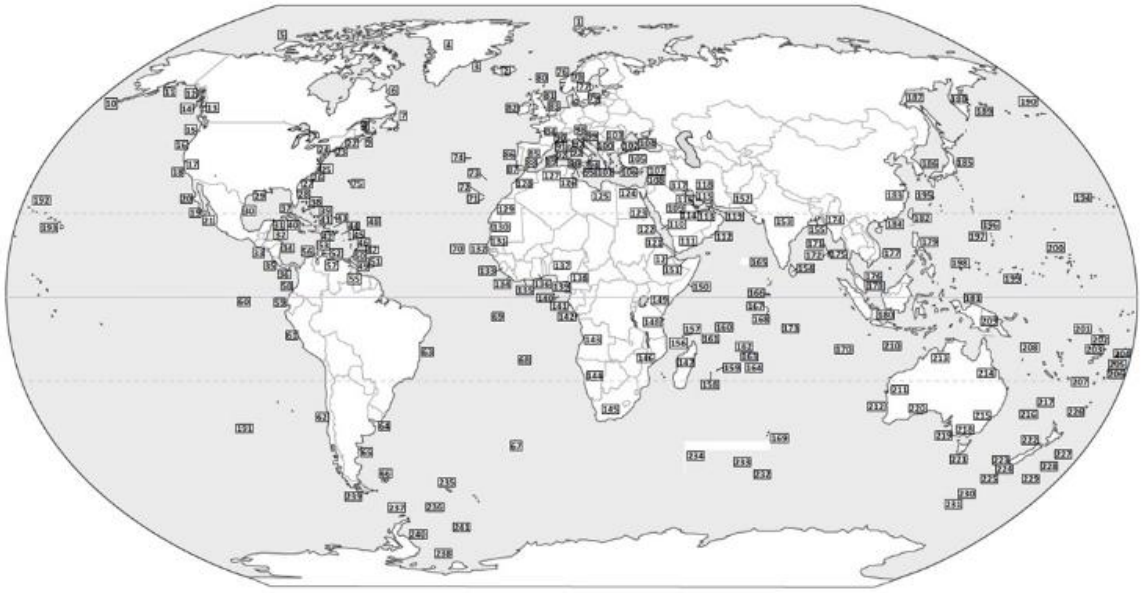

Figure 1.6: Showing the global records of coralline algae families (*Corallinaceae, Hapalidiaceae* and *Sporolithaceae*). Taken from van der Heijden and Kamenos (2015).

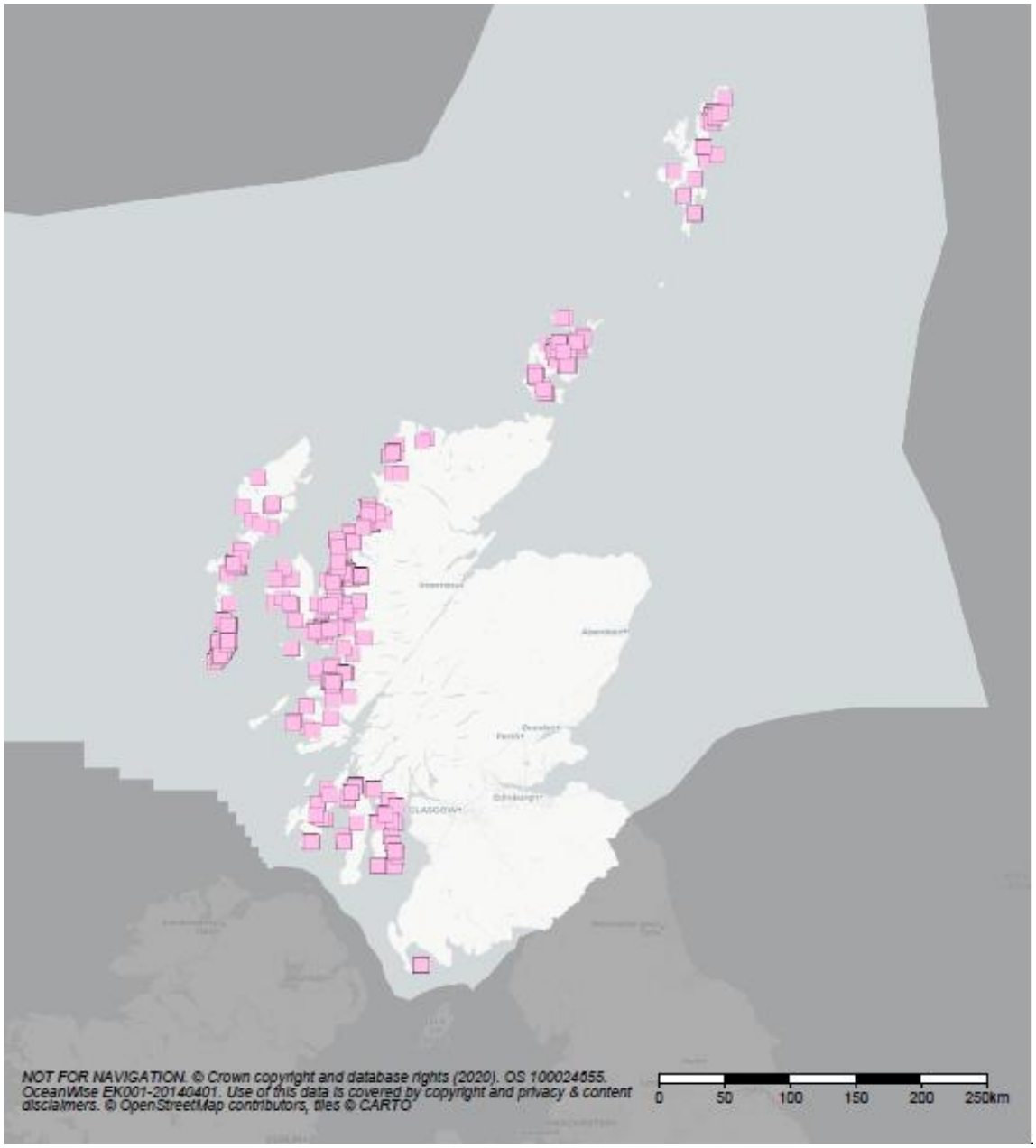

Figure 1.7: The distribution of rhodolith beds around Scotland. Pink squares represent records of rhodolith beds. The map is taken from Scotland's National Marine Plan Interactive (Marine Scotland - National Marine Plan Interactive, 2020).

1.3.2 Blue carbon storage in rhodolith beds

Previously, coralline algae have been discounted as BC repositories, as the process of calcification releases CO_2 (Frankignoulle and Canon 1994; Gattuso *et al.*, 1998; Howard *et al.*, 2017; Lovelock and Duarte 2019). However, recent research suggests that while calcifiers do release CO_2 during calcification, autotrophic calcifiers can directly recycle a portion of that CO_2 via photosynthesis (Mao 2019). Furthermore, as calcium carbonate systems often form complex 3D habitats, they also can entrain large quantities of allochthonous organic material (Fodrie *et al.*, 2017; Mao *et al.*, 2020). Therefore, rhodolith beds do have the capacity to act as a BC store.

Coralline algae can store carbon at an organism level within their skeleton, with algae that form rhodolith beds able to store carbon at an ecosystem level within both community and sediment (Figure 1.8). As coralline algae are autotrophic calcifying organisms they can store both OC and IC within the tissue of the coralline algae itself (autochthonous pathway). Globally, it is estimated that coralline algae can sequester 330 g C m^{-2} yr^{-1} of OC within their tissues (van der Heijden and Kamenos 2015). This autochthonous carbon can then go on to be buried and locked away with subsequent sedimentation (Mao *et al.*, 2020). As coralline algae are widespread (estimated habitat area of 0.45-0.49.4 x 10^{12} m^{-2}), this results in the global potential of rhodolith beds to sequester 0.7×109 t C yr^{-1} (van der Heijden and Kamenos 2015).

OC can enter the ecosystem through the burial of allochthonous and autochthonous material, which can make up a large component of OC stored within the coralline algae deposit (van der Heijden and Kamenos 2015, Mao *et al.*, 2020). Allochthonous material can come from a variety of marine and terrestrial sources including macroalgae, marine fauna, terrestrial soils and terrestrial plants (Mao *et al.*, 2020). The source of carbon buried in rhodolith beds can vary temporally with land use, with a previous study finding that the amount of marine-derived carbon can shift from 51% to over 69% following a reduction of land use and input of terrestrial carbon (Mao *et al.*, 2020).

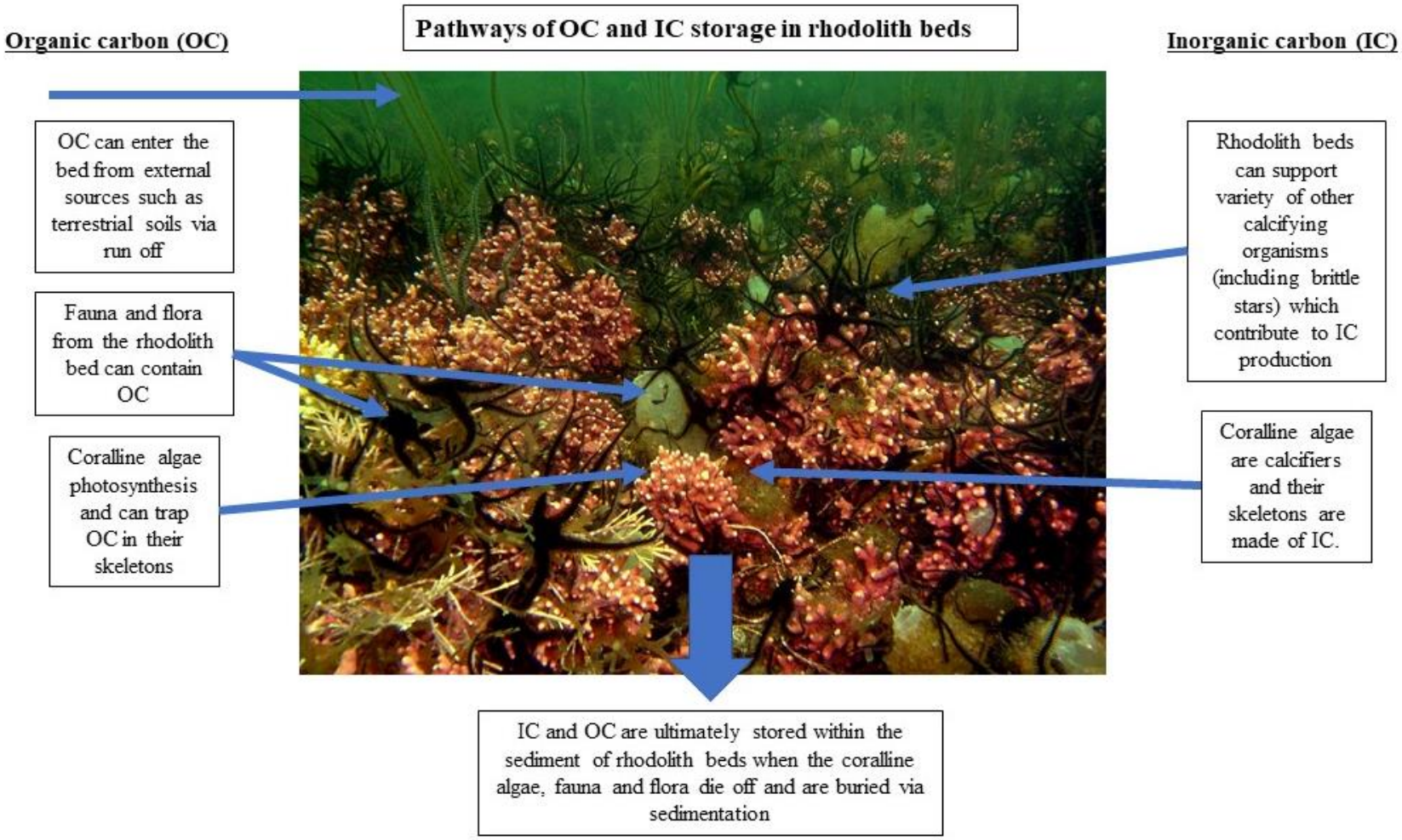

Figure 1.8: A schematic showing the different pathways of organic carbon (OC) and inorganic carbon (IC) storage in rhodolith beds.

Few studies have calculated the OC standing stock of rhodolith beds (Burrows *et al.,* 2014; Mao *et al.,* 2020). However, one study found that Scottish rhodolith beds from a sheltered environment have a standing stock of 7.23 ± 1.30 Mg OC ha^{-1} in the top 25cm of sediment (**Error! Reference source not found.**; Mao *et al.,* 2020). This is likely an underestimate, as the average depth of rhodolith bed deposits remains unknown (Burrows *et al.,* 2014). As current estimates of the amount of OC stored in rhodolith are based on one study (Mao *et al.,* 2020) the spatial variability in rhodolith bed BC remains unknown. Once buried, carbon can be locked away in rhodolith beds for millennia, thus they may present a large BC store (Mao *et al.,* 2020).

The current SOC stock of Scottish rhodolith beds is lower than classical blue carbon habitats but comparable to non-classical blue carbon habitats in Scotland. With regards to classical blue carbon habitats, Scottish seagrass beds have an estimated SOC stock of 54.79 ± 35.02 Mg OC ha^{-1} over 50cm depth (Potouroglou *et al.,* 2021) and Scottish salt marshes have a SOC 54.9 – 98.6 t C h^{-1} over 15cm depth (Austin *et al.,* 2021). Comparisons between the SOC estimates is limited by the different depths used in the studies. However, even when taking the different depths into account, both seagrass beds and saltmarshes appear to store a significantly more OC. Extrapolating the rhodolith core data to 50cm would unlikely result in a SOC comparable to Potouroglou *et al.,* (2021) with the majority of in rhodolith beds stored in the top 10cm of the sediment (Mao *et al.,* 2020). With regards to non-classical blue carbon, the current rhodolith bed SOC stock is comparable to marine sediments, with muddy sediments storing 6-123 Mg OC ha^{-1} in the top 1m and sandy sediments, 4 to 76 Mg OC ha^{-1} (Parker *et al.,* 2020). Whilst the SOC of rhodolith beds is small, they are still able to contribute to the national BC inventory partly due to their large distribution (predicted available distribution of 7130km^{-2}; Simon-Nutbrown *et al.,* 2020). For example, in Orkney rhodolith beds are one of the main contributors to the local BC budget (Porter *et al.,* 2020).

1.3.3 Rhodolith beds in a changing world

As rhodolith beds are globally distributed commercially important ecosystems that can store BC, understanding how rhodolith beds will function in the future world is important (Simon-Nutbrown *et al.,* 2020; van der Heijden and Kamenos 2015) To date, the majority of research has focussed on the effects of temperature and OA on individual coralline algae species, with few studying the effects on the whole ecosystem (Legrand *et al.,* 2017; Burdett *et al.*, 2018). It is now known that changes to the ocean's climate, including OA and temperature, can have a large effect on the physiology and survival of coralline algae species (Brodie *et al.,* 2014; McCoy and Kamenos 2015; Cornwall *et al.,* 2019). Rhodolith species are especially vulnerable to changes, with species often having long generation times and thus reduced capacity to acclimatise over multiple generations (Cornwall *et al.,* 2019). In a future warmer, more acidic world, the distribution of rhodolith beds is anticipated to decrease over the coming century (Brodie *et al.*, 2014; Simon-Nutbrown *et al.*, 2020).

As the process of calcification is dependent on seawater pH (Feely *et al.,* 2014), current research has primarily focused on the effects of OA on rhodolith species, which are calcifying organisms (Koch *et al.,* 2013; Brodie *et al.,* 2014; McCoy and Kamenos 2015). Although the effects of OA are species-specific (Martin *et al.,* 2013; Noisette *et al.,* 2013a), in general, OA has been found to negatively impact many aspects of rhodolith species physiology and life cycle stages (McCoy and Kamenos 2015) including calcification (Kamenos *et al.*, 2013; Brodie *et al.,* 2014; McCoy and Kamenos 2015; Burdett *et al.,* 2018), calcite skeleton structure and thickness (Ragazzola *et al.,* 2012; Kamenos *et al.,* 2013; McCoy and Ragazzola 2014). OA can also affect photosynthesis, however, the effects of this are species-specific (Noisette *et al.,* 2013a), with some species experiencing an increase in photosynthesis (Noisette *et al.,* 2013a; Burdett *et al.,* 2018), and others a decrease or no change at all under elevated pCO_2 (Anthony *et al.,* 2008; Martin *et al.,* 2013; Noisette *et al.,* 2013a; Sordo *et al.,* 2018). There is little understanding of the impacts of OA on the whole rhodolith bed ecosystem, however, some studies have found that rhodolith beds shift to favour net dissolution under elevated pCO_2 (Legrand *et al.,* 2017; Burdett *et al.,* 2018). This in turn could result in the dissolution of both live and dead rhodolith beds globally (Brodie *et al.,* 2014).

Water temperature can also have a significant impact on rhodolith bed ecosystems (Brodie *et al.,* 2014; Simon-Nutbrown *et al.,* 2020). Similarly to other algae species, coralline algae have

thermal optimums (Brodie *et al.*, 2014), with evidence that temperature can have a negative effect on calcification (Kamenos and Law 2010, Cornwall *et al.*, 2019) and cause bleaching, where the coralline algae lose photosynthetic pigments (Martone *et al.*, 2010). Whilst some species are more tolerant to changes in temperature than OA (Cornwall *et al.*, 2019), temperature is anticipated to particularly affect the distribution of Arctic non-geniculate coralline algae species, such as *Lithothamnion glaciale*, at the southerly edge of their thermal ranges (Simon-Nutbrown *et al.*, 2020).

As both oceanic warming and OA will occur simultaneously (along with other effects such as hypoxia and sea-level rise) understanding the interactive effects of multiple stressors is a crucial stage in coralline algae research (Koch *et al.*, 2013). Interactions between OA and temperature have been found to reduce the ability of individual coralline algae species to tolerate adverse conditions. For example, interactions between pCO_2 and temperature can reduce tissue growth (McCoy and Kamenos 2015), and productivity when beyond a species' thermal optimum (Martin *et al.*, 2013). Furthermore, whilst some species have enhanced productivity under future conditions, species may experience reduced calcification rates negatively affecting rhodolith bed structure (Brodie *et al.*, 2014; Qui-Minet *et al.*, 2019). Although the resilience of coralline algae to changing conditions varies between species, rhodolith-forming coralline algae species are often long-lived species with a long generation time and may be particularly vulnerable to change (Noisette *et al.*, 2013a, 2013b; Brodie *et al.*, 2014; McCoy and Kamenos 2015; Cornwall *et al.*, 2019). Research has found that future climate change may have a significant impact on future rhodolith bed distributions with declines of up to 84% (under the RCP 8.5 scenario) by 2100 in Scotland (Simon-Nutbrown *et al.*, 2020).

Climate change may affect rhodolith beds' capacity to act as BC repositories, with the potential of beds to store both autochthonous and allochthonous carbon reduced. For example, if rhodolith bed distribution decreases with climate change, beds will no longer be able to support a biodiverse community of autotrophs which may produce autochthonous OC. Furthermore, it is currently not known if the carbon already stored in rhodolith bed deposits will be protected from climate change, or if the carbon will start to be remineralised and re-enter the atmosphere. Understanding the effects of climate change on rhodolith bed communities and their capacity as BC repositories represents a crucial research gap in rhodolith bed research (Mao *et al.*, 2020).

1.4 Current uncertainties regarding blue carbon storage in rhodolith beds

Rhodolith beds can act as BC stores, however, there are several areas of uncertainty that need to be resolved. In particular, research is required to investigate the spatial variability of rhodolith bed BC, with the carbon stored in other BC systems such as seagrasses varying by several magnitudes (Lavery *et al.,* 2013; Röhr *et al.,* 2016, 2018; Potouroglou *et al.,* 2021). It is also not known if carbon stores vary temporally, with previous research showing that historic changes in land use can have an impact on the amount of carbon stored. Whilst BC can mitigate climate change, it is currently not known if systems will continue to sequester and store BC in a future world. Further research is required to investigate changes to autochthonous carbon production and allochthonous carbon burial and storage by the rhodolith bed community, with the potential of carbon that has previously been locked away remineralised under future warming and re-introduced into the atmosphere.

1.4.1 How does carbon storage vary spatially and temporally?

Currently, previous studies measuring carbon storage in Scottish rhodolith beds have focussed on one study site in Loch Sween (56°01.99’ N, 05°36.13’ W; Mao *et al.,* 2020). However, the structure and health of coralline algae can vary quite drastically between beds. For example, whilst the coralline algae bed in Loch Sween is situated in a sheltered environment (referred to as “tidal formed” beds), there are beds elsewhere in Scotland (including the Sound of Barra and Wyre Sound, Orkney) that are situated in exposed environments (referred to as “wave formed” beds). In exposed environments, bed formation is driven by wave energy, with waves causing ripples of peaks and troughs in the rhodolith bed (Figure 1.9; Bosence and Wilson 2003). Currently, no studies have measured the carbon stored in wave-formed beds, and it is not certain how the high-energy environment will impact carbon burial.

a)  b) 

Figure 1.9: a) A tidal formed coralline algae bed in Loch Sween. Photo credit: Nick Kamenos. b) A wave formed coralline algae bed in the Sound of Barra. Photo credit: Kelly James.

Whilst there has been little research into carbon stock variability in rhodolith beds, findings from other BC systems can be used to predict the potential drivers of variability in rhodolith bed carbon stocks. Within classical BC systems, carbon stocks are known to vary spatially on both large and small scales (Lavery *et al.*, 2013; Hunt *et al.*, 2020; Smeaton *et al.*, 2017, 2016). Abiotic factors, including sediment type and grain size (Serpetti *et al.*, 2012; Hunt *et al.*, 2020), hydrodynamical activity (Lohse *et al.*, 1995; Dahl *et al.*, 2018), and sediment oxygen dynamics (Burdige 2007; Glud 2008) can influence carbon burial and subsequent storage. Fine-grained sediments, which can be more abundant in areas with low hydrodynamical energy, can store more OC% (Dahl *et al.*, 2016; Serrano *et al.*, 2016). This is due to fine grain-sized particles having a higher affinity to bind to OC and lower oxygen exchange and bacterial remineralization within sediments (Kell *et al.*, 1994; Hedges and Keil 1995; Dauwe *et al.*, 2001; Burdige 2007). Biotic factors, including bioturbation, can also drive changes in carbon stocks, with frequent bioturbation from fauna reducing burial efficiency by increasing the decomposition rate of organic matter (Mazarrasa *et al.*, 2018; Thomson *et al.*, 2019).

Anthropogenic activities and climate change can also affect the capacity of systems to store BC (Macreadie *et al.*, 2012, 2013, 2019b; Sasmito *et al.*, 2019; Mao *et al.*, 2020). The effects of disturbance on the BC habitat and the carbon stored are complex. For example, dredging can expose ancient sediment to microbial attack, reducing the quantity of carbon stored within the bed (Macreadie *et al.*, 2019b; Sala *et al.*, 2021). However, the degree to which the carbon is remineralised can depend on the reactivity of the carbon, with organic material that is recalcitrant and refractory less vulnerable to bacterial remineralisation than labile organic material (Black *et al.*, 2022; Smeaton and Austin 2022a). Furthermore, whilst adjacent land change and eutrophication may degrade BC habitats (Diaz and Rosenberg 2008), they can

increase allochthonous carbon storage via elevated sedimentation rates (Macreadie *et al.,* 2012; Asmala *et al.,* 2018). Whilst degraded systems may sequester autochthonous carbon at a reduced rate (if at all) carbon already stored may continue to be locked away if not disturbed (Sasmito *et al.,* 2019). Understanding the effects of disturbance on BC storage and sequestration is crucial if we are to predict the capacity of habitats to act as BC repositories in a changing world (Macreadie *et al.,* 2019a; McLeod *et al.,* 2011).

Within rhodolith beds, the ratio of dead to living coralline algae thali on the surface of the bed may also vary (Foster 2001). Whilst the coralline algae bed at Loch Sween is formed of predominantly live thalli, other beds in Scotland are formed of predominantly dead thali (for example in the Sound of Eriskay and the Firth of Clyde). It is currently not known if dead beds continue to act as traps of allochthonous carbon and if the carbon stored within the bed remains locked away.

The current BC inventory for Scottish rhodolith beds is 20 million tonnes OC (Mao *et al.,* 2020; Simon-Nutbrown *et al.,* 2020) with 33.5-607 t C yr^{-1} sequestered annually (Burrows *et al.,* 2014). However, this value is likely an underestimate for several reasons. Within the Burrows and co-authors (2014) report, only carbon storage within the top 25cm was only considered. However, rhodolith bed deposits can be a range of depths with beds as thick as 125cm found in the Wyre Sound (Prof John Baxter, *per coms*). As OC continues to be stored below 60cm (Mao *et al.,* 2020), I anticipate the amount of OC locked away in Scottish rhodolith beds to be much higher (Mao *et al.,* 2020). Furthermore, the Burrows and co-authors (2014) report only considered carbon stored within the individual coralline algae. It is now known that coralline algae can store a large quantity of allochthonous carbon from a variety of sources, with a large amount of allochthonous carbon stored within rhodolith beds (Mao *et al.,* 2020).

1.4.2 How will Scottish rhodolith beds function as blue carbon repositories in a changing world?

As BC is a NBS for mitigating pCO_2 increases, understanding how carbon storage is affected by climate change is a crucial question in BC science (Macreadie *et al.,* 2019a). Currently, very little is known about the effects of climate change on carbon storage, sequestration, and the stability of rhodolith bed BC stores; however, knowledge of this is crucial for understanding the future role of rhodolith beds as BC repositories (Macreadie *et al.,* 2019a, 2019b). Such information can be used to inform conservation management, for example, by identifying large

rhodolith beds BC repositories that are under threat from climate change (Macreadie *et al.,* 2019a). Climate change may impact rhodolith bed BC in several ways: for example, by shifting the distribution of the rhodolith bed habitat (See 5.3; Macreadie *et al.,* 2019a), by altering biogeochemical mechanisms involved in carbon storage (for example, microbial dynamics within the sediment; Macreadie *et al.,* 2019b), and by affecting the source of carbon (Mao *et al.,* 2020).

As discussed in section 1.3.3, the distribution of live rhodolith beds is predicted to decrease in the Northern Hemisphere in the coming century (Brodie *et al.,* 2014; Simon-Nutbrown *et al.,* 2020). Whilst a reduction in live coralline algae on the surface of rhodolith beds will likely reduce their ability to sequester autochthonous carbon, it is not known if dead beds still accumulate carbon from external sources (allochthonous carbon). Whilst these habitats still maintain a rugged 3D structure, they may still promote the storage of allochthonous carbon in the short term. However, as the dead coralline algae fragments start to corrode in more acidic water (Brodie *et al.,* 2014), the 3D structure may degenerate and this may result in less allochthonous carbon being stored in the long term. As discussed in 1.4.1, it is currently not known whether dead beds continue to store ancient carbon already locked away within the beds. Therefore, although the distribution of rhodolith beds may change in the coming century, ancient carbon stores already locked away within the sediment may not.

Climate change can also affect carbon storage by altering biogeochemical mechanisms, such as carbon remineralisation, within the habitat (Macreadie *et al.,* 2019a). Carbon remineralisation occurs when the labile fraction of OC is broken down by microbes and takes place both in the water column and the upper layers of sediment (Glud 2008). Carbon remineralisation is influenced by several abiotic and biotic processes including water depth, temperature, oxygen concentration, and bioturbation (Glud 2008; Bourgeois *et al.,* 2017; Macreadie *et al.,* 2019b). Currently, the effects of climate change on carbon remineralisation within rhodolith beds are unknown, with the effects of climate change on remineralisation likely complex. For example, whilst high temperatures increase remineralisation rates (Arnosti *et al.,* 1998; Thamdrup *et al.,* 1998), low oxygen concentrations decrease remineralisation rates (Glud 2008). Furthermore, as remineralisation rates are strongly influenced by a range of other factors (for example, water depths, and food availability), the effects of climate change may be site-specific and depend on a multitude of interactions (Bourgeois *et al.,* 2017). Understanding

how carbon remineralisation will be impacted by climate change is a crucial step in BC science and inferring how carbon sequestration will change in a future world.

Within many BC habitats, allochthonous carbon can represent a large proportion of the carbon buried (Kennedy *et al.,* 2010; á Norði *et al.,* 2018; Oreska *et al.,* 2018; Queirós *et al.,* 2019); therefore, the effects of climate change on the source of carbon must be considered. Allochthonous carbon can come from the terrestrial or marine environment and can travel considerable distances between being deposited in the BC habitat (Krause-Jensen *et al.,* 2018; Queirós *et al.,* 2019). The proportion of allochthonous carbon buried can be high – for example, allochthonous carbon in seagrass meadows can account for ~50% of the OC pool (Kennedy *et al.,* 2010). As climate change affects marine and terrestrial environments, the effect of climate change on the source of allochthonous must be considered. In rhodolith beds, there has been little work investigating the effects of climate change on allochthonous carbon sources; however, historic changes in local land use have been found to alter the source of allochthonous carbon (Mao *et al.,* 2020). As rhodolith beds can store a large proportion of carbon from the adjacent terrestrial environment further work is necessary to determine the effects of climate change on the sources of allochthonous carbon in rhodolith beds.

Currently, the effects of climate change on Scottish rhodolith bed BC are poorly understood. Further research is needed to predict the role of rhodolith beds as BC repositories in a future world.

1.5 Aims

Although previous research has identified that rhodolith bed habitats are currently carbon repositories, BC research in rhodolith beds is still developing. The overall aim of this thesis "Scottish rhodolith bed BC in a changing world" is to investigate past, present, and future carbon storage in Scottish rhodolith beds. The thesis aimed to 1) investigate how carbon storage is influenced by bed type and structure, 2) contribute to the current rhodolith bed BC inventory for Scotland, and 3) provide context for future Scottish rhodolith bed blue carbon storage.

To address this aim, I explored rhodolith bed BC through four research objectives:

1) understand the characteristics of rhodolith beds that allow them to act as BC repositories (Chapter 2);

2) investigate the spatial variability in rhodolith BC and contribute to the current BC inventory for Scotland (Chapter 3);

3) investigate rhodolith bed community metabolism, organic carbon (OC) and inorganic carbon (IC) production under future conditions (elevated temperature and ocean acidification; Chapter 4);

4) explore how the burial and storage of allochthonous carbon will change under elevated temperature and ocean acidification (Chapter 5).

In chapter 2, I first discuss the role of non-classical systems (including rhodolith beds, bivalve beds, sediments, and mud flats) as BC stores in the form of a literature review. I discuss the characteristics of non-classical systems that allow them to store BC and future research priorities in BC research. In chapter 3, I investigated how carbon storage varies with bed health and structure around Scotland. I collected sediment cores from various locations and used OC%, the carbon reactivity index, and stable isotopes to measure the quantity, vulnerability and source of carbon in Scottish rhodolith beds. In chapters 4 and 5 I ran *in vitro* experiments to investigate carbon sequestration and burial under future conditions. In chapter 4, I investigated the effects of climate change on rhodolith bed community metabolism using measurements including respiration/photosynthesis and calcification/dissolution to quantify OC and IC production. In chapter 5, I investigated the effects of climate change on the burial

and storage of labile (biodegradable) and refractory (less biodegradable) carbon using the teabag index as a proxy for the different carbon types (Keuskamp *et al.*, 2013). I again used metabolism measurements to measure OC and IC production.

With climate change resulting in a current climate crisis, and BC as a way of mitigating climate change, understanding how current and future carbon stores vary spatially and temporally is of the utmost importance (IPCC 2022; Macreadie *et al.*, 2021). Information can be used to better refine management strategies to protect large carbon stocks and those vulnerable to disturbance. This thesis aims to further the understanding of BC storage in rhodolith beds to contribute to the knowledge used to manage and protect such systems.

Chapter 2 Non-classical blue carbon ecosystems are key stores of marine organic carbon

This paper is under revision for One Earth. Submitted on the 12th of September 2022. I have submitted it to SSRN – a pre-print repository accepted by One Earth – and the PDF is available at http://ssrn.com/abstract=4301771. Authors include Kelly James[1], Peter I. Macreadie[2], Heidi L. Burdett[3, 4], Ian Davies[5], John Baxter[6], and Nicholas A. Kamenos[7, 8*]

[1]School of Geographical and Earth Sciences, University of Glasgow, Glasgow, UK.

[2]Centre for Integrative Ecology, School of Life and Environmental Sciences, Deakin University, Burwood, Australia.

[3]The Lyell Centre for Earth and Marine Science and Technology, Edinburgh, United Kingdom

[4]School of Energy, Geoscience, Infrastructure and Society, Heriot-Watt University, Edinburgh, UK

[5]Marine Scotland Science, Aberdeen, UK

[6]School of Biology, Faculty of Science, University of St Andrews, St Andrews, United Kingdom.

[7]Umeå Marine Sciences Centre, Umeå University, Norrbyn, Sweden.

[8]Department of Ecology and Environmental Sciences, Umeå University, Umeå, Sweden

*Communicating author: nick.kamenos@umu.se

2.1 Summary

Blue carbon (BC) is receiving much attention within Agenda 2030 as a nature-based solution (NBS) to climate change, but classically focuses only on seagrass meadows, mangrove forests, and tidal marshes – these are characterised by 2 key ecosystem features (high primary productivity and organic sediment accumulation). However, other ecosystems could also be important but remain neglected in NBS strategic planning. Using meta-analysis, we have identified four additional ecosystem features that enable other non-classical systems – including intertidal mud flats, coralline algae beds / rhodoliths and shallow seabed sediments (particularly fjords) – to play a major role in global BC burial. A paucity of empirical evidence for other coastal systems (coral reefs, bivalve beds, rocky reefs and polar zoobenthos), currently prevents an objective assessment of their role in BC storage. Informed by this, we propose a real-world application framework, including research and management priorities, for fully integrating BC as a NBS to climate change across ecosystems; this will "close the loop" on carbon burial including all contributing non-classical BC ecosystems. Failure to do so will risk a major weakness in the global BC inventory, limiting the effectiveness of any implemented NBS strategies.

2.2 Background

Nature-based solutions (NBSs) to climate change are recognised mechanisms for drawing down carbon from the atmosphere for long-term environmental storage (Ahmed and Glaser 2016; Griscom *et al.*, 2017). Together with geoengineering, this natural solution could enable a reduction of anthropogenic carbon dioxide (CO_2) concentrations in the atmosphere (Griscom *et al.*, 2017; Anderson *et al.*, 2019), specifically addressing Climate Action targets within the UN Sustainable Development Goals (SDGs). At the land-sea interface and continental shelf, sequestration and storage of carbon by marine ecosystems (BC) has gained momentum as a globally significant process that locks away carbon for hundreds, and sometimes thousands, of years (Macreadie *et al.*, 2019a; Mao *et al.*, 2020) and is endorsed by the United Nations as a transformative ocean science solution for sustainable development (www.oceandecade.org). However, although more BC is stored per unit area compared to terrestrial soils (Pidgeon 2009; McLeod *et al.*, 2011), uncertainty over the complexity of BC capture and storage processes has limited its implementation as an NBS (Williamson and Gattuso 2022). By contrast, the contribution of the deep ocean interior to carbon sequestration and burial via the biological pump is much better understood (e.g. Middelburg 2019).

The presence of both carbon sequestration and efficient burial are required for BC ecosystems to be effective nature-based solutions (Macreadie et al., 2012; van der Heijden and Kamenos 2015; Mao *et al.*, 2022; i.e. both capture and storage of atmospheric carbon). Dissolved CO_2 is sequestered by marine plants and algae on biological timescales, (i.e. hours to decades (Howard *et al*., 2017) and a portion of that carbon may be recycled and released back into the water column, but some will become incorporated into the bottom sediments, either locally (autochthonous carbon) or elsewhere via export (allochthonous carbon). At present, ecosystems with two key features, (1) high primary productivity and (2) high localised organic sediment accumulation rates (e.g. seagrass meadows, mangrove forests, saltmarshes) that can bury significant quantities of largely autochthonous carbon (Chmura *et al.*, 2003; Bouillon *et al.*, 2008; Fourqurean *et al.*, 2012; Kirwan *et al.*, 2012) have been the focus of much BC science and policy discussions. Systems with high productivity but low sediment accumulation, such as kelp forests, have also been accepted as playing important roles in BC sequestration and 'donation' (Macreadie *et al.*, 2019a; Queirós *et al.*, 2019) despite a likely negligible role in carbon burial and storage (Hill *et al.*,2015; Krause-Jensen *et al.*, 2018).

With an international BC policy framework currently in development (www.bluecarbonpolicy.org), we are now in a timely position for leveraging a coordinated approach to accelerate the implementation and success of BC as a sustainable NBS to climate change. However, despite growing acknowledgement for BC science as a NBS tool, a knowledge gap is becoming apparent: there is now growing evidence that other ecosystems may bury comparable quantities of carbon to the 'classic' BC systems, but generally remain unaccounted for in BC inventories and under-represented in policy processes. These potential 'non-classic' BC ecosystems are likely shallow sedimentary systems (i.e. fjords (Smith *et al.*,2015; Smeaton *et al.,* 2016), intertidal mudflats (Chen *et al.,* 2020; Sasmito *et al.,* 2020)), calcifying ecosystem engineers (i.e. coralline algal, bivalve and coral reefs (Wild, *et al.*,2005; Fodrie *et al.*,2017; Mao *et al.,* 2020), rocky reefs (Porter *et al.,* 2020) and polar zoobenthos (Barnes 2017; Figure 2.1 and Figure 2.2). These systems have particular features that enable them to bury organic carbon (OC) which are not necessarily the two features present in classic BC systems. These features include: the burial of OC despite the presence of calcification (Wild, *et al.*,2005; Fodrie *et al.*,2017; Mao *et al.,* 2020); the burial of significant allochthonous carbon (e.g. Smith *et al.,* 2015; Smeaton *et al.,* 2016); the presence of high burial efficiency (e.g. Nilsson *et al.,* 2019); and highly depositional settings (e.g. Moritsch *et al.,* 2021). However, the contribution of these systems to net BC burial is complicated by potentially conflicting processes including calcification which produces CO_2 (Macreadie *et al.,* 2019a) or low carbon burial efficiency (Nilsson *et al.,* 2019). Critically, should these other ecosystems perform BC functions, then failure to account for these non-classical systems, and manage activities detrimental to their carbon stocks, mean there are likely weakness in the global BC inventory, limiting the effectiveness of any NBS strategies that are implemented solely based on classical BC ecosystems.

Many of the literature-proposed non-classical systems, are however, characterised by multiple or differing combinations of features, complicating the use of more simple unified descriptors to characterise BC ecosystems. Here, using literature meta-analysis, we show that the presence and relative balance of particular ecosystem features means we need to reconsider the current attributes that are used to classify systems as important in a BC context. Using these features along with priorities for future management and research, we propose a real-world application framework, for a holistic integration of BC as a NBS to climate change across ecosystems.

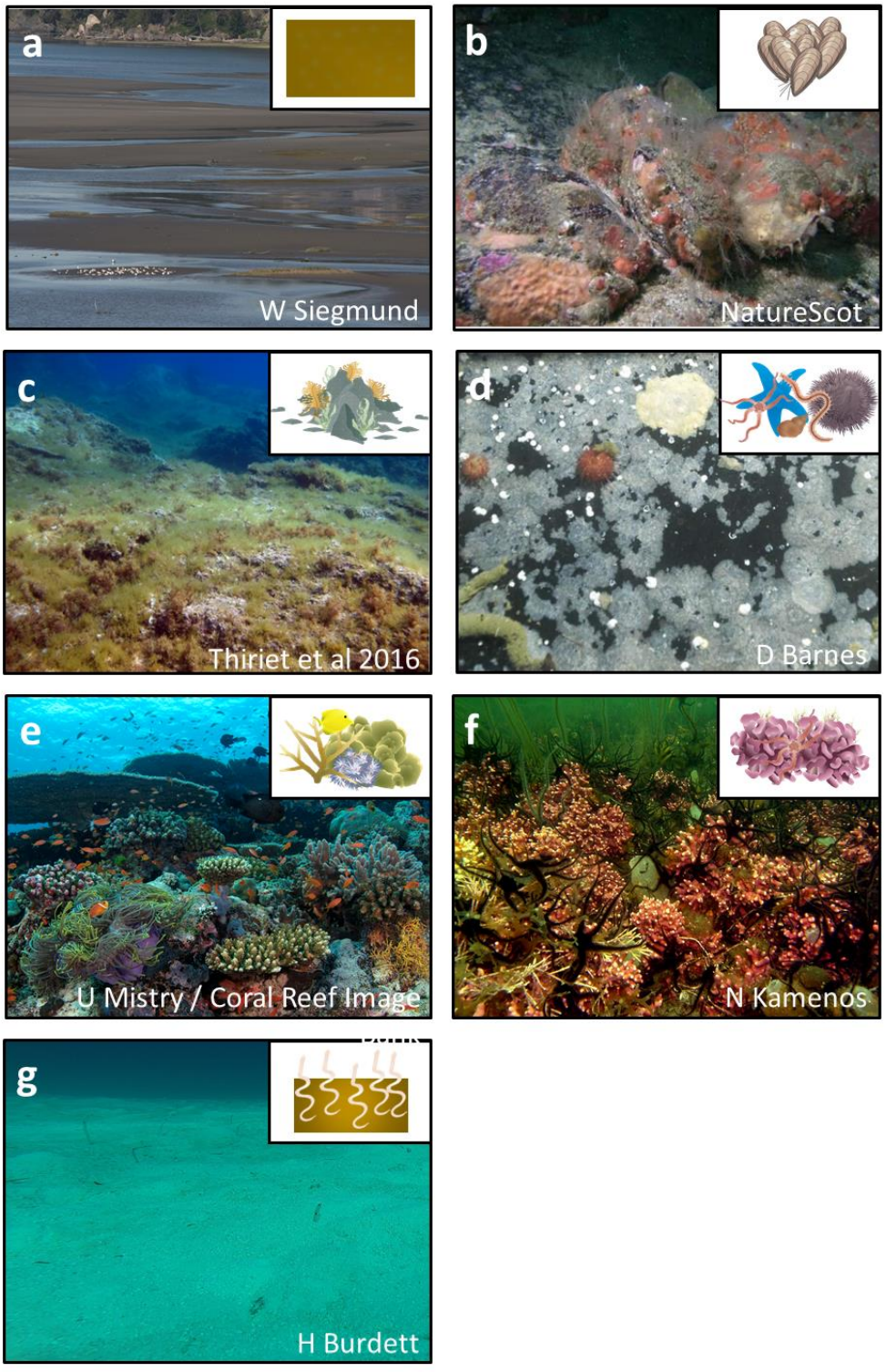

Figure 2.1: Non-classical systems that may perform BC functions. a. Mud / tidal flat (frame width = 20m). b. Bivalve bed (frame width = 10cm). c. Rocky reef (frame width = 1m). d. Polar zoobenthos (frame width = ca. 1m). e. Coral reef (frame width = 3m). f. Coralline algal bed (frame width = 20cm). g. Sedimentary system (frame width = 50 cm). Inset graphic representative of ecosystem category in Figure 2.4.

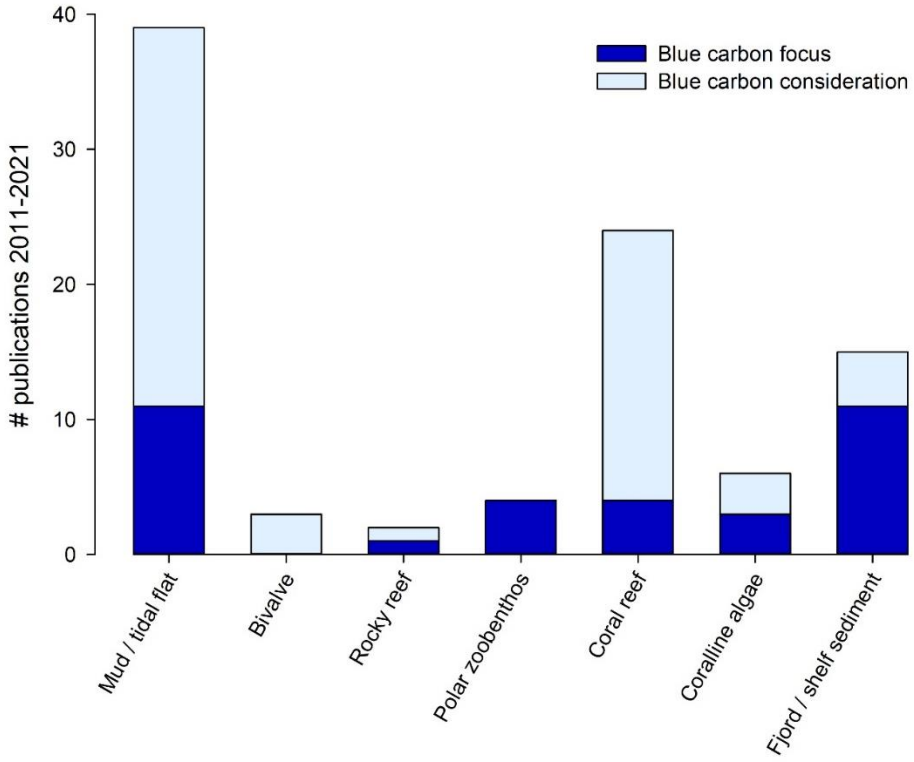

Figure 2.2. Number of peer-reviewed publications on non-classical systems 2011-2021, either primarily focused on quantifying BC processes in the target system (dark blue), or giving consideration to their BC role (light blue), based on Web of Science searches (see Methods).

2.3 Methods

2.3.1 Peer reviewed papers on non-classical systems: number of publications

To quantify the number of articles published on non-classical systems within a blue carbon context, a literature search was performed using Web of Science. Publication dates were limited to 1 January 2011 – 31 December 2021, with the search terms "blue carbon" AND the following system terms: "mudflat" / "tidal flat" ("mud flat" yielded no results); "bivalve"; "rocky shore" / "rocky coast"; "polar zoobenthos" / "zoobenthos"; "coral reef"; "coralline algae" / "coralline"; "fjord" / "shelf sediment*". Those papers whose primary focus was on blue carbon processes of the target system (as opposed to only a consideration for their blue carbon role) were manually identified from the resultant hits.

2.3.2 Meta-analysis of key features

Using a meta-analysis framework we assess if, based on four key features, candidate non-classical marine ecosystems (i.e. ecosystems other than seagrass meadows, saltmarshes and mangrove forests) also function as blue carbon repositories. We focussed on systems where i) the emergent literature indicates they may be candidate blue carbon systems, and ii) where historic terminology or differing disciplinary definitions mean such systems may not yet have been assessed in the context of blue carbon.

Literature search: We searched for scientific and grey literature in Web of Science and Google Scholar. Title and text keywords were used for searches, based on terms associated with the blue carbon research (complete term list in Appendix 1.1). The literature search was conducted between Aug-2020 and May-2021 (complete reference list used in this metanalysis in Appendix 1.2).

Quantitative data: to assess the extent to which each non-classical system was represented by each feature, we assessed the following (Figure 2.2):

Feature 1: Photosynthetic carbon uptake may balance carbon release from calcification: In some systems photosynthetic carbon uptake is driven by different organisms to those that release carbon by calcification (e.g. bivalve beds). Thus, we assessed community and

ecosystem level responses which integrated those processes rather than organism-specific responses. In the context of blue carbon, it is the integrated responses that are relevant. Carbon uptake was quantified from measurements of photosynthesis or net community / ecosystem metabolism (NC/EM). Calcification-related carbon release was quantified from measurements of calcification in the same system but not necessarily the same organism. Balance was determined by comparison of pairs of either NC/EM-calcification or photosynthesis-calcification. In all cases, we only used pairs of data that were integrated over the full diel range. All units were converted to carbon equivalents (C mol m^{-2} yr^{-1}) using a 1:1 oxygen to carbon conversion (e.g. as in Glud *et al.,* 2000, 2002).

Feature 2. High rates of external carbon supply and burial: We assessed the literature for quantification of the source proportions of OC buried within each system. In most cases this was categorised as ranges of % marine and % terrestrial contribution. Where more granularity was available, we re-categorised those data as ranges of % marine and % terrestrial. While simplified, this broader categorisation encompasses the majority of the available data.

Feature 3. Systems that exhibit low carbon remineralisation rates: Remineralisation occurs at various stages between sequestration and burial and the stage at which this occurs can vary between systems. To standardise between systems, we used OC burial efficiency (as the % of carbon buried of that reaching the sea floor) as a cross-system proxy to indicate the degree to which each system exhibited lower carbon remineralisation rates. Calculated burial efficiency was available in some literature; where not calculated and where data were available, we calculated it as the % of carbon buried of that reaching the sea floor.

Feature 4. Systems in a highly depositional setting: Rates of sediment accumulation indicating the extent of deposition in each system were converted to m ky^{-1}. For coral reef systems, we specifically targeted reef lagoons in this context.

Qualitative data and incomplete data: Many papers assessed either contained qualitative data and narratives or did not contain all the information required to make quantitative assessments. Where available we assessed the raw data provided in paper supplementary materials, if not available, we used the data as presented in the published papers. If qualitative data and/or narratives were available, we included that information in our assessment overview (text and Table 2.1), but not in the qualitative assessment in Figure 2. Where there was only limited

availability of quantitative data, these data were included in Figure 2 but we note more data are required for a complete assessment. Where data could not be converted to units relevant to all systems, these data were considered qualitatively (Table 2.1).

Habitat descriptors:

- *Mud flats and tidal flats:* Intertidal depositional systems characterised by fine sediments.
- *Bivalve beds:* populations of bivalves creating beds. For example, oysters, mussels and flame shells.
- *Rocky reefs:* subtidal reefs engineered by rocky substrata <200m deep.
- *Polar zoobenthos:* communities of polar organisms dominated by rock-dwelling bryozoans structuring the seabed in coastal waters as defined by Barnes (2017).
- *Coral reefs:* communities generated by tropical hermatypic coral reefs including the reef slope, crest, flat and lagoon, but excluding associated mangrove forests or seagrass meadows.
- *Coralline algal systems:* coralline algal beds composed of communities generated by coralline algal ecosystem engineers - generally free-living thalli.
- *Sedimentary ecosystems:* continental shelf (<200m), fjords, deltas and other non-biogenic sedimentary systems in <200m. Many fjords have inner regions extending to >200 m depth; these were also included due to their coastal location.

Allochthonous and autochthonous definitions: In the context of this assessment we use the following definitions: autochthonous OC is formed in situ (e.g. fleshy macroalgae attached to a coral reef and providing the source of OC buried in a reef lagoon) while allochthonous OC is not formed in situ (e.g. marine phytoplanktonic blooms or terrestrially derived organic material that is subsequently deposited on/in marine sediments).

2.4 Ecosystem features promoting blue carbon status in non-classical systems

Carbon uptake vs calcification carbon release: Calcifying systems release carbon dioxide during the calcification process: in seawater, theoretically 0.6 mol of CO_2 is released for each mol of $CaCO_3$ deposited (Ware *et al.,* 1992; Frankignoulle *et al.,* 1994). Thus, the role of calcifying systems as a nature-based solution to climate change has previously been questioned (Macreadie *et al,* 2017, 2019a). Calcifying organisms, including coralline algae and bivalves, can also make up a significant proportion of the community of other vegetated systems such as seagrass meadows. Calcification may therefore also lessen the extent of net carbon sequestration and storage in these classical BC ecosystems (Saderne *et al.,* 2019). Carbon released during the creation of their carbonate structures (i.e. shells and skeletons) may mean that the autochthonous carbon flux, particularly in heterotrophic systems, represents a carbon source rather than a carbon sink. However, these structures are also a geologically-important long-term store of inorganic carbon (IC; Skudder *et al.,* 2006; Fodrie *et al.,* 2017; Coppari *et al.,* 2019; Lee *et al.,* 2020; Mao *et al.,* 2020) and biological reprocessing can enhance carbonate sedimentation and burial (Perry *et al.,*2015). Across contemporary timescales, photosynthetic carbon uptake within the ecosystem communities may be able to, in part, offset some calcification-derived carbon release of the ecosystem engineers themselves (Figure 2.3 and Figure 2.4)

In calcifying photoautotrophs (such as corals and coralline algae), calcification occurs simultaneously with photosynthesis in the presence of light (Goreau 1961; Gattusso *et al.,* 1999, 2000). Community composition is therefore important in determining the reef-scale fate of OC. In coral reefs where scleractinian corals are dominant, high rates of particulate organic matter release may also enable higher carbon storage in sediments (Wild *et al.,* 2005; Tanaka *et al.,* 2008; Naumann *et al.,* 2012) as photosynthetically-derived OC may be released as particulate or dissolved organic matter and incorporated into sediments (Tanaka *et al.,* 2008; Tremblay *et al.,* 2012). Where net autotrophy occurs at the community level (e.g. on a macroalgal dominated coral reef), this may offset some calcification-derived carbon loss (Takeshita *et al.,* 2016). However, organic matter can also be returned back into the water column through processes such as microbial respiration (Tanaka *et al.,* 2008), the so-called 'sponge-loop' (Rix *et al.,* 2017) and fish herbivory (Atwood *et al.,* 2018) – features which may be enhanced in degraded or macroalgal-dominated reefs (Gattuso *et al.,* 1999, 1998, Costa *et*

al., 2020). There is also evidence for photosynthesis-calcification interactions in coralline algal beds at the individual and community scales that at least partially offset calcification-derived carbon release (Mao 2019). Recycling/reuse of calcification-derived carbon for photosynthesis by individual alga results in twice as much carbon being locked away than is released (Mao 2019). Similarly to coral reefs, coralline algal beds are net-autotrophic (with net calcification) at the community level in the daytime because of the high proportion of photosynthetic organisms, with net respiration and dissolution at night (Burdett *et al.,* 2018).

The pathway of calcium carbonate formation is thus important. However, where systems contain multiple contrasting pathways of calcification this may alter the carbon release-uptake balance further (e.g. heterotrophic vs autotrophic). Coral reef lagoons often contain carbonate sands which are derived from fish (via grazing of corals (e.g. Perry *et al.,* 2015) or physiological calcification (e.g. Walsh *et al.,* 1991), heterotrophs with and without symbionts (e.g. foraminifera (Yamano *et al.,* 2000)) and autotrophs (e.g. *Halimeda* sp. (e.g. Multer 1998; Rees *et al.,* 2007)). Estimates suggest that up to 85% of the sediments may be derived from fish (Perry *et al.,* 2015), 30% from foraminifera (Yamano *et al.,* 2000) and 65% from *Halimeda* (Rees *et al.,*2007) at different locations. Each of these pathways, and sediment proportions, will have a different impact on the carbon-balance in coral reef systems. Thus, there is evidence that carbon released by calcifying systems may not be to the extent theoretically predicted due to calcification alone (Figure 2.3).

High rates of external carbon supply and burial: Physical and biological connectivity between terrestrial and marine ecosystems underpins many ecosystem services (Macreadie *et al.,* 2012; Townsend *et al.,* 2018). Marine inter-habitat connectivity and terrestrial-marine connections are both crucial for BC storage, because neighbouring ecosystems may each play a key role in the sequestration-storage process (Smale *et al.,* 2018) and terrigenous carbon may be entrained and buried within marine systems (Macreadie *et al.,* 2015; Mao *et al.,* 2020). The three-dimensional structures created in reef-like systems such as bivalve and coralline algal beds can be key in facilitating entrainment of allochthonous particulates for subsequent incorporation and burial into the underlying sediments (Fodrie *et al.,*2017; Ridge *et al.,* 2017; Mao *et al.,* 2020). This represents a form of marine carbon additionality including the trapping of carbon lost from terrestrial systems. Many non-classical candidate BC ecosystems are dominated by ecosystem engineers (e.g. corals, bivalves, coralline algae) and are often co-located with classical BC ecosystems (Costa *et al.,*2020). The three-dimensional habitat they

create encourages high biodiversity, including BC-relevant organisms, especially macrophytes (Krause-Jensen and Duarte 2016), and facilitates the entrainment of allochthonous particulate organic matter (Mao *et al.*, 2020). For example, pseudofaeces deposition in bivalve beds (Dame *et al.*, 1984; Waldbusser *et al.*, 2013; Chambers *et al.*, 2018) can enhance the quantity of OC buried within the habitat. Similarly, by reducing wave energy along a coastline (Barbier *et al.*, 2011; Manis *et al.*, 2015; Lunt *et al.*, 2017), biologically-engineered systems can promote leeward carbon storage with reduced carbon turnover (Chen *et al.*, 2017) – this has been observed in saltmarshes protected by oyster reefs(Ridge *et al.*, 2017). The quantity of allochthonous carbon burial may be sufficient to partially offset calcification-derived carbon release (Figure 2.4), even in heterotrophic ecosystems such as bivalve beds (Norling *et al.*, 2008; Fodrie *et al.*, 2017; Ridge *et al.*, 2017; Chambers *et al.*, 2018). High rates of external carbon supply and burial to systems with relatively low autochthonous carbon generation may thus facilitate high carbon burial when in combination with other features (Figure 2.3).

Low rates of carbon remineralisation: The quantity of carbon stored in marine ecosystems is in part governed by rates of organic matter consumption and bacterial recycling and remineralisation in the water column (Feely *et al.*, 2004; Henson *et al.*, 2019), on the sediment surface (Marzocchi *et al.*, 2018) and within the sediment (Ståhl *et al.*, 2004; Glud *et al.*, 2016; Hall *et al.*, 2017; Luo *et al.*, 2018). When consumption and remineralisation rates within the marine water column are low, the efficiency of carbon export from the water column to the seabed is high (i.e. reduced biological consumption pre deposition; Buesseler *et al.*, 2007; Henson *et al.*, 2019). If remineralisation rates (and biological consumption) within the sediment are also low, a large proportion of OC (e.g. kelp landing on the seabed) will be preserved for long-term storage (Macreadie *et al.*, 2012). Thus, low remineralisation rates within both the water column and sediment could enable that habitat to act as a BC store (Figure 2.4). In general, export efficiency is higher at higher latitudes (Henson *et al.*, 2019), driven by cooler temperatures that limit bacterial activity rates (Rivkin and Legendre 2001), and defined seasonality in primary productivity and carbon sequestration rates (Harrison and Cota 1991; Henson *et al.*, 2019). Several environmental variables also affect remineralisation rates including sediment permeability, depth, temperature, sediment oxygenation, resource availability and faunal activity (Canfield *et al.*,1993; Piepenburg *et al.*, 1995; Hulthe *et al.*, 1998; Ståhl *et al.*, 2004; Middelburg and Levin 2009; Kristensen *et al.*, 2012; Glud *et al.*, 2016;

Bourgeois *et al.,* 2017; Hall *et al.,* 2017; Luo *et al.,* 2018; Nilsson *et al.,* 2019; Thomson *et al.,* 2019). Combined with highly depositional environments (above), high-latitude sedimentary systems including fjords, estuaries, deltas, mud flats and continental shelves often have low remineralisation rates (Burdige 2005; Smith *et al.,* 2015; Smeaton *et al.,* 2016; Sheilds *et al.,* 2017), enabling the storage of considerable quantities of OC (e.g. Smith *et al.,* 2015). This may be further enhanced in the coming decades due to increased upwelling and productivity resulting from glacial retreat, sea-ice melt and sediment ageing (Peck *et al.,* 2010; Bourgeois *et al.,* 2017; Hopwood *et al.,* 2019). Thus, low rates of carbon remineralisation may facilitate high carbon burial particularly when combined with other features (Figure 2.3).

***Highly depositional settings*:** Although not necessarily associated with high seabed complexity, systems characterised by high depositional rates (e.g. fjords, mud flats and deltas) can be key recipients and stores of allochthonous OC (Macreadie *et al.,* 2012; Smith 2013; Bianchi *et al.,* 2020). Carbon supply characteristics, and links to the recipient depositional environment, can govern the potential for carbon burial (Figure 2.4). Where carbon supply and deposition are high, this enables significant burial of both OC and IC, the latter of which can be derived from terrestrial weathering and therefore not subject to *in situ* carbon production (e.g. Smeaton *et al.,* 2016). Significantly, there is evidence that the proportion of buried OC of allochthonous marine and terrigenous sources can vary through time in these depositional systems. For example, present-day and historical land use practices have been shown to affect the quantity of allochthonous terrigenous material available for BC burial (Macreadie *et al.,* 2012; Mao *et al.,* 2020), driving the proportions of marine/terrestrial carbon buried in the sediment (Macreadie *et al.,* 2015; Mao *et al.,* 2020). This has implications for the management of human activities that affect BC systems which rely on allochthonous carbon donations as combined management of both the source and repository of carbon is needed. Thus, highly depositional settings may facilitate high carbon burial particularly when combined with other features (Figure 2.3).

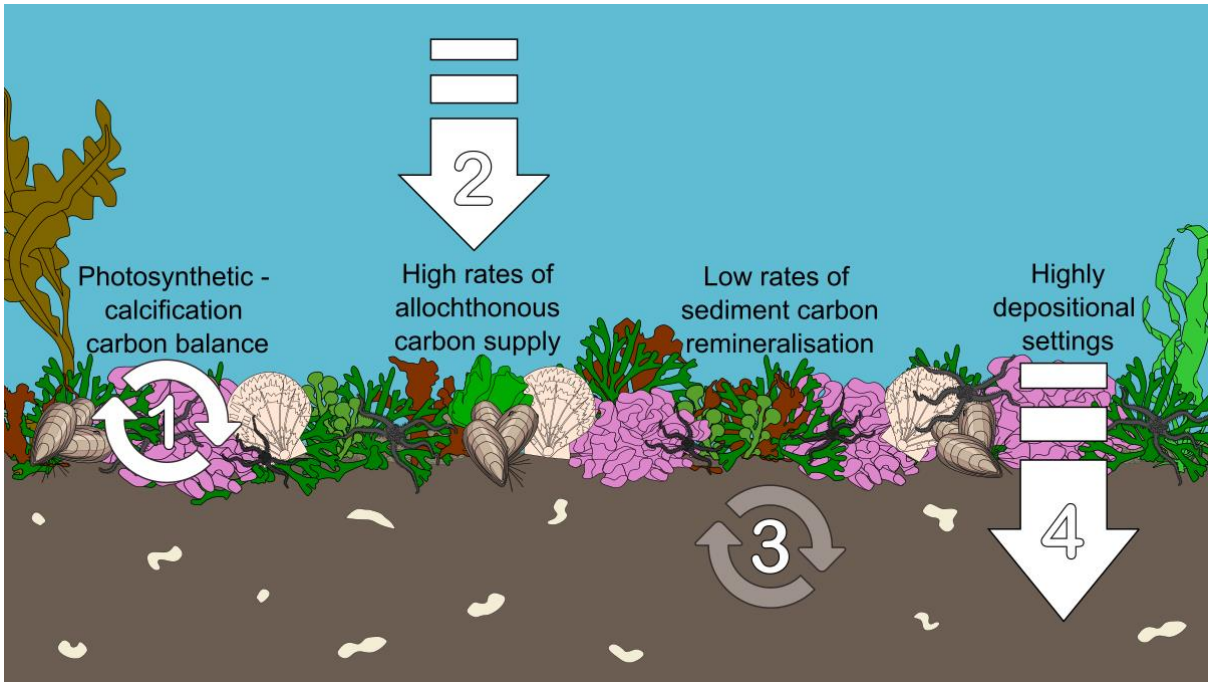

Figure 2.3: Key features promoting carbon burial in non-classical BC systems; 1. Balancing of carbon release by calcification via carbon uptake at the individual and ecosystem levels. 2. High rates of allochthonous organic carbon supply to systems that may not be characterised by high autochthonous production. 3. Low rates of sediment carbon remineralisation once carbon has been buried promoting longevity of carbon storage. 4. Systems in highly depositional geomorphological settings. Figure from James *et al.,* (*in* review). Figure concept by all authors, figure creation by Burdett.

2.5 Non-classical blue carbon ecosystems with a balance of features promoting blue carbon storage

Using both quantitative and qualitative evidence derived from literature meta-analysis, at present three of the assessed ecosystems have the potential to be important stores of BC because they exhibit a balance of the literature-proposed features promoting carbon burial: mud / tidal flats, sedimentary ecosystems including fjords and coralline algal beds (Table 2.1). This is despite the presence of potentially conflicting processes in those ecosystems including low burial efficiency and carbon release from calcification (Table 2.1; Figure 2.4). Given the large geographical extents of these ecosystems worldwide, it is therefore likely that current global BC storage estimates are substantially underestimated. It is possible of quantify carbon stocks in non-classical systems at local scales (e.g. Mao *et al.,* 2020), however, spatiotemporal variability is an important consideration for all BC ecosystems (Mao *et al.,* 2020; Williamson *et al.,* 2022) and thus global scale quantification remains challenging (Macreadie *et al.,* 2019). While there is evidence that the other systems considered (bivalve beds, polar zoobenthos and coral reefs) exhibit some of the features, at present insufficient quantitative data are available to determine if a balance of features are met that would promote carbon burial (Table 2.1). Much of the available information indicates that while these systems may be capable of sequestering carbon, there is little current evidence to indicate what proportion of the sequestered carbon is eventually buried for long term storage. Further, systems dominated by benthic heterotrophs (e.g. polar zoobenthos) require more consideration. In particular, the balance of heterotrophic carbon released over the organism's lifetime should be balanced against the autochthonous carbon biomass stored at any time.

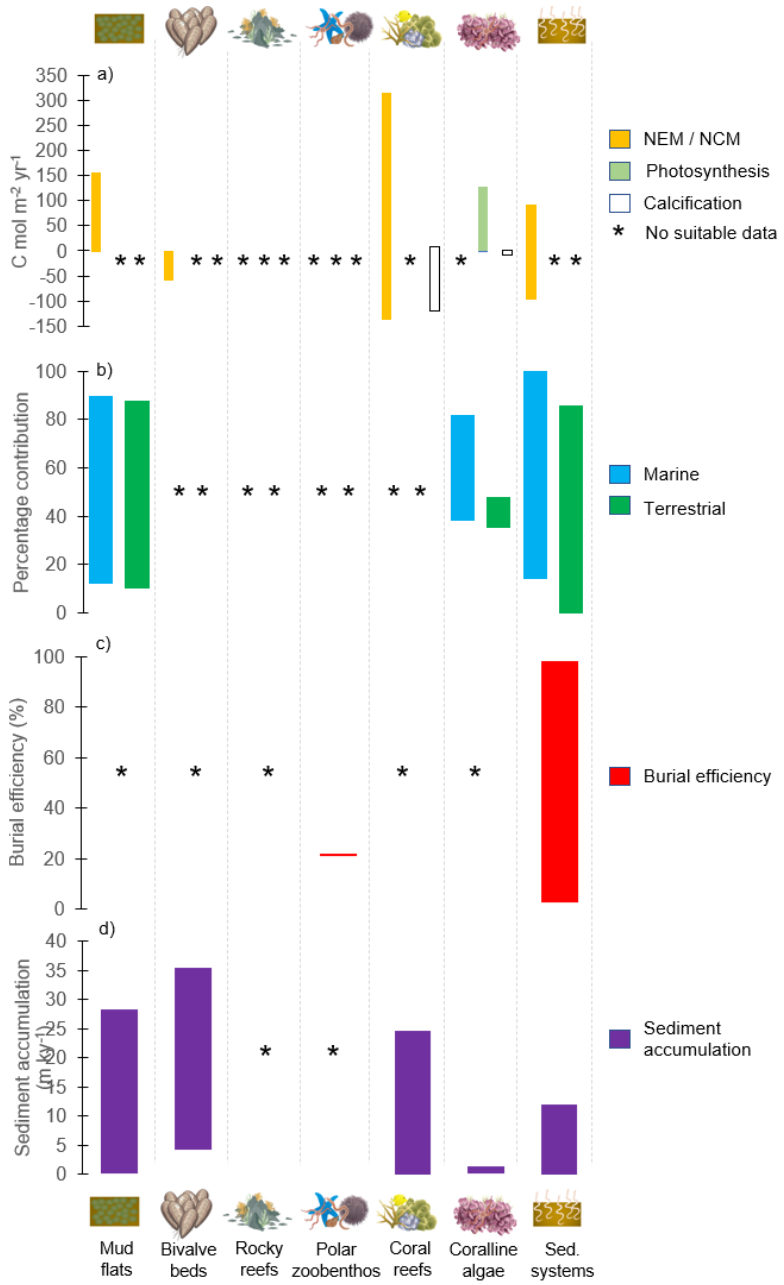

Figure 2.4: Carbon balance associated with carbon sequestration and burial in mud flats, bivalve beds, rocky reefs, polar zoobenthos, coral reefs, coralline algal beds, shelf sedimentary systems (including fjords). a) *Feature 1: Photosynthetic carbon uptake may balance carbon release from calcification.* Range of carbon exchange processes (Net Ecosystem Metabolism (NEM) / Net Community Metabolism (NCM), photosynthesis and calcification) in carbon equivalents (assuming 1:1 oxygen to carbon following [91]. b) *Feature 2. High rates of external carbon supply and burial.* Range of contributed organic carbon (as %) derived from marine and terrestrial sources in each system. c) *Feature 3. Systems that exhibit low carbon remineralisation rates.* Range of organic carbon burial efficiencies as the % of carbon buried of that reaching the sea floor. d) *Feature 4. Systems in a highly depositional setting.* Range of sediment accumulation rates indicating extent of depositional environment; sediment accumulation for corals reefs refers to lagoon sediments. Black * indicates no data available or experimental design / units not appropriate for quantitative comparison. All data based on the quantitative literature. Figure from James *et al.,* (*in* review). Figure concept by all authors, figure creation by Kamenos and Burdett.

Table 2.1: Synthesis of the presence of features that promote non-classical systems to store BC, based on the currently available qualitative and quantitative evidence. ✓ = preponderance of literature support, (✓) = some qualitative evidence for at least periodic process occurrence, X = not likely in the system, ? = not enough evidence to make assessment. Balance of calcification released C refers to the balance of C released by calcification by other uptake processes in that ecosystem (e.g. photosynthesis). Classes were qualitative and based on the prevailing literature. Figure from James *et al.,* (*in* review) – concept and creation by all authors.

	Classical BC ecosystem features		Non-classical BC ecosystem features				**Synthesis: balance of features promoting organic carbon burial?**
System	High primary productivity	High localised sediment accumulation rate	Balance of calcification-released C	Allochthonous C burial	Low C remineralization rates (high burial efficiency)	Highly depositional environment	
Mud flats	✓	(✓)	X	✓	?	✓	✓
Bivalve beds	(✓)	?	X	(✓)	?	✓	**?**
Rocky reefs	✓	?	?	(✓)	?	?	**?**
Polar zoobenthos	(✓)	?	?	?	✓	?	**?**
Coral reefs	✓	(✓)	X	(✓)	X	(✓)	**?**
Coralline algae	✓	✓	✓	✓	(✓)	(✓)	✓
Sedimentary ecosystems	(✓)	✓	X	✓	✓	✓	✓

2.6 Management considerations to promote sustained carbon burial by non-classical systems

The ability to recognise and acknowledge systems that bury carbon is vital to ensure their continued provision of nature-based services. Central to this recognition, will be our ability to manage such systems, beginning locally, in a way that enables their continued service provision. More widely, international policy frameworks enable the inclusion of marine and coastal systems providing nature-based solutions into policy. For example, via the Paris Agreement, BC can be included in nationally determined (carbon) contributions. Countries can include such systems in their national-level adaptation strategies for sustainable development. For these frameworks, marine spatial planning is an invaluable instrument for managing coastal and marine activities linked to BC (e.g. Cisneros-Montemayor *et al.,* 2019; Lovelock and Duarte 2019). This is particularly pertinent when considering non-classical BC systems in the context of climate change. For example, consideration has been given to the relative merits of protection vs restoration during marine spatial planning of BC systems (Moritsch *et al.*, 2021). While both restoration and protection have value to both preserve the carbon already buried and to enable continued sequestration, capture and storage, a focus on protection over restoration is more effective (Moritsch *et al.,* 2021). This effect will be magnified where systems accrete particularly slowly and/or bury carbon over extended geologic periods (Mao *et al.,* 2020). For example, where calcifying biota accrete OC-bearing deposits over millennia, remobilisation of such carbon via damage to the ecosystem represents a temporally greater release than the short-term sequestration increase over the coming century through ecological restoration. For the non-classical systems identified here, it would seem there is an unequivocal remit of protection over restoration in the marine spatial planning process (which would also benefit biodiversity). For this to happen effectively, marine spatial planning should provide, by default, capacity for the protection of any identified BC systems beyond seagrass, mangroves and saltmarshes, yet also have scope to legislate the restoration or enhancement of those systems where damage has already occurred (for example in Europe the EU Habitats Directive and OSPARCOM). This is particularly pertinent where nations may not be governed by the REDD++ framework but where local conservation initiatives are guided or governed by wider international frameworks. In this context, we propose a flexible management framework that balances BC storage capacity against alternative management priorities at the local, but also international, scales (Figure 2.5).

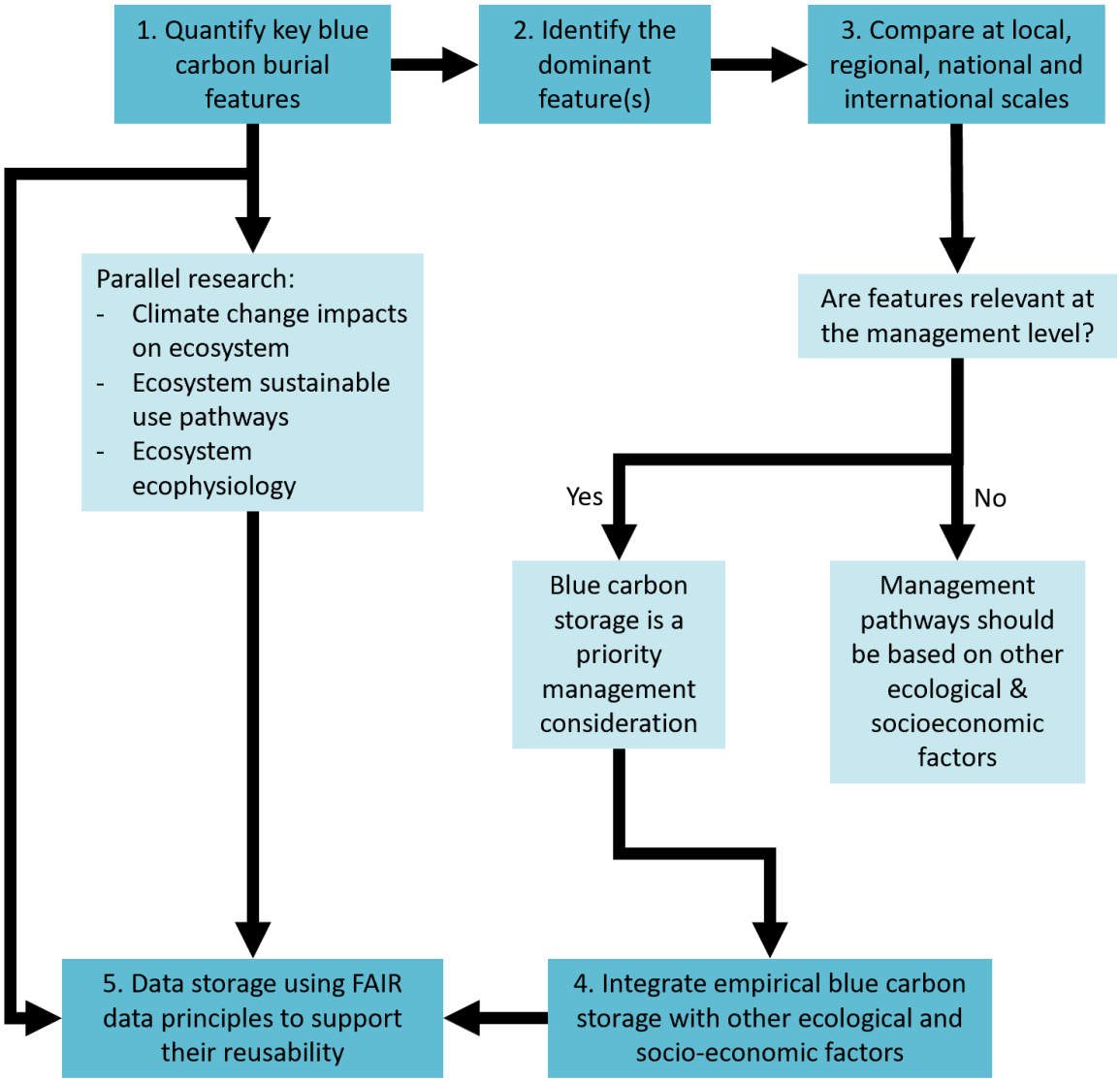

Figure 2.5: Proposed evidence-based framework for inclusive BC storage management. Initial BC storage assessment is quantified based on the four key ecosystem features (c.f. Figure 2.3). These empirical data can then be placed in the local-international context - with flexibility depending on the management viewpoint - to guide the prioritisation of BC storage as a management consideration, as well as parallel research to improve our knowledge of other socio-ecological processes within the system. Adopting the ICON science principles to be Integrated, Coordinated, Open and Networked [94], will maximise stakeholder benefit during policy implementation and facilitate cross-system transferability of science outcomes. Figure from James *et al.,* (*in* review) – concept and creation by all authors.

2.7 Moving forward: research and management priorities over the coming decade for non-classical blue carbon repositories

Given recent momentum in the application of BC storage as a natural climate change mitigation measure (Griscom *et al.,* 2017), efforts to address knowledge gaps at local-global scales are required to ensure more robust assessment of BC ecosystem spatio-temporal distribution and dynamics (Figure 2.5). To address this, we present 15 priorities for the coming decade to resolve BC dynamics:

A. Several non-classical BC ecosystems capture and bury marine and/or terrigenous allochthonous carbon. Thus, their function as a nature-based solution to climate change depends, in varying degrees, on continued supply of OC from other systems or the wider depositional environment in which they occur. This may represent a form of unquantified carbon, so long as it can be demonstrated that the carbon would otherwise end up in the atmospheric CO_2 pool if not captured and stored long-term within these non-classical BC ecosystems. Determining allochthonous pathways and contributions will be critical for the management of carbon stores in the future, as well as determining alternative fates of allochthonous carbon if these non-classical BC ecosystems weren't present. Priorities in this context are:

    1. For each system, determine the burial efficiency of different donor carbon types (e.g. labile vs refractory) to help rank the most dominant contributions to buried carbon.

    2. Determine the spatio-temporal variability in local carbon supply chains to non-classical burial hotspots (e.g. via isotopic, eDNA or biomarker fingerprinting approaches). For example, if the majority of carbon buried in a marine system is terrigenous, then the carbon donor, donor pathway and recipient repository all need to be protected.

    3. Where losses of terrigenous carbon are buried in marine systems, determine the implications for carbon accounting (e.g. double accounting) where carbon stocks allocated to terrestrial systems are in reality buried in the marine environment, or

alternative fates of allochthonous carbon for scenarios where non-classical BC ecosystems are degraded or lost.

B. A key characteristic required of all nature-based solutions to climate change is a net OC burial. This information is only partially available for many ecosystems, and may be particularly complex to determine in some cases due to the links between systems, including carbon donor-store relationships. A first step should be quantification of such balances, both now and for the future, via more complete carbon budgets. This is particularly pertinent for heavily calcified systems including coral reefs and bivalve beds. This is not a trivial task as processes may be spatio-temporally variable, particularly where the ecosystem incorporates multiple biotopes or undergoes periodic phase shifts. In this context, while many incubation experiments for either net ecosystem metabolism or calcification do exist (as do theoretical carbon budgets) quantification of carbon recycling, and importantly burial efficiency is still lacking at suitably long timescales. Priorities are:

    1. Quantifying recycling of carbon released during calcification via autotrophic processes in autotrophic calcifying systems. This should be considered at both ecosystem and individual levels.

    2. While we consider OC primarily, in the context of B1), systems that contain multiple pathways of calcification (coral reef lagoons with mixed carbonate sediments in particular) require that the relative role of each of these pathways on the carbon-balance is better quantified (a predominance of autotrophic pathways will be more likely to show a balance of carbon release (calcification) and uptake (photosynthesis)).

    3. Determining longer term carbon burial efficiency via remineralisation assessments. If buried carbon is rapidly remineralised and recycled, this detracts from the ecosystem's role in longer term carbon burial.

C. Projected climate change provides an added level of complexity to Priorities A and B. We already know that climate change affects the capacity for ecosystems to store carbon (e.g. Mao *et al.,* 2020). We now need to assess both the current storage capacity

(in the context of carbon balances in Priorities A and B) and project the magnitude of change due to a range of inter-connected, rapidly changing, factors over the coming century (e.g. altered community composition and sediment biogeochemistry). Whether carbon storage will be positively or negatively affected by these factors remains uncertain, even for classical BC ecosystems. Site-specific changes will further influence the complexity of BC storage processes, necessitating a clear understanding of spatio-temporal drivers of BC storage across ecosystems. One approach to determining the interaction of such complex environmental and human stressors in the future is to investigate historical changes in carbon burial in areas with accurately recorded or reconstructed environmental and human histories. Such data could be used in predictive models of future carbon burial. These factors have significant potential to alter carbon burial over the coming century and should be the focus of future scientific research:

1. Changes in carbon input (Behrenfeld *et al.*, 2006; Smoak *et al.*, 2013; Barnes *et al.*, 2020),
2. A breakdown of carbonate structures (Kamenos *et al.*, 2013; Mollica *et al.*, 2018),
3. Altered community composition (e.g. Brodie *et al.*, 2014),
4. Associated ecophysiology (e.g. Harley *et al.*, 2012; Burdett *et al.*, 2018),
5. Shifts in habitat distribution (e.g. Brodie *et al.*, 2014; Simon-Nutbrown *et al.*, 2020),
6. Changes to sediment and water biogeochemistry (e.g. Brodie *et al.*, 2014; Ravaglioli *et al.*, 2019),
7. Changes in coastal habitation and development (e.g. Macreadie *et al.*, 2013; Mao *et al.*, 2020)

D. Cross-cutting the research-orientated Priorities 1-3 is the role of management. If ecosystems are not appropriately acknowledged for their BC storage capacity, they risk reduced protection, exposing them to disturbance that may cause the release of carbon that in some cases has been locked away for millennia (e.g. Macreadie *et al.*, 2013; Moritsch *et al.*, 2021). Omitting systems from global BC estimates due to a paucity of information and / or making assumptions about biogeochemical processes could thus lead to substantial underestimates in total global OC storage and in assessments of its spatial variation. Priorities in this context are:

1. Spatially resolved cost-benefit analysis of enhanced management of activities affecting current (classical) BC ecosystems over incorporation of non-classical ecosystems.

2. Generally non-classical BC ecosystems are slower to accrete with respect to classical ecosystems. However, non-classical ecosystems also have the capacity to store OC over millennia creating significant carbon repositories of low turnover. Quantifying millennial-scale carbon inventories will be required to enable D1).

We show that closing the loop on carbon burial by including all contributing non-classical BC ecosystems is critical if we are to avoid major weakness in the global BC inventory. Imperative to ensuring the effectiveness of implemented NBS strategies will be the management of activities detrimental to carbon stocks. We provide a framework for implementing this management approach that can be applied across any coastal ecosystem that functions as a BC repository.

Chapter 3 Organic carbon quantity and reactivity is linked to hydrodynamic conditions and carbon source in Rhodolith beds

3.1 Introduction

Previous research has identified that rhodolith beds are blue carbon (BC) repositories (Mao *et al.,* 2020), with the current Scottish rhodolith bed BC inventory estimated as 20 million tonnes OC (Mao *et al.,* 2020; Simon-Nutbrown *et al.,* 2020). However, as current organic carbon (OC) storage estimates are based on one study site in Scotland (56°01.99' N, 05°36.13' W; Mao *et al.,* 2020), little is known of the spatial variability of rhodolith bed carbon stocks. In particular, it is not known how the quantity, reactivity, and source of OC vary between different bed types. As rhodolith beds are globally abundant benthic communities (Foster 2001; van der Heijden and Kamenos 2015), existing in a variety of environments, depths and latitudes, with differing levels of live and dead coralline algae (van der Heijden and Kamenos 2015; Riosmena-Rodríguez *et al.,* 2017), carbon storage is likely to vary between beds. This represents a critical knowledge gap and could result in rhodolith bed BC not being protected from human disturbance. For example, rhodolith beds that store a large quantity of carbon, that has accumulated over millennia (Mao *et al.,* 2020), may not be protected by current measures and are vulnerable to degradation (e.g. through calcium carbonate mining (Riosmena-Rodríguez *et al.,* 2017) and bottom trawling fishing (Hall-Spencer and Moore 2000; Tauran *et al.,* 2020; Fragkopoulou *et al.,* 2021). Similarly, other bed types, including beds primarily made of dead coralline algae, may not be protected, however, may still store a vast quantity of OC that is vulnerable to disturbance (Macreadie *et al.,* 2019). Currently, legislation does consider the effects of land change and development on rhodolith bed BC, with the potential of land-based activities adjacent to rhodolith beds causing long-term change to the terrestrial carbon supplied to the system (Macreadie *et al.,* 2012; Mao *et al.,* 2020).

3.1.1 Organic carbon quantity

There are several ways in which carbon storage can vary between rhodolith beds, the first being the quantity of OC stored in the sediments (here on defined as sedimentary OC (SOC)). Globally, rhodolith beds can be found in a variety of depositional settings from sheltered fjords to exposed coastal sites (Riosmena-Rodríguez *et al.,* 2017). The hydrodynamical energy at

these sites can vary drastically, with exposed sites characterised as having higher hydrodynamical energy than sheltered sites (Riosmena-Rodríguez *et al.,* 2017). As hydrodynamical activity is known to affect SOC storage in other systems (Samper-Villarreal *et al.,* 2016; Dahl *et al.,* 2018), the quantity of OC stored will likely vary between sites with different levels of exposure.

Hydrodynamical energy can influence the SOC through sediment resuspension and sediment grain size. Increased hydrodynamical activity can cause sediment resuspension (Dahl *et al.,* 2018), introducing the SOC into the water column where it is either remineralized by bacteria or transported elsewhere (Macreadie *et al.,* 2013). Sediment resuspension can also increase oxygen exposure within the sediments. As, thermodynamically, O_2 is the most favourable electron acceptor for carbon mineralization, oxygen exposure increases the remineralisation of SOC resulting in SOC loss from the sediment (Glud 2008; Zhao *et al.,* 2018; Macreadie *et al.,* 2019). If fresh material is reintroduced into sediments following resuspension, it can result in microbial priming, where the fresh carbon provides sufficient energy to microbes for the enhanced degradation of the SOC (Trevathan-Tackett *et al.,* 2018; Chen *et al.,* 2022). Hydrodynamical energy also influences sediment type, which in turn can also affect SOC storage (Serpetti *et al.,* 2012; Hunt *et al.,* 2020). Low-energy environments can facilitate the settlement of fine-grained sediment (including mud, silt and clay; Dahl *et al.,* 2018). These fine-grained sediments have a high affinity to OC, with the increased surface area providing more area for the sorption of OC (Kell *et al.,* 1994; Hedges and Keil 1995). Furthermore, fine-grained sediments can have lower oxygen exchanges and shallower redox potentials, limiting aerobic remineralisation and favouring the preservation of OC within sediments (Hedges and Keil 1995; Dauwe *et al.,* 2001; Burdige 2007; Glud 2008).

The quantity of OC stored in rhodolith beds may also vary between live and dead beds. Rhodolith beds can consist of both live and dead coralline algae, with the algae dying off due to natural and anthropogenic causes (for example, bottom trawling fishing; Fragkopoulou *et al.,* 2021). Once the coralline algae die, deposits can remain with dead coralline algae gravel present on the sediment surface (Riosmena-Rodríguez *et al.,* 2017). It is currently not known if dead rhodolith beds continue to accumulate organic material, or if the OC already stored remains locked away within the sediment.

As rhodolith bed deposits can be several meters thick (de Grave *et al.,* 2000), it is likely that if left undisturbed, dead rhodolith beds may continue to store carbon previously locked away (Mao *et al.,* 2020). Whilst dead coralline algae on the surface of the bed undergo the dissolution of calcium carbonate, losing structure (Martin *et al.,* 2007; Kamenos *et al.,* 2013; Brodie *et al.,* 2014), the SOC within the bed may remain unchanged, with previous research finding that at a certain depth SOC concentration remain relatively constant (Mao *et al.,* 2020). SOC preservation may also be affected by changes to the epibenthos, with dead rhodolith beds harbouring lower biodiversity than live beds in some locations (Sheehan *et al.,* 2015; Riosmena-Rodríguez *et al.,* 2017). In terms of carbon already stored within the sediment, this may favour preservation in the upper layers of the sediment, with reduced bioturbation from the epifaunal community (Mazarrasa *et al.,* 2018; Thomson *et al.,* 2019). Over time, dead coralline algae gradually undergo dissolution, weakening the bed structure (Martin *et al.,* 2007; Kamenos *et al.,* 2013; Brodie *et al.,* 2014). Therefore, over centuries to millennia, dead rhodolith deposits may experience a loss in the OC stored as the bed gradually dissipates. On the other hand, the collapse of the bed structure may help retain the SOC stock, with the sediment becoming more compacted.

3.1.2 Organic carbon reactivity

The reactivity of OC stored within rhodolith beds is another parameter of carbon storage that may vary between bed types, with carbon reactivity playing an important role in the preservation of SOC. SOC is made up of a mix of labile, recalcitrant and refractory fractions (Burdige 2007; Smeaton and Austin 2022a). Compared to recalcitrant and refractory carbon, labile carbon is more biodegradable, made of molecules with a small molecular weight that can be remineralised by both aerobic and anaerobic processes (Burdige 2007; Arndt *et al.,* 2013). Recalcitrant and refractory carbon, on the other hand, is made of more resistant complex compounds with higher molecular weights, which can only be remineralised in the presence of oxygen (Burdige 2007). Therefore, the proportion of labile, refractory, and recalcitrant carbon that makes up the SOC influences its vulnerability to bacterial remineralisation with OM with a higher proportion of labile material more vulnerable to degradation (Kell *et al.,* 1994; Goldstein *et al.,* 2020; Smeaton and Austin 2022a).

SOC reactivity can be affected by several factors, including carbon source and bacterial degradation (Burdige 2007; Smeaton and Austin 2022a). Marine carbon is typically more

labile than terrestrial carbon, being made of simple sugars and amino acids rather than complex resistant compounds including lignin and cellulose (Burdige 2007; Arndt *et al.*, 2013; Hill *et al.*, 2015; Trevathan-Tackett *et al.*, 2020). Furthermore, unlike marine carbon, terrestrial carbon can undergo pre-ageing, when labile terrestrial carbon is degraded in the water column, or the terrestrial carbon is processed and undergoes physical protection (i.e. encapsulation) before being buried in sediment (Burdige 2005; Arndt *et al.*, 2013; Hemingway *et al.*, 2019). SOC reactivity can also change with depth due to bacterial degradation, with OM processes within the sediment having a lower proportion of labile material and therefore being less reactive (Canfield 1994; Arndt *et al.*, 2013). Understanding the reactivity of OM can give a valuable insight into how vulnerable carbon stocks are to disturbance, with sediments that have a higher proportion of labile carbon more vulnerable to bacterial degradation if exposed (Black *et al.*, 2022; Smeaton and Austin 2022a).

3.1.3 Source of organic carbon to the sedimentary carbon stock

A further parameter that may vary between rhodolith beds is the relative contribution of marine and terrestrial allochthonous carbon. Current estimates of the ratio of marine to terrestrial carbon in rhodolith beds are limited to one site, with terrestrial and marine contributions ranging from 32-49% and 51-69% respectively (Mao *et al.*, 2020). In other systems, terrestrial and marine contributions can vary by several magnitudes (Bianchi 2011; Lafon *et al.*, 2014; Smith *et al.*, 2015; Cui *et al.*, 2016). For example, in fjord systems, terrestrial contributions can be near 100% when riverine input is high, and near 0% when high surface water circulation transports a high proportion of terrestrial carbon to the continental shelf (Lafon *et al.*, 2014). Marine carbon contributions, on the other hand, can be linked to ecosystem primary productivity, with high productivity increasing the proportion of marine carbon stored within sediments (Koziorowska *et al.*, 2016; Mao *et al.*, 2020). Understanding the major carbon donor pathways to a system is important, with changes in carbon sources linked to changes in climate and land use (Blake *et al.*, 2007; Mao *et al.*, 2020; Inglis *et al.*, 2022). For example, elevated rainfall can increase runoff and the proportion of terrestrial carbon supplied to coastal systems (Inglis *et al.*, 2022). Investigating the relative contributions of marine and terrestrial carbon to BC storage can also inform policy, with the potential of on-land and marine developments having unintended consequences for BC storage (Sasmito *et al.*, 2019, 2020).

3.1.4 Chapter aims

Several different parameters must be investigated when assessing a system's ability to act as a BC repository. Systems must bury OC, with a high proportion of the OC preserved after it is remineralised by bacteria. Understanding the dominant sources of carbon in a system is also important, with terrestrial carbon typically less reactive and vulnerable to bacterial degradation than marine carbon (Burdige 2007; Hill *et al.,* 2015; Trevathan-Tackett *et al.,* 2020). Furthermore, assessing the source of carbon to a system can give an insight into the main carbon donor pathways, allowing for predictions to be made about changes to contributions under climate change, and allowing for policy to be put in place to protect pathways. This chapter investigates how the quantity, reactivity and source of OC vary with rhodolith bed structure and health. Scotland was used as a model system, with live, dead and mixed (live/dead) rhodolith beds present in a variety of sheltered and exposed environments. Furthermore, there are rhodolith beds present in Scotland that are interlinked with seagrass meadows, offering a unique opportunity to investigate carbon storage in areas that have multiple BC systems. As rhodolith beds are currently considered BC systems by the Scottish Government (Burrows *et al.,* 2014; Turrell 2020), investigating spatial variability between bed types also contributes to the Scottish BC inventory.

Sediment cores were collected from four locations in Scotland to:

a) identify if carbon storage varied between sheltered and exposed beds,

b) identify if carbon continued to be stored in beds where the coralline algae are dead, and

c) characterise carbon storage in a rhodolith-seagrass interlinked bed.

3.2 Methods

3.2.1 Study sites

Sites at Upper Loch Torridon, Sound of Barra, Sound of Eriskay and Tingwall (Orkney) were chosen to reflect different types of rhodolith beds: sheltered, exposed, inter-linked and dead (Table 3.1; Figure 3.1). A detailed description of each site, including coring coordinates, bed type and status (live/dead), depositional environment, depth of coring site, surrounding terrestrial organic soil content, and dominant terrestrial land types can be found in Table 3.1.

Table 3.1: Description of study sites including coordinates (latitude, longitude), details on bed type (with exposure index ranging from most sheltered (1.7 units) to most exposed (4.5 units)) and status, depositional environment, depth of coring site (m), organic soil content, and dominant land types .[1]Burrows et al, (2008), [2]UK Soil Observatory (2022), [3]Campbell and Marchbank, (2013), [4]Smeaton and Austin (2022b), [5]Richards (1998), [6]Land Use Consultants (1998), [7]Scottish Natural Heritage (1996)

Site	Coordinates (Lat, Long)	Bed Type (Exposure Index)[1]	Bed Status	Depositional Environment	Depth of coring site	Surrounding Terrestrial Organic Soil Content[2]	Dominant Terrestrial Land Types
Upper Loch Torridon	57.541167, -5.532167	Sheltered (2.51)	Live	Fjordic	20 m	Organo-mineral (12-35%) to organic (>35%)	Dry and wet heath habitats[3,4]
Sound of Barra	57.052356, -7.415361	Exposed (3.37)	Live and Dead	Open Ocean	7 m	Low (<1.5%)	Grassland and machair. Crofting present[5]
Sound of Eriskay	57.094361, -7.297278	Exposed (3.13)	Dead	Open Ocean	7 m	Moderate (1.5-3%) to organic (>35%)	Grassland and machair. Crofting present[5]
Tingwall (Orkney)	59.087722, -3.038861	Exposed (2.94)	Live and Dead.	Shallow coastal site, inter-linked with seagrass meadow[3]	4 m	Humose (5-12%)	Moorland and limited tree cover[6]
Loch Sween	56.031837, -5.601581	Sheltered (2.07)	Live	Fjordic	6 m	Humose (5-12%)	Grassland, moorland and farmland[7]

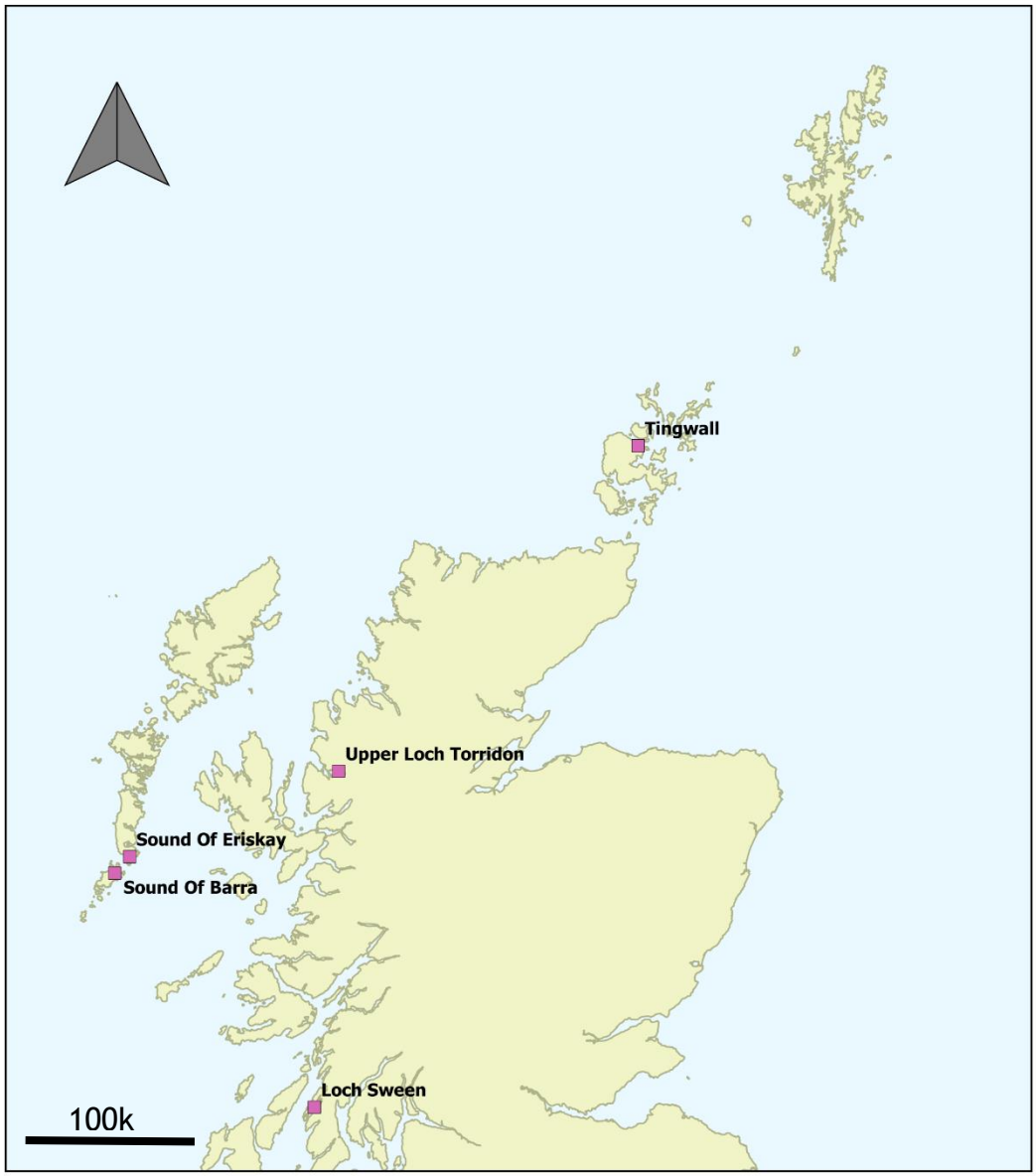

Figure 3.1: Map of sampling sites with Upper Loch Torridon, the Sound of Barra, Tingwall, the Sound of Eriskay and Loch Sween labelled.

3.2.2 Core collection

Cores of a maximum of 30cm depth were collected with scuba using a drop hammer. Once extracted, cores were kept in an upright position during transportation to the shore to minimise the mixing of sediment within the core. They were then placed into a freezer (-18°C) within 30 minutes of collection and were kept frozen until returned to the laboratory for processing.

3.2.3 End-member sampling

At each study site, samples of terrestrial and marine organic materials were collected to enable the identification of carbon sources within the coralline algae beds. Sample types collected were: terrestrial soil (n= 5 for each site, collected every 30m in altitude from sea level), terrestrial plants, marine macroalgae (from both the coralline algae bed and the intertidal zone), and marine fauna (collected from the coralline algae bed). Terrestrial samples were frozen (-18°C) immediately after collection, whilst marine macroalgae samples were first washed gently with deionised water before being frozen (-18°C). Marine fauna was depurated in filtered seawater for 12 hours to remove the gut contents and then rinsed in deionised water before being subsequently frozen. I was unable to obtain enough material for marine particulate organic matter (POM), and terrestrial POM end-member samples. As $\delta^{13}C$ and $\delta^{15}N$ are similar for marine and freshwater POM (Mao *et al.,* 2020), literature samples were not included in the stable isotope model.

3.2.4 Preparation of samples

Sediment cores were cut into 1cm horizons whilst frozen using a diamond-bladed band saw. Horizons were then dried in a freeze-dryer for 72 hours. The wet and dry weight of each horizon was measured (2 d.p), and the horizons were subsequently sieved into four fractions (<63 µm, 63-250 µm, 250-500 µm, and >500 µm). Before sieving, a small subsample (~2g) was removed for ^{210}Pb dating. For selected horizons (3 per core ranging from the bottom to the middle of the core), small bivalves were removed from the >500 µm fraction and sent away for radiocarbon dating.

For stable isotope analysis, samples were milled into a small powder using a ball and mill grinder. A small portion (0.5-2g) of the sample was then acidified using 1mol HCl and washed

with deionised water until a neutral pH was reached to remove calcium carbonate from the sample. Samples were then dried in a freeze-dryer for 72 hours.

End member samples were dried at 40°C for 72 hours before being ground using a ball and mill grinder. Using the same method as above, 0.5-2g of the sample was then acidified and then washed with deionised water and freeze-dried for 72 hours.

3.2.5 Core dating

3.2.5.1 Lead-210 dating

Dried marine sediment samples from the sediment cores were analysed for ^{210}Pb, ^{226}Ra, ^{137}Cs and ^{241}Am by direct gamma assay in the Environmental Radiometric Facility at University College London, using ORTEC HPGe GWL series well-type coaxial low background intrinsic germanium detector. ^{210}Pb was determined via its gamma emissions at 46.5keV and ^{226}Ra by the 295keV and 352keV gamma rays emitted by its daughter isotope ^{214}Pb following 3 weeks of storage in sealed containers to allow radioactive equilibration. ^{137}Cs and ^{241}Am were measured by their emissions at 662kev and 59.5kev (Appleby et al, 1986). The absolute efficiencies of the detector were determined using calibrated sources and sediment samples of known activity. Corrections were made for the effect of self-absorption of low-energy gamma rays within the sample (Appleby et al, 1992). A constant state of supply model (CRS) was used to obtain calendar ages, with the CRS assuming that there is a constant influx of ^{210}Pb over time and that variation in ^{210}Pb activity is proportional to the variation in concentration and sediment influx.

3.2.5.2 Radiocarbon dating

Radiocarbon determinations were obtained for Upper Loch Torridon (at 24.9 cm (core base), 21.1 cm and 17 cm) and the Sound of Barra (at 28.4 cm (core base) and 19.4 cm). Radiocarbon determinations were obtained from small bivalves, with surficial calcareous encrustations removed and samples washed with deionised before being dried at 40°C for 24 hours.

Radiocarbon samples were sent to the Scottish Environmental Research Centre AMS Laboratory. For a detailed description of methods employed by the laboratory, refer to Dunbar and co-authors (2016).

3.2.5.3 Age model

Bayesian age-depth models were created for the sediment sequences retrieved from the Sound of Barra and Upper Loch Torridon using Oxcal version 4.4 (Bronk Ramsey 2021) using the '*P-Sequence'* depositional model. A variable *k* parameter of 1 was used to account for variation in sedimentation rate with depth. the *C_Date* function was used to incorporate calendar ages derived from the 210Pb constant rate of supply age model. For Torridon, an additional C_Date was included to mark the Chernobyl nuclear disaster (1986AD) based on a sustained peak in the ^{137}Cs and ^{241}Am data (Appendix 2.1). The ^{14}C dates were included using the *R_Date* function, with local deviations in the Marine Reservoir Effect accounted for using a Delta-R of −150 ± 52 (Reimer *et al.,* 2013). For Barra, an additional ^{14}C date at 19.4cm (SUERC-105078) was positioned as an outlier outside the p-sequence, as it was older than the ^{14}C date at 28.4cm (SUERC-95320). For both cores, the core top had live coralline algae growth so was considered to be 0 years (2019). Modelled ages were given as mean values ± σ ka AD.

3.2.6 Stable isotope analysis

Stable isotope analysis (with δ^{13}C and δ^{15}N) was conducted at the NEIF Stable Isotope Laboratory (at SUERC) and used to determine the main source of OC in the cores. By using end-member samples collected from the study sites, sediment δ^{13}C and δ^{15}N values can be compared with end-member δ^{13}C and δ^{15}N values to determine the OC source (marine fauna, macroalgae, soil, terrestrial plants, sheep faecal pellets, and seagrass). Four aliquots of USGS40 were analysed each day (average and standard deviation (SD) for USGS 40 over 13 analytical runs, spanning a period of 6 months (n = 54) were δ^{13}C −26.37 ± 0.11‰ and δ^{15}N −4.43 ± 0.40‰, accepted values are −26.39 ± 0.04‰ and −4.52 ± 0.06‰ respectively). For each site, δ^{13}C and δ^{15}N were calculated for the <63 µm, 63-250 µm, and 250-500 µm fractions within each 1cm section of the core.

3.2.7 Organic carbon wt% and calcium carbonate wt%

Stable isotope analysis was used to obtain the %wt of OC in each acidified fraction. The OCwt% for the fraction was calculated by:

$$OCwt\%_{Fraction} = \frac{OC\ in\ acidified\ fraction\ (\%\ wt) \times acidified\ fraction\ weight\ (g)}{non - acidified\ fraction\ weight\ (g)}$$

The total OCwt% in each section was calculated by:

$$OCwt\%_{section} = \frac{\sum OCwt\%_{Fraction} \times non-acifidied\ fraction\ weight\ (g)}{section\ weight\ (g)}$$

For $CaCO_3$, samples were weighed before and after acidification to determine the % weight of calcium carbonate in each fraction. The total $CaCO_3$wt% in the section was calculated by:

$$CaCO_3\text{wt}\%_{section} = \frac{\sum CaCO_3\text{wt}\%_{Fraction} \times non-acifidied\ fraction\ weight\ (g)}{section\ weight\ (g)}$$

3.2.8 Sedimentary organic carbon stock

The mass of OC in the sediment samples was calculated by multiplying the wt% of OC in each sample, by the mass of the samples after acidification. The OCwt% in each sediment sample was calculated by dividing the mass of OC by the weight of the sample before acidification. The OCwt% for each horizon of the core was calculated by calculating the mass of OC in the <500µm fractions and dividing that by the total mass of the <500µm fractions before acidification. For Upper Loch Torridon and the Sound of Barra, the SOC stock (Mg/ha) in the top 25cm was calculated by:

$$SOC\ stock = \sum_{i} S_i \times A$$

Where *i* refers to the number of sections of the core, S_i is the mass of OC in that section and *A* the core surface area.

The wt% of calcium carbonate in each sample was calculated by dividing the mass lost from acidification by the total mass of the sample before acidification.

3.2.9 Carbon reactivity index

The carbon reactivity index (CRI; Smeaton and Austin 2022a), was used to assess how vulnerable the SOC was to bacterial remineralisation. The CRI is based on the lability of

carbon, with a value of 0 corresponding to material that is fully labile and biodegradable, and a value of 1 corresponding to material that is fully recalcitrant/refractory and non-biodegradable (Smeaton and Austin 2022a). The CRI was determined via Thermogravimetric Analysis (TGA). Approximately 20mg of milled sediment was placed into 70 mL aluminium oxide crucibles before being placed into a Mettler Toledo TGA2. Here the samples were heated at 10°C min−1 from 40°C to 1000°C under a constant stream of N2. Mass loss between 200-400°C was due to the decomposition of organic material (OM) that was labile in nature, whilst recalcitrant OM decomposed between 400-550°C and refractory OM between 550-650°C. The following calculation was used to determine the CRI:

$$CRI = \frac{\%OM_R}{\%Total\ OM}$$

Where %OMR represents the percentage of the sample that was recalcitrant and refractory, and %Total OM represents the total % of OM in the sample (Smeaton and Austin 2022a).

In each section, the CRI was calculated for each fraction size (<63µm; 63-250µm; 250-500µm) as well as for a bulk sediment sample that had not been sieved.

3.2.10 Isotope mixing model – the source of organic carbon to rhodolith beds

The relative proportion of the different sources of carbon (terrestrial soil, terrestrial plants, macroalgae, marine fauna, sheep faecal pellets, seagrass) found in sediments was quantified using a Bayesian Stable Isotope Mixing Model (SIMM). A SIMM was run in R version 4.1.1 in R Studio (Version 1.4.1717) using the package MixSiar (Stock and Semmens 2016; Stock *et al.*, 2018). MixSIAR uses a Markov chain Monte Carlo method estimates the relative contributions of organic material in sediment samples. Contributions are expressed as posterior probability distributions, with a generalist prior (1:1). Both $\delta^{13}C$ and $\delta^{15}N$ were used as isotopic markers in the SIMM model, with fraction size used as a factor to investigate contributions of sources with fraction size. For Upper Loch Torridon, age was used as a continuous variable to investigate how carbon sources changed with time. Age could not be used as a continuous variable for the other sites as there was either evidence of sediment mixing (Sound of Barra), or the core was relatively modern (Sound of Eriskay and Tingwall). Trophic enrichment factors of -1.5‰ for $\delta^{13}C$ and -1.2‰ for $\delta^{15}N$ were used to account for the altercation of organic

material during burial (Kelleway *et al.,* 2022; Lehmann *et al.,* 2002). The MCMC algorithm parameters employed were chain length = 100,000; burn in = 50,000; thin = 50; and chains = 3. MCMC convergence was assessed based on Gelman-Rubin diagnostic statistics and Geweke statistic calculations (Stock and Semmens 2016) with variables considered insignificant if the models failed to converge. Separate SIMM models were used for each site.

3.2.11 Statistical analysis

Data analysis was conducted using R version 4.1.1 in R Studio (Version 1.4.1717). Shapiro Wilk tests and Levene's test were used to assess the distribution of the data and the heterogeneity of variance. Kruskal Wallace tests and ANOVAs (analysis of variance) were used to investigate the effects of the continuous variables age and depth and the discrete variable fraction size on OCwt%, $CaCO_{3wt}$% and CRI index with separate models run for each site. Medians (IQR duration) were given for non-parametric data and mean (±standard deviation) was given for parametric data. In all models, a significance level of 0.05 was used. With regards to the ANOVA results, R^2 refers to adjusted R^2. The package ggplot2 was used to plot the graphs.

3.3 Results

3.3.1 Age models

The sediment core at Upper Loch Torridon was 24.9 cm and spanned the last 900 years. The age model contains 3 radiocarbon dates. The base of the sequence is dated to 1122AD±79AD (Figure 3.2) and the top of the core is assigned the year the core was retrieved 2019±0AD. There are 2 intervals in the model; the bottom interval has age uncertainties ranging between 956 and 1286 (95.4% CI). The interval above is comprised of calendar ages derived from ^{210}Pb dating. ^{210}Pb activity was 108.91±5.31Bq kg^{-1} in the surface sediment and decreased exponentially with depth (Appendix 2.1). The topmost 13.1 cm (green interval in Figure 3.2) contains 13 calendar ages derived from the constant rate of supply model (Appendix 2.1). Age uncertainties for this interval range between 2 and 26. A broad peak in ^{137}Cs activity between 2.9 and 5 cm are likely from the Chernobyl accident which resulted in an increase in atmospheric ^{137}Cs in 1986AD (Appendix 2.1). The peak in ^{137}Cs agreed with the CRS model for the ^{210}Pb dates (Appendix 2.1). The sedimentation rates derived from the Bayesian model suggest there is a gradual increase in sedimentation rate between 1890 – 1930.

The sediment core from the Sound of Barra was 28.4 cm. The age model contains 3 radiocarbon dates, of which 1 is an outlier. The base of the sequence is dated to 1791AD±85AD and the top of the core is assigned the year the core was retrieved 2019±0AD (Figure 3.2). An outlier radiocarbon measurement from a single shell at 19.4cm is dated 1676AD±94AD (Figure 3.2). There are 2 intervals in the model; the bottom interval has age uncertainties ranging between 1639 and 1938 (95.4% CI). The interval above is comprised of calendar ages derived from 210Pb dating. 210Pb activity was 33.49±4.58Bq kg-1 in the surface sediment and decreased exponentially with depth (Appendix 2.1). The topmost 14.8 cm (green interval in Figure 3.2) contains 14 calendar ages derived from the constant rate of supply model (Appendix 2.1). Age uncertainties for this interval range between 2 and 28. As the age model suggested mixing, I was unable to estimate the ages for each section of the core. Instead, the depth of the core is used to explain patterns in core OC%, CRI, and source. The ^{137}Cs record of the core is poor (Appendix 2.1) and is not sufficient for dating. ^{241}Am activities were relatively low and constant throughout the top 14.8 cm and were not used in the age model. As mixing was present, sediment accumulation rates were not calculated for this site.

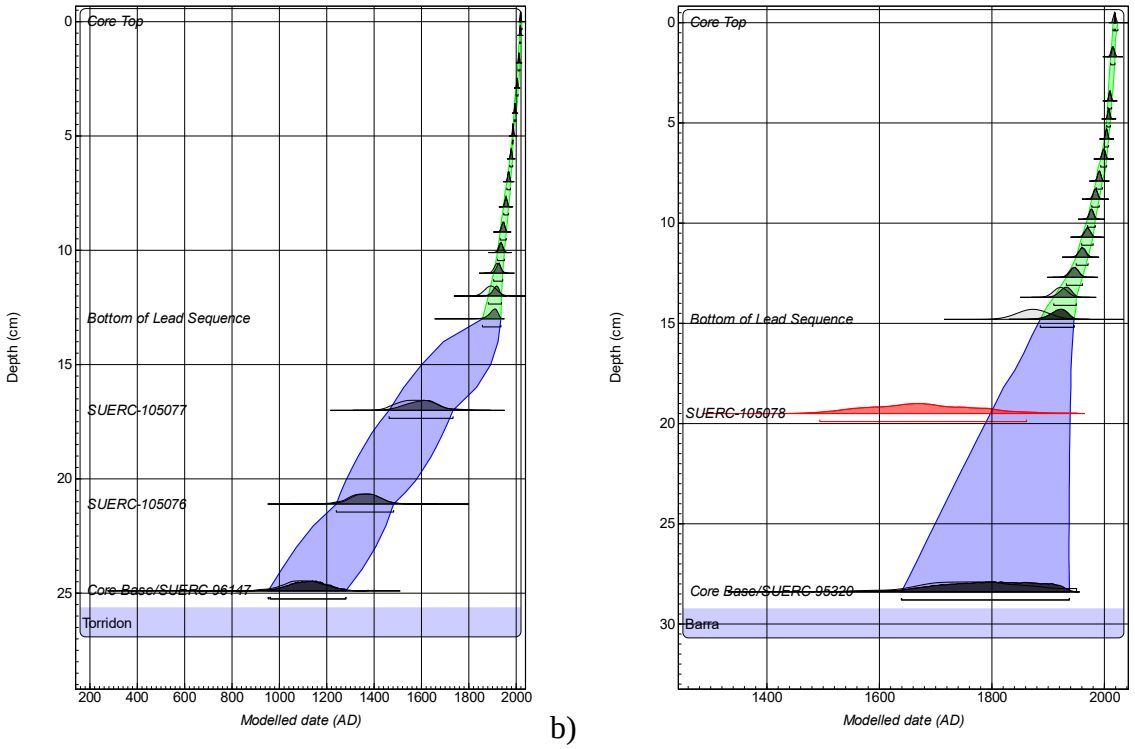

Figure 3.2: OxCal Bayesian age-depth model for a) Upper Loch Torridon and b) the Sound of Barra. The 95.4% confidence intervals are given by the green and blue envelopes, with the green envelopes representing the ^{210}Pb dates and the blue envelope the ^{14}C dates. For the Sound of Barra, the red 14C date was an outlier and suggested sediment mixing was present in the core.

The sediment core from Tingwall was 12c m. ^{210}Pb activity was 16.64±3.62Bq kg^{-1} in the surface sediment and decreased exponentially with depth (Appendix 2.1). Only a single low ^{137}Cs activity was detected at 9.55 cm (Appendix 2.1), which is insufficient for dating. Low and relatively flat ^{241}Am activities in the sediments cannot provide a reliable chronostratigraphic date as well (Appendix 2.1). ^{210}Pb activity was used to obtain an age model till 5.3 cm, with 5.3 cm aged at 1942±17AD. However, as the total depth of the sediment core was only 12 cm, a sample for ^{14}C dating was not submitted as the ^{210}Pb data suggested that it would not give a definitive radiocarbon value (Figure 3.3). Sediment accumulation rates (from the CRS model) rapidly increased from 0.013 g cm^{-2} yr^{-1} in the 1940s to 0.059 g cm^{-2} yr^{-1} in the 2000s; Figure 3.3).

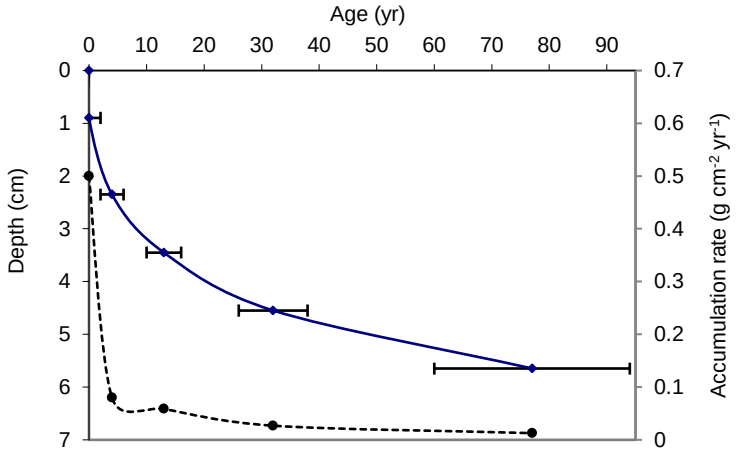

Figure 3.3: Radiometric chronology of the core from Tingwall, showing the CRS model ^{210}Pb dates and accumulation rates. The solid line shows age while the dashed line indicates accumulation rate.

The sediment core from Eriskay was 7.15 cm. ^{210}Pb activity was 45.97±5.68Bq kg^{-1} in the surface sediment and decreased exponentially with depth (Appendix 2.1). Both ^{137}Cs and ^{241}Am activity were low and could not provide reliable chronostratigraphic dates (Appendix 2.1). ^{210}Pb activity was used to obtain an age model for the whole core, with the core base aged to 1972±13AD. Sediment accumulation rates (from the CRS model) were relatively stable, with a mean of 0.142 g cm^{-2} yr^{-1} (Figure 3.4).

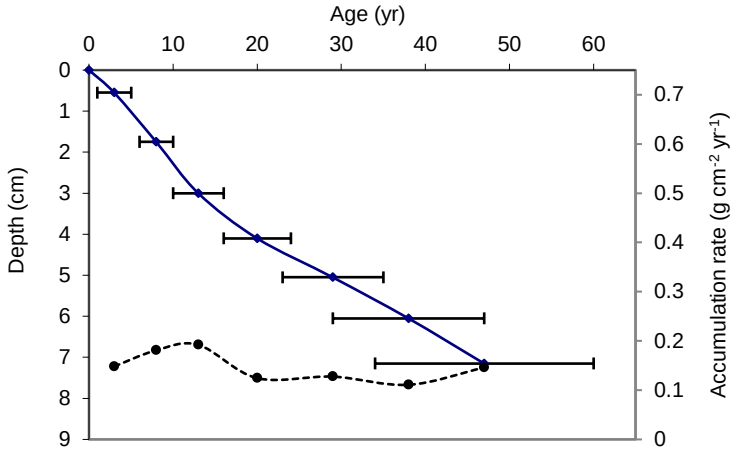

Figure 3.4: Radiometric chronology of the core from Eriskay, showing the CRS model ^{210}Pb dates and accumulation rates. The solid line shows age while the dashed line indicates accumulation rate.

3.3.2 Organic carbon %, calcium carbonate %, and organic carbon reactivity within rhodolith beds

At Upper Loch Torridon, the sediment was primarily made of >500µm particles (53.5±10.0%), followed by 250-500µm particles (24.2±4.43%), 63-250µm particles (16.8±4.24%), and <63 particles (5.46±1.98%; Figure 3.5). OC wt% did not vary with fraction size ($p>0.05$), with an average OC wt% of 2.14±0.79% across all fractions (Figure 3.5). Changes in OC wt% with age were confirmed by a significant breakpoint at 1786 ($R^2= 0.82$, $p<0.05$). Average OC wt% was relatively stable from 1184AD (1.46±0.47%) to 1786AD (1.70±0.9%) where it then increased rapidly to 3.23±0.25% at present-day (Figure 3.7, Figure 3.8)

$CaCO_3$ wt% increased with fraction size for Upper Loch Torridon ($F_{(2,63)}= 35.95$, $R^2= 51.8\%$, $p<0.001$; Figure 3.5), with bulk $CaCO_3$ wt% decreasing from 1122AD to present day (Figure 3.7, Figure 3.8; **Error! Reference source not found.**$F_{(1,20)}= 9.00$, $R^2= 0.28$, $p<0.01$). CRI index increased with fraction size ($F_{(2,71)}= 4.87$, R2= 9.5%, $p<0.05$; Figure 3.5), and decreased with age ($F_{(1,23)}= 62.06$, $R^2= 72\%$, $p<0.001$), with the CRI of a bulk sediment sample of 0.80 in 1122AD decreasing to 0.68 at the present day (Figure 3.7, Figure 3.8**Error! Reference source not found.**). The average bulk CRI at Upper Loch Torridon was 0.76±0.3.

Compared to Upper Loch Torridon, the sediment at the Sound of Barra had a higher proportion of >500µm particles (82.3±7.41%) and a smaller proportion of 250-500µm (7.86±2.66%), 63-250µm (7.56±3.99%), and <63µm particles (2.29±1.08%; Figure 3.). OC wt% was higher in the <63µm fraction compared to the 63-250 and 250-500µm fractions ($X^2(2)= 12.15$, $p<0.001$; Figure 3.5). OC wt% did not vary significantly with depth ($p>0.05$; Figure 3.7, Figure 3.8).

In the Sound of Barra, $CaCO_3$ wt% increased with fraction size ($X^2(2)= 26.54$, $p<0.001$), with more $CaCO_3$ wt% compared to Upper Loch Torridon in all three fraction sizes (Figure 3.6). Bulk $CaCO_3$ wt% also increased with depth (Figure 3.7, Figure 3.8; $F_{(1,23)}= 22.37$,$p<0.001$). CRI index decreased with fraction size ($F_{(2,73)}= 11.53$, R2= 22.0%, $p<0.001$; Figure 3.5), and increased with depth ($F_{(1,25)}= 54.45$, R2= 67.3%, $p<0.001$), with the CRI of a bulk sediment sample of 0.81 at the core base decreasing to 0.66 at the present day (Figure 3.7, Figure 3.8). The average bulk CRI at the Sound of Barra was higher than Upper Loch Torridon at 78.0±0.4.

The sediment at Tingwall was similar to the Sound of Barra, with 76.3±6.70% of >500µm particles, 9.83±3.13% of 250-500µm particles, 10.7±3.74% of 63-250µm particles, and

3.14±0.96% of <63 µm particles (Figure 3.5). OC wt% decreased with increasing fraction size and was highest in the <63µm fraction ($X^2(2)= 6.37$, $p<0.05$; Figure 3.5). OC wt% also decreased with depth ($F_{(1,12)}= 23.28$, $R^2 = 63.2\%$, $p<0.05$; Figure 3.7, Figure 3.8), with an OC wt% of 1.77% at the core top, and 0.63% at the core base.

At Tingwall, $CaCO_3$ wt% increased with fraction size ($X^2(2)= 24.55$, $p<0.001$), with more $CaCO_3$ than Upper Loch Torridon, but less than the Sound of Barra (Figure 3.6). Bulk $CaCO_3$ wt% did not vary with depth for Tingwall ($p>0.05$; Figure 3.7, Figure 3.8), with an average bulk $CaCO_3$% of 83.1±4.27%). Similarly to the Sound of Barra, CRI decreased with fraction size ($X^2(2) = 12.201$, $p<0.01$; Figure 3.6), and increased with depth ($F_{(1,11)}= 54.45$, R2= 75.7%, $p<0.001$), with the CRI of a bulk sediment sample of 0.81 at the core base decreasing to 0.56 at the present day (Figure 3.7, Figure 3.**Error! Reference source not found.**8). The average bulk CRI at the Tingwall was lower than Upper Loch Torridon and the Sound of Barra at 0.72±0.08.

The sediment in the Sound of Eriskay rhodolith bed compromised of 53.7±4.59% of >500µm particles, 21.2±4.21% of 250-500µm particles, 21.0±3.41% of 63-250µm particles, and 4.14±1.05% of <63 particles (Figure 3.5). OC wt% did not significantly vary with fraction size ($p>0.05$; Figure 3.5), or depth ($p>0.05$; Figure 3.7, Figure 3.8**Error! Reference source not found.**), with a median bulk OC wt% of 1.54(IQR = 1.49)%.

At the Sound of Eriskay, $CaCO_3$ varied with fraction size ($F_{(2,18)}= 9.25$,$p<0.01$), however, conversely to the other sites, $CaCO_3$ wt% was smaller in the 250-500µm fraction compared to the <63µm and 63-250µm fractions (Figure 3.6). Bulk $CaCO_3$ wt% decreased with depth at the Sound of Eriskay ($F_{(1,5)}= 48.28$,$p<0.05$; Figure 3.7, Figure 3.8). CRI did not vary with fraction size ($X^2(2) = 1.89$, $p= 0.39$), however, bulk CRI increased with core depth ($F_{(1,5)}= 47.14$, R2= 88.5%, $p<0.05$) with a CRI of 0.73 at the core base and 0.69 at the core top (Figure 3.7, Figure 3.8). Out of all the sites, bulk CRI index was the lowest at the Sound of Eriskay at 0.71±0.02.

CRI was obtained for samples at Loch Sween. CRI varied with fraction size ($X^2(2) = 19.51$, $p<0.01$), however, conversely to the other sites, the 63-250µm fraction was found to have the lowest CRI index followed by the <63µm fraction and then the 250-500µm fraction (Figure 3.6). Bulk CRI were not obtained for Upper Loch Sween with samples separated into fraction

sizes for a previous study. Samples could not be manually recombined to form a bulk sample as there were no data on the proportion of >500µm fraction in the sample.

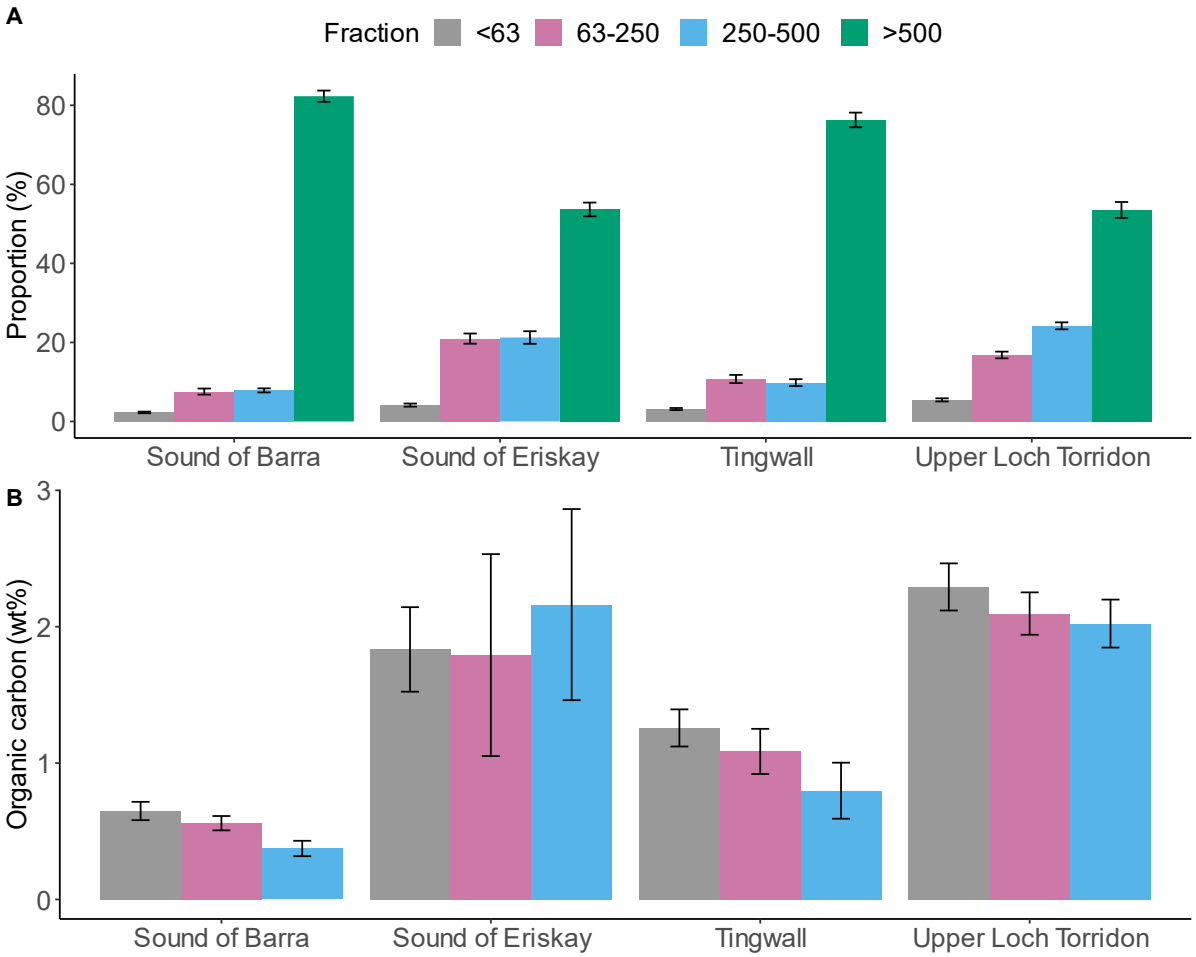

Figure 3.5: Showing A) the proportion (%) of each fraction at each site, and B) the OC wt% of each fraction at each site. Grain sizes are <63 µm (grey bar), 63-250 µm (pink bar), 250-500 µm (blue bar) and >500 µm (green bar). Data represent mean±standard error across all sediment sections. For graph A, the sample size for each fraction is as follows: Sound of Barra = 27, Sound of Eriskay = 7, Tingwall = 13, Upper Loch Torridon = 25. For graph B, the sample size for each fraction is as follows: Sound of Barra = 25, Sound of Eriskay = 7, Tingwall = 13, Upper Loch Torridon = 22.

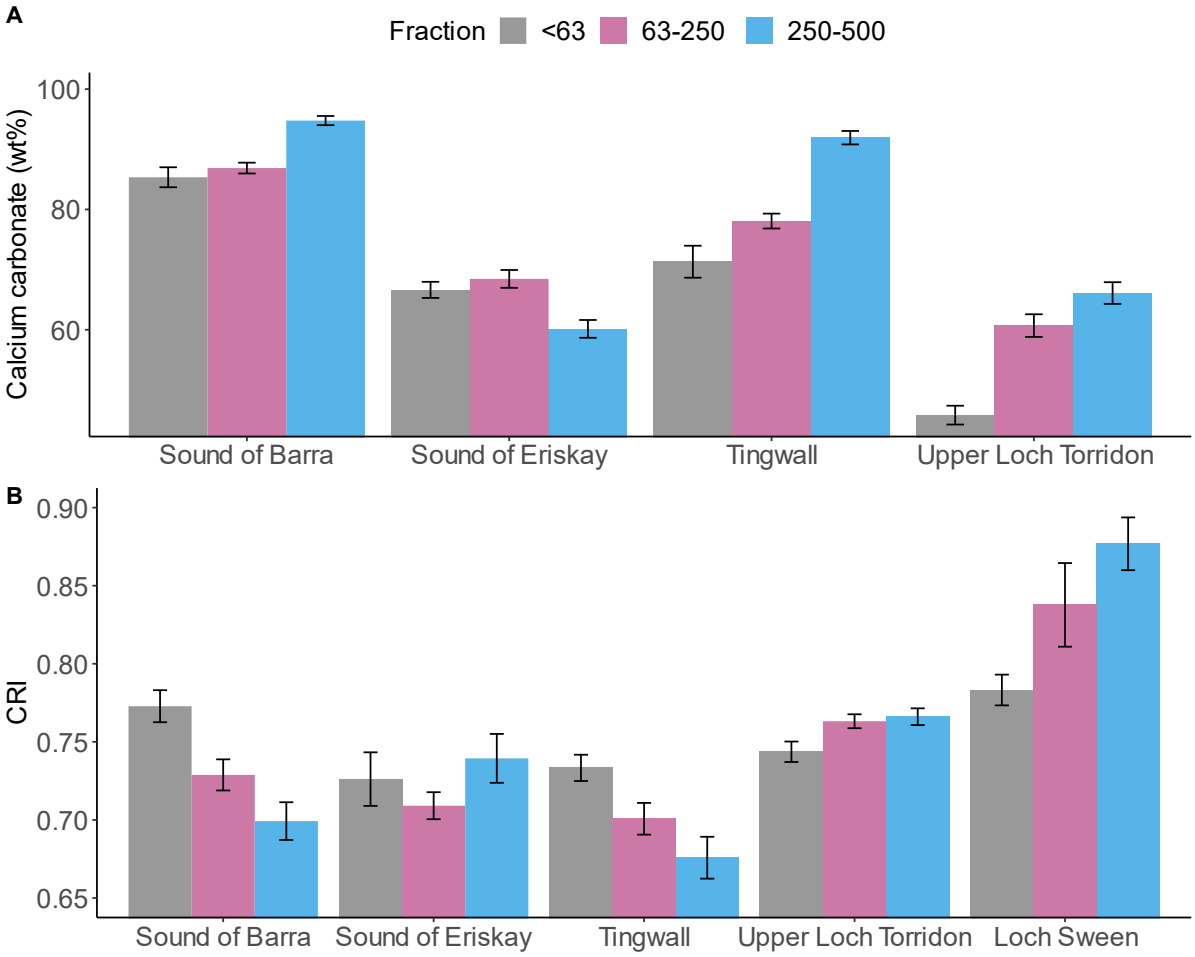

Figure 3.6: Showing A) the Calcium carbonate wt% of each fraction, and B) the CRI of each fraction at each site. Data represent mean±standard error across all sediment sections. For graph A, the sample size for each fraction is as follows: Sound of Barra = 25, Sound of Eriskay = 7, Tingwall = 13, Upper Loch Torridon = 22. For graph B, the sample size for each fraction is as follows: Sound of Barra = 25, Sound of Eriskay = 7, Tingwall = 13, Upper Loch Torridon = 24, Loch Sween = 28.

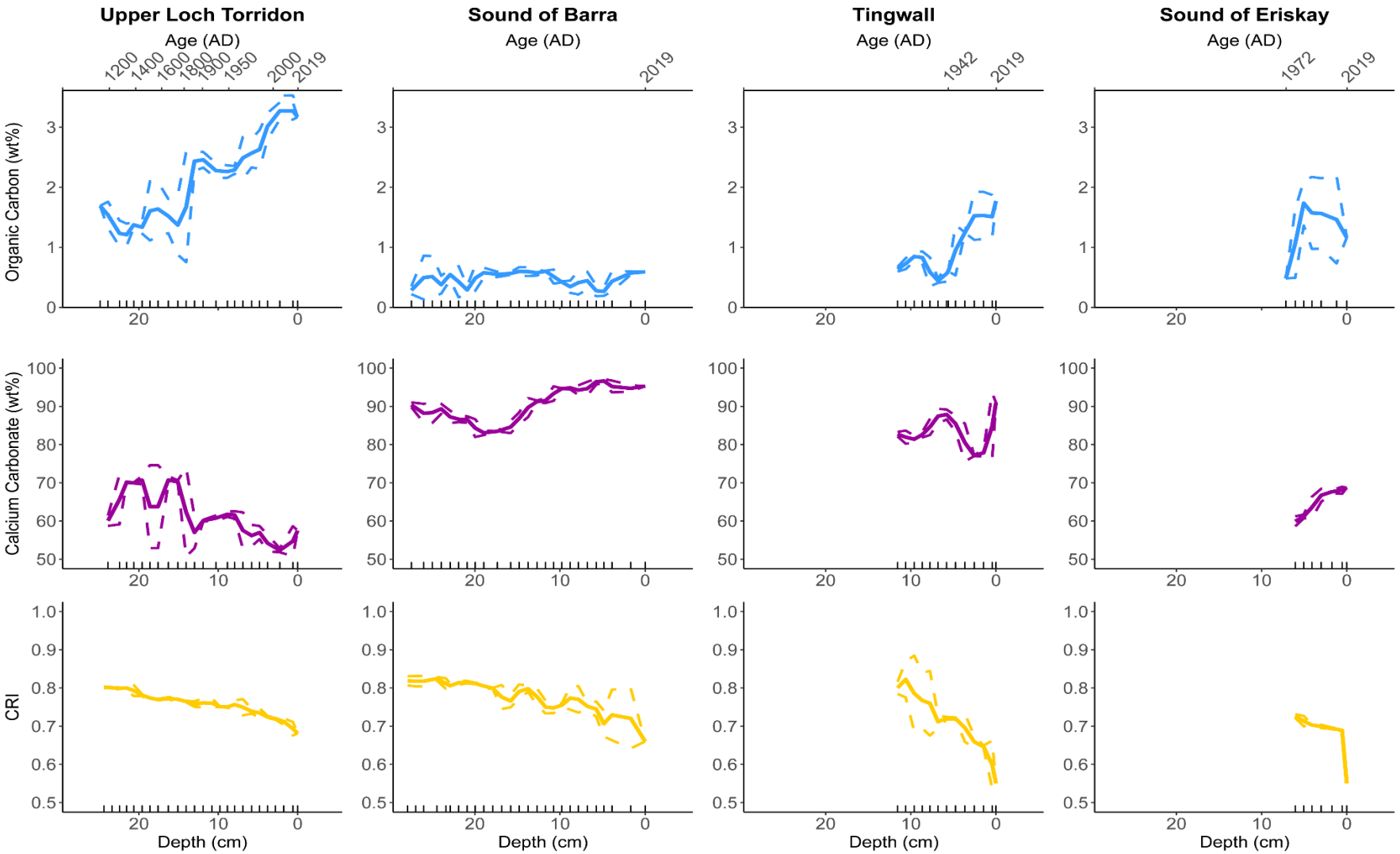

Figure 3.7: Showing organic carbon wt% (blue line), calcium carbonate wt% (purple line) and CRI (yellow line) for Upper Loch Torridon, Sound of Barra, Tingwall and the Sound of Eriskay. Data is plotted against depth (cm) for all sites, with age included as a secondary x-axis for Upper Loch Torridon, Tingwall and the Sound of Eriskay. Full lines represent the rolling average, and dashed lines represent a rolling standard deviation (n= 2 for each point). Ticks on the x-axis represent datapoints.

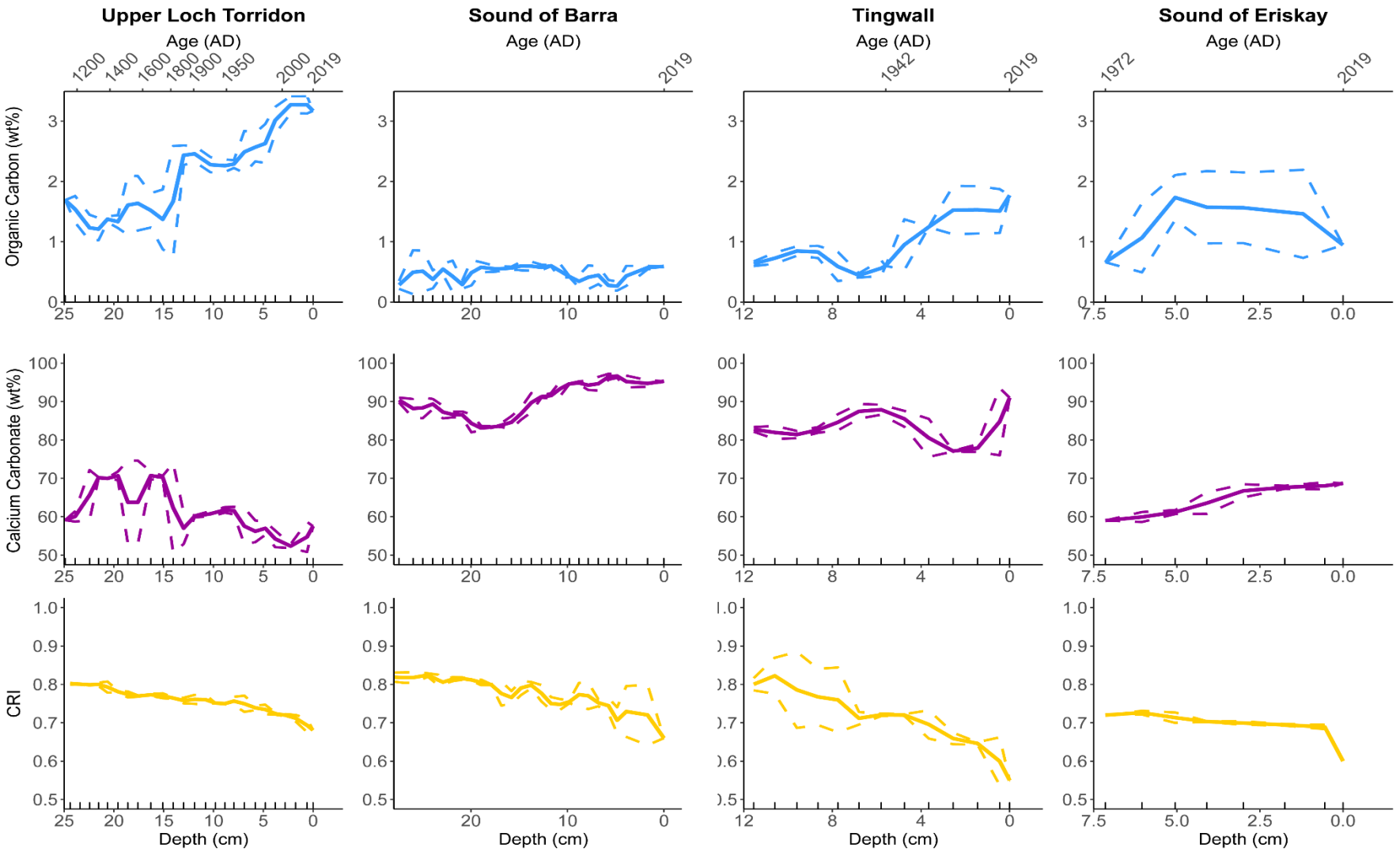

Figure 3.8: Showing data from Error! Reference source not found.**7 with x-axis spanning length of core at each site. Ticks on the x-axis represent datapoints.**

3.3.3 Carbon stock in Scottish rhodolith beds

Carbon Stocks were calculated for Upper Loch Torridon and the Sound of Barra, with the sediment length at each site >25cm. Carbon stocks were not calculated for Tingwall or the Sound of Eriskay with core lengths of 12cm and 6.6cm respectively.

At Upper Loch Torridon 17.21 Mg OC ha^{-1} was stored within the top 25cm of sediment. On the other hand, 1.67 Mg OC ha^{-1} was stored within the rhodolith bed at the Sound of Barra, with the stock approximately 10x lower than Upper Loch Torridon. Compared to the carbon stock at Loch Sween (7.23±1.30 Mg OC ha^{-1}), 2.4x more carbon was stored at Upper Loch Torridon, and 4x less carbon was stored at the Sound of Barra (Figure 3.9).

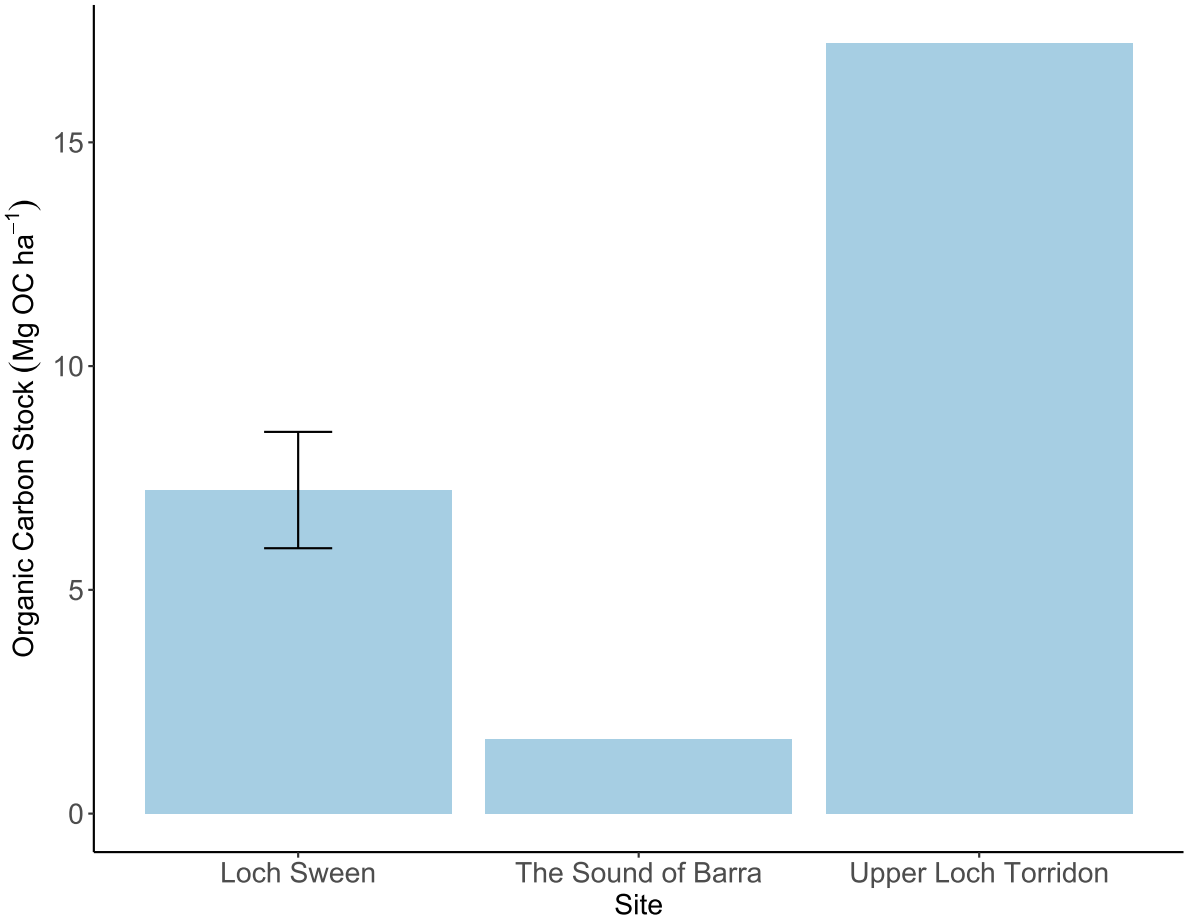

Figure 3.9: The organic carbon stock (Mg OC ha^{-1}) for Upper Loch Torridon (this study), Sound of Barra (this study), and Loch Sween (Mao *et al.,* 2020). Mean±sd are given for Loch Sween with the carbon stock calculated over 3 cores. In this study, only 1 core was analysed per site and therefore no standard deviations are given. For the Sound of Barra, the top 25cm of sediment was used for SOC calculations. For Loch Torridon the SOC of the core (24.9cm) was rounded to 25cm.

3.3.4 Source of organic carbon to rhodolith beds

For all sites, end-member samples provided a distinct separation between marine and terrestrial inputs along the $\delta^{13}C$ axis (Figure 3.10).

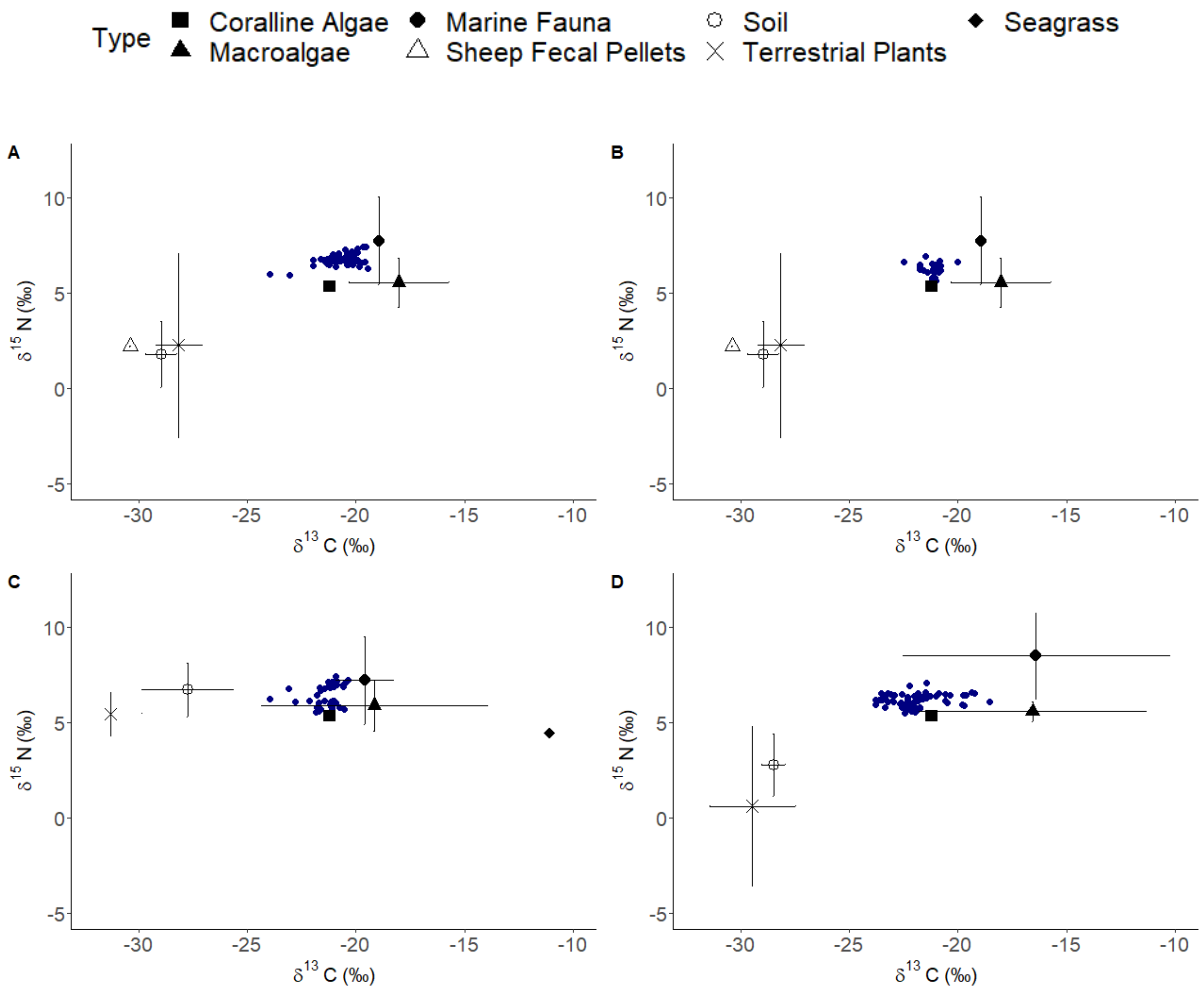

Figure 3.10: Crossplots of $\delta^{13}C$ and $\delta^{15}N$ for the established end–member baseline (black symbols (terrestrial end-members are open symbols, marine are closed) with standard deviations as error bars) and for sediment data from all three fraction groups (<63,63-250,250-500). Showing data from A) Sound of Barra, B) Sound of Eriskay, C) Tingwall and D) Upper Loch Torridon.

The source of carbon was found to vary with site (Figure 3.11). At all sites, OC was dominated by marine carbon, with the Sound of Barra containing the most marine-derived carbon (96.6±1.5%), followed by the Sound of Eriskay (92.1±2.7%), and then Tingwall (90.8±4.6%). Upper Loch Torridon had the least marine-derived carbon at 84.2±6.3%, with other carbon coming from terrestrial soil (9.8±6.7%) and terrestrial plants (6±4.7%). At all sites, marine-derived carbon primarily came from marine fauna, with smaller contributions from macroalgae, coralline algae and seagrass also (See Appendix 2.2 for more details).

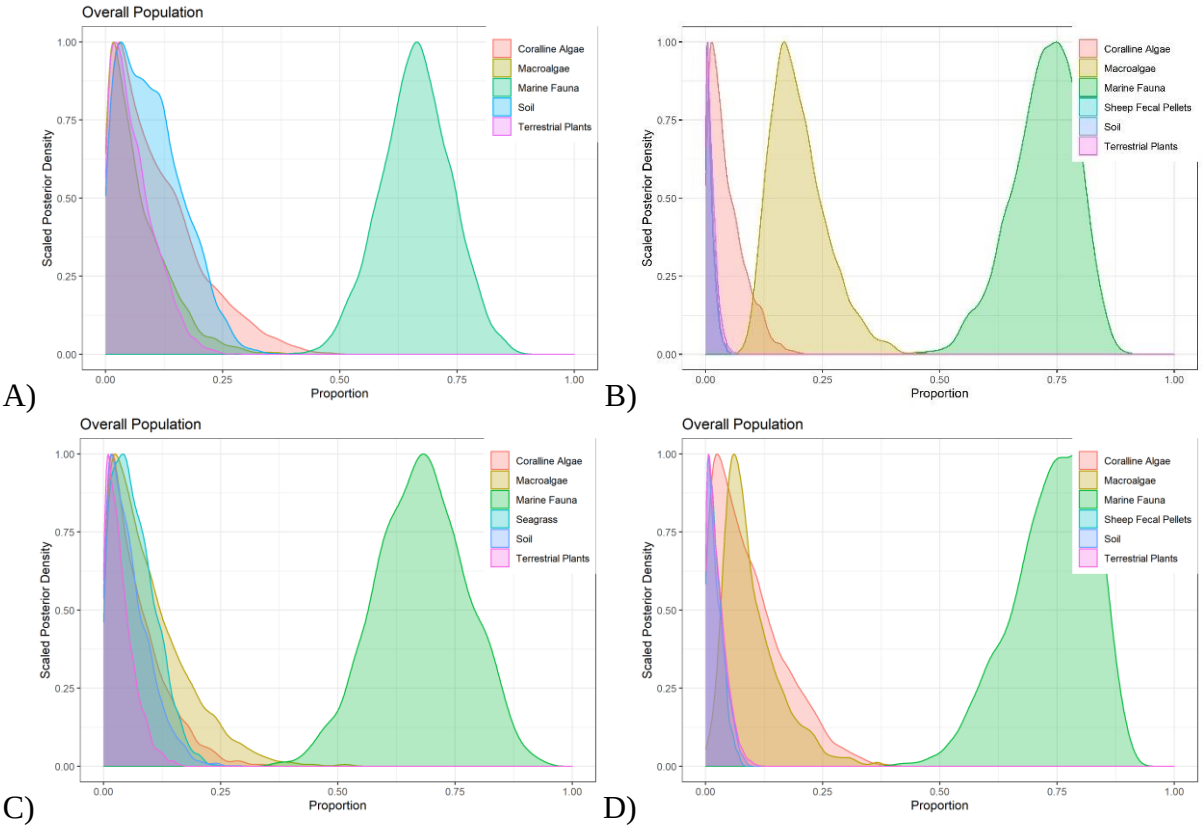

Figure 3.11: Proportional contribution of end members to observed isotopic patterns. The proportional contribution of terrestrial plants and soil, sheep fecel pellets, marine fauna, macroalgae, coralline algae, and seagrass. Sites are, A) Upper Loch Torridon, B) Sound of Barra, C) Tingwall, and D) Sound of Eriskay.

At Upper Loch Torridon and the Sound of Barra, there was evidence that carbon source varied with fraction size (Figure 3.12, Figure 3.13). There was no difference in carbon source between fractions for Tingwall and the Sound of Eriskay, with models failing to converge.

At Upper Loch Torridon, all fractions contained a large proportion of material from marine fauna (63µm = 66.9±8.2%, 63-250µm = 70.8±8.6%, 250-500µm = 71.4±9.4%; Figure 3.12), with the smaller fractions containing more organic material from terrestrial soil (63µm = 10.0±6.7%, 63-250µm = 9.6±7.5%, 250-500µm = 6.7±5.7%). Contributions from coralline algae were similar across all fraction sizes (63µm = 11.1±9.0%, 63-250µm = 9.7±9.7%, 250-500µm = 10.6±10.2%). Contributions from marine plants and terrestrial plants were low in all fractions (Macroalgae: 63µm = 6.2±5.7%, 63-250µm = 4.6±5.3%, 250-500µm = 7.0±7.6%; Terrestrial Plants: 63µm = 5.8±4.5%, 63-250µm = 5.2±4.8%, 250-500µm = 4.2±4.1%).

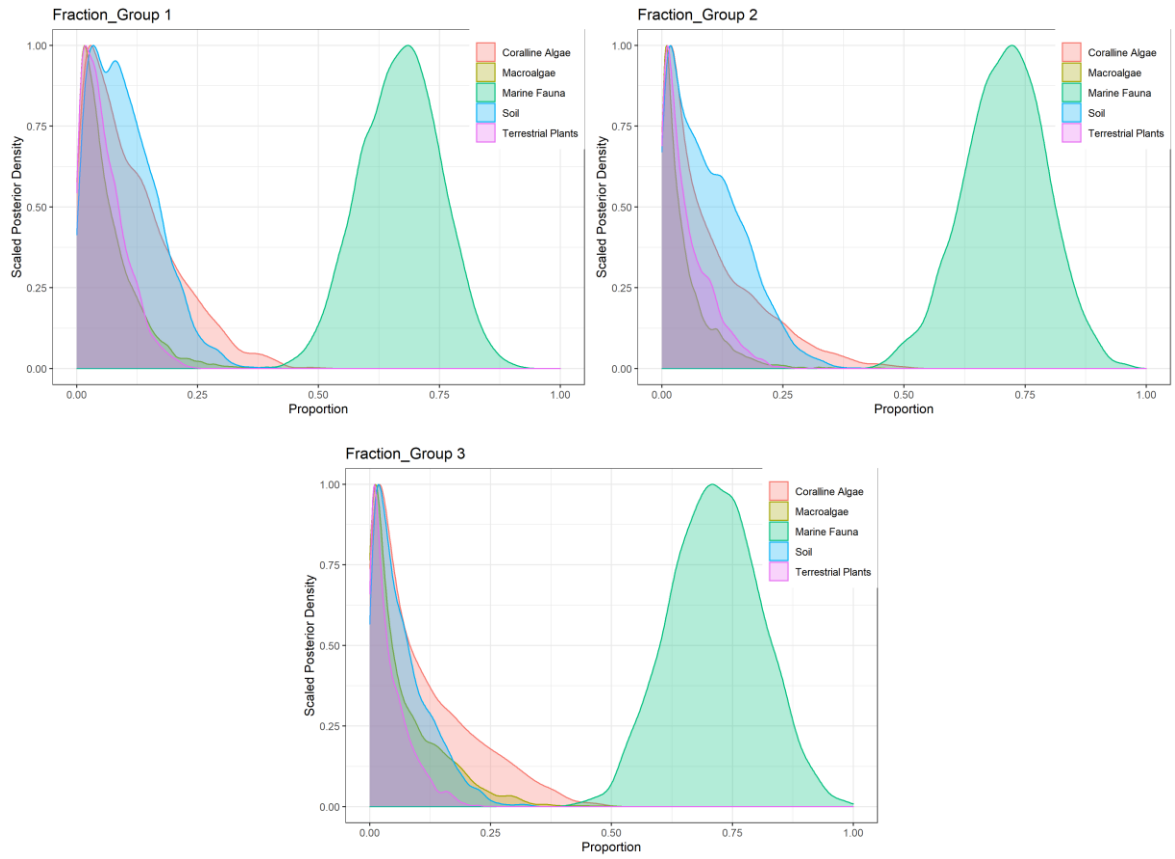

Figure 3.12: Proportional contribution of end members to observed isotopic patterns. The proportional contribution of terrestrial plants (purple curve) and soil (blue curve), marine fauna (red curve) and macroalgae (green curve) to each fraction group at Upper Loch Torridon. Fraction Group 1 = <63µm, Fraction Group 2 = 63-250µm, Fraction Group 3 = 250-500µm.

At the Sound of Barra, the largest fraction size also had the highest contribution from marine fauna (Figure 3.13; 63µm = 81.8±8.3%, 63-250µm = 83.4±9.4%, 250-500µm = 90.6±8.5%). Macroalgae was a further source of carbon to all fractions (63µm = 9.6±7.4%, 63-250µm = 11.6±9.4%, 250-500µm = 6.0±7.4%), with small contributions from coralline algae (<4%) terrestrial carbon (soil, terrestrial plants, sheep fecal pellets; <1.5%) in all fractions.

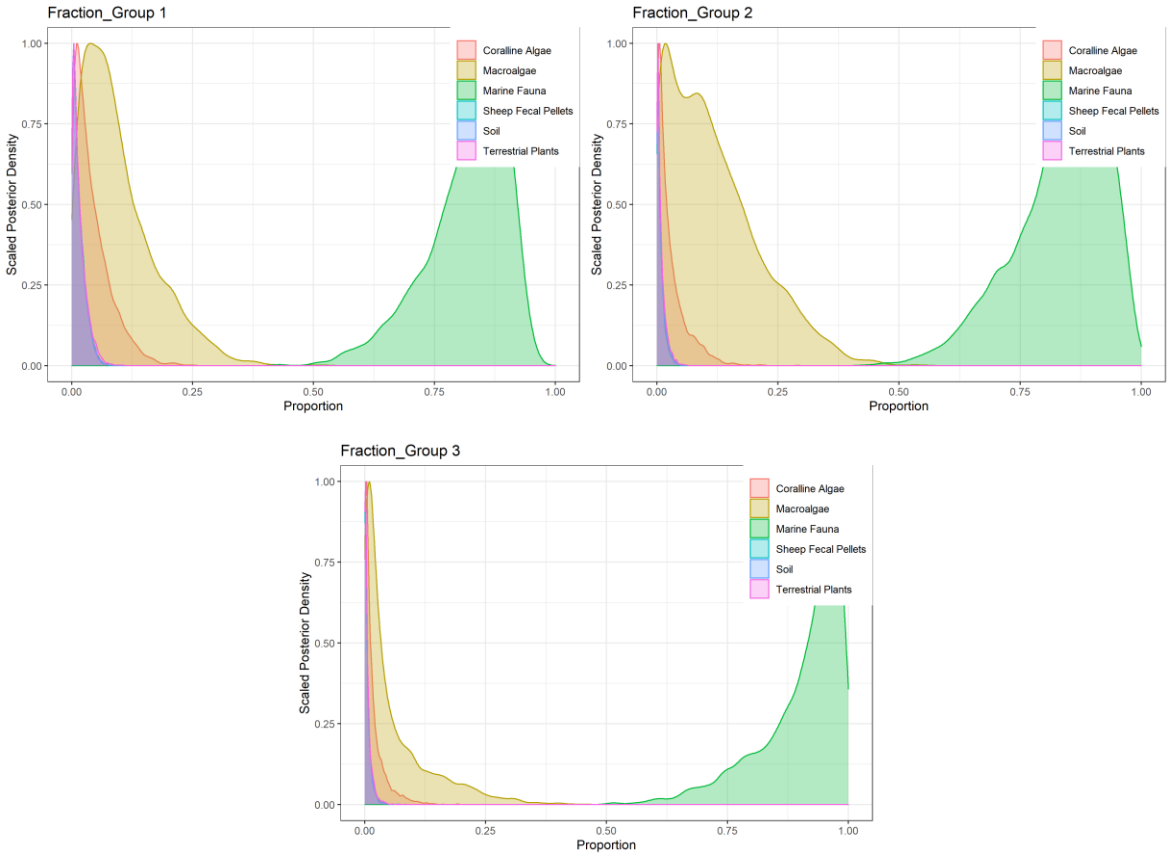

Figure 3.13: Proportional contribution of end members to observed isotopic patterns. The proportional contribution of terrestrial plants (purple curve) and soil (blue curve), sheep fecal pellets (turquoise curve), marine fauna (green curve), macroalgae (yellow curve), and coralline algae (red curve) to each fraction group at the Sound of Barra. Fraction Group 1 = <63µm, Fraction Group 2 = 63-250µm, Fraction Group 3 = 250-500µm.

For all sites, when using the mixing model, the source of carbon was not linked to core depth or age, with models failing to converge (Appendix 2.2). On the other hand, at the Sound of Barra, when using only the $\delta^{13}C$ data, sediment $\delta^{13}C$ values increased with depth ($X^2(26)$ = 49.96, $p<0.01$; Appendix 2.2), suggesting that there may be more carbon from coralline algae and terrestrial carbon (who have lower $\delta^{13}C$ values) at the surface of the core.

3.4 Discussion

Carbon storage in Scottish rhodolith beds appeared to be influenced by both wave exposure and the source of carbon entering the bed. When comparing the top 25cm of sediment, the sheltered beds in the fjordic systems were a larger BC repositories, storing a higher proportion of terrigenous carbon, compared to the exposed bed in the oceanic system. Carbon reactivity was linked to carbon source and exposure, with more reactive marine carbon stored in non-fjordic beds which appeared to be remineralized to a greater degree in exposed beds.

3.4.1 Sheltered rhodolith beds in fjordic systems store more organic carbon

In this study, the sheltered bed at Upper Loch Torridon stored the most OC with the SOC stock in the top 25cm of the sediment 10x higher than the Sound of Barra and 2.4x higher than Loch Sween (Mao *et al.,* 2020). The disparities in the SOC stock between the sites appeared to be driven by differences in hydrodynamical energy, carbon reactivity and carbon source. Further work collecting sediment cores from other sites is needed to confirm this association, with this conclusion is only based on 3 sites (and cores).

Hydrodynamical energy varied largely between the study sites which could, in part, explain differences in the SOC. Out of the five study sites, Loch Sween had the lowest wave exposure (exposure index of 2.07; as calculated by Burrows 2008), followed by Loch Torridon (2.51). On the other hand, the Sound of Barra experienced the highest wave exposure, with an index of 3.37. Hydrodynamical energy can influence sediment type, with low hydrodynamical energy increasing the proportion of fine-grained particles within the sediments (Dahl *et al.,* 2018). Differences in grain size between the sheltered and exposed sites were evident in this study, with Upper Loch Torridon having over 2x more fine-grained particles (<63µm) than the Sound of Barra. Grain size has been linked to the carbon content in other BC systems (Dahl *et al.,* 2016; Serrano *et al.,* 2016), with fine-grained particles having a higher affinity to OC (Kell *et al.,* 1994; Hedges and Keil 1995; Bergamaschi *et al.,* 1997), and fine-grained sediments favouring OC preservation with lower oxygen exchanges and shallower redox potentials (Hedges and Keil 1995; Dauwe *et al.,* 2001; Burdige 2007; Glud 2008). Therefore, the greater proportion of fine-grained particles in Upper Loch Torridon may partially explain why the SOC at Upper Loch Torridon is 10x larger than the Sound of Barra.

Compared to both the Sound of Barra and Upper Loch Torridon, Loch Sween had a lower proportion of fine-grained particles (Mao *et al.,* 2020). This was unexpected, with Loch Sween having the lowest wave exposure out of the three sites. However, whilst the wave exposure index considers wind fetch and wave exposure (Burrows 2008), it does not include other parameters such as wave height, water depth and current direction which can all affect sediment type, erosion and OC content (Samper-Villarreal *et al.,* 2016; Dahl *et al.,* 2018). Differences in these additional parameters may explain why Loch Sween has a lower proportion of fine-grained particles than Upper Loch Torridon (and in turn a smaller SOC stock), with Loch Sween a shallower site compared to Upper Loch Torridon (6m compared to 20m depth). As the surface sediment at shallower sites can be more vulnerable to wave action and current flows (Dahl *et al.,* 2018), Loch Sween may experience greater particle resuspension in turn storing less OC. A further variable that is not considered in the wave exposure index is water movement from rivers (Burrows 2008). Unlike Upper Loch Torridon and the Sound of Barra, Loch Sween has a large river entering the site which may increase water movement in the bed removing fine-grained particles. Finally, rhodolith thalli shape/size was not considered in this study, with thalli shape and size potentially altering hydrodynamical movement near the bed. Therefore, whilst the wave exposure index may provide some indication of site exposure (Burrows 2008), other variables, including depth, freshwater movement into the system, and rhodolith thalli shape/size, should also be considered when assessing a system's ability to store SOC (Samper-Villarreal *et al.,* 2016; Dahl *et al.,* 2018).

The absence of sediment mixing, as a result of low hydrodynamical energy, may further explain why both Upper Loch Torridon and Loch Sween stored more SOC than the Sound of Barra. Low hydrodynamical energy can further favour OC preservation, with limited to no sediment mixing maintaining redox potentials and reducing the exposure of OC within the sediment to O_2 (Canfield 1994; Glud 2008). Both the age model and downcore OC% concentrations at Upper Loch Torridon and Loch Sween (Mao *et al.,* 2020), suggest that sediment mixing is not present at these sites, with OC preserved. At both sites, OC% concentrations decreased downcore, until roughly 15cm, where OC% concentrations remain constant (Mao *et al.,* 2020). The initial decrease in OC% concentrations suggested that bacterial remineralisation may have been present, with both labile and refractory carbon remineralized in the oxic and suboxic zone (Canfield 1994; Glud 2008). OC degradation slowed (particularly evidence at Loch Sween; Mao *et al.,* 2020), before remaining constant from ~15cm, suggesting a shift from the suboxic to a reduced zone where the sediment is characterised as anaerobic (Glud 2008). In this zone,

recalcitrant and refractory carbon cannot be processed (Burdige 2007; Canfield 1994), and is effectively preserved and 'locked away'. The bacterial remineralisation of labile carbon downcore is further supported by the CRI data, with the bulk CRI increasing with depth at Upper Loch Torridon. At 15cm depth (1750AD), when remineralization appears to stop labile carbon is still present in the SOC. This suggests that whilst the labile fraction of the SOC is more vulnerable to degradation, a proportion of it may be preserved, potentially with the labile compounds physically protected by the encapsulation of protective organic matrices (Burdige 2007). The degradation of OC slowed at 1750AD at Upper Loch Torridon, and 1625AD at Loch Sween, with a higher proportion of fine grain-sized particles at Upper Loch Torridon potentially resulting in a shallower redox gradient, with OC preserved 100 years earlier than Loch Sween (Mao *et al.,* 2020).

At the exposed bed at the Sound of Barra, a significantly lower mass of OC was stored with radiocarbon measurements and ^{241}Am activities indicating sediment mixing throughout the sediment core. Sediment mixing was also evident when collecting the core, with distinct waves and ripples of live coralline algae typical of a high-exposure environment (Harris *et al.,* 2007). The high hydrodynamical activity at the Sound of Barra may partially explain why the SOC is low with high hydrodynamical activity resulting in the rapid bacterial degradation of OC throughout the mixed layer (Burdige 2007; Jankowska *et al.,* 2016; Dahl *et al.,* 2018; Zhao *et al.,* 2018) and the transport of SOC elsewhere (Macreadie *et al.,* 2013). Furthermore, conversely to Upper Loch Torridon, high wave exposure resulted in sediment with a lower proportion of fine grain-sized particles and a higher proportion of calcium carbonate, reducing the ability of sediment to bind to and preserve OC (Kell *et al.,* 1994; Bergamaschi *et al.,* 1997).

Disparities in the SOC stock between Upper Loch Torridon, Loch Sween and the Sound Of Barra may have also been linked to carbon source. At both Upper Loch Torridon and Loch Sween, terrestrial inputs were higher than the Sound of Barra (16% (this study) and 32% (Mao *et al.,* 2020) vs 3% (this study)). Terrestrial carbon typically contains more refractory carbon than marine, thus less reactive and vulnerable to bacterial remineralization (Kristensen 1990; Burdige 2007; Hill *et al.,* 2015; Trevathan-Tackett *et al.,* 2020). Therefore, the larger SOC stock at Upper Loch Torridon and Loch Sween may be linked to high input of terrigenous carbon, with a larger proportion of carbon preserved (Canfield 1994). Terrestrial inputs at Upper Loch Torridon and Loch Sween (Mao *et al.,* 2020) were from both terrestrial soils and plants. Upper Loch Torridon (~10%) stored more carbon from terrestrial soils than Loch Sween

(~8%). As the elevation around Upper Loch Torridon is steeper, this may be due to high runoff from the surrounding landscape (Smeaton and Austin 2022b). Furthermore, the terrestrial soils around Upper Loch Torridon have a higher OC% (UKSO 2022), resulting in more organic-rich soils entering the rhodolith bed than Loch Sween. On the other hand, Upper Loch Torridon stored less carbon from terrestrial plants (~8%) than Loch Sween (~24%; Mao *et al.,* 2020). Loch Sween is dominated by grassland, moorland and farmland (Scottish Natural Heritage 1996) which may shed material more abundantly than dry and wet heath as present at Upper Loch Torridon (Campbell and Marchbank 2013).

At the Sound of Barra, the SOC was primarily marine-derived (97%), with marine-derived contributions from fauna (~72%), macroalgae (~20%) and coralline algae (4.5%). Marine fauna contributions were high (as they were at the other sites), which is likely due to the diverse and abundant faunal community, including crustaceans, bivalves, and echinoderms (Barbera *et al.,* 2003; Kamenos *et al.,* 2004b; Attard *et al.,* 2015), which when deceased end up buried within the sediment (Mao *et al.,* 2020). Although the OC of marine fauna is typically low, with shells and calcareous skeletons made of a high proportion of inorganic carbon, the OC supplied from the soft body of fauna can be more relatively refractory (Kristensen 1990). This may explain that, whilst low, the Sound of Barra did store some OC which was composed of refractory carbon (~80%). At the Sound of Barra, OC contributions from macroalgae were the highest of all the sites. Macroalgae contain a high proportion of labile carbon, which can be remineralized by bacteria both within the water column and sediment or grazed on by fauna (Kristensen 1994; Vichkovitten and Holmer 2004; Hill *et al.,* 2015; Krause-Jensen and Duarte 2016). Thus, whilst macroalgae act as a carbon donor at the Sound of Barra, the majority of this carbon is likely remineralised, resulting in a small SOC stock at the Sound of Barra. Similarly to Upper Loch Torridon, the SOC at the Sound of Barra was to some degree labile (~20%), suggesting that the labile component may have been physically protected to come degree from degradation (Burdige 2007).

3.4.2 Dead rhodolith beds continue to store organic carbon

This study provides the first evidence that dead rhodolith beds continue to store OC once the coralline algae within the bed die off. Unfortunately, when collecting the cores only 6cm of sediment could be obtained, with large pieces of rock within the sediment making core extraction difficult. However, even when only investigating 6cm of sediment, OC was present,

suggesting that beds continue to act as BC repositories when the coralline algae die. Compared to the Sound of Barra, which connects to the Sound of Eriskay, more OC% was stored in the top 6cm of sediment. This may be linked to hydrodynamical energy with the Sound of Eriskay less exposed than the Sound of Barra (exposure index is 3.13 vs 3.37) resulting in a higher proportion of fine-grained sediment at the Sound of Eriskay. Similarly to above, the higher proportion of fine-grained sediments may result in a higher concentration of OC compared to the Sound of Barra, with fine-grained sediments having a higher affinity to OC (Kell *et al.,* 1994; Hedges and Keil 1995), and lower oxygen exchanges and shallower redox potentials favouring the preservation of OC within sediments (Hedges and Keil 1995; Dauwe *et al.,* 2001; Burdige 2007; Glud 2008). There was also no evidence of sediment mixing in the top 6cm of sediment at the Sound of Eriskay, with ^{210}Pb concentrations decaying with depth, meaning that once buried, the OC may be protected from resuspension where it could be exposed to O_2 or transported elsewhere (Macreadie *et al.,* 2013). Compared to the Sound of Barra, more terrestrial carbon and less macroalgae-derived carbon was stored at the Sound of Eriskay, which could result in more refractory carbon present and preserved in the sediment (Kristensen 1990; Canfield 1994; Burdige 2007).

There was also evidence that the Sound of Eriskay continues to accumulate allochthonous carbon after the coralline algae die off. At the Sound of Eriskay, the construction of the Eriskay causeway in 2000-2001AD caused a reduction in hydrodynamical energy with coralline algae dying as a consequence (Mercer *et al.,* 2015). In the core, the top 4cm of sediment accumulated after 2000AD, with an average OC concentration of ~1.5% OC. As reduced water velocity facilitates sedimentation (as evident in the ^{210}Pb age model) and the deposition of organic material, this could have caused the continued accumulation of allochthonous carbon even after the coralline algae had died (Burdige 2007; Jankowska *et al.,* 2016; Dahl *et al.,* 2018). As the coralline algae only died 20 years ago, it is still not known if the bed continues to store OC over long periods, as the dead coralline algae gradually undergo dissolution, weakening the bed structure (Martin *et al.,* 2007; Kamenos *et al.,* 2013; Brodie *et al.,* 2014).

3.4.3 Interlinked rhodolith-seagrass bed stores fresh marine carbon

The final site studied was an interlinked rhodolith-seagrass bed at Tingwall, with 12 cm of sediment extracted before bedrock was hit (multiple attempts were made to obtain longer cores at this site). This bed was unique to the other sites, with patches of rhodolith bed and *Zostera*

meadows found throughout the site. Additionally, the bed was the shallowest of all the sites (4m) and was close to the coast being accessed by scuba divers from the shore. Due to the wave exposure index (average wave exposure of 2.94), depth and proximity to shore, the site was considered relatively exposed. However, no ripples of live and dead coralline algae were observed and therefore the site appeared to be less exposed than the Sound of Barra. Currently, there have been no studies relating wave exposure index to bed exposure, thus a wave exposure of index of 2.94 may be too low to evoke sediment resuspension.

At Tingwall, the OC concentration at the top of the core was higher than the Sound of Barra but lower than Upper Loch Torridon and Loch Sween, with 1.77% of OC stored. Similarly to the previous sites, OC% concentrations may be linked to hydrodynamical energy, with more fine-grained particles than in the Sound of Barra, but less than in Upper Loch Torridon. The presence of *Zostera* and rhodolith fragments within the site may have further reduced wave velocities within the rhodolith bed (Duarte *et al.,* 2011; Infantes *et al.,* 2012; Githaiga *et al.,* 2019), in turn reducing resuspension and sediment mixing, enhancing OC stocks (Kennedy *et al.,* 2010; Hansen and Reidenbach 2013; Githaiga *et al.,* 2019). The lack of sediment mixing at Tingwall is supported by the ^{210}Pb dating with an exponential decrease in activity with depth.

At Tingwall, the CRI was the lowest compared to other sites. The low CRI may be due to the input of fresh labile marine carbon from both macroalgae and seagrass deposited at the top of the core (Burdige 2007; Trevathan-Tackett *et al.,* 2020). When collecting cores, Tingwall appeared to be the most productive of all the sites, with a rich community of autotrophs in the rhodolith-seagrass bed. Stable isotope analysis confirmed that the autotrophs contributed to the SOC with carbon originating from both macroalgae and seagrass. This is in agreement with other studies from *Zostera* meadows which have found carbon buried within the sediments originating from a variety of autotrophs including *Zostera*, macrophytes, macroalgae and epiphytes (Kennedy *et al.,* 2004; Serrano *et al.,* 2016; Röhr *et al.,* 2018). Both macroalgae and *Zostera* leaves and rhizomes are both made of a high proportion of labile material, with macroalgae more labile than *Zostera* (Kristensen 1994), thus could result in a low CRI at the top of the core. On the other hand, carbon buried at the Sound of Barra and the Sound of Eriskay, whilst also originating from marine sources, may be more degraded before being buried with the bed (Kristensen 1994; Vichkovitten and Holmer 2004), therefore having a lower CRI. At Tingwall, OC% and CRI appeared to be closely linked with OC% decreasing with depth and CRI increasing. This suggests that whilst fresh labile material was deposited in

the bed, this was gradually degraded by bacteria, resulting in more refractory OC stored deeper in the core (Canfield 1994).

3.4.4 Conclusions

This chapter aimed to investigate how the quantity, reactivity and source of OC vary with rhodolith bed structure and status. By using Scotland as a model system this study found that:

a) Carbon storage varied 10-fold between exposed and sheltered rhodolith beds, with sheltered beds in a fjordic depositional environment storing significantly more carbon. At the sheltered sites, lower hydrodynamical energy resulted in the deposition of fine-grained particles and limited sediment mixing which favoured the preservation of OC. Furthermore, OC degradation slowed over time, with the potential for OC to be preserved and 'locked away' after a certain depth. Disparities in the SOC stock were also linked with carbon source, with more terrestrial carbon, which is less reactive, stored in fjordic systems.

b) Dead rhodolith beds still act as BC repositories once the coralline algae have died. In this study, the dead bed not only protect OC that was previously stored whilst the bed was alive, but, continued to bury allochthonous carbon. The OC stored within the dead beds was to some degree labile, and thus if exposed to O_2 through activities such as bottom trawling fishing, could be partially remineralized into the atmosphere.

c) In a rhodolith-seagrass interlinked bed, carbon originated from a variety of autotrophs including *Zostera*. OC at the top of the core appeared to originate from the bed itself, with the sediment consisting of fresh labile carbon resulting in a lower CRI. Whilst the bed appeared to be in an exposed environment, being close to shore at a shallow depth, the OC within the sediment appeared to be protected. This is potentially a consequence of *Zostera* which can reduce water movement, protecting OC stocks from resuspension.

Chapter 4 Response of Rhodolith Bed Community Blue Carbon Sequestration to Ocean Acidification and Elevated Temperature

4.1 Introduction

4.1.1 Autochthonous organic carbon production in rhodolith beds

Any effect of climate change on blue carbon (BC) community metabolism should be considered – specifically the balance of autochthonous organic carbon (OC) and inorganic carbon (IC) production. Currently, whilst there have been several studies that have examined the effects of climate change (particularly elevated pCO_2 resulting in ocean acidification (OA) and elevated temperature) on rhodolith species photosynthesis/respiration and calcification/dissolution rates (i.e Kamenos *et al.,* 2013; Martin *et al.,* 2013; Noisette *et al.,* 2013a, 2013b), few have discussed such metrics in terms of their autochthonous carbon budget (i.e. Martin *et al.,* 2007; Burdett *et al.,* 2018; Sordo *et al.,* 2019). Furthermore, whilst rhodoliths are foundation stone species - supporting a whole ecosystem of calcifiers, grazers and autotrophs (Barbera *et al.,* 2003; Kamenos *et al.,* 2004b; Martin *et al.,* 2005; Attard *et al.,* 2015) few studies have investigated the effects of climate change on rhodolith beds at a community level (Legrand *et al.,* 2017; Burdett *et al.,* 2018). These two points represent knowledge gaps. As rhodolith beds can store allochthonous BC (Mao *et al.,* 2020), understanding autochthonous carbon production, and the balance of OC and IC, is important when assessing their role as BC repositories. Furthermore, as the rhodolith beds support a diverse community of autotrophs and calcifiers, which contribute significantly to the production of autochthonous OC and IC (Martin *et al.,* 2007; Qui-Minet *et al.,* 2022), the effects of climate change on these components must also be considered (Legrand *et al.,* 2017).

At the community level, both autochthonous OC and IC can be produced in rhodolith beds. Autochthonous OC production is the balance of photosynthesis to respiration, with photosynthesis absorbing CO_2 and respiration releasing CO_2 (van der Heijden and Kamenos 2015). On the other hand, IC carbon production is the balance of calcification to dissolution, with the process of calcification theoretically releasing CO_2 and the dissolution of calcium carbonate absorbing CO_2 (Ware *et al.,*1992; Frankignoulle and Canon, 1994; van der Heijden and Kamenos 2015; Macreadie *et al.,*2017). The ability of rhodolith beds to store

autochthonous BC depends on the balance of OC and IC, with the dissolution of IC absorbing CO_2 and the production of IC releasing CO_2 where it can be reintroduced into the atmosphere (Frankignoulle and Canon, 1994; Macreadie *et al.*, 2017). Whilst previous studies have discounted rhodolith beds as BC repositories (Macreadie *et al.*, 2017, 2019), the calcification-derived CO_2 may be recycled within the community by autotrophs (for a more in-depth discussion, see Chapter 2). Few studies have quantified both OC and IC carbon in rhodolith beds (Martin *et al.*, 2007; van der Heijden and Kamenos 2015; Burdett *et al.*, 2018), thus the current and future role of rhodolith beds as BC repositories is not well defined.

Under current oceanic pH and temperature conditions, rhodolith beds can be highly productive systems (Martin *et al.*, 2005), with rhodolith beds harbouring a variety of autotrophs (e.g. coralline algae, macroalgae, and microalgae) which can contribute to community-level OC production (Barbera *et al.*, 2003; Martin *et al.*, 2005; Attard *et al.*, 2015; Qui-Minet *et al.*, 2022). Rhodolith beds also produce a significant amount of IC (in the form of calcium carbonate), with calcifiers including coralline algae, molluscs, crustaceans, annelids and bryozoans all contributing to community IC production (Bosence and Wilson, 2003; Martin *et al.*, 2007; Legrand *et al.*, 2017). The ability of rhodolith beds to act as a BC source or sink depends on a variety of factors including the community assemblage (i.e. the biomass of autotrophs and calcifiers), depth/irradiance (which influences primary production and calcification; Martin *et al.*, 2005, 2007), and temperature (which influences respiration, photosynthesis and calcification; Martin *et al.*, 2007). Under current conditions, rhodolith beds are considered to be net sources of CO_2 (Martin *et al.*, 2007), with community IC production often exceeding OC production (Burdett *et al.*, 2018; Legrand *et al.*, 2017; Martin *et al.*, 2007). However, such studies do not consider the recycling of calcification-derived CO_2 by other autotrophs, with evidence that community-scale photosynthesis may partially offset calcification-derived carbon release (Mao 2019; See chapter 2 for a more in-depth discussion).

4.1.2 Autochthonous organic carbon production in a future world

Currently, little is known about how the ability of rhodolith beds to act as a carbon source or sink will change with future conditions. To my knowledge, only two studies have investigated rhodolith bed community metabolism under future conditions, with one *in situ* study (Burdett *et al.*, 2018), and one *in vitro* study (Legrand *et al.*, 2017). With regards to the *in situ* study, short-term OA (<1 day) shifted the community from net respiration to net photosynthesis, and

net calcification to net dissolution (Burdett *et al.,* 2018). This resulted in the system shifting from a carbon source to a carbon sink, with net photosynthesis and net dissolution under OA absorbing CO_2 (Burdett *et al.,* 2018). Whilst this may be beneficial for BC storage in the short term, it is important to consider that prolonged CO_2 enrichment may result in the long-term dissolution of rhodolith beds, with the system only partially recovering when ambient conditions were returned (Burdett *et al.,* 2018). This may in turn influence the community of autotrophs and calcifiers supported by the rhodolith bed, which play an important role in community carbon cycling (Martin *et al.,* 2007; Brodie *et al.,* 2014; Attard *et al.,* 2015). Whilst this study provided important evidence of the effects of pCO_2 on a rhodolith bed community, the effects of elevated temperature were not investigated. As temperature is known to affect rhodolith species (Martin and Gattuso 2009; Noisette *et al.,* 2013b; Qui-Minet *et al.,* 2019), the effects of elevated temperature, and the interaction between elevated temperature and pCO_2, on OC and IC production must also be considered.

A further study by Legrand *et al.,* (2017) has investigated the effects of both elevated temperature and pCO_2, and a combination of the two stressors, on rhodolith bed community metabolism. By running the experiment *in vitro* the study was able to maintain treatment conditions over 3 months, allowing for the longer-term effects of OA and temperature on the rhodolith bed community to be explored (Legrand *et al.,* 2017). Furthermore, by measuring both whole assemblage and individual species metabolism, the study allowed for both single-species and community-level responses to climate change to be observed (Legrand *et al.,* 2017). When comparing the response of live coralline algae (*Lithothamnion coralloides)* and the rhodolith bed assemblage to climate change, responses differed, highlighting the importance of investigating the effects of OA and global warming on metabolism at a community level (Legrand *et al.,* 2017). Differences in responses were driven by changes in interactions between calcifying and fleshy algae, and algae and grazers (Legrand *et al.,* 2017). For calcifying and fleshy algae interactions, under elevated pCO_2, epiphytic algal growth increased with more CO_2 available for photosynthesis (Koch *et al.,* 2013; Legrand *et al.,* 2017). Epiphytic algae growth in turn increased community respiration, and decreased calcification, with algal overgrowth shading the coralline algae, limiting O_2, nutrients and light, reducing coralline algae calcification rates (Martin and Gattuso 2009; Legrand *et al.,* 2017). Epiphyte-grazer interactions were altered by both OA and warming, with changes in respiration and excretion rates indicating that some species were stressed under future conditions, whilst others benefited from the increased food supply provided by the epiphytic algae growth (Jokiel *et al.,*

2008; Legrand *et al.,* 2017, 2020). In terms of IC and OC storage, the results are in agreement with Burdett *et al.,* (2018), with the community experiencing an increase in OC and a decrease in IC production, shifting from a carbon source to a carbon sink (Legrand *et al.,* 2017).

The results from Legrand et al (2017) and Burdett *et al.,* (2018) highlight the need to investigate the effects of climate change on the whole community, with single-species experiments not fully encapsulating how rhodolith beds will fair under future conditions. Unlike Legrand et al (2017), Burdett *et al.,* (2018) did not compare differences in the response of the whole community and single species to OA, with the experiment run *in situ*. However, differences in species and community responses can be observed when comparing the results of Burdett *et al.,* (2018) to the literature. For example, when investigating a rhodolith bed consisting of the coralline algae *L. glaciale* and other components (fauna, macroalgae and sediment), net photosynthesis increased under OA (Burdett *et al.,* 2018). However, in a single species experiment with *L. glaciale,* there were no observed effects of OA on photosynthesis rates, with growth from epiphytic algae not observed in this experiment (Kamenos *et al.,* 2013). With regards to calcification, evidence from single-species experiments on how *L. glaciale* will fair with OA is contradictory. Whilst some single-species experiments suggest that *L. glaciale* may increase calcification rates under OA, with algae compensating for nighttime dissolution (Kamenos *et al.,* 2013), others suggest that *L. glaciale* calcification rates will decrease (Büdenbender *et al.,* 2011; Ragazzola *et al.,* 2012), or remain unchanged (Ragazzola *et al.,* 2013). However, whilst the pH for OA conditions is similar for these experiments, temperature differed (Büdenbender *et al.,* 2011; Ragazzola *et al.,* 2012, 2013, Kamenos *et al.,* 2013), with increased calcification under OA found under warmer temperatures, with more energy potentially available to compensate for nighttime dissolution (Kamenos *et al.,* 2013). Furthermore, whilst these experiments give an insight into how individual coralline algae will fair under future conditions, they do not consider changes to species interactions and may not reflect the real world, with calcifying fauna also sensitive to OA (Wood *et al.,* 2010; Smith 2014). Thus, future experiments must investigate the effects of climate change on the whole rhodolith bed community.

4.1.3 Chapter aims

There is a lack of evidence of how the ability of rhodolith beds to act as a carbon source or sink will change in a future world. With different components of the community contributing to OC and IC production, the effects of climate change on the community as a whole must be considered. In this study, elevated pCO_2 and temperature were used to investigate the ability of rhodolith beds to function as BC systems under future climate conditions. Rhodolith bed samples contained live *L. glaciale*, rhodolith bed sediment (containing biofilm), calcifying fauna (primarily the brittle stars *Ophiocomina nigra* and *Opiothix fragilis*), and small pieces of macroalgae and algae so that the samples represented a whole community. Experiments were run over the summer and winter, with previous research finding that responses of species, and interaction between species, can vary with season (Legrand *et al.,* 2017; Martin *et al.,* 2013).

In this study, experiments were run *in vitro* allowing for experimental parameters to be controlled throughout the experiment. *In situ* experiments can offer the opportunity to investigate the effects of climate change in a natural setting (Burdett *et al.,* 2018). However, increasing temperature and acidifying the marine environment *in situ* in the long term is incredibly difficult with experiments suffering from low statistical replication. For example, whilst natural CO_2 vents offer a unique opportunity to explore the long-term effects of OA, changes in pH can be extreme and not representative of future change (Hall-Spencer *et al.,* 2008). Additionally, elevating temperature artificially *in situ* is incredibly difficult, with experiments investigating the effects of elevated temperature relying on either season or latitude (known as a space-for-time approach; (Pickett 1989) to explore environmental changes (Krause-Jensen and Duarte 2014; Olesen *et al.,* 2015).

In this study, elevated pCO_2 and temperature were used to identify if under future conditions:

a) Community OC production increased, with elevated pCO_2 facilitating higher photosynthesis rates from autotrophs.
b) Community IC production decreased, with dissolution rates increasing the amount of CO_2 absorbed by the system.
c) Rhodolith beds will shift from carbon sources to sinks, with increased dissolution rates suggesting that bed structure may be at risk under future conditions.

4.2 Methods

4.2.1 Experimental set-up

Experiments were run in parallel with Chapter 5 during the summer (2021) and winter (2021-2022). Sediment cores were collected using scuba from a rhodolith bed at Loch Sween, Scotland (56°01.99' N, 05°36.13' W). Samples were collected by coring 10cm of sediment in a clear Perspex drainpipe (diameter = 10cm, n= 40). Around 60-100g of coralline algae (*Lithothamnion glaciale*) was present on top of the sediment. Small marine fauna and flora (brittle stars, gastropods and macroalgae) were retained on top of the sediment in the cores so that each core represented an *in situ* rhodolith bed community as closely as possible. Cores were kept in an upright position and were then transported back to the mesocosm facility at the University of Glasgow.

Perspex pipes (here on defined as cores) were placed in large holding tanks (100 L; n= 5 per tank), with the tanks primarily used to maintain the internal water temperature of the cores. The cores were maintained at an ambient temperature (14°C in the summer, and 6°C in the winter; (Attard *et al.,* 2015)), with the light intensity and diel cycle within the range of that season (Summer: 12L:12D, light intensity = 7.35 mol m^{-2} d^{-1}; Winter: 8L:16D, light intensity = 1.08 mol m^{-2} d^{-1}; Attard *et al.,* 2015). Cores were bubbled constantly with ambient air (400ppm, present-day concentration as measured using a Licor CO_2 analyser), with conditions maintained for a week to allow the rhodolith cores to stabilise post-collection (Kamenos *et al.,* 2013).

After a week, conditions were gradually altered over 2 weeks to the following treatment combinations (n= 10 for each treatment):

- Ambient: Ambient pCO_2 (Bubbled gas composition = 400ppm) and temperature
- +T: Ambient pCO_2 (400ppm) and elevated temperature (+3°C)
- +CO2: Elevated pCO_2 (750ppm) and ambient temperature
- +T +CO2: Elevated pCO_2 (750ppm) and elevated temperature (+3°C)

An elevated pCO_2 of 750ppm and a temperature of +3°C were chosen as they are in the range of the most likely climate scenario for the end of the century (Meinshausen *et al.,* 2011; Peters and Hausfather 2020; IPCC 2022).

The sediment cores were maintained at treatment conditions for 4 weeks with ~30% of the water refreshed twice weekly with water bubbled with the corresponding pCO_2 concentration and at the same temperature. The Perspex plastic of the cores was cleaned every 2-3 weeks to remove any biofilm, with biofilm growth on the coralline algae and sediment undisturbed. Background parameters (temperature, pH, salinity and dissolved oxygen (DO)%) were monitored using a YSI Pro Plus Quatro throughout the experiment.

4.2.2 Rhodolith bed community metabolism

After 4 weeks, rhodolith bed community metabolism (photosynthesis, respiration, production and calcification) was calculated using O_2 dissolved IC (DIC), and $CaCO_3$ (using total alkalinity (TA)) fluxes. Fluxes were calculated via *in vitro* light and dark incubations, with incubations lasting approximately 2 hours. During incubations, cores were incubated using a closed system so that no air could enter. Water was stirred constantly using a magnetic stirrer. Oxygen sensor spots (Manufacturer = PreSens; product code = SP-PSt3-NAU) were used to determine O_2 concentrations (using a Fibrox 3 PreSens monitoring system) at the start and end of the incubation. Water samples were also taken at the start and end of each incubation so that changes in DIC and A_T could be calculated. Samples were filtered using 1.6 um filter paper before being placed in pre-acid washed exetainers and spiked with 0.06% saturated mercuric chloride solution. All samples were stored at 4°C until the analysis date.

A_T was measured on a Metrohm 848 Titrino Plus using the 2-stage open-cell potentiometric titration method on 12 ml sample volumes with 0.01 M HCl (Dickson *et al.*, 2007). Samples were kept at room temperature, which was measured and accounted for later in the TA calculations. Seawater Reference Materials (batches 189 and 196) were used as standards (supplied from Dickson's Laboratory, Scripps Institution of Oceanography). Two water samples were analysed for each measurement, with the average A_T value reported. The average instrument precision (from here on calculated as the sd from the standard value) across the analysis period is 24 (µmol kg^{-1}).

DIC was determined using an Automated Infra-Red Inorganic Carbon Analyser (AIRICA) (Marianda, model number 21) fitted with a Licor 820. The Licor was calibrated immediately before the analysis period, with 400 ppm and 1000 ppm certified carbon dioxide gas (mixtures of CO_2 and N_2). On the AIRICA, 1 ml of sample was reacted with approximately 60 ul, 10%

phosphoric acid. The evolved gas was dried using a NafionTM drier (Perma pure) before reaching the Licor. Peak areas were converted to a concentration of DIC using Seawater Reference Materials (batches 189 and 196) supplied from Dickson's Laboratory, Scripps Institution of Oceanography. Three repeated measurements were made per sample and an average of the last two measurements is the reported value of DIC. The average instrument precision across the analysis period is 26 (µmol kg^{-1}).

Additional carbonate chemistry parameters (pH_{NBS}, pCO_2, $[HOC_3^-]$, $[CO_3^{-2}]$, aragonite saturation state [Ω_{Arg}], calcite saturation state [Ω_{Cal}]) were calculated from A_T and C_T using the *seacarb* package in RStudio (Gattuso *et al.,* 2022) with dissociation constants from Lueker *et al.,* (2000), and KSO4 using Dickson (1990).

O_2 fluxes were calculated via the below equation:

$$O_2\text{flux} = \frac{\Delta O_2 \times v}{s \times \Delta t}$$

where ΔO_2 is the change in oxygen concentration (mmol/L), v is the volume (L), s is the surface area of the community (m^2), and t is time (hours). Light O_2 flux corresponded to net daytime production (NDP) and dark O_2 flux corresponded to respiration (R). Benthic gross primary production (GPP; mmol O_2 m^{-2} h^{-1}) was calculated as NDP + |R|. GPP was calculated with the assumption that respiration rate is light-dependent, however, GPP should be regarded as a minimum estimate as R can be higher during the daytime compared to the night-time (Glud 2008). Net community metabolism (NCM, mmol O_2 m^{-2} d^{-1}) corresponded to the net O_2 flux and was calculated by multiplying light and dark hourly fluxes by the respective time the mesocosms spent in light and dark conditions. A positive NCM value signified that the system was net autotrophic, whilst a negative value signified that the system was net heterotrophic.

DIC and $CaCO_3$ fluxes were calculated via the below equations:

$$\text{DIC flux} = \frac{\Delta DIC \times v}{s \times \Delta t} - G$$

$$CaCO_3 \text{ flux (G)} = \frac{\Delta A_T \times v}{2 \times s \times \Delta t}$$

where ΔDIC is the change in dissolved DIC (mmol/kg), ΔA_T is the change in TA (mmol/kg), and G is $CaCO_3$ flux. Light, dark and net fluxes were calculated for DIC and $CaCO_3$ data.

4.2.3 Organic and inorganic carbon production

O_2 and DIC fluxes were used as a proxy of production, with DIC decreasing by one mole, and O_2 increasing by one mole for the production of 1 mol of OC (van der Heijden and Kamenos 2015):

$$CO_2 + H_2O \rightarrow CH_2O + O_2$$

Light fluxes represented OC production through photosynthesis, whilst dark fluxes represented breakdown via respiration. Daily O_2 production represented net OC production, with every 1 mol of O_2 presenting 1 mol of OC production. A -DIC:O_2 ratio of 1 suggests that DIC absorbed during the experiment is due to OC production through photosynthesis.

$CaCO_3$ fluxes were used as a measure of calcification and dissolution. For each decrease of 2 moles of TA, $CaCO_3$ precipitated increased by 1 mole (van der Heijden and Kamenos 2015):

$$Ca^{2+} + 2HCO_3^- \rightarrow CaCO_3 + CO_2 + H_2O$$

As the carbon contained in $CaCO_3$ is inorganic, for every 1 mol of $CaCO_3$ produced, 1 mol of IC is also produced.

As 1 mol of CO_2 is absorbed for each mol of OC produced and 1 mol of CO_2 is released for each mol of IC produced, the total CO_2 drawdown was determined for each core by:

$$CO_2\ drawdown = OC - IC$$

Annual CO_2 drawdown was calculated by:

$$\begin{aligned} Annual\ CO_2\ drawdown \\ &= (176\ days\ x\ Summer\ OC\ net\ production) \\ &+ (176\ days\ x\ Winter\ OC\ net\ production) \end{aligned}$$

A positive CO_2 drawdown value corresponded to the system acting as a CO_2 sink, and a negative value, a CO_2 source.

All flux measurements were corrected for considering seawater blanks from both light and dark cores.

4.2.4 Statistical analysis

Data analysis was conducted using R version 4.1.1 in R Studio (Version 1.4.1717). Tank had no significant random effect (using mixed models) for any parameters in this analysis ($p>0.05$) and was not used as a factor in the analysis. Shapiro Wilk tests and Levene's test were used to assess the distribution of the data and the heterogeneity of variance. Kruskal Wallace tests and ANOVAs (analysis of variance) were used to investigate the effects of treatment, temperature, and CO_2 on the flux measurements. As multiple hypotheses were tested with the same dataset, Holm's Sequential Bonferroni Procedure was used to detail family-wise error rates. When investigating correlations between DIC flux and O_2 flux, a Pearson's or Spearman's rank correlation test was used. Models were run on raw flux data, and on flux data that had been scaled to per g of live coralline algae.

Medians (IQR duration) were given for non-parametric data and mean (±standard deviation) was given for parametric data. In all models, a significance level of 0.05 was used. The package ggplot2 was used to plot the graphs.

4.3 Results

4.3.1 Environmental parameters

The average temperature, salinity and DO% are shown in Table 4.1. For both summer and winter experiments, average temperature varied between ambient and +T treatments (Summer = $X^2(1) = 28.58$, $p<0.001$); Winter $X^2(1) = 16.07$, $p<0.001$), but not within ambient or +T treatments ($p>0.05$). Salinity and DO% did not vary between treatments for either summer or winter experiments ($p>0.05$). Water chemistry parameters are also summarised in Table 4.1.

Table 4.1: Environmental parameters under ambient, elevated temperature (+T), elevated CO_2 (+CO2), and elevated temperature with elevated CO_2 (+T +CO2). Values are given for both light and dark, with samples taken before incubations commenced. Water temperature, salinity, total alkalinity (A_T) and dissolved inorganic carbon (C_T) were all directly measured. All other parameters were calculated with dissociation constants from Lueker *et al.*, (2000), and KSO_4 using Dickson (1990). Carbonate parameters are pH (pH_{NBS}), pCO_2, HCO_3^-, CO_3^{2-}, aragonite saturation state (Ω_{Arg}), and calcite saturation state (Ω_{Cal}). Data presented are mean±sd, with n = 5 for each treatment (n= 10 when averaged across light and dark incubations).

	Ambient		+T		+CO2		+T +CO2	
	Light	Dark	Light	Dark	Light	Dark	Light	Dark
Summer								
Temperature (°C)	13.9±0.5		16.2±1.2		13.9±0.5		16.0±1.2	
Salinity	34.7±0.9		35.3±0.8		35.0±0.6		35.7±0.5	
DO (%)	100.8±2.5		101.1±5.3		101.4±2.8		99.6±2.3	
A_T (µmol kg^{-1})	1088.6±269.5	1300.7±250.1	1467.9±218.5	1715.4±378.9	1556.1±316.9	1880.4±489.4	2064.2±304.8	1692.6±237.6
C_T (µmol kg^{-1})	1023.4±242.7	1277.5±289.2	1376.3±218.8	1602.4±350.7	1495.8±324.2	1820.1±441.5	1984.8±181.8	1766.6±193.3
pH_{NBS}	7.72±0.13	7.54±0.2	7.76±0.08	7.83±0.04	7.67±0.26	7.64±0.19	7.6±0.53	7.12±0.18
pCO_2 (µatm)	418.1±116.4	881.4±569.8	530.4±158	511.9±60.9	846±667.7	908.3±243	1854.8±2306.1	2951.3±857.2
HCO_3^- (µmol kg^{-1})	966.9±223	1213.5±274.5	1295.3±209.2	1503.1±323	1410.9±308.4	1723.9±412.8	1823.7±132.1	1642.7±213.7
CO_3^{2-} (µmol kg^{-1})	40.6±21.5	30.3±6.6	62.4±11.7	81.1±25.7	53.1±24.7	61.3±35.3	96.6±85.4	19.1±9.7
Ω_{Arg}	0.62±0.33	0.47±0.1	0.95±0.18	1.26±0.4	0.81±0.38	0.94±0.53	1.49±1.32	0.29±0.15
Ω_{Cal}	0.97±0.51	0.73±0.16	1.48±0.27	1.96±0.62	1.26±0.59	1.47±0.83	2.3±2.04	0.46±0.23
Winter								
Temperature (°C)	7.4±1.4		9.2±1.0		7.1±1.2		8.9±1.3	
Salinity	36.0±0.7		35.6±0.6		36.5±0.7		36.2±0.4	
DO (%)	102.0±1.0		100.0±1.3		101.2±0.7		99.2±2.2	
A_T (µmol kg^{-1})	2359.2±327.7	2086.6±465	2337.9±332.6	1794.5±106.9	2724.9±509.3	2373.3±419.8	2810.6±472.2	2549.5±439.8
C_T (µmol kg^{-1})	2227.9±358.2	1981.7±436.7	2173.5±279.1	1739.3±112	2584.9±431.6	2266.9±365.2	2660.5±413.9	2453.8±416.8
pH_{NBS}	7.93±0.13	7.87±0.05	8±0.08	7.73±0.12	7.89±0.11	7.83±0.11	7.91±0.08	7.81±0.07
pCO_2 (µatm)	579.7±295.2	548.9±86.1	442.5±43.1	708.3±227.1	682.3±71.1	684.6±118.5	668.7±57.8	797.6±192.3
HCO_3^- (µmol kg^{-1})	2096.7±354.5	1872.5±407	2029.3±238.4	1654.4±107.9	2431.9±377.4	2141.8±327.3	2501.7±368.6	2326.3±389
CO_3^{2-} (µmol kg^{-1})	104.6±13.8	83.8±28.5	123.7±42.6	52.9±10.3	121.2±59.3	93.2±45.2	128.1±49.3	90.8±29
Ω_{Arg}	1.58±0.21	1.26±0.43	1.86±0.65	0.8±0.16	1.82±0.89	1.4±0.68	1.92±0.74	1.37±0.44
Ω_{Cal}	2.48±0.33	1.99±0.67	2.93±1.02	1.26±0.25	2.86±1.39	2.2±1.07	3.02±1.15	2.15±0.69

4.3.2 Rhodolith bed community metabolism

The rhodolith bed community was a net source of O_2 during the day (as measured through net daytime production (NDP)), and a sink at night (as measured through respiration (R)) for both seasons, with no statistically significant differences between treatments for either season (Figure 4.1a, Table 4.2). NDP was statistically higher in the summer (Table 4.2) with a median NDP of 2.24 (IQR = 3.33) O_2 mmol m^{-2} h^{-1} in the summer and 0.34 (IQR = 1.31) O_2 mmol m^{-2} h^{-1} in the winter. R on the other hand was statistically lower in the summer (-3.17±1.77 O_2 mmol m^{-2} h^{-1}) compared to the winter (-1.55±1.07 O_2 mmol m^{-2} h^{-1}; Table 4.2). Whilst there were significant differences in NDP and R with season, there were not for NCM, with a mean of -0.10±3.13 O_2 mmol m^{-2} d^{-1} in the summer and -1.12±1.66 O_2 mmol m^{-2} d^{-1} in the winter (Figure 4.1b). Whilst GPP did not vary with treatments within each season, it did between seasons with autotrophs within the bed being most active during the summer (Summer = 6.38(IQR = 3.08) O_2 mmol m^{-2} h^{-1}; Winer = 2.20(IQR = 1.50) O_2 mmol m^{-2} h^{-1}). Scaling O_2 fluxes per g of coralline algae did not change any trends observed (Appendix 3.2).

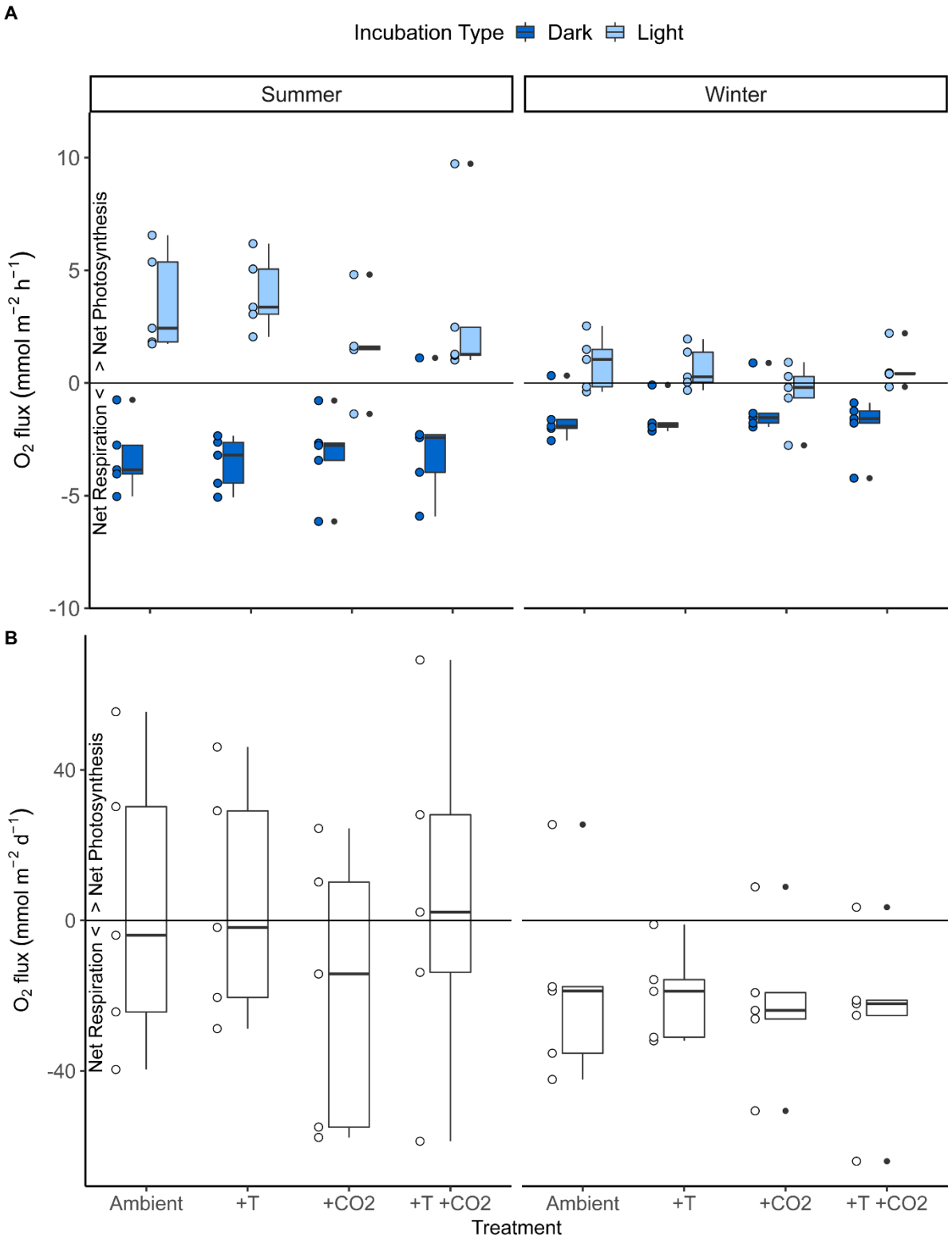

Figure 4.1: Showing A) light (NDP) and dark (R) O_2 flux and B) net O_2 flux (NEM) for the rhodolith bed community for both summer and winter experiments. Treatments are ambient conditions, elevated temperature (+T), elevated CO_2 (+CO2), and elevated temperature with elevated CO_2 (+T +CO2). Points to the left of the bar charts correspond to raw data. Boxplot bars represent median and interquartile ranges, and whiskers represent minimum and maximum values.

Table 4.2: Summary of statistical analysis (ANOVA and Kruskal Wallace test results) testing the effects of treatment for the rhodolith bed community in summer and winter experiments, and differences between seasons. Showing net daytime production (NDP, from light fluxes), respiration (R, from dark fluxes), gross primary productivity (GPP, NDP + |R|) and net community metabolism (NCM, NDP + R). Units for NDP, R and GPP are O_2 mmol m^{-2} h^{-1}. Units for NCM are O_2 mmol m^{-2} d^{-1}. n= 20 for summer and winter experiments. X^2 refers to chi-squared, indicating that a Kruskal-Wallace test was used as the data was non-parametric. *data was not homogenous and was transformed by log(data+5) before the test was run.

	Net Daytime Production NDP		**Respiration R**		**Gross Production GPP**		**Net Community Metabolism NCM**	
	F	***p***	***F***	***p***	***F***	***p***	***F***	***p***
Summer								
T	4.418	0.425	0.015	0.903	0.673	0.424	0.507	0.487
pCO_2	9.493	0.248	0.326	0.576	1.621	0.221	0.369	0.552
T x pCO_2	1.692	0.619	0.178	0.697	0.120	0.734	0.410	0.531
Winter								
T	0.782	0.390	X^2 = 1.691	0.638	1.114	0.307	0.004	0.953
pCO_2	1.869	0.190	X^2 = 0.091	0.762	1.078	0.315	0.744	0.401
T x pCO_2	1.853	0.192	X^2 = 1.463	0.227	2.854	0.111	0.143	0.711
Season	**X^2 = 15.384**	**P<0.001**	**12.22**	**<0.001**	**X^2 = 20.652**	**P<0.001**	0.052	0.821*

Similarly to O_2 flux measurements, whilst there was no significant association between DIC flux and treatment for light, dark, and net measurements, DIC flux did vary between seasons (Figure 4.2, Table 4.3). In the summer rhodolith beds exhibited a positive flux during the day (median = 1.60 DIC mmol m^{-2} h^{-1}, IQR = 3.59; Figure 4.2), and a negative flux at night (median = -7.24 DIC mmol m^{-2} h^{-1}, IQR = 2.72; Figure 4.2), with a negative net flux of -60.24 (IQR = 7.01) DIC mmol m^{-2} d^{-1}. In the winter this trend was reversed with DIC flux negative during the day (median = -0.42 DIC mmol m^{-2} h^{-1}, IQR = 3.98; Figure 4.2) and positive during the night (1.19±2.70 DIC mmol m^{-2} h^{-1}; Figure 4.2) with a positive net flux of 8.44±62.4 mmol m^{-2} d^{-1}. Similarly to the O_2 fluxes, scaling per g of coralline algae did not change any trends observed (Appendix 3.2).

DIC flux did not follow a 1:1 quotient with O_2 flux and was not significantly correlated for either the light or dark incubations during the summer and winter experiments ($p>0.05$; Figure 4.3).

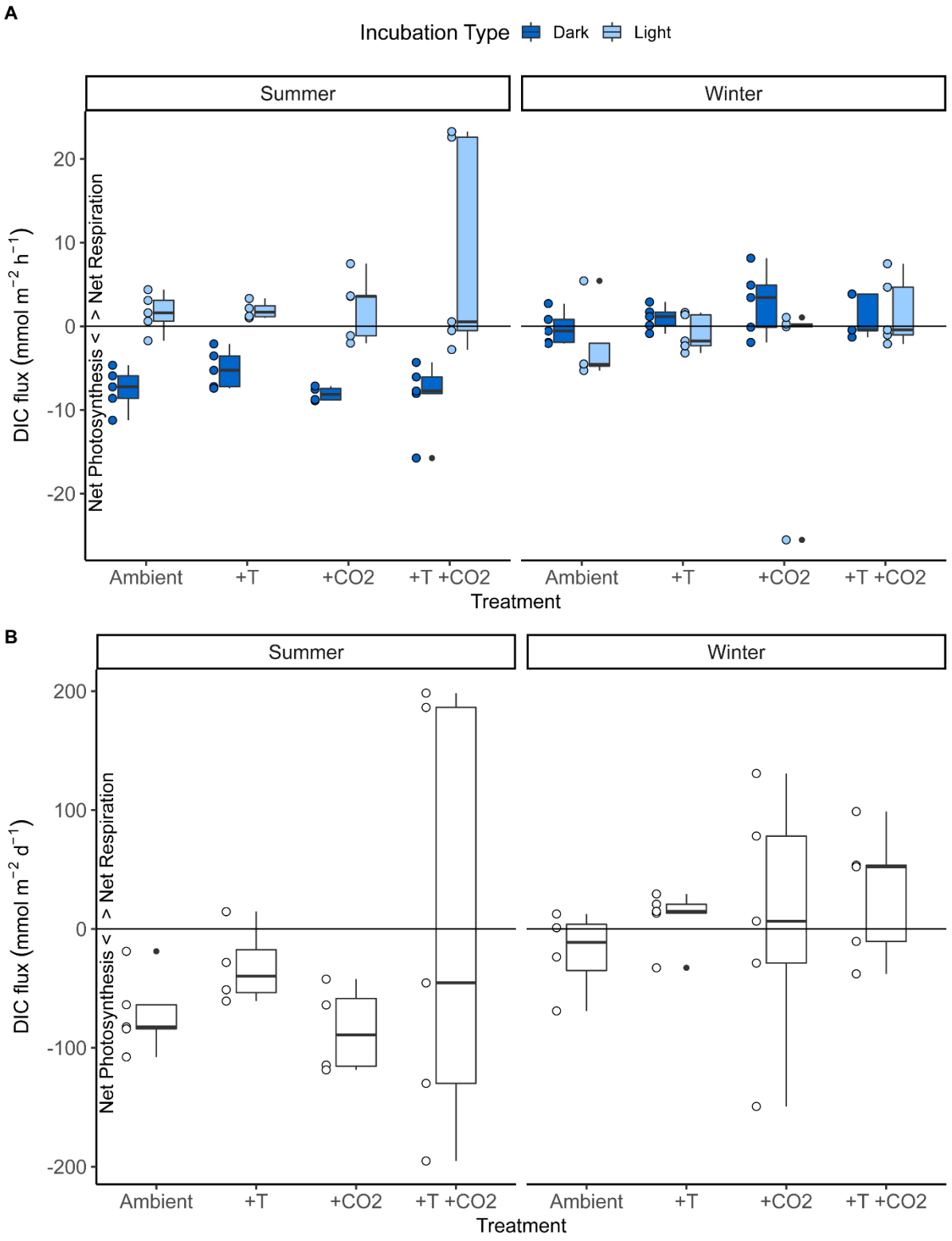

Figure 4.2: Showing a) light (NDP) and dark (R) DIC flux and b) net DIC flux for the rhodolith bed community for both summer and winter experiments. Treatments are ambient conditions, elevated temperature (+T), elevated CO_2 (+CO2), and elevated temperature with elevated CO_2 (+T +CO2). Points to the left of the bar charts correspond to raw data. Boxplot bars represent median and interquartile ranges, and whiskers represent minimum and maximum values.

Table 4.3: Summary of statistical analysis (ANOVA and Kruskal Wallace test results) testing the effects of treatment on DIC fluxes (light, dark and net) for the rhodolith bed community in summer and winter experiments, and differences between seasons. Units for light and dark fluxes are DIC mmol m^{-2} h^{-1}. Units for net fluxes are DIC mmol m^{-2} d^{-1}. n= 20 for summer and winter experiments. X^2 refers to chi-squared, indicating that a Kruskal-Wallace test was used as the data was non-parametric.

	Light DIC Flux		**Dark DIC Flux**		**Net DIC Flux**	
	F	***p***	***F***	***p***	***F***	***p***
Summer						
T	$X^2 = 0.000$	1	$X^2 = 1.707$	0.191	$X^2 = 1.873$	0.171
pCO_2	$X^2 = 0.007$	0.935	$X^2 = 2.407$	0.121	$X^2 = 0.438$	0.508
T x pCO_2	$X^2 = 0.065$	0.996	$X^2 = 4.675$	0.197	$X^2 = 2.615$	0.455
Winter						
T	$X^2 = 0.96$	0.327	1.779	0.201	0.754	0.399
pCO_2	$X^2 = 1.127$	0.288	0.060	0.809	0.589	0.455
T x pCO_2	$X^2 = 2.25$	0.522	1.563	0.229	0.007	0.934
Season	**$X^2 = 5.119$**	**0.024**	**86.1**	**<0.001**	3.904	0.056

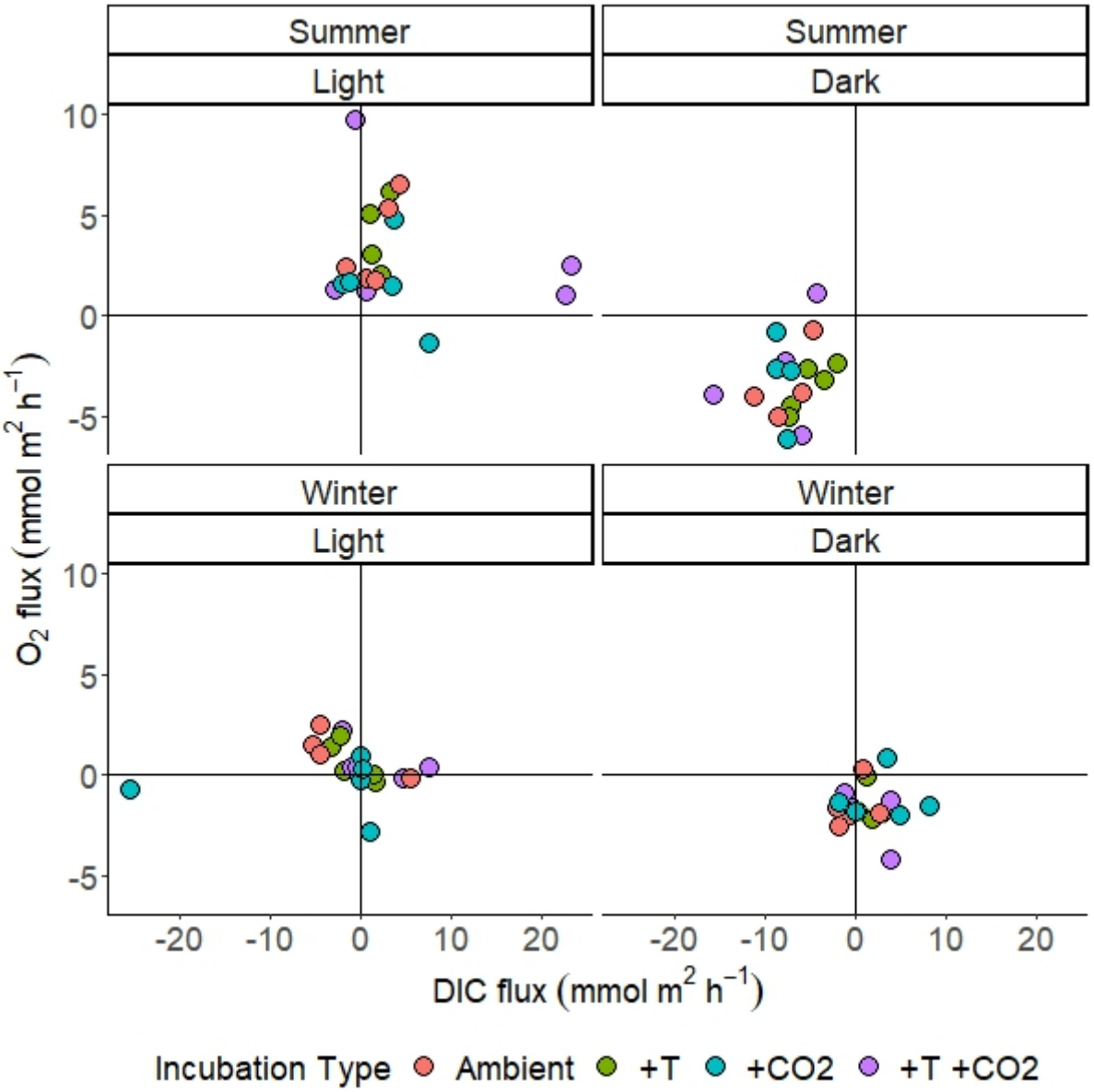

Figure 4.3: O2 flux vs DIC flux for light and incubations during summer and winter experiments for the rhodolith bed community. Treatments are ambient conditions, elevated temperature (+T), elevated CO_2 (+CO2), and elevated temperature with elevated CO_2 (+T +CO2).

Across both seasons, rhodolith beds exhibited net calcification during the light, and dissolution in the dark, with net dissolution observed across both treatments (Figure 4.4). In the summer, net $CaCO_3$ flux was significantly lower in the elevated temperature treatments (Table 4.4), with a mean flux of -22.9±18.5 $CaCO_3$ mmol m^{-2} d^{-1} under ambient temperatures, and -53.2±34.6 $CaCO_3$ mmol m^{-2} d^{-1} under elevated temperatures (Figure 4.4). In the summer, light $CaCO_3$ flux varied with treatment (Table 4.4), however, no significant differences were observed when running a Tukey Post Hoc test, with the Post Hoc test less sensitive to the small sample size. With the Post Hoc test, the smallest p-value (0.08) was between the ambient treatment and the elevated CO_2 treatment. This suggests that differences in light $CaCO_3$ flux between these two treatment groups may drive the significance observed in the ANOVA test, with the ambient treatment having higher calcification rates in the light (Figure 4.4). $CaCO_3$ flux did not vary with treatment for the dark incubations during the summer experiments (Table 4.4).

In the winter, light $CaCO_3$ flux was affected by pCO_2 (Table 4.4), with daytime calcification lower in the elevated pCO_2 treatments (Figure 4.4). There was no significant difference with treatment for light or net fluxes (Figure 4.4, Table 4.4).

Dark and net $CaCO_3$ fluxes varied with season (Figure 4.4, Table 4.4), with more dissolution experienced at night in the summer resulting in more dissolution throughout the day.

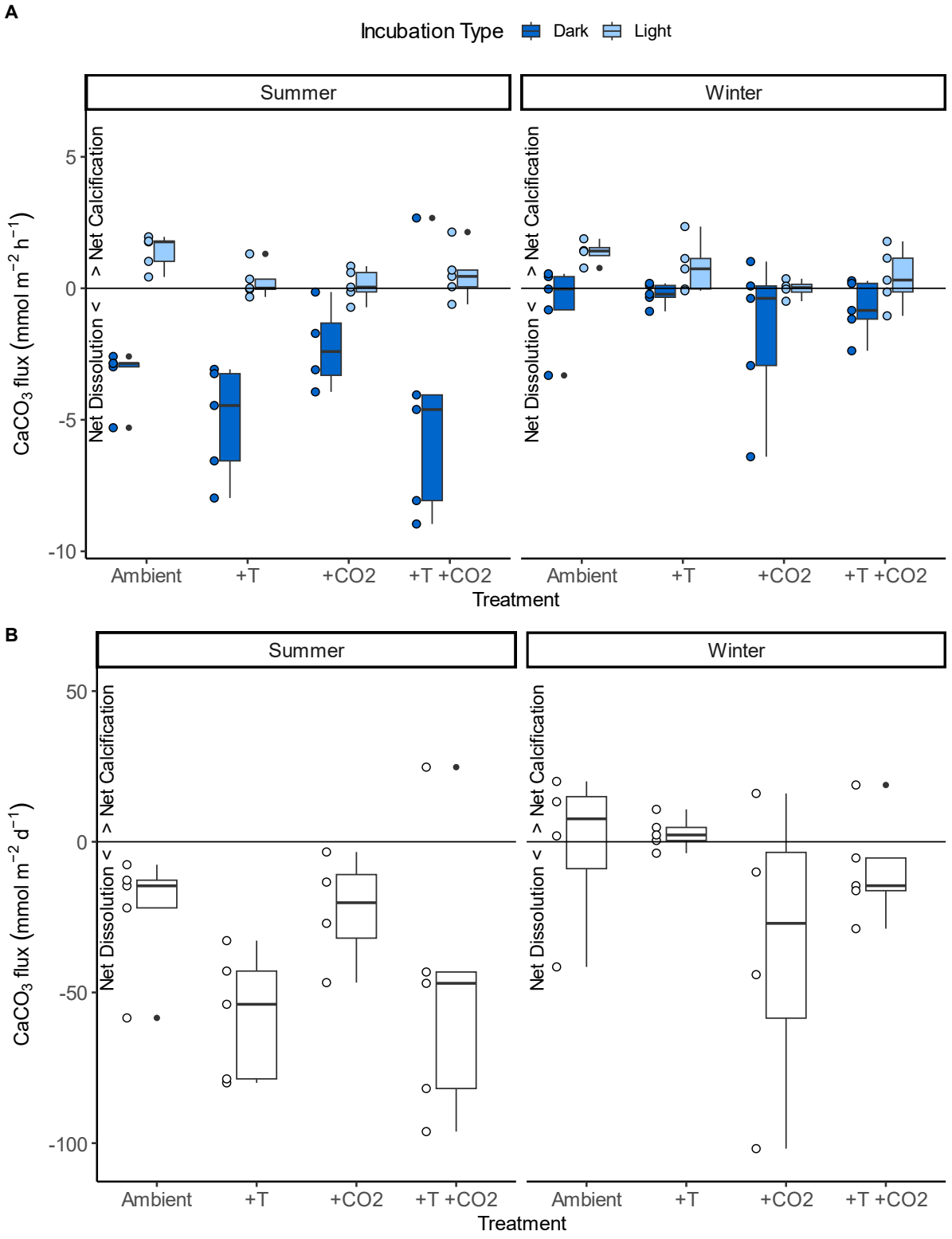

Figure 4.4: Showing a) light (NDP) and dark (R) $CaCO_3$ flux and b) net $CaCO_3$ flux for the rhodolith bed community for the summer and winter experiments. Treatments are ambient conditions, elevated temperature (+T), elevated CO_2 (+CO2), and elevated temperature with elevated CO_2 (+T +CO2). Points to the left of the bar charts correspond to raw data. Boxplot bars represent median and interquartile ranges, and whiskers represent minimum and maximum values.

Table 4.4: Summary of statistical analysis (ANOVA and Kruskal Wallace test results) testing the effects of treatment on $CaCO_3$ fluxes (light, dark and net) for the rhodolith bed community for summer and winter experiments, and differences between seasons. . Units for light and dark fluxes are $CaCO_3$ mmol m^{-2} h^{-1}. Units for net fluxes are $CaCO_3$ mmol m^{-2} d^{-1}. n= 20 for summer and winter experiments. X^2 refers to chi-squared, indicating that a Kruskal-Wallace test was used as the data was non-parametric. ↓ represent that the elevated condition had a negative effect on the parameter.

	Light $CaCO_3$ Flux		**Dark $CaCO_3$ Flux**		**Net $CaCO_3$ Flux**	
	F	***p***	***F***	***p***	***F***	***p***
Summer						
T	1.136	0.302	2.557	0.131	**4.977**	**0.041↓**
pCO_2	2.150	0.162	0.255	0.621	0.057	0.815
T x pCO_2	**5.408**	**0.034**	0.061	0.808	0.097	0.760
Winter						
T	0.023	0.880	$X^2 = 1$	1	$X^2 = 0.071$	0.790
pCO_2	**4.575**	**0.051↓**	$X^2 = 0.571$	0.450	$X^2 = 2.965$	0.085
T x pCO_2	1.524	0.237	$X^2 = 0.623$	0.891	$X^2 = 3.142$	0.370
Season	$X^2 = 0.256$	0.613	**$X^2 = 13.965$**	**P<0.001**	**8.231**	**<0.01**

4.3.3 Organic and inorganic carbon production

OC and IC production values were plotted against each other to determine how a system's ability to act as a carbon source or sink varied with season or treatment (Figure 4.5) In the summer, treatments were typically carbon sinks with dissolution rates larger than photosynthesis rates. IC production varied with treatment, with IC production lower in the summer with elevated temperature (Table 4.4, Figure 4.5). In the winter, cores were typically carbon sources, with respiration rates higher than calcification rates (Figure 4.5). CO_2 drawdown did not vary with treatment for summer or winter experiments but did vary with season (Table 4.5), with CO_2 drawdown positive in the summer (40.64±41.80 mmol m^{-2} d^{-1}), and negative in the winter (-12.39±33.14 mmol m^{-2} d^{-1}). When averaged across all treatments, the annual CO_2 drawdown across all treatments was 169 mmol m^{-2} yr^{-1}, with rhodolith beds acting as a net carbon sink.

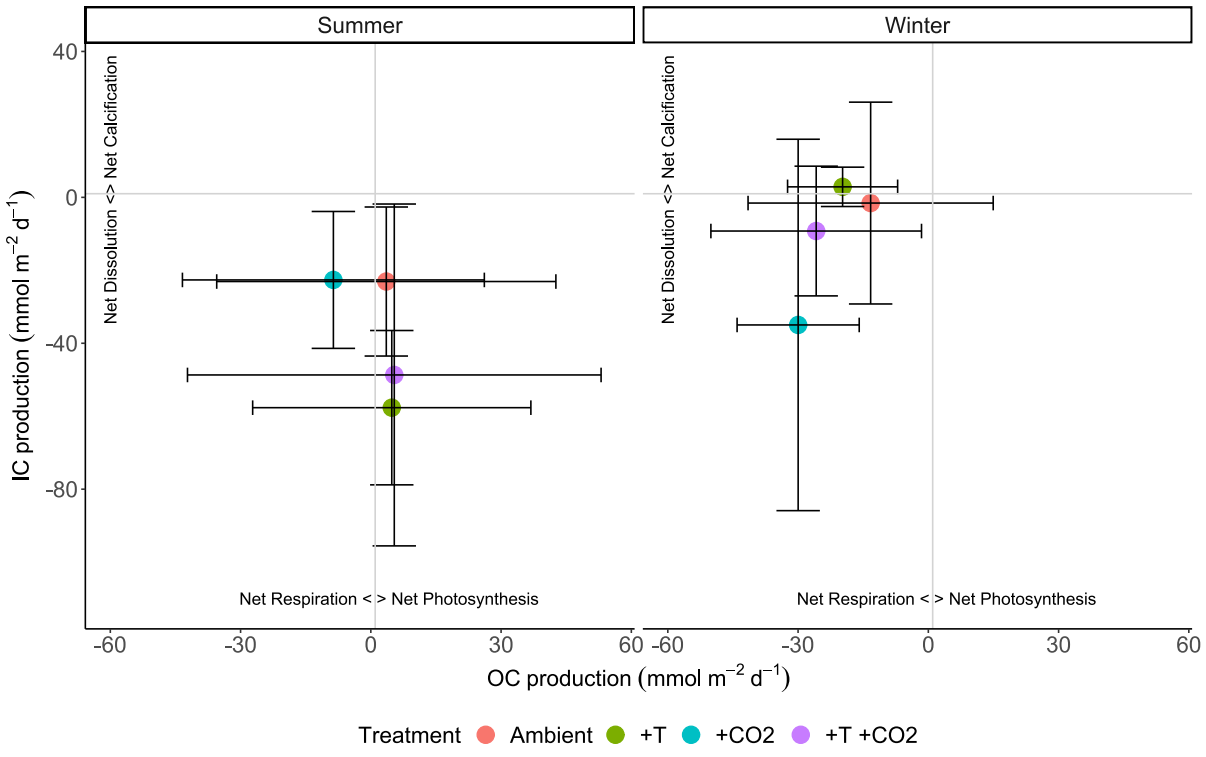

Figure 4.5: Inorganic carbon (IC) vs organic carbon (OC) production for the rhodolith bed community for summer and winter experiments. Treatments are ambient conditions, elevated temperature (+T), elevated CO_2 (+CO2), and elevated temperature with elevated CO_2 (+T +CO2).

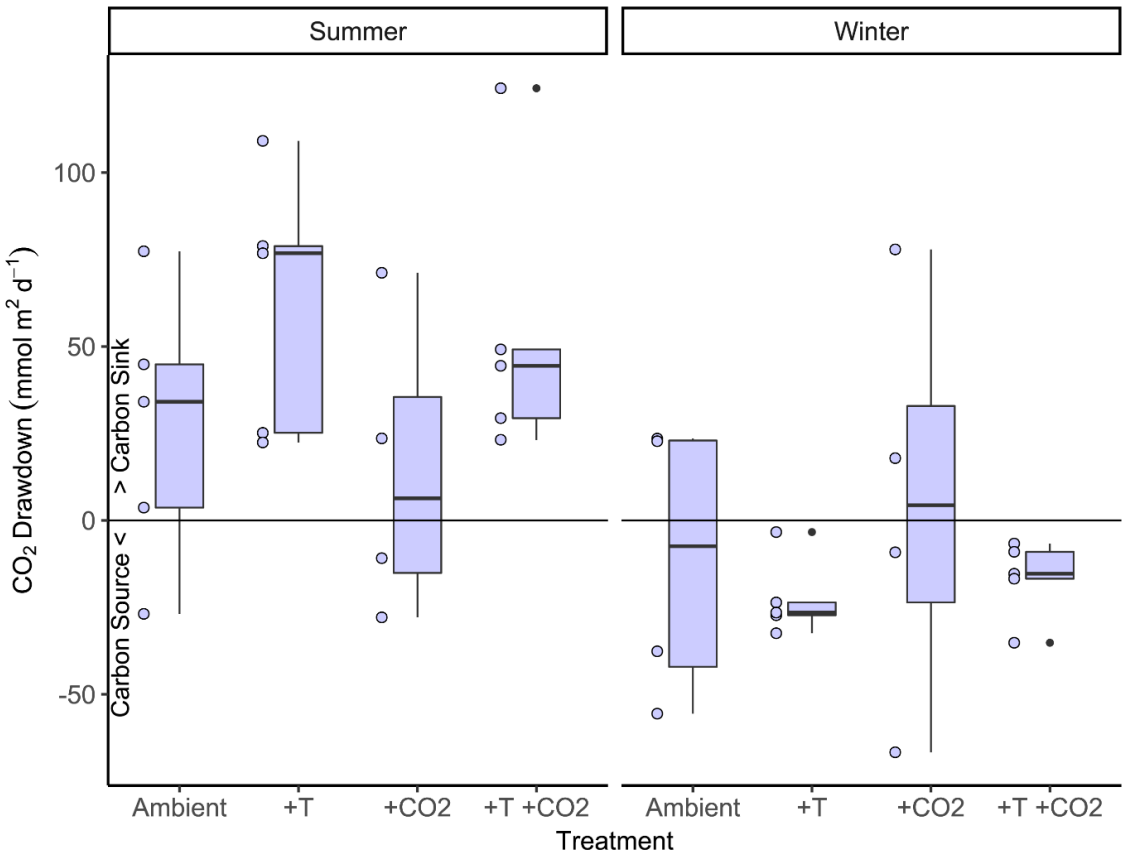

Figure 4.6: CO_2 drawdown for the rhodolith bed community for summer and winter experiments. Treatments are ambient conditions, elevated temperature (+T), elevated CO2 (+CO2), and elevated temperature with elevated CO2 (+T +CO2). Points to the left of the bar charts correspond to raw data. Boxplot bars represent median and interquartile ranges, and whiskers represent minimum and maximum values.

Table 4.5: Summary of statistical analysis (ANOVA) testing the effects of treatment for the rhodolith bed community in summer and winter experiments, and differences between seasons. Showing CO_2 Drawdown. n= 19 for summer and 18 for winter experiments.

	CO_2 Drawdown	
	F	***p***
Summer		
T	4.053	0.062
pCO_2	0.314	0.584
T x pCO_2	0.013	0.918
Winter		
T	0.975	0.34
pCO_2	0.435	0.52
T x pCO_2	0.105	0.75
Season	**18.15**	**<0.001**

4.4 Discussion

Climate change can affect an ecosystem's ability to sequester autochthonous carbon, however, few studies have investigated the effects of climate change on autochthonous carbon production in rhodolith beds at a community level (Legrand *et al.*, 2017; Burdett *et al.*, 2018). In this study, whilst elevated temperature and pCO_2 had no significant effect on rhodolith bed community OC flux, some patterns were apparent. On the other hand, IC flux was sensitive to both OA and temperature, with daylight calcification lower under OA and net calcification lower under elevated temperature. Large variations in O_2, DIC and $CaCO_3$ fluxes within treatment groups, likely due to the variability in the community assemblages, may have masked the effects of treatments. For all treatments, rhodolith beds acted as annual carbon sinks, in part due to net dissolution experienced in both the summer and the winter.

4.4.1 Organic carbon production may not change with global warming or ocean acidification

At a community level, OC production (as measured by O_2) did not significantly vary with temperature or pCO_2. Whilst there was no significant difference, some patterns were apparent in the figures with NDP and NCM potentially lower under OA. Conversely to previous literature, DIC flux did not follow a 1:1 ratio with O_2 flux (Martin *et al.*, 2005, 2007). As DIC is also influenced by other processes within the sediment and water column, including methanogenesis and sulphate reduction (Wu *et al.*, 2016; Meister *et al.*, 2019), DIC fluxes did not necessarily represent OC production from photosynthesis and were not used to measure OC production, with O_2 flux data used instead.

At a community level, there was no significant effect of temperature or OA on OC production, with photosynthesis and respiration rates similar amongst treatments. Although NDP and NCM were potentially lower under OA, the results are still in disagreement with other community-level studies, with previous research observing an increase in OC production under OA due to increased photosynthesis by autotrophs (Burdett et al., 2018; Legrand et al., 2017). There are several reasons why the results in this study contradict previous research. To start, large variations were observed for all OC measurements within treatment groups which may mask small changes between treatment groups. In this study, cores contained live *L. glaciale*, rhodolith bed sediment (containing biofilm), calcifying fauna (primarily the brittle stars *Ophiocomina nigra* and *Opiothix fragilis*), and algae, with each component contributing to OC

flux (Martin *et al.*, 2007; Attard *et al.*, 2015). As the mass of each component was not controlled for, with the cores reflecting the natural variability of a rhodolith bed system, the different ratios of components in each core likely contribute to the large variations in OC production observed in each treatment. Controlling for the mass of coralline algae did not reduce variations in O_2 data, suggesting that other components within the rhodolith bed (e.g. sediment, macroalgae, epiphytic algae, fauna), have a large effect on oxygen dynamics within the community (Chapter 5; Attard *et al.*, 2015). The large variability between cores may also be caused by sediment surface area, with large variation in O_2 flux measurements previously exhibited in rhodolith beds when flux measurements were calculated from small surface areas (Attard *et al.*, 2015). Future studies could either use larger cores to provide more surface area, or a higher sample size to provide more precise average values.

Another reason for the differences between this study and the literature is that whilst no changes in OC production were observed at a community level, temperature and OA may still impact the different components of the community, altering species interactions (Legrand et al., 2017). Changes in species interactions were particularly prominent in the summer, where epiphyte algal growth was observed on the sediment and coralline algae in some cores. Whilst the biomass of the epiphyte was not measured, growth may alter how OC is produced within the cores (Legrand et al., 2017), with OC primarily produced by *L. glaciale* in some cores and by epiphytic algae in others. Rhodolith bed sediment may also contribute to OC production, with the sediment containing biofilm which is photosynthetically active (Chapter 5). As OC production is influenced by many components of the community, variations in community OC production may not reflect changes to community composition. Thus, whilst measuring community OC production under OA and elevated temperature can be used to predict the capacity of a system as a carbon sink or source, investigating the changes to individual components of the system independently can provide further insight into how the system will operate in the future. Furthermore, as each core compromised or differing amounts of each component (e.g. 60-100g of coralline algae, 2-5 brittle stars of varying sizes), variability between cores within the same treatment may have been too large to show any effects of OA on community level OC production, albeit representative of a real rhodolith bed community.

Cores were kept at treatment conditions for different periods compared to previous research (Legrand *et al.*, 2017; Burdett *et al.*, 2018), which may have resulted in disparities between the results. Whilst the water pH and temperature for this study under elevated pCO_2 were similar

to previous studies (Legrand *et al.,* 2017; Burdett *et al.,* 2018), the time scale was different. In this experiment, cores were kept at treatment conditions for 1 month before OC and IC production was measured. This was longer than Burdett *et al.,* (2018), with samples acidified for <1 day, and shorter than Legrand *et al.,* (2017), with samples kept at treatment levels for 3 months. Both studies attribute the increase in OC production to different factors, with short-term acidification providing more CO_2 for photosynthesis by coralline algae and other autotrophs (Koch *et al.,* 2013; Burdett *et al.,* 2018), and longer-term acidification resulting in the growth of photosynthetically epiphytic algae, which contributes to OC production (Qui-Minet *et al.,* 2022). As this study was run for 1 month, the coralline algae may not experience enhanced photosynthesis, with the algae instead negatively impacted by treatment conditions, as seen in the calcification data. Additionally, although epiphyte algae were present, growth may not be high enough to enhance OC production beyond the variability seen under ambient conditions. Therefore, whilst the results from this study can be used to explore the effects of 1-month warming and OA, they may not be representative of how the system will react to future conditions, with changes to the ocean's climate occurring gradually over decadal timescales. Future work is therefore needed to establish if there is a link between OC production and future climate conditions, with experiments ran over multiple years, and the rate much more gradual than this study, Legrand *et al.,* (2017), and Burdett *et al.,* (2018).

A final explanation as to why no significant change in OA was observed in this study, is that the rhodolith bed may be tolerant to change. Previous single-species studies using individual coralline algae have similarly found no change in O_2 fluxes under elevated temperature and OA (Noisette *et al.,* 2013a, 2013b). Over a 24-hour rhodolith beds tolerate significant changes in both pH and temperature (Kamenos *et al.,* 2013; Mao 2019), with coralline algae having a large influence on seawater chemistry (Martin and Hall-Spencer 2017). Perhaps the changes in temperature and pCO_2 used in this study were not high enough or kept elevated for long enough to evoke changes in O_2 fluxes within the community. Whilst this is a possibility, this reason is unlikely, with ample evidence at community and species level of the effects of elevated pCO_2 and temperature on coralline algae metabolism (Hall-Spencer *et al.,* 2008; Martin *et al.,* 2013; Noisette *et al.,* 2013b; Legrand *et al.,* 2017; Burdett *et al.,* 2018). Additionally, in this study, there were negative effects of both OA and temperature on calcification rates further providing evidence that the rhodolith bed is susceptible to the effects of climate change.

When comparing the measurements of this study, with previous measurements from Loch Sween, where the samples were taken (Attard *et al.*, 2015; Burdett *et al.*, 2018), OC production measurements followed a similar trend with overall net heterotrophy experienced across both seasons. However, compared to such studies, NDP measurements in this study were higher, and R lower, resulting in a higher average NCM in both the summer and winter compared to *in situ* measurements (Attard *et al.*, 2015; Burdett *et al.*, 2018). Instead, NCM values were within the lower range measured at the rhodolith bed at the Bay of Brest, France (Martin *et al.*, 2007), a site with irradiance levels ~8-fold higher than Loch Sween. Whilst this study matched irradiance levels with previous records from Loch Sween (Attard *et al.*, 2015), the laboratory lighting was static and had no diel gradient in light intensity. Therefore, differences between field and laboratory metabolic rates may be a consequence of laboratory lighting, with irradiance levels having a large effect on O_2 production (Martin *et al.*, 2005, 2007; Attard *et al.*, 2015). This inference is further supported by GPP values, which were again larger than Loch Sween field measurements, suggesting a more active phototroph community within the laboratory cores (Attard *et al.*, 2015).

4.4.2 Inorganic carbon production is sensitive to ocean acidification and global warming

Community-level IC production decreased with both elevated temperature and ocean acidification, providing evidence that the rhodolith bed community changed in response to climate change. Calcification rates during the light experiments were particularly sensitive to OA, with ambient treatment significantly higher than the elevated pCO_2 treatments. Several factors may have contributed to changes in community-level calcification rates. For example, the presence of epiphyte growth on the coralline algae in some cores may have reduced calcification rates, with shading limiting O_2 and nutrients reaching the coralline algae (Garrabou and Ballesteros 2000; Martin and Gattuso 2009; Legrand *et al.*, 2017). *L. glaciale* may also have experienced reduced calcification rates irrespective of algal growth, with OA previously found to reduce the growth rate, wall-thickness, and cell density of calcium carbonate skeletons (Ragazzola *et al.*, 2012). Other components of the rhodolith bed likely also contributed to reduced calcification rates, with calcifying fauna sensitive to OA (Wood *et al.*, 2010; Smith, 2014), and the rhodolith bed sediment containing a high proportion of dead coralline algae which can undergo enhanced dissolution with OA (Kamenos *et al.*, 2013).

Temperature also influenced community IC production, with net calcification rates decreasing with elevated temperature. Whilst this is contrary to single-species experiments regarding *L. glaciale* and other rhodolith species (Büdenbender *et al.,* 2011; Riosmena-Rodríguez *et al.,* 2017), it may be due to changing interactions between the epiphyte and coralline algae communities. As discussed above, shading from the epiphyte community can reduce calcification (Garrabou and Ballesteros 2000; Martin and Gattuso 2009; Legrand *et al.,* 2017). As the epiphyte biomass can increase with temperature, with more energy for photosynthesis (Koch *et al.,* 2013), epiphyte biomass may have been higher under elevated temperature, significantly reducing calcification rates. Changes in net calcification rates under temperature also appeared to be linked to an increase in dissolution rates in the dark. Rhodolith bed sediment can contain high amounts of dead coralline algae, and net dissolution experienced in both seasons in this experiment is likely due to the dissolution of dead coralline algae in the underlying sediments (Martin *et al.,* 2007; Kamenos *et al.,* 2013). There is limited research on the effects of temperature on dead coralline algae dissolution, with research primarily focussing on OA (Kamenos *et al.,* 2013; Brodie *et al.,* 2014), therefore future research is needed to establish if there is a link, with the increased dissolution of dead coralline algae having the potential to damage the structure and function of rhodolith beds.

4.4.3 Rhodolith beds can act as blue carbon sinks under current and future conditions

Whilst there was no significant change in the ability of rhodolith beds to act as a carbon sink or source with elevated temperature and OA, patterns were apparent with CO_2 drawdown higher with elevated temperature in the summer, and lower with elevated temperature in the winter. Changes in CO_2 drawdown appeared to be driven by changes in calcium carbonate dissolution rather than OC production. As discussed above, increases in carbonate dissolution may be due to several factors including epiphyte growth (Garrabou and Ballesteros 2000; Martin and Gattuso 2009; Legrand *et al.,* 2017), reduced calcification rates (Ragazzola *et al.,* 2012), and reduced calcification by calcifying fauna (Wood *et al.,* 2010; Smith, 2014).

CO_2 drawdown also varied with season, with beds acting as a carbon sink in the summer and a source in the winter. Similarly to above, changes from sink to source appeared to be driven by calcium carbonate dissolution, with OC production negative for both experimental campaigns. This is in agreement with previous studies, with beds generally net heterotrophic and organic

carbon entering beds from elsewhere to balance the organic carbon deficit (Martin *et al.,* 2007; Attard *et al.*, 2015; Burdett *et al.*, 2018). Theoretically, this could mean that once established, rhodolith bed community dissolution from dead fragments of coralline algae in the bed may offset CO_2 released from the calcification of live coralline algae. However, as such arguments are based on calcification/dissolution processes at an ocean scale (i.e. Macreadie *et al.*, 2017), this may not be the case with the potential for CO_2 to be recycled both by the ecosystem and in the water column (see Chapter 2 for more discussion). Furthermore, as other studies from the field have found net calcification in rhodolith beds under ambient conditions (Martin *et al.,* 2007; Burdett *et al.*, 2018), this finding may be an artefact of the laboratory environment with the coralline algae less densely packed in the cores than in the field. Furthermore, whilst dissolution may result in the net uptake of CO_2, it can also damage the structure of rhodolith beds (Brodie *et al.,* 2014). Not only would this affect the ability of rhodolith beds to support the diverse community of autotrophs that contribute to OC production in the bed, but it would also affect the ability of beds to store allochthonous carbon (Brodie *et al.,* 2014). DIC flux indicated that other biological processes, such as methanogenesis, may have occurred during the incubation. As methane is a more potent greenhouse gas compared to CO_2, future work is needed to determine the rhodolith bed's contribution to methane emissions which may partially offset their contributions as a BC sink (Al-Haj and Fulweiler, 2020).

4.4.4 Conclusion

This chapter aimed to investigate how the ability of rhodolith beds to act as a carbon source or sink varied with climate change. This study found that:

a) After being exposed to a CO_2 concentration of 750ppm and warming of 3°C, community OC production was not significantly affected by elevated temperature or ocean acidification. Whilst some patterns were apparent, these were not in agreement with previous literature. The results do not mean that rhodolith bed communities are tolerant of climate change, with epiphyte algal growth observed in some cores. Furthermore, as the rhodolith bed community had calcification rates under future conditions, there was evidence that the community was negatively impacted by OA and temperature. With treatment conditions only maintained for one month before the experiments, there is the potential that OC production will change over the long term, with OC production increasing if rhodolith beds are replaced by fleshy algae, as seen in some areas with naturally high pCO_2 conditions (Porzio *et al.*, 2013, 2011).

b) Community IC production was affected by both global warming and OA. Decreased IC production may have been due to lower calcification rates by the coralline algae and calcifying fauna as well increased dissolution from dead coralline algae within the sediment.

c) Whilst there was no significant effect of elevated temperature of OA on the ability of rhodolith beds to act as a carbon source or sink, there were significant changes between seasons. There were also some patterns apparent between treatment groups within seasons, with CO_2 drawdown higher with elevated temperature in the summer, and lower with elevated temperature in the winter. The dissolution of dead coralline algae within the sediment likely had a large effect on the ability of rhodolith beds to act as a source or sink. Whilst this may, in part, offset the CO_2 released via the calcification of live coralline algae, increased dissolution of dead bed change may result in long-term damage to rhodolith beds reducing their capacity to act as BC repositories.

Chapter 5 Warming and ocean acidification reduces the burial and storage of labile carbon in rhodolith beds

5.1 Introduction

Chapter 3 showed that the sedimentary OC (SOC) stock compromised of both labile and refractory (including refractory and recalcitrant) carbon types. Labile and refractory carbon react differently, with labile carbon more vulnerable to bacterial remineralisation (Burdige 2007; Canfield 1994; Burdige 2007; Arndt *et al.,* 2013; Keuskamp *et al.,* 2013; Djukic *et al.,* 2018). Labile carbon remineralisation is also sensitive to climate change, increasing with global warming (Glud 2008; Keuskamp *et al.,* 2013; Djukic *et al.,* 2018; Mueller *et al.,* 2018; Trevathan-Tackett *et al.,* 2020). Currently, it is not known if OC storage in rhodolith beds will be affected by climate change however it is likely that any effects of climate change will vary with carbon source and reactivity. Rhodolith beds receive carbon from both marine (typically more labile; Burdige 2007; Hill *et al.,* 2015; Trevathan-Tackett *et al.,* 2020) and terrestrial (typically more refractory; Burdige 2005, 2007) sources (Chapter 3; Mao *et al.,* 2020), and responses are therefore likely to differ between beds. Furthermore, while the rhodolith bed SOC stock contains both labile (~20-40%) and refractory carbon (Chapter 3), it is not known if the current SOC stock of rhodolith beds will decrease with climate change. Understanding the ability of rhodolith beds to act as future BC repositories is critical. For example, changes in the rates of degradation of labile and refractory carbon in response to climate change may result in less labile allochthonous carbon being buried within rhodolith beds. Furthermore, if the SOC stock is vulnerable to bacterial remineralisation under future climate change, carbon accumulated in the SOC stock may be partially remineralized and reintroduced into the atmosphere.

5.1.1 Effects of global warming on carbon burial

One way in which climate change may affect rhodolith bed BC storage is through the increased degree of degradation of carbon entering the bed. Carbon degradation within sediments is driven by a multitude of enzymatic reactions (Chen *et al.,* 2022), with reactions changing downcore as O_2 availability decreases (Glud 2008; Arndt *et al.,* 2013). Temperature can affect the breakdown of carbon, with temperature theoretically increasing the rate of enzymatic

reactions responsible for breakdown (Arndt *et al.*, 2013; Chen *et al.*, 2022). There is evidence that temperature can affect carbon breakdown, with a strong association between seasonal temperature and degradation rates in several temperate environments, with degradation rates higher in the summer (Middelburg *et al.*, 1996; Tabuchi *et al.*, 2010; Arndt *et al.*, 2013; Xue *et al.*, 2015; Chen *et al.*, 2022). Regionally, although some studies have found degradation rates to be higher in warmer climates (Ainley and Bishop, 2015; Trevathan-Tackett *et al.*, 2021), generally this pattern is weaker, with other studies finding that degradation rates are not notably different between warmer and cooler biomes (Arndt *et al.*, 2013; Djukic *et al.*, 2018; Mueller *et al.*, 2018). This may be because the microbial community is adapted to local temperatures (Robador *et al.*, 2009, 2016), with decomposition being driven instead by a suite of abiotic factors, including ecosystem/sediment type, salinity, humidity, and pH (Djukic *et al.*, 2018; Mueller *et al.*, 2018, 2020; Behera *et al.*, 2019; Marley *et al.*, 2019; Balmonte *et al.*, 2020; Trevathan-Tackett *et al.*, 2021) and biotic factors including the faunal activity (Arndt *et al.*, 2013; Ravaglioli *et al.*, 2019; Lee *et al.*, 2022).

Organic material type is another driver of degradation rates, with labile carbon remineralized at a faster rate and sensitive to temperature (Glud 2008; Keuskamp *et al.*, 2013; Djukic *et al.*, 2018; Mueller *et al.*, 2018; Trevathan-Tackett *et al.*, 2020). As labile carbon types are easier to consume and are preferred food resources by the microbial community (Burdige 2007; Arndt *et al.*, 2013; Kelleway *et al.*, 2022), increasing temperatures result in the increase in the degradation of labile carbon compounds (Keuskamp *et al.*, 2013; Trevathan-Tackett *et al.*, 2020). Refractory carbon may also experience more degradation with elevated temperatures. However, the mass loss may be less than that of labile carbon, (Trevathan-Tackett *et al.*, 2020). The differences in the effects of global warming on carbon type may result in a smaller proportion of labile carbon buried within the system, ultimately resulting in systems storing less carbon. On the other hand, as labile carbon can be physically protected from remineralisation (i.e. encapsulation; Burdige 2005; Arndt *et al.*, 2013; Hemingway *et al.*, 2019), the effects of temperature on the mass of carbon stored within a system may not be as large as suggested.

5.1.2 Effects of global warming on the current sedimentary carbon stock

As elevated temperature can enhance degradation rates, climate change may also affect the current SOC stock. The effects of temperature on the SOC are complex. In the upper layers of the sediment, carbon is processed by both oxic and anoxic oxidation pathways (Glud 2008). However, downcore microbial activity, and therefore degradation activity, slow as O_2 availability and the proportion of labile carbon decreases (Glud 2008). Ultimately a proportion of carbon is not degraded and is preserved and if undisturbed can remain "locked away" in sediments indefinitely (Canfield 1994; Burdige 2005; Mao *et al.,* 2020). Currently, little is known about how ancient carbon stores will be affected by climate change, with previous studies suggesting carbon that is already locked away in BC system sediments may be resilient to warming (Macreadie *et al.,* 2019b). On the other hand, there is evidence that under elevated temperatures, refractory carbon is remineralised at a faster rate in the anoxic zone, with anaerobic microbial activity increasing with elevated temperatures (Keuskamp *et al.,* 2013; Trevathan-Tackett *et al.,* 2020). If microbial activity increased with temperature within the anoxic zone of the sediment, this could result in the loss of ancient carbon from BC systems globally, with carbon reintroduced as CO_2 into the atmosphere (Macreadie *et al.,* 2019b). As this would reduce the ability of BC systems to act as a NBS for pCO_2 increases, more research is needed to establish the resilience of ancient carbon stocks to global warming.

5.1.3 Effects of ocean acidification the current sedimentary carbon stock

Currently, there has been little research on the effects of ocean acidification (OA) on degradation and burial rates (Ravaglioli *et al.,* 2019; Lee *et al.,* 2022), with rates primarily driven by the other factors as discussed above (Glud 2008; Arndt *et al.,* 2013; Chen *et al.,* 2022). Whilst OA is anticipated to have a smaller effect on the SOC stock than global warming, it may still alter carbon dynamics, with OA shown to cause changes to detritivore and microbial communities (Ravaglioli *et al.,* 2019; Yuan *et al.,* 2021; Lee *et al.,* 2022). Detritivores play an important role in the carbon cycle, consuming organic material, and altering O_2 dynamics by reworking the sediment (de Goeij *et al.,* 2013; Mazarrasa *et al.,* 2018; Thomson *et al.,* 2019). There is evidence that in response to OA, detritivores increase the consumption of labile and refractory OC to compensate for the adverse effects of OA (Ravaglioli *et al.,* 2019; Lee *et al.,* 2022). Whilst this may result in more carbon being buried within the sediment, with

consumption increasing the production of particulate organic matter which is subsequently buried within the sediments (Ravaglioli *et al.*, 2019), it may also result in a loss of OC from the system, with the consumed carbon respired into the water column, ultimately entering the atmosphere (Lee *et al.*, 2022).

OA may also affect carbon dynamics through changes to the microbial community. There is ample evidence that ocean acidification can affect microbial community composition, with some species more vulnerable to changes in pH than others (Liu *et al.*, 2010; Witt *et al.*, 2011; Nagelkerken and Connell, 2015; Malits *et al.*, 2021). The effects of this on OC can vary. As OA increases the amount of CO_2 available for photosynthesis, ecosystem primary productivity increases (Witt *et al.*, 2011; Yuan *et al.*, 2021). On one hand, this can result in more OC stores, with elevated primary productivity resulting in the production of more OC (Witt *et al.*, 2011). However, increased ecosystem productivity can result in the enhanced remineralisation of both labile and refractory carbon, with more carbon providing energy for bacterial consumption via bacterial priming (Trevathan-Tackett *et al.*, 2018; Ravaglioli *et al.*, 2020; Yuan *et al.*, 2021; Chen *et al.*, 2022).

5.1.4 Chapter aims

As rhodolith beds can store a large amount of OC, the effects of climate change on the system's ability to bury and store labile and refractory OC must be investigated. If the burial of OC is negatively impacted by elevated temperatures and OA then beds may bury less carbon in the future. Furthermore, if climate change results in the degradation of the current SOC stock, this could result in ancient carbon being reintroduced into the atmosphere as pCO_2 which would reduce the capacity of the system to act as a BC repository. In this chapter, labile and refractory litter was buried in rhodolith bed sediment, with sediment exposed to different temperatures and OA treatments. Using both litter types allowed for the effects of climate change to be investigated on fresh labile and refractory carbon newly buried in the BC system. The results allowed for inferences to be made of the stability of refractory carbon already locked away in the SOC stock to future climate change. O_2 fluxes were also measured to determine if changes to tea litter were a consequence of increased aerobic or anaerobic microbial activity within the sediments using total oxygen uptake (TOU; Glud 2008). O_2, dissolved inorganic carbon (DIC) and calcium carbonate ($CaCO_3$) fluxes were used to investigate climate-driven change to microbial activity within the sediment, with OC and IC production also quantified to measure changes to the rhodolith bed sediment under future climate conditions.

I hypothesised that in response to elevated temperature and pCO_2:

a) The decomposition of labile material (biodegradable) will decrease due to an increase in microbial activity in the rhodolith bed sediment.

b) The decomposition of refractory material (less biodegradable) will be unaffected, with the potential for the SOC to be preserved under future climate scenarios.

c) Net OC production by the sediment community will decrease, with more microbial activity within the sediment in response to warming.

d) Net IC production will decrease, with more dissolution of dead coralline algae and other shell fragments within the rhodolith bed sediment in response to lowered OA.

5.2 Methods

The TBI index (see Keuskamp *et al.,* 2013) was used as a proxy for carbon storage and burial with Lipton Green tea (EAN 87 10908 90359 5 or EAN 87 22700 05552 5) and Rooibos tea (EAN 87 22700 18843 8) used to represent labile and refractory carbon types respectively. Tea bags were buried both *in situ* and *in vitro*, with *in situ* measurements representing real-time carbon burial and storage and used to validate *in vitro* burial. Teabags were also buried *in vitro* to assess how OC burial and storage changed with global warming and OA.

5.2.1 *In situ* carbon burial and storage

Teabags were buried in a rhodolith bed at Loch Sween, Scotland (56°01.99' N, 05°36.13' W; tea buried 8cm depth into sediment). Teabag burial occurred during the summer (May-July) and winter (December-February) sampling campaigns and was left undisturbed for 92 days. During this time, a Tinytag (TG-4100) Temperature Data Logger was placed on the surface of the rhodolith bed to measure hourly water temperature. Upon retrieval, samples were dried at 35°C for 72 hours. Dry mass loss was measured for each tea bag, and tea material was milled into a powder with a 10mg subsample analysed for OC wt% (measurements carried out by the University of St Andrews using an Elementar EL Vario, following the methodology of Verardo *et al.,* (1990)). The stabilisation factor (S) and decomposition rate (k) were calculated using equations by Keuskamp and co-authors (2013), with S representing the amount of labile material not broken down, and k representing the rate at which labile and refractory material is broken down. The equations for S and K are given below in Eq. 4 and Eq. 5 respectively.

Eq. 4 $$S = 1 - \left(\frac{a_g}{H_g}\right)$$

Where a_g is the decomposable fraction and H_g is the hydrolysable fraction of green tea.

Eq. 5 $$k = log_e\left(\frac{a_r}{Wt-(1-a_r)}\right) / t$$

Where a_r is the decomposable fraction of rooibos tea, Wt is the weight of the substance after incubation time and t is time in days.

5.2.2 *In vitro* carbon burial and storage

Experiments were run over two seasons: Summer (2021) and Winter (2021-2022). Sediment cores were collected using scuba from a rhodolith bed alongside *in situ* tea burial. Samples were collected by coring 10cm of sediment in a clear Perspex drainpipe (diameter = 10cm, n= 40). Around 60-100g of coralline algae (*Lithothamnion glaciale*) was present on top of the sediment, with calcifying fauna (primarily the brittle stars *Ophiocomina nigra* and *Opiothix fragilis*) retained on top of the sediment so that each core represented an *in situ* rhodolith bed community as closely as possible. Cores were kept in an upright position and were then transported back to the mesocosm facility at the University of Glasgow.

Perspex pipes (here on defined as cores) were placed in large holding tanks (100 L; n= 5 per tank), with the tanks primarily used to maintain the internal water temperature of the cores. The cores were maintained at an ambient temperature (14°C in the summer, and 6°C in the winter; Attard *et al.,* 2015), with the light intensity and diel cycle within the range of that season (Summer: 12L:12D, light intensity = 7.35 mol m^{-2} d^{-1}; Winter: 8L:16D, light intensity = 1.08 mol m^{-2} d^{-1}; Attard *et al.,* 2015). Cores were bubbled constantly with ambient air (400ppm CO_2 as measured using a Licor CO_2 analyser), with conditions maintained for a week to allow the rhodolith cores to stabilise post-collection (Kamenos *et al.,* 2013).

After a week, conditions were gradually altered over 2 weeks to the following treatment combinations (n= 10 for each treatment):

- Ambient: Ambient pCO_2 (Bubbled gas composition = 400ppm CO_2) and temperature
- +T: Ambient pCO_2 (400ppm) and elevated temperature (+3°C)
- +CO2: Elevated pCO_2 (750ppm) and ambient temperature
- +T +CO2: Elevated pCO_2 (750ppm) and elevated temperature (+3°C)

An elevated pCO_2 of 750ppm and a temperature of +3°C were chosen as they are in the range of the most likely climate scenarios for the end of the century (Meinshausen *et al.,* 2011; Peters and Hausfather 2020; IPCC 2022).

The sediment cores were maintained at treatment conditions for 4 weeks with ~30% of the water refreshed twice weekly with water bubbled with the corresponding pCO_2 concentration and at the same temperature. The Perspex plastic of the cores was cleaned every 2-3 weeks to

remove any biofilm, with biofilm on the coralline algae and sediment left undisturbed. Background parameters (temperature, pH, salinity and dissolved oxygen (DO)%) were monitored using a YSI Pro Plus Quatro throughout the experiment.

For each treatment, 3 cores had green tea bags and 3 cores had rooibos tea bags buried within the sediment of the core. Two cores were left undisturbed, and 2 cores were disturbed in the same manner as adding the tea but with no tea bags inserted as a procedural control. Similarly to the teabags buried *in situ*, bags were buried at 8cm depth with dry mass loss, OC wt% loss, S and k calculated at the end of the 92 days.

Throughout the experiment, TOU was measured to validate that any changes to the tea were due to processes within the sediment, rather than surficial carbon remineralisation. TOU is used as a proxy of carbon remineralisation and is calculated using the below calculation (Glud 2008):

$$\text{Total oxygen uptake (TOU)} = \frac{\Delta O_2 \times v}{s \times \Delta t}$$

TOU was measured on days 1, 3, 7, 14, 30, 60 and 90 (Keuskamp *et al.,* 2013). To establish a baseline benthic oxygen uptake rate, 3 incubations were run before the tea was added. An average of these 3 values was taken for each core and included as a measurement on day 0.

5.2.3 Organic and inorganic carbon production

Before tea burial, OC and IC production were calculated for each sediment core. For OC production, O_2 and DIC fluxes were used, with an increase in O_2 of 1 mol, and a decrease in DIC of 1 mol, representing 1 mol of OC production (van der Heijden and Kamenos 2015). For IC production, $CaCO_3$ fluxes were used (using total alkalinity (TA)), with A_T decreasing by 2 moles for every 1 mol of $CaCO_3$ and IC precipitated (van der Heijden and Kamenos 2015).

O_2, DIC and $CaCO_3$ fluxes were calculated via *in vitro* incubations (n= 5 per treatment), with each incubation lasting approximately 2 hours. Both light and dark incubations were run so that net fluxes could be calculated, with cores left for 1 week between light and dark incubations as the diel cycle was adjusted. The light experiments were conducted at midday, whereas the dark experiments were carried out 1 hour after the light was turned off (sundown).

As this chapter was focussed on the response of rhodolith bed sediment to future climate conditions, coralline algae pieces were removed from the cores 1 week before incubations started so that only sediment was present.

Cores were incubated using a closed system so that no air could enter. Water was stirred constantly using a magnetic stirrer. Oxygen sensor spots (Manufacturer = PreSens; product code = SP-PSt3-NAU) were used to determine O_2 concentrations (using a Fibrox 3 PreSens monitoring system) at the start and end of the incubation. Water samples were also taken at the start and end of each incubation so that changes in DIC and A_T could be calculated. Samples were filtered using 1.6 µm filter paper before being placed in pre-acid washed exetainers and spiked with 0.06% saturated mercuric chloride solution. All samples were stored at 4°C until the analysis date.

A_T was measured on a Metrohm 848 Titrino Plus using the 2-stage open-cell potentiometric titration method on 12 ml sample volumes with 0.01 M HCl (Dickson *et al.,* 2007). Samples were kept at room temperature, which was measured and accounted for later in the TA calculations. Seawater Reference Materials (batches 189 and 196) were used as standards (supplied from Dickson's Laboratory, Scripps Institution of Oceanography). Two water samples were analysed for each measurement, with the average A_T value reported. The average instrument precision across the analysis period is 24 (µmol kg^{-1}).

DIC was determined using an Automated Infra-Red Inorganic Carbon Analyser (AIRICA) (Marianda, model number 21) fitted with a Licor 820. The Licor was calibrated immediately before the analysis period, with 400ppm and 1000ppm certified carbon dioxide gas (mixtures of CO_2 and N_2). On the AIRICA, 1ml of sample was reacted with approximately 60ul, 10% phosphoric acid. The evolved gas was dried using a NafionTM drier (Perma pure) before reaching the Licor. Peak areas were converted to a concentration of DIC using Seawater Reference Materials (batches 189 and 196) supplied from Dickson's Laboratory, Scripps Institution of Oceanography. Three repeated measurements were made per sample and an average of the last two measurements is the reported value of DIC. The average instrument precision across the analysis period is 26 (µmol kg^{-1}).

Additional carbonate chemistry parameters (pH_{NBS}, pCO_2, $[HCO_3^-]$, $[CO_3^{2-}]$, aragonite saturation state [Ω_{Arg}], calcite saturation state [Ω_{Cal}]) were calculated from A_T and C_T using the

seacarb package in RStudio (Gattuso *et al.,* 2022) with dissociation constants from Lueker *et al.,* (2000), and KSO4 using Dickson (1990).

O_2, DIC, and $CaCO_3$ fluxes were calculated via the below equations:

$$O_2\text{flux} = \frac{\Delta O_2 \times v}{s \times \Delta t}$$

$$\text{DIC flux} = \frac{\Delta DIC \times v}{s \times \Delta t} - G$$

$$CaCO_3 \text{ flux} = \frac{\Delta A_T \times v}{2 \times s \times \Delta t}$$

where ΔO_2 is the change in oxygen concentration (mmol/L), ΔDIC is the change in dissolved inorganic carbon (mmol/kg), ΔA_T is the change in TA (mmol/kg), v is volume (L), s is surface area (m^2), and t is time (hours), and G is net calcification. Net fluxes were calculated by multiplying light and dark hourly fluxes by the respective time the cores spent in light and dark conditions.

Light and dark fluxes of O_2 and DIC represent photosynthesis and respiration respectively, whilst net fluxes of O_2 and DIC represent net production. $CaCO_3$ fluxes represent calcification and dissolution.

An annual estimate of OC production was calculated by:

$$\begin{aligned} &Annual\ OC\ production \\ &\quad = (176\ days\ x\ Summer\ OC\ net\ production) \\ &\quad + (176\ days\ x\ Winter\ OC\ net\ production) \end{aligned}$$

5.2.4 Statistical Analysis

Data analysis was conducted using R version 4.1.1 in R Studio (Version 1.4.1717). For both the physiological measurements and tea bag measurements, tank had no significant random effect (using mixed models). Therefore, Kruskal Wallace tests and ANOVAs (analysis of variance) were used to investigate the effects of treatment, temperature, and CO_2 on the

physiological measurements. Data were checked for normality using a Shapiro-Wilk test, and, due to the small sample size, the heterogeneity of variance was checked using Levene's test. Kruskal Wallace tests and ANOVAs (analysis of variance) were used to investigate the effects of treatment, temperature, and CO_2 on the physiological measurements. As multiple hypotheses were tested with the same dataset, Holm's Sequential Bonferroni Procedure was used to detail family-wise error rates. The same procedure was used when exploring the difference in tea mass loss, k, S and OC wt% loss between treatments. When investigating correlations between DIC flux and O_2 flux, and OC wt% and mass loss, a Pearson's or Spearman's rank correlation test was used. Medians (IQR duration) were given for non-parametric data and mean (±standard deviation) was given for parametric data. All graphs were plotted using ggplot2.

5.3 Results

5.3.1 *In situ* carbon burial and storage

In the summer (May-July), the average bottom water temperature at Loch Sween was 13.34°C with a maximum of 17.94°C and a minimum of 8.62°C. The average water temperature was lower in the winter (December-February) at 7.89°C with a maximum of 10.17°C and a minimum of 6.20°C.

Green tea mass loss and OC loss varied significantly between seasons, with the mass loss being 10% higher in the summer, and OC wt% 84% higher in the winter. On the other hand, rooibos tea mass and OC wt% loss did not vary between seasons. The stability factor (S) was significantly higher in the winter, whilst, there was no significant difference in decomposition rate (k), with large variations within each season. Over both seasons mass loss was higher and OC wt% loss was lower for green tea than rooibos tea (Mass loss: $X^2(1)= 50.95$, $p<0.001$; OC wt% Loss: $F_{(1,51)}= 5.925$, $R^2 = 8.65\%$, $p<0.05$). (Figure 5.1, Table 5.1)

Table 5.1: Summary statistics and results from ANOVA and Kruskal tests for differences in green and rooibos tea mass loss (%) and OC loss (wt%) and decomposition rate (k) and Stability factor (S) between the summer and winter sampling campaigns. Values are given as mean±sd. Significant values (p<0.05) are highlighted in bold.

	Season		
	Summer	Winter	Summary Statistics
Green Tea			
Mass Loss (%)	64.3±4.71	58.8±4.79	**$F_{(1,34)}= 11.75$, $p<0.01$**
OC Loss (wt%)	10.0±7.43	18.4±4.84	**$F_{(1,24)}= 15.6$, $p<0.01$**
Rooibos Tea			
Mass Loss (%)	10.8±5.15	14.0±12.3	$F_{(1,35)}= 0.120$, $p= 0.731$
OC Loss (wt%)	17.2±6.26	15.9±4.73	$F_{(1,25)}= 0.322$, $p= 0.576$
k	0.003±0.002	0.004±0.001	$F_{(1,36)}= 1.839$, $p= 0.183$
S	0.24±0.06	0.35±0.1	**$F_{(1,32)}= 20.46$, $p<0.01$**

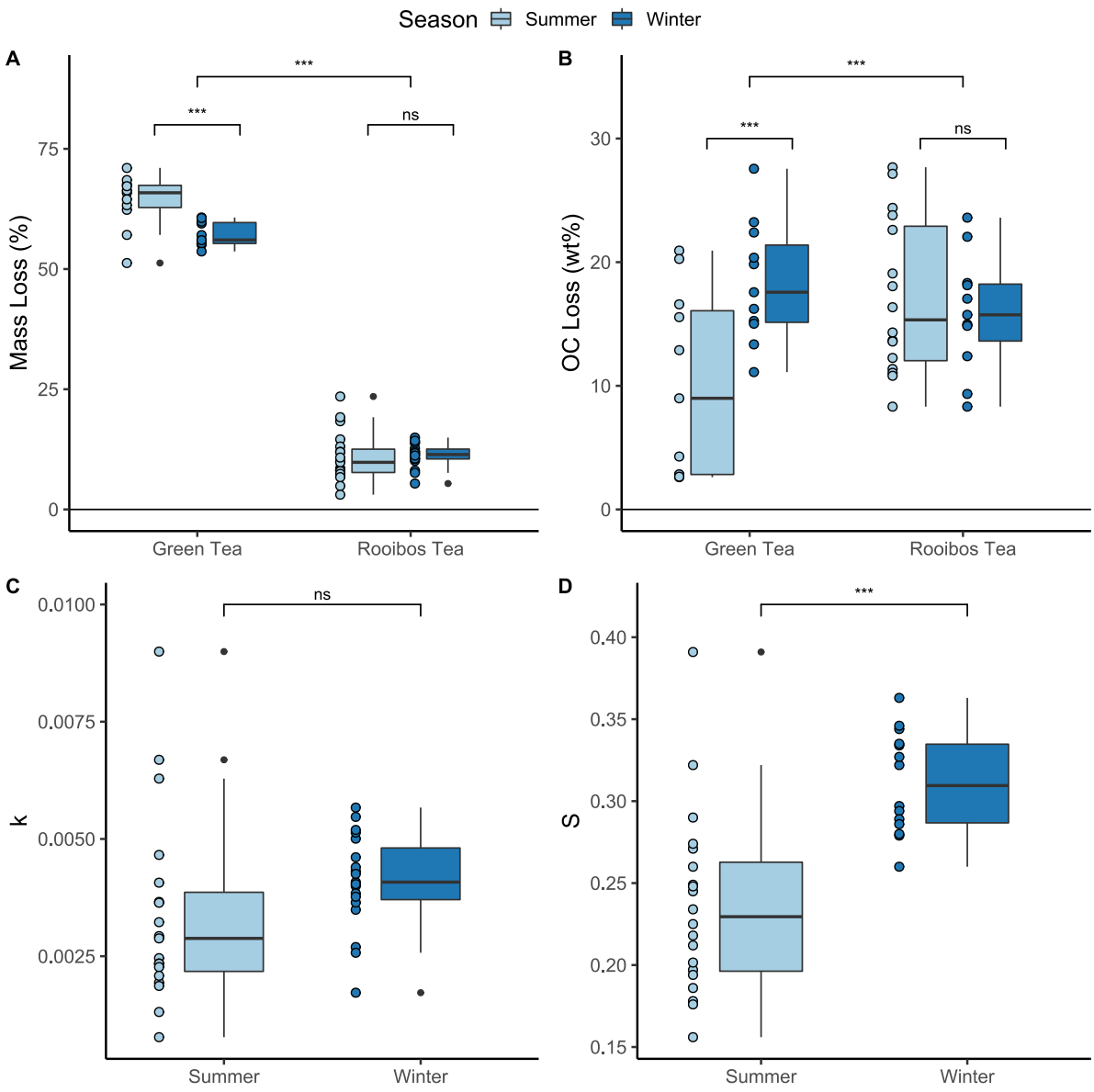

Figure 5.1: A) mass loss (%) for green and rooibos tea B) OC wt% loss for green and rooibos tea C) k (decomposition rate) and D) S (stability factor), for *in situ* summer and winter field campaigns. Each box represents the median and IQR, with points to the left of each box representing the raw data. Significance bars are placed on each plot to show if parameters vary with season. Mass loss and OC wt% loss are also compared between tea types. * = significant result (<0.05), ns = non-significant result (>0.05).**

5.3.2 *In vitro* carbon burial and storage

5.3.2.1 Environmental Parameters

The average temperature, salinity, and DO% are shown in Table 5.2. The average summer temperature was 7°C higher than the winter. For both summer and winter experiments, the average temperature was higher for the +T treatments (Summer = $X^2(1) = 18.984$, $p<0.001$; Winter = $X^2(1) = 16.68$, $p<0.001$) and did not vary within temperature treatments ($p>0.05$). Salinity and DO% did not vary between treatments for either summer or winter experiments ($p>0.05$). Water chemistry parameters are also summarised in Table 5.2.

Table 5.2: Environmental parameters under ambient (T CO2), elevated temperature (T+ CO2), elevated CO_2 (T CO2+), and elevated temperature with elevated CO_2 (T+ CO2+). Values are given for both light and dark, with samples taken before incubations commenced. Water temperature, salinity, dissolved oxygen (DO), total alkalinity (A_T) and dissolved inorganic carbon (C_T) were all directly measured. All other parameters were calculated with dissociation constants from Lueker *et al.,* (2000), and KSO4 using Dickson (1990). Carbonate parameters are pH (Ph_{NBS}), pCO_2, HCO_3^-, CO_3^{2-}, aragonite saturation state (Ω_{Arg}), and calcite saturation state (Ω_{Cal}). Data presented are mean±sd, with n = 5 for each treatment (n= 10 when averaged across light and dark incubations).

	Ambient		+T		+CO2		+T +CO2	
	Dark	Light	Dark	Light	Dark	Light	Dark	Light
Summer								
Temperature (°C)	13.58±0.32		16.50±0.21		13.53±0.24		16.48±0.19	
Salinity	34.64±2.24		34.68±2.26		35.10±2.09		35.47±2.25	
DO (%)	98.99±1.86		96.89±3.42		98.46±1.39		96.48±2.33	
A_T (µmol kg-1)	1868.8±273.7	1979.2±150	1971.6±247.9	1895±136.4	1556.1±316.9	1880.4±489.4	2064.2±304.8	1692.6±237.6
C_T (µmol kg-1)	1683.7±203.7	1836.1±137.5	1775.1±172	1754.7±121.5	1495.8±324.2	1820.1±441.5	1984.8±181.8	1766.6±193.3
pH_{NBS}	8.01±0.14	7.93±0.02	7.98±0.18	7.87±0.27	7.67±0.26	7.64±0.19	7.6±0.53	7.12±0.18
pCO_2 (µatm)	348.9±96.2	461±32.8	414.2±153.3	607.5±404.1	846±667.7	908.3±243	1854.8±2306.1	2951.3±857.2
HCO_3^- (µmol kg-1)	1545.2±157.8	1713.9±126.4	1623.7±129.9	1628.6±133	1410.9±308.4	1723.9±412.8	1823.7±132.1	1642.7±213.7
CO_3^{2-} (µmol kg-1)	125.2±49.7	104.6±12.8	136.8±57.9	104.3±47	53.1±24.7	61.3±35.3	96.6±85.4	19.1±9.7
ΩArg	1.91±0.75	1.62±0.19	2.1±0.89	1.62±0.73	0.81±0.38	0.94±0.53	1.49±1.32	0.29±0.15
ΩCal	2.97±1.17	2.53±0.29	3.26±1.38	2.52±1.15	1.26±0.59	1.47±0.83	2.3±2.04	0.46±0.23
Winter								
Temperature (°C)	6.41±0.43		9.34±0.37		6.41±0.45		9.33±0.43	
Salinity	35.80±2.06		35.97±0.87		36.26±1.58		36.64±0.97	
DO (%)	99.73±3.38		99.43±2.89		98.15±6.23		98.92±2.94	
A_T (µmol kg-1)	2480.9±40.1	2330.6±406.3	2604±452.4	2213.4±380.7	2724.9±509.3	2373.3±419.8	2810.6±472.2	2549.5±439.8
C_T (µmol kg-1)	2284.6±57.6	2180.4±360.4	2431.5±317.6	2068±314.3	2584.9±431.6	2266.9±365.2	2660.5±413.9	2453.8±416.8
pH_{NBS}	8.07±0.03	7.96±0.1	7.93±0.3	7.95±0.13	7.89±0.11	7.83±0.11	7.91±0.08	7.81±0.07
pCO_2 (µatm)	390.3±35.3	492.4±87.1	651.9±425.1	481.3±92.2	682.3±71.1	684.6±118.5	668.7±57.8	797.6±192.3
HCO_3^- (µmol kg-1)	2120.6±66.6	2042.1±324.8	2258.7±243.4	1935.1±268.8	2431.9±377.4	2141.8±327.3	2501.7±368.6	2326.3±389
CO_3^{2-} (µmol kg-1)	145.6±12.3	115.8±39.5	142.5±96.8	111±52.5	121.2±59.3	93.2±45.2	128.1±49.3	90.8±29
ΩArg	2.19±0.19	1.75±0.59	2.14±1.46	1.68±0.79	1.82±0.89	1.4±0.68	1.92±0.74	1.37±0.44
ΩCal	3.46±0.29	2.75±0.93	3.37±2.29	2.64±1.24	2.86±1.39	2.2±1.07	3.02±1.15	2.15±0.69

5.3.2.2 Total Oxygen Uptake (TOU) measurements

For both the summer and winter experiments, there was no significant difference in TOU for any of the tea types during any of the treatments ($p>0.05$; Figure 5.2, Figure 5.3).

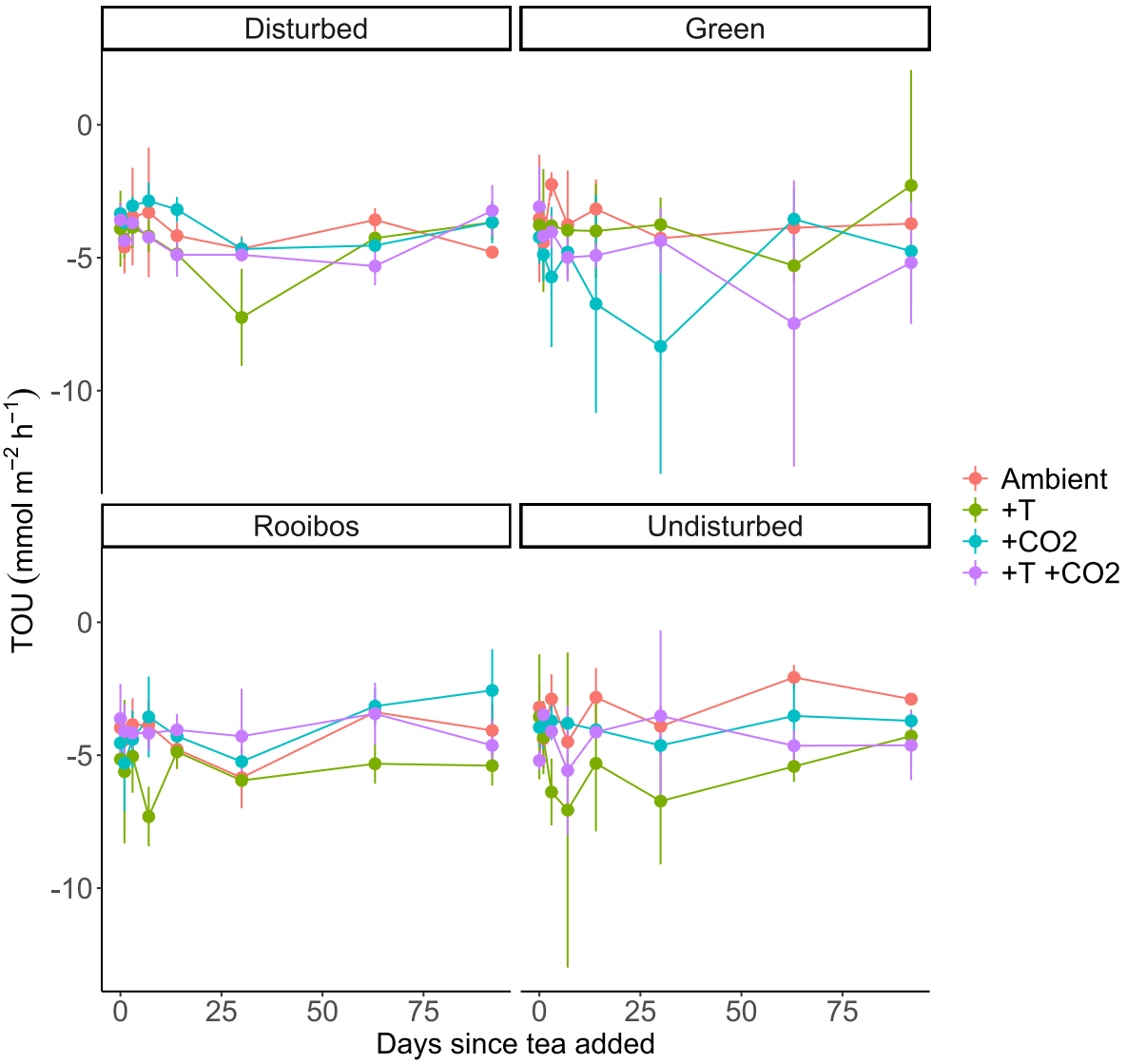

Figure 5.2: Summer experiments, showing total oxygen uptake measurements against days since tea was added. Treatments are ambient, elevated temperature (+T), elevated CO_2 (+CO2), and elevated temperature and CO_2 (+T +CO2). For each treatment, tea types are Green tea, Rooibos tea, disturbed (sediment was disturbed in a similar manner to adding tea) and undisturbed (sediment was undisturbed). Points represent means and vertical lines represent sd. n = 3 for each time point.

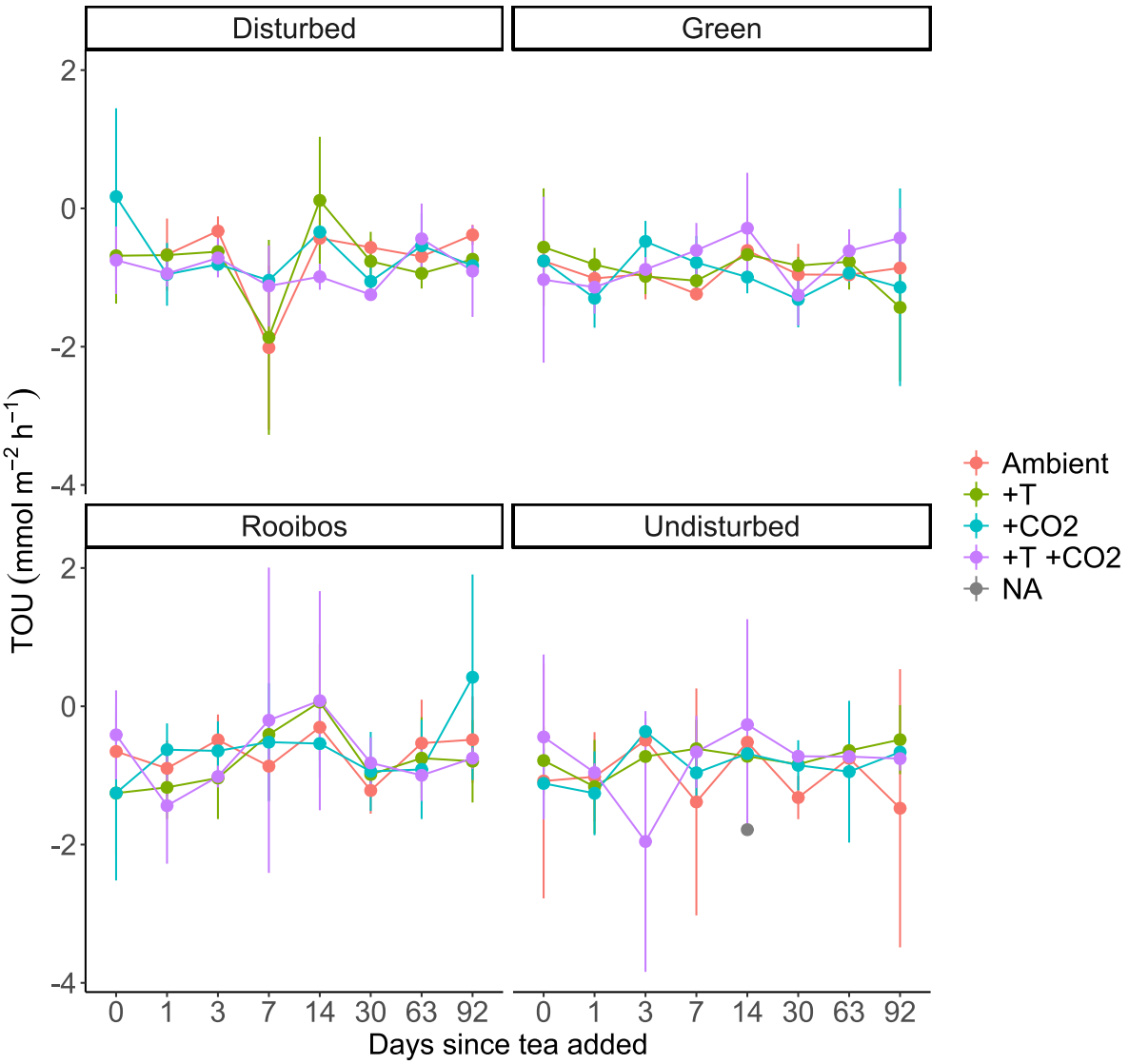

Figure 5.3: Winter experiments, showing total oxygen uptake measurements against days since tea was added. Treatments are ambient, elevated temperature (+T), elevated CO_2 (+CO2), and elevated temperature and CO_2 (+T +CO2). For each treatment, tea types are Green tea, Rooibos tea, disturbed (sediment was disturbed in a similar manner to adding tea) and undisturbed (sediment was undisturbed). Points represent means and vertical lines represent sd. n = 3 for each time point.

5.3.2.3 Effects of temperature and pCO_2 on organic material mass

In the summer, green tea mass loss significantly varied with treatment (Figure 5.4), with mass loss lower under ambient conditions compared to +T and +T +CO2 treatments (Tukey HSD $p<0.05$ for those comparisons; Table 5.3, Figure 5.4). Conversely, green tea OC wt% loss was significantly higher at ambient temperatures (13.2±10.3%) compared to elevated temperatures (0.3±6.7%; Table 5.3, Figure 5.4). Rooibos tea mass loss and OC wt% loss did not significantly vary between treatments, with an average mass loss of 22.2±0.9% and an average OC wt% loss of 6.8±10.5% for all lab treatments (Figure 5.4).

In the winter, green tea mass loss was on average 5% higher at elevated temperatures with an average mass loss of 45.5±1.20% at ambient temperature conditions, and 50.7±2.8% at elevated temperature conditions (Table 5.3, Figure 5.4). On the other hand, OC wt% loss did not vary with treatment, with an average OC wt% loss of 13.3±4.9%, (Table 5.3, Figure 5.4). Rooibos tea mass loss and OC wt% loss did not significantly vary between treatments (Table 5.3) with an average mass loss of 12.1±4.2% and an OC wt% loss of 11.3±2.6%. (Figure 5.4).

Green tea and rooibos tea mass loss, and green tea OC wt% loss were significantly lower in the winter than in the summer (Table 5.3). There was no difference in rooibos tea OC wt% loss between seasons (Table 5.3).

OC% and mass loss were not correlated for either the green tea or rooibos tea types during the summer and winter experiments (Figure 5.5; $p>0.05$ for all comparisons).

Table 5.3: Summary of statistical analysis (ANOVA) testing the effects of treatment on tea mass loss and OC wt% loss in summer and winter experiments, and differences between seasons. Significant results are highlighted in bold.

	Green Tea				Rooibos Tea			
	Mass Loss		OC wt% Loss		Mass Loss		OC wt% Loss	
	F	***p***	***F***	***p***	***F***	***p***	***F***	***p***
Summer								
T	**3.785**	**<0.01**	**6.423**	**0.044**	-0.432	0.679	-1.319	0.229
pCO_2	**2.986**	**0.020**	0.314	0.596	-0.263	0.876	-1.175	0.278
T* pCO_2	**-2.279**	**0.025**	2.422	0.171	1.22	0.299	1.323	0.227
Winter								
T	**2.935**	**0.019**	2.426	0.158	0.591	0.573	-1.658	0.141
pCO_2	0.406	0.696	0.920	0.366	-1.021	0.341	-0.678	0.519
T* pCO_2	-0.351	0.735	1.833	0.213	-0.05	0.934	1.677	0.137
Season	**86.71**	**<0.001**	**5.55**	**0.030**	**59.58**	**<0.001**	1.86	0.188

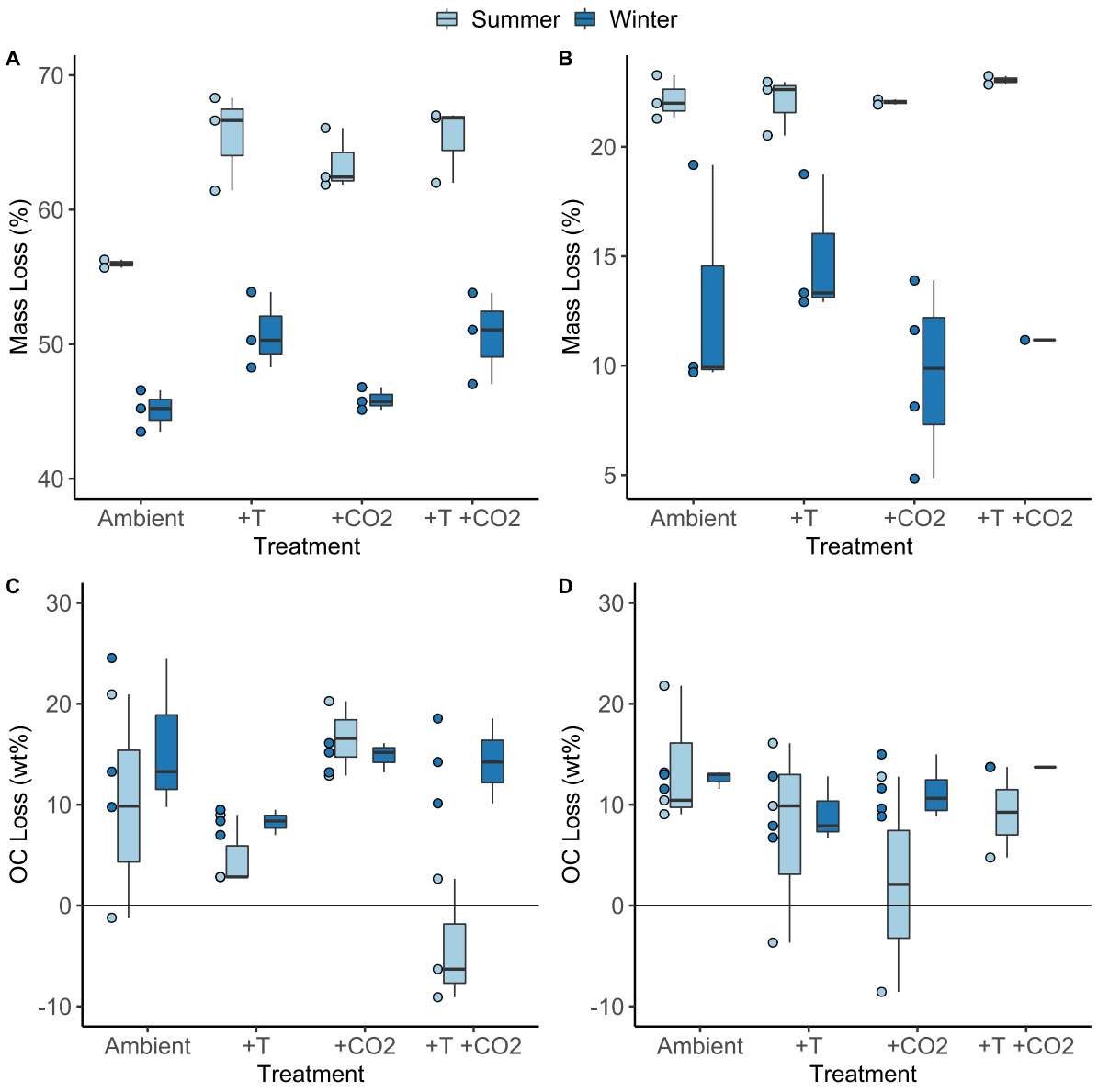

Figure 5.4: A) Green Tea mass loss, B) Rooibos Tea mass loss, C) Green Tea OC wt% Loss, D) Rooibos Tea OC wt% Loss for summer (light blue) and winter (dark blue) experiments. Treatments are ambient (Ambient), elevated temperature (+T), elevated CO_2 (+CO2), and elevated temperature and CO_2 (+T +CO2). Data represents medians, IQR, and minimum and maximum values. Points to the left of the boxes represent raw data.

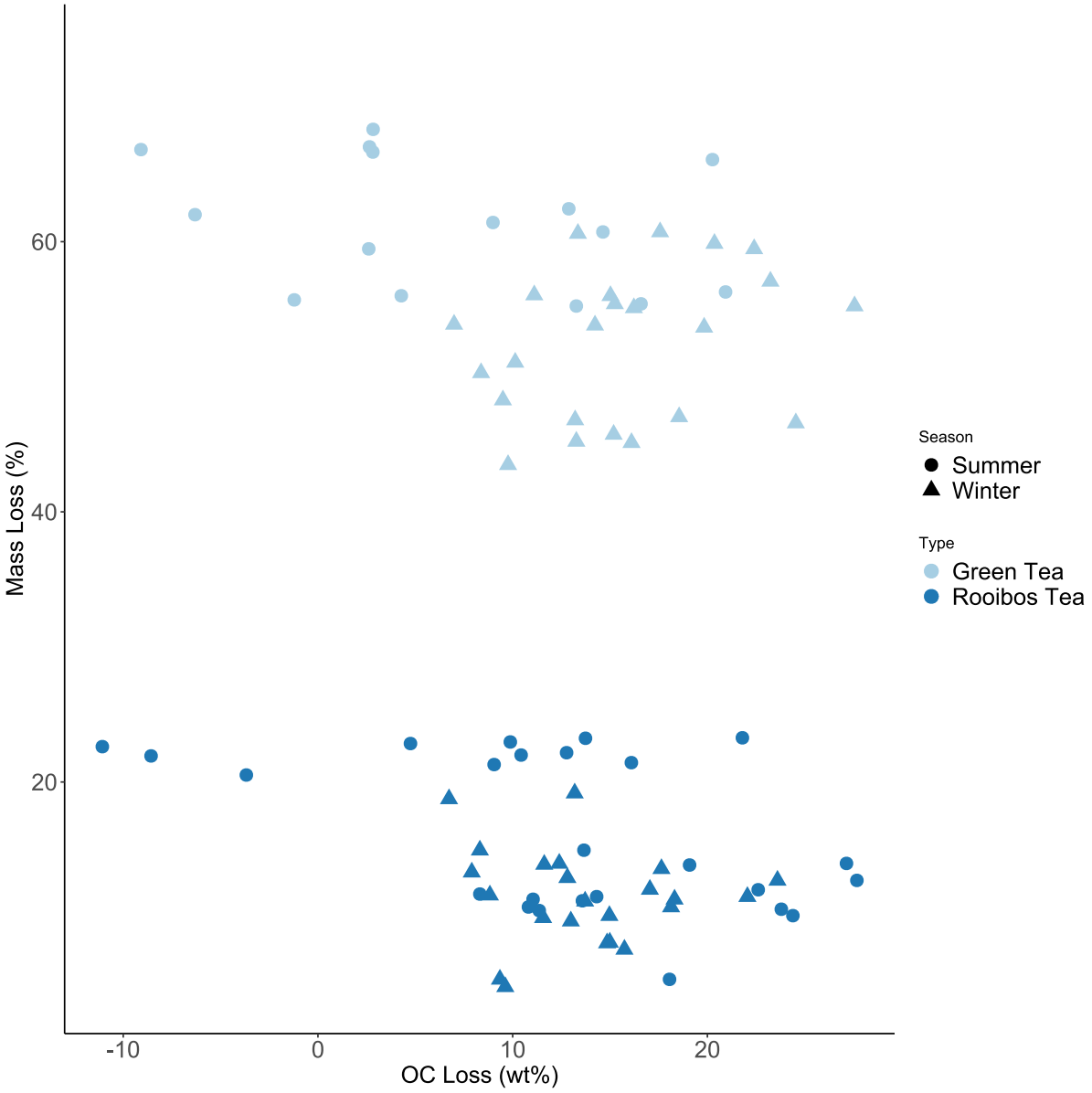

Figure 5.5: OC loss (wt%) vs Mass Loss for summer and winter experiments. Green points represent green tea and red points represent rooibos tea.

5.3.2.4 Effects of temperature and pCO_2 on sediment decomposition rate (k) and stability factor (S)

In the summer, k was higher under ambient conditions (0.010±0.0007) than at elevated temperatures (0.08±0.006; Table 5.4, Figure 5.6). k was significantly lower in the winter, compared to the summer, and did not vary significantly between the lab treatments in the winter with an average decomposition rate of 0.006±0.003 (Table 5.4, Figure 5.6).

S was significantly lower with elevated temperatures for both summer (0.22±0.03 vs 0.28±0.05) and winter experiments (0.40±0.03 vs 0.46±0.14; Table 5.4, Figure 5.6). In the summer, S also varied with CO_2, with S higher in the ambient CO_2 treatment group (0.34±0.005; Table 5.4, Figure 5.6). Across all treatments, S was significantly lower in the summer experimental campaign (Table 5.4, Figure 5.6).

Table 5.4: Summary of statistical analysis (ANOVA) testing the effects of treatment on k (decomposition rate) and S (stability factor) in summer and winter experiments, and differences between seasons. *Tukey Post Hoc test showed no differences between treatment groups, however, the Post Hoc test is sensitive to the small sample size. When the smallest p-value for the Post Hoc test was between the ambient treatment and +T treatment (p= 0.059), the difference between these treatment groups is considered significant. Significant results are highlighted in bold.

	k		S	
	F	***p***	***F***	***p***
Summer				
T	0.150	0.709	**-3.767**	**<0.001**
pCO_2	2.642	0.143	**-2.985**	**0.030**
T* pCO_2	**7.499**	**0.026***	2.267	0.057
Winter				
T	0.334	0.581	**-2.937**	**0.019**
pCO_2	2.289	0.174	-0.418	0.687
T* pCO_2	0.290	0.607	0.356	0.731
Season	**7.495**	**0.012**	**9.295**	**<0.001**

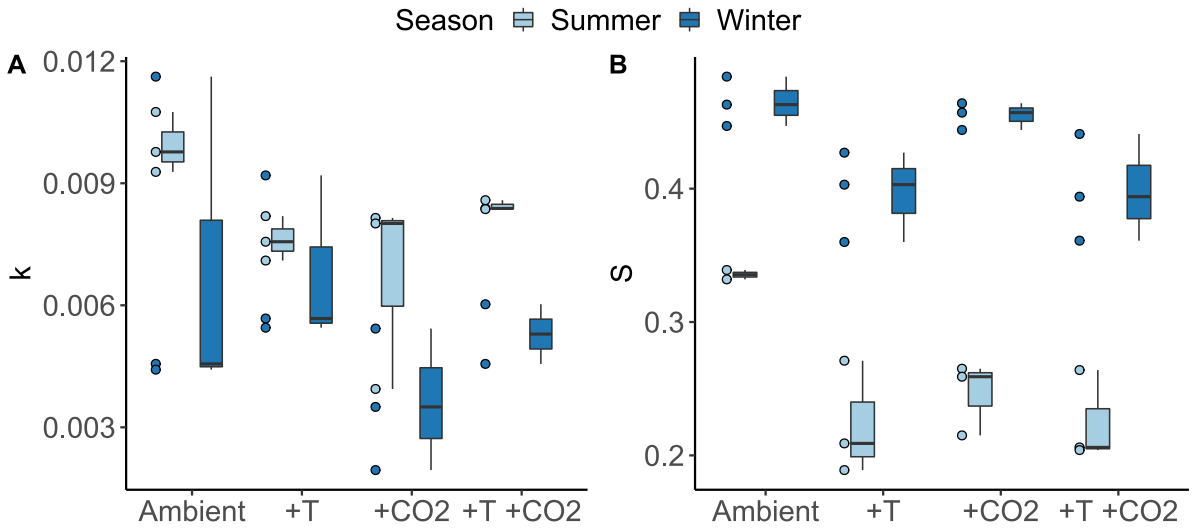

Figure 5.6: k (decomposition rate) and S (stability factor) for summer and winter experiments. Treatments are ambient (T CO2), elevated temperature (T+ CO2), elevated pCO_2 (T CO2+), and elevated temperature and CO2 (T+ CO2+). Data represents medians, IQR, and minimum and maximum values. Points to the left of the boxes represent raw data.

5.3.2.5 Comparisons between *in situ* and *in vitro* carbon burial and storage

For some parameters, *in vitro* measurements for the ambient treatments were not similar to *in situ* measurements. Whilst mass loss for rooibos teabags was similar between lab and field experiments in the winter, it differed for green and rooibos tea bags in the summer and green tea bags in the winter, with rooibos tea losing more mass and green tea losing less mass under ambient *in vitro* conditions. S was significantly lower *in situ* during both sampling periods, as was k in the summer, but not the winter. OC wt% loss was not significantly different between the lab and field experiments for both tea types in the summer and winter. (Table 5.5)

Table 5.5: Summary statistics and results from ANOVA and Kruskal tests for differences in green and rooibos tea mass loss (%), OC loss (wt%), and k (decomposition rate) and S (stability factor) between the field and lab (ambient treatment) during summer and winter sampling campaigns. ANOVA tests are referred to using F-value, whilst Kruskal Wallace is referred to using the X^2 value. Significant results are highlighted in bold.

	Summer	Winter
Green Tea		
Mass Loss (%)	**$F_{(1,20)}$= -2.442, p= 0.024**	**$F_{(1,17)}$= 23.26, p<0.001**
OC Loss (wt%)	$F_{(1,14)}$= 0.659, p= 0.431	$F_{(1,12)}$= 0.500, p= 0.494
Rooibos Tea		
Mass Loss (%)	**$X^2(1)$ = 5.95, p= 0.015**	$X^2(1)$ = 2.43, p= 0.119
OC Loss (wt%)	$F_{(1,17)}$= 0.721, p= 0.408	$F_{(1,11)}$= 1.079, p= 0.321
k	**$X^2(1)$ = 7.43, p<0.01**	$X^2(1)$ = 2.492, p= 0.144
S	**$F_{(1,20)}$= 6.02, p= 0.023**	**$X^2(1)$ = 5.34, p= 0.021**

5.3.3 Rhodolith bed sediment metabolism

In the summer, dark incubations showed that the sediment was net heterotrophic (-2.52±1.33 O_2 mmol m^{-2} h^{-1} across all treatments), light incubations showed net autotrophy (1.53±2.47 O_2 mmol m^{-2} h^{-1} across all treatments). In the summer, both light and net O_2 flux was higher under elevated temperature, with net heterotrophy experienced at ambient temperatures (-3.16±31.6 O_2 mmol m^{-2} d^{-1}), and net autotrophy experienced at elevated temperatures (26.2±28.4 O_2 mmol m^{-2} d^{-1}). (Figure 5.7, Table 5.6)

In the winter experiments, light O_2 flux varied with treatment, with the +T group having the highest O_2 flux. O_2 production was lower in the winter, with both light and dark O_2 generally showing net heterotrophy. Winter dark and net O_2 flux did not vary with treatment, with a negative median daily flux of -25.5 (IQR = 12.0) O_2 mmol m^{-2} d^{-1}, suggesting that the sediment was net heterotrophic. (Figure 5.7, Table 5.6)

The results show that at ambient temperatures, annual OC production is -4.93 mol of OC m^{-2} yr^{-1}, whilst at elevated temperatures, annual OC production is 0.24 mol of OC m^{-2} yr^{-1}.

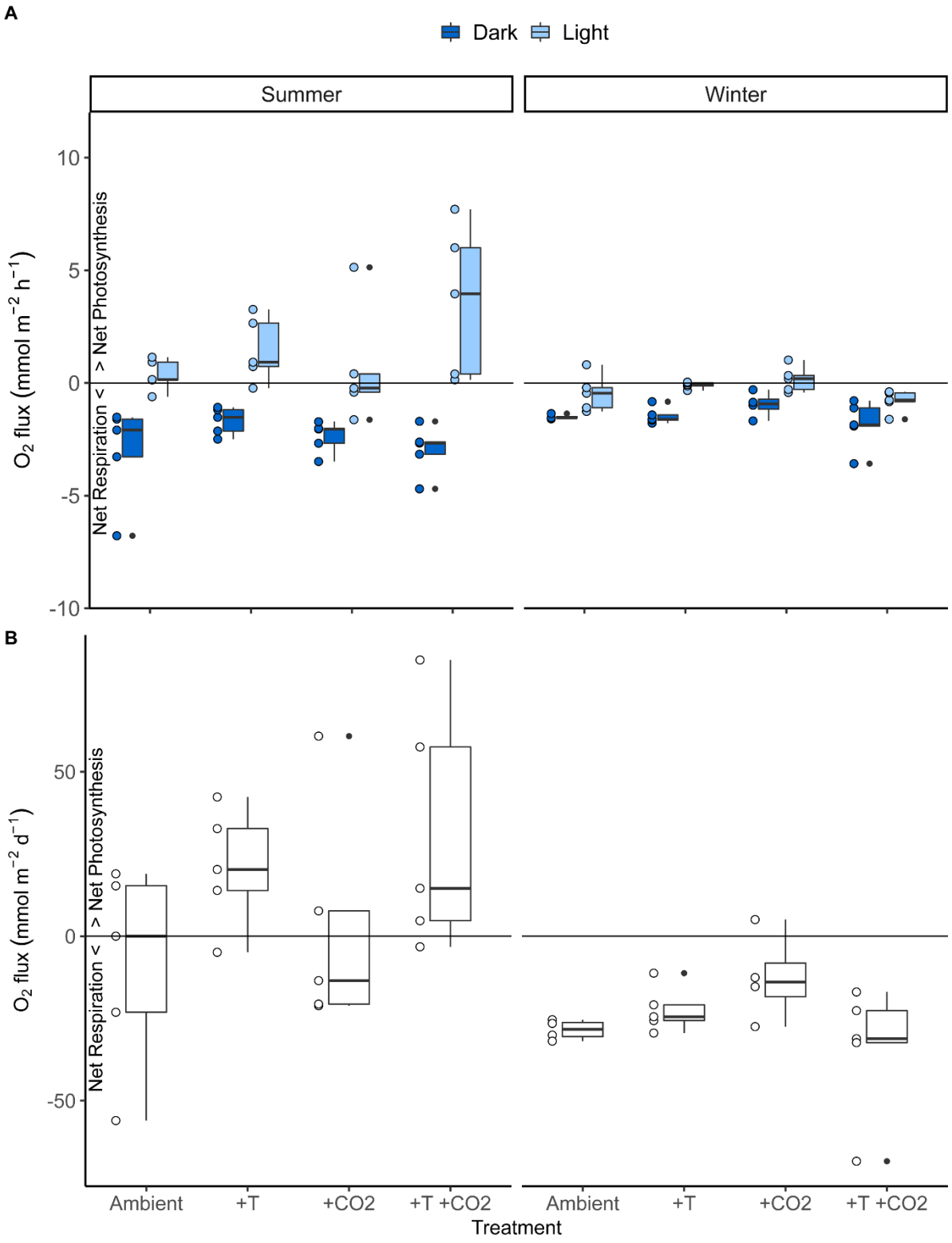

Figure 5.7: a) light (NDP) and dark (R) and b) net O_2 flux for rhodolith bed sediment for both summer and winter experiments. Treatments are ambient conditions, elevated temperature (+T), elevated CO_2 (+CO2), and elevated temperature with elevated CO_2 (+T +CO2). Points to the left of the bar charts correspond to raw data. Boxplot bars represent median and interquartile ranges, and whiskers represent minimum and maximum values.

Table 5.6: Summary of statistical analysis (ANOVA and Kruskal Wallace test results) testing the effects of treatment on O_2 fluxes (light, dark and net) in rhodolith bed sediment for summer and winter experiments, and differences between seasons. n= 20 for summer and winter experiments. X^2 refers to chi-squared, indicating that a Kruskal-Wallace test was used as the data was non-parametric.

	Light O_2 Flux		**Dark O_2 Flux**		**Net O_2 Flux**	
	F	***p***	***F***	***p***	***F***	***p***
Summer						
T	**X^2 = 3.86**	**0.049**	X^2 = 0.28	0.597	**4.781**	**0.042**
pCO_2	X^2 = 0.05	0.820	X^2 = 2.29	0.131	0.636	0.564
T x *p*CO_2	X^2 = 4.49	0.214	X^2 = 4.42	0.220	0.001	0.057
Winter						
T	1.553	0.231	X^2 = 1.78	0.183	X^2 = 0.28	0.594
pCO_2	0.041	0.843	X^2 = 0.05	0.825	X^2 = 0.10	0.757
T x *p*CO_2	**6.853**	**0.020**	X^2 = 2.74	0.433	X^2 = 6.09	0.107
Season	X^2 = 9.68	**<0.001**	X^2 = 10.16	**<0.001**	X^2 = 16.27	**<0.001**

Contrary to O_2 flux data, light DIC flux significantly varied with CO_2 in the summer, with elevated CO_2 treatments having a positive DIC flux (4.09±5.13 DIC mmol m^2 h^{-1}), and ambient CO_2 treatments, a negative flux (-4.09±6.92 DIC mmol m^2 h^{-1}). On the other hand, both dark and net DIC flux was not found to vary between treatments ($p>0.05$), with both fluxes negative. (Figure 5.8, Table 5.7)

Light, dark and net DIC flux did not vary significantly between treatments for the winter experiments ($p>0.05$). Whilst the average DIC flux for the light incubations was negative (-9.89±6.30 DIC mmol m^2 h^{-1}), it was positive for the dark incubations (0.47±7.81 DIC mmol m^2 h^{-1}), suggesting that OC was produced in the light. The average net flux was negative across all treatments with an average of -71.3±58.4 DIC mmol m^2 d^{-1}. (Figure 5.8, Table 5.7)

Annual OC production was 14.9 mol m^{-2} yr^{-1}, with no difference in production between temperature or CO_2 treatments.

DIC flux and O_2 were not found to be correlated for either the light and dark incubations during the Summer and Winter experiments (Figure 5.9; $p>0.05$ for all comparisons).

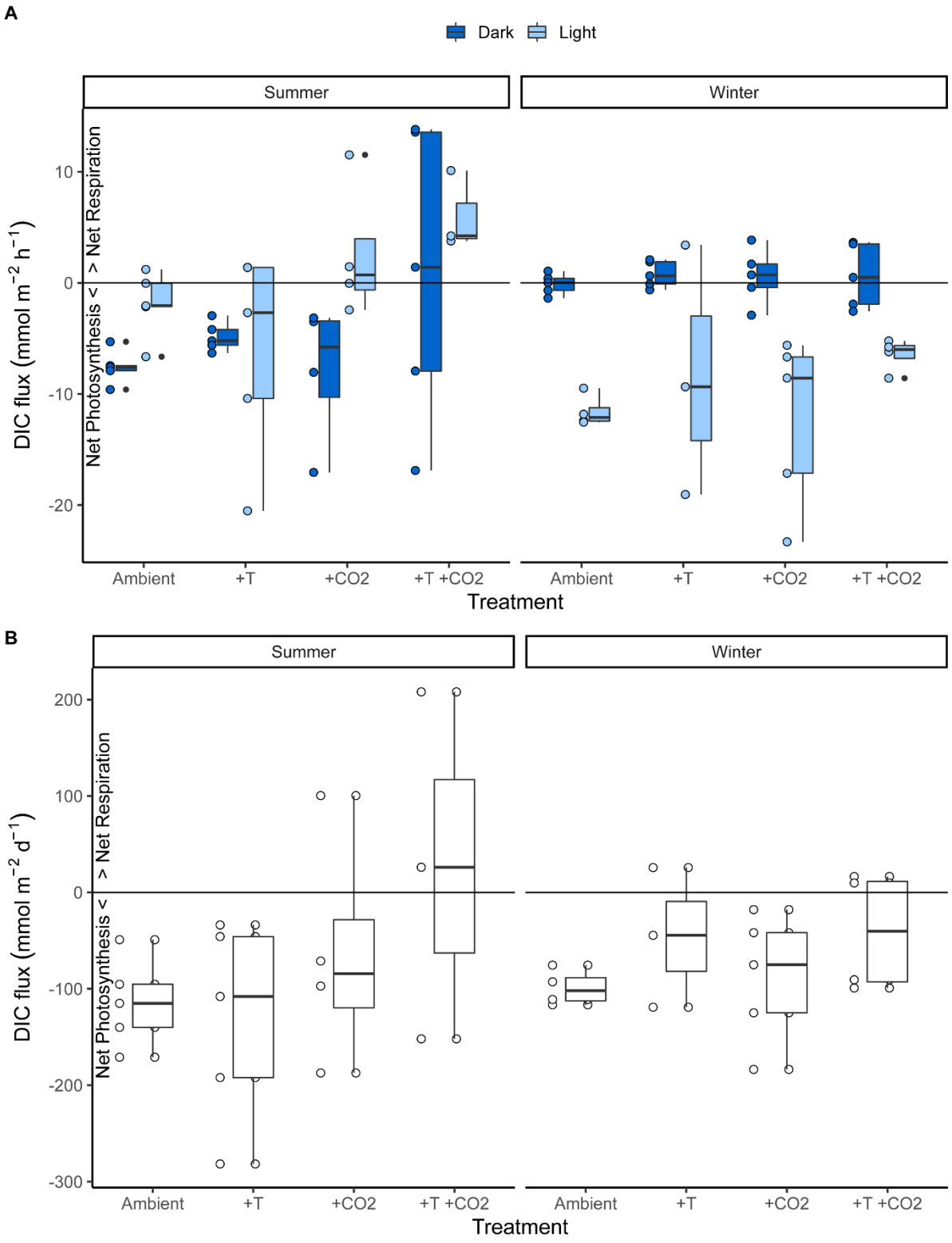

Figure 5.8: A) light and dark and B) DIC fluxes for rhodolith bed sediment for both summer and winter experiments. Treatments are ambient conditions, elevated temperature (+T), elevated CO_2 (+CO2), and elevated temperature with elevated CO_2 (+T +CO2). Points to the left of the bar charts correspond to raw data. Boxplot bars represent median and interquartile ranges, and whiskers represent minimum and maximum values.

Table 5.7: Summary of statistical analysis (ANOVA and Kruskal Wallace test results) testing the effects of treatment on DIC fluxes (light, dark and net) in rhodolith bed sediment for summer and winter experiments, and differences between seasons. n= 20 for summer and winter experiments. X^2 refers to chi-squared, indicating that a Kruskal-Wallace test was used as the data was non-parametric.

	Light DIC Flux		**Dark DIC Flux**		**Net DIC Flux**	
	F	***p***	***F***	***p***	***F***	***p***
Summer						
T	-0.460	0.652	$X^2 = 2.94$	0.087	0.236	0.095
pCO_2	2.635	0.019	$X^2 = 0.16$	0.683	3.236	0.635
T x pCO_2	**2.787**	**0.083**	$X^2 = 3.10$	0.376	0.987	0.339
Winter						
T	0.655	0.252	0.682	0.505	0.090	0.769
pCO_2	-0.160	0.875	0.536	0.599	2.889	0.115
T x pCO_2	0.393	0.701	-0.458	0.653	0.008	0.931
Season	$X^2 = 14.83$	**<0.001**	$X^2 = 14.60$	**<0.001**	0.123	0.728

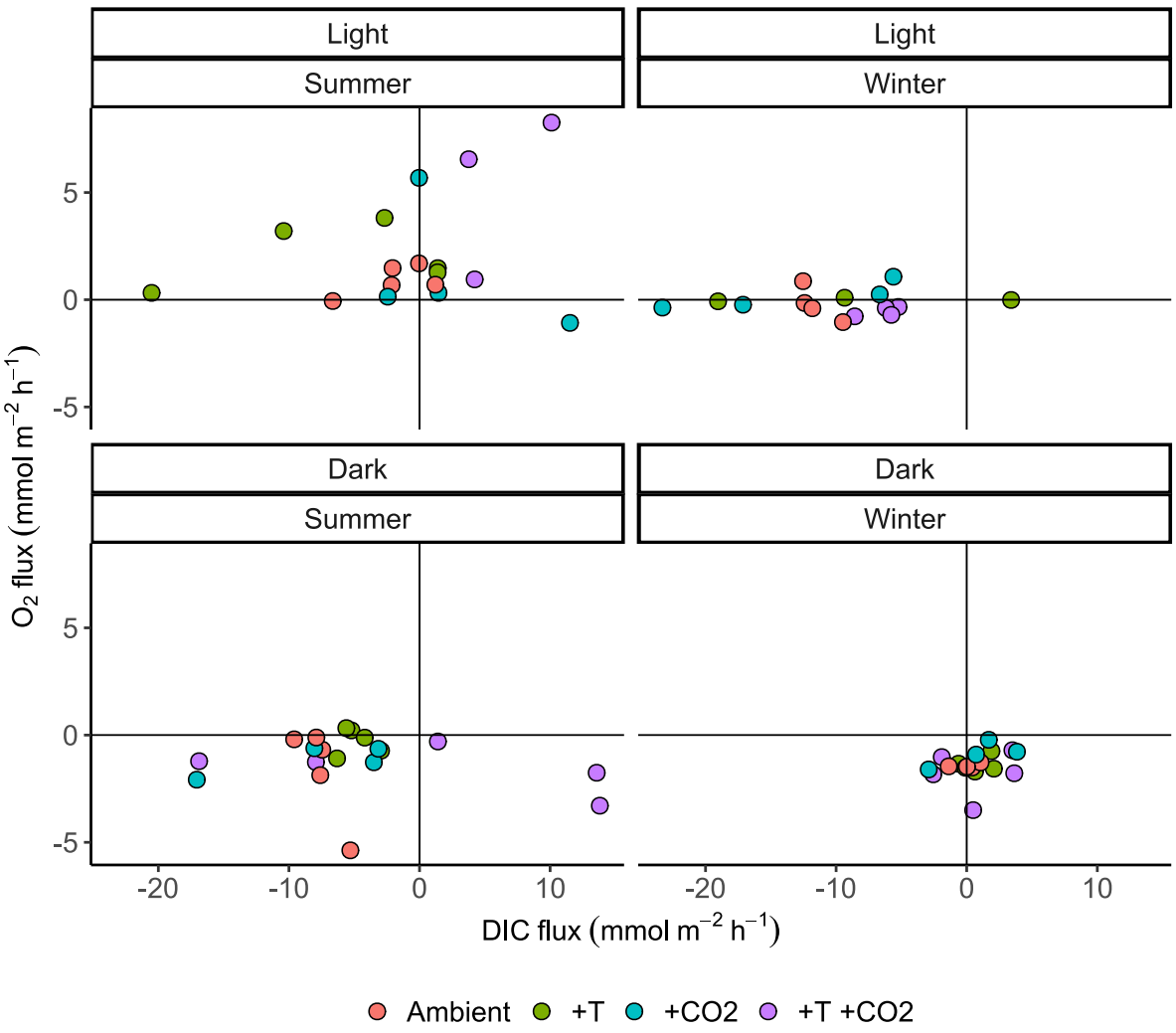

Figure 5.9: O_2 flux vs DIC flux for the rhodolith bed sediment. Data is separated for light and dark incubations for summer and winter experiments. Treatments are ambient, elevated temperature (+T), elevated CO_2 (+CO2), and elevated temperature and CO_2 (+T +CO2). For O_2 fluxes, a negative flux corresponds to net respiration and a positive flux corresponds to net photosynthesis. This is the reverse for DIC data, with a positive flux corresponding to net respiration and a negative flux corresponding to net photosynthesis. DIC fluxes can be influenced by other processes including methanogenesis.

In the summer, light and dark $CaCO_3$ flux did not significantly vary with treatment, with a net dissolution for both incubations (Figure 5.10Median light flux = -0.786 (IQR = 1.67) $CaCO_3$ mmol m^2 h^{-1}; Median dark flux =-2.60 (IQR = 2.12) $CaCO_3$ mmol m^2 h^{-1}). Net flux also did not vary with treatment with a net medium dissolution of -50.2 (IQR = 103.0) $CaCO_3$ mmol m^2 d^{-1} across all treatments. (Figure 5.10, Table 5.8)

Dark $CaCO_3$ flux was higher in the winter, with net dissolution observed for both light and dark incubations (Median light flux = -0.563 (IQR = 0.78) $CaCO_3$ mmol m^2 h^{-1}; Median dark flux = -0.39 (IQR = 0.52) $CaCO_3$ mmol m^2 h^{-1}) and did not vary between treatments. Whilst winter net flux was significantly higher than the summer, there was no difference between treatments, with the cores experiencing a net medium dissolution of -10.7 (IQR = 14.1) $CaCO_3$ mmol m^2 d^{-1}. (Figure 5.10, Table 5.8)

The results suggest annual IC production is -11.0 mol of IC m^{-2} yr^{-1}, with no difference in IC production with temperature or CO_2 treatment.

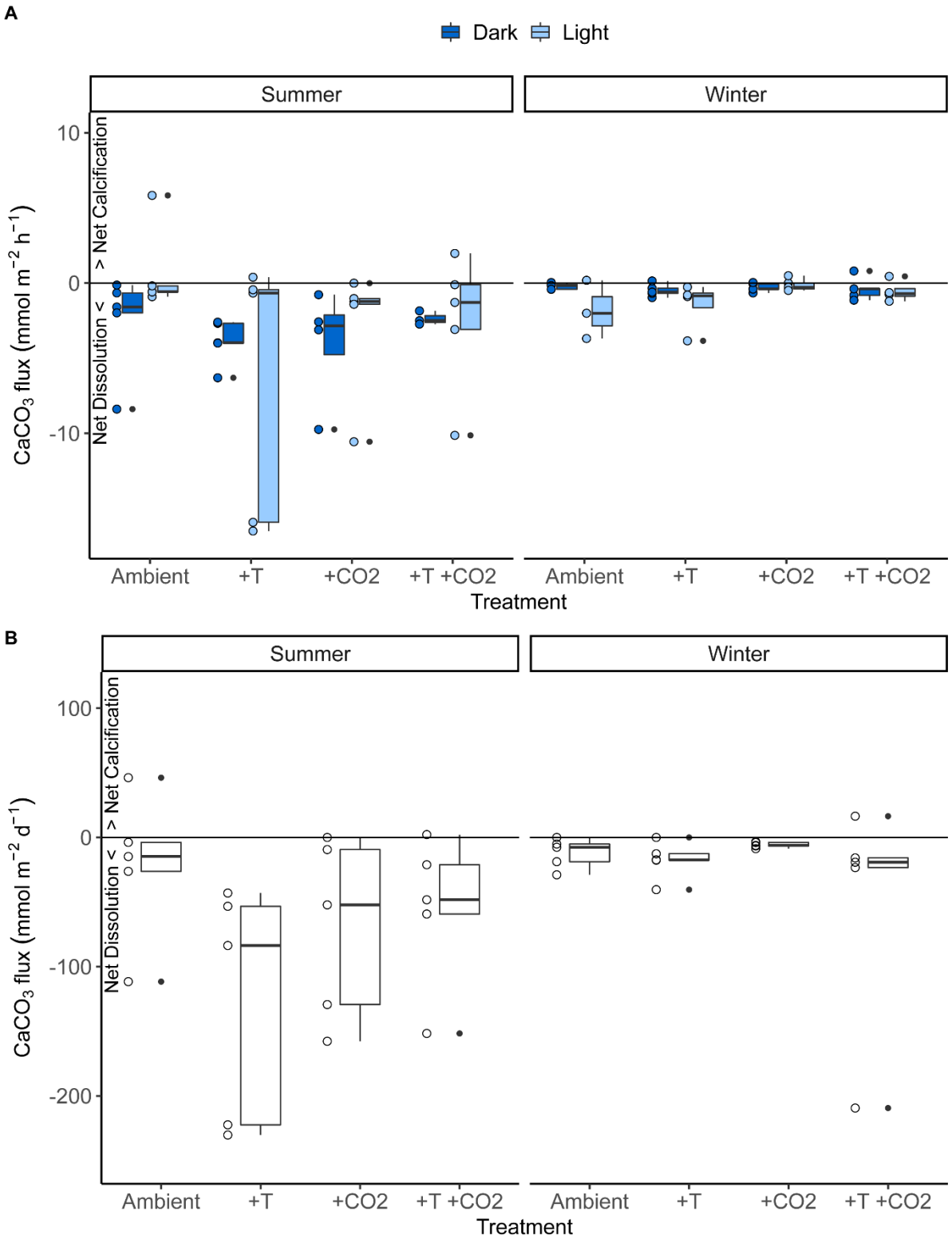

Figure 5.10: A) light and dark and B) $CaCO_3$ fluxes for rhodolith bed sediment for both summer and winter experiments. Treatments are ambient conditions, elevated temperature (+T), elevated CO_2 (+CO2), and elevated temperature with elevated CO_2 (+T +CO2). Points to the left of the bar charts correspond to raw data. Boxplot bars represent median and interquartile ranges, and whiskers represent minimum and maximum values.

Table 5.8: Summary of statistical analysis (ANOVA and Kruskal Wallace test results) testing the effects of treatment on $CaCO_3$ fluxes (light, dark and net) in rhodolith bed sediment for summer and winter experiments, and differences between seasons. n= 20 for summer and winter experiments. X^2 refers to chi-squared, indicating that a Kruskal-Wallace test was used as the data was non-parametric.

	Light $CaCO_3$ Flux		**Dark $CaCO_3$ Flux**		**Net $CaCO_3$ Flux**	
	F	***p***	***F***	***p***	***F***	***p***
Summer						
T	$X^2 = 0.37$	0.545	$X^2 = 1.33$	0.248	2.013	0.175
pCO_2	$X^2 = 0.69$	0.406	$X^2 = 0$	1	0.133	0.720
T x pCO_2	$X^2 = 2.52$	0.472	$X^2 = 4.38$	0.223	3.467	0.811
Winter						
T	$X^2 = 1.10$	0.294	0.807	0.382	$X^2 = 2.40$	0.121
pCO_2	$X^2 = 3.05$	0.081	0.004	0.948	$X^2 = 0.14$	0.705
T x pCO_2	$X^2 = 4.13$	0.248	0.199	0.661	$X^2 = 3.30$	0.347
Season	$X^2 = 0.74$	0.39	**$X^2 = 20.34$**	**<0.001**	**$X^2 = 6.06$**	**0.014**

5.4 Discussion

Rhodolith beds are able to bury and store BC, however, currently it is not known if their ability to store BC will be affected by climate change. Here, I show that OA and temperature may reduce the capacity of rhodolith beds to store OC, with a lower mass of labile carbon preserved. Rhodolith bed sediment OC and IC production were not affected by OA or temperature, with large variations in production measurements between treatment groups.

5.4.1 Increased labile carbon loss under elevated temperature and CO_2

Field decomposition rates and stability factors were in agreement with other studies globally. Field decomposition rates of 0.003 in the summer, and 0.004 in the winter were in line with studies within freshwater and marine environments (Yousefi Lalimi *et al.,* 2018; Seelen *et al.,* 2019; Simpson *et al.,* 2021) as well as marsh ecosystems (Mueller *et al.,* 2018). Freshwater, marine and marsh sediments are typically water-logged which creates anoxic conditions favouring preservation. This is contrary to terrestrial porous sediments, where decomposition rates have been found to typically be above 0.01 (Keuskamp *et al.,* 2013). Low decomposition rates are also driven by low temperatures (Mueller *et al.,* 2018; Seelen *et al,* 2019) which could explain why the results from the field incubations are on the lower end of the scale seen within freshwater and marine environments (Yousefi Lalimi *et al.,* 2018; Seelen *et al.,* 2019; Simpson *et al.,* 2021). Stability factors of 0.24 in the summer and 0.35 in the winter were within the higher range of other freshwater and marine environments meaning that more labile carbon was preserved (Seelen *et al.,* 2019). As above, this may be a result of the water logged conditions and lower temperatures favouring a higher degree of preservation compared to other studies.

5.4.2 Increased labile carbon loss under elevated temperature and CO_2

In this study, temperature affected the preservation of labile material, with labile mass loss higher and S lower under elevated temperature. Additionally, summer experiments showed higher labile carbon breakdown and lower S than winter experiments, further supporting the association between temperature and the preservation of labile carbon. Research regarding the effects of temperature on the microbial breakdown of labile carbon is well established, with previous studies using the TBI index also finding an increased breakdown of labile material under elevated temperatures (Keuskamp *et al.,* 2013; Mueller *et al.,* 2018;

Trevathan-Tackett *et al.,* 2020). Temperature can increase the rate of enzymatic reactions responsible for carbon degradation (Arndt *et al.,* 2013; Chen *et al.,* 2022), with microbes favouring labile carbon, which is easier to consume than refractory carbon (Burdige 2007; Arndt *et al.,* 2013; Kelleway *et al.,* 2022). Whilst previous studies found increased labile carbon degradation when temperature change was ≥5°C (Keuskamp *et al.,* 2013; Trevathan-Tackett *et al.,* 2020), here differences were observed when the temperature was raised by only 3°C, highlighting the sensitivity of carbon burial to changes in the environment. As a large proportion of carbon within the coastal environment is labile (Vichkovitten and Holmer 2004; Trevathan-Tackett *et al.,* 2020), the results suggest that increases in temperature in line with current climate predictions could significantly reduce the capacity of BC systems to bury carbon.

To my knowledge, only 1 study (Lee *et al.,* 2022) have used litter bags to investigate the effects of elevated pCO_2 on carbon burial in a marine system . Here the decomposition of labile carbon was increased under elevated pCO_2, which is likely due to changes to the microbial biome (Liu *et al.,* 2010; Witt *et al.,* 2011; Nagelkerken and Connell 2015; Malits *et al.,* 2021), with little bioturbation observed from the calcifying fauna present in the cores. Elevated pCO_2 can result in increased productivity by the microbial community, resulting in more energy for the remineralization of organic material (Trevathan-Tackett *et al.,* 2018; Ravaglioli *et al.,* 2020; Yuan *et al.,* 2021; Chen *et al.,* 2022). In previous studies, decreases in OC concentration in response to increased productivity have been observed at shallow depths (0-2cm of sediment; Trevathan-Tackett *et al.,* 2018; Ravaglioli *et al.,* 2020), whilst in this study, a decrease in labile carbon concentrations was observed at depths of 8cm in the sediment. It is not known if OA results in an increase in microbial activity at depths greater than 0-2cm, however, as the sediment at 8cm is aphotic, the decrease in labile carbon concentrations observed in this study may be due to other changes to microbial activity driven by OA (Liu *et al.,* 2010), with OA able to alter species interactions at a microbial level (Malits *et al.,* 2021). Regardless, the results from this study further support the reduced capacity of BC systems to bury carbon under climate change (Lee *et al.,* 2022), and additional work is needed to establish the links between labile carbon decomposition and elevated pCO_2.

Whilst this experiment suggests that the burial and preservation of labile carbon may be reduced with global warming, other factors may limit the vulnerability of labile carbon to increased degradation. The analysis conducted in chapter 3 shows that under anaerobic conditions, labile carbon is protected to some degree from remineralisation, with ~20% of

labile carbon preserved within the sediment. This suggests that the labile carbon present has been physically protected from remineralisation through processes such as encapsulation, or sorption to minerals within the sediment (Burdige 2005; Arndt *et al.,* 2013; Hemingway *et al.,* 2019). As labile carbon may be protected from remineralisation, the effects of temperature on labile carbon already stored within the rhodolith bed may not be as large are found in this study. This is because the green tea was not processed in the water in the same manner as naturally derived labile organic matter. Thus the SOC stock may remain unaffected by warming of +3°C and a pCO_2 concentration of 750ppm.

In contrast to labile carbon, refractory carbon mass loss was not influenced by elevated temperature and pCO_2, with the breakdown of rooibos material low in both summer and winter experiments. This is not in agreement with another TBI study (Trevathan-Tackett *et al.,* 2020), where refractory carbon mass was found to decrease with temperature. However, with decomposition rates lower than previous studies (0.003-0.008 in this study, vs ~0.01 in Trevathan-Tackett *et al.,* (2020)), and in line with other TBI studies from freshwater and marine environments (Yousefi Lalimi *et al.,* 2018; Seelen *et al.,* 2019; Simpson *et al.,* 2021), the results suggest that the sediment properties within the rhodolith bed samples in this study may favour OC preservation. Typically, decomposition rates are low in freshwater and marine systems, with water-logged conditions within the sediment, and sediment grain size reducing decomposition rates (Yousefi Lalimi *et al.,* 2018). As finer-grained sediments can have shallower redox gradients (Hedges and Keil 1995; Dauwe *et al.,* 2001; Burdige 2007; Glud 2008), the refractory carbon in this study may have been decomposing within a fully anoxic environment, favouring preservation and reducing the effects of temperature on degradation rates. This suggests that refractory carbon already locked away within rhodolith beds may be protected by future climate change as long as they remain undisturbed (Macreadie *et al.,* 2019b; Smeaton and Austin 2022a), with a low k suggesting that the sediment properties of rhodolith beds contribute to a large amount of OC stored within rhodolith beds (Mao *et al.,* 2020).

Similarly to other studies, mass loss and OC wt% loss were not correlated (O'Meara *et al.,* 2018; Marley *et al.,* 2019). Whilst OC wt% loss was positive for some samples, I do not think this reduces the validity of the TBI index as a proxy for carbon degradation. In this study, initial OC wt% values were based on Keuskamp and co-authors (2013), as I was unable to obtain independent starting OC wt% values for each teabag as this would require breaking apart the bags. With the contents of tea bags not standardised to be used for science and the filling made from ground samples rather than leaves, the starting OC wt% in each

bag may have differed. This experiment suggests that mass loss (with independent mass measurements for each teabag before and after burial) is a more reliable proxy of carbon degradation, with loss representing changes in organic material mass. The use of the TBI as a proxy of organic material breakdown was further verified by the TOU data, suggesting that changes in organic material mass were due to breakdown by anaerobic (rather than aerobic) bacteria, in the sediment, with no change in O_2 concentration when the teabags were introduced into the sediment (Trevathan-Tackett *et al.*, 2020). Not all *in vitro* and *situ* measurements agreed with each other, likely due to difficulties burying teabags *in situ* resulting in resuspension of sediment and uneven covering of teabags.

Whilst TBI provided a proxy of carbon degradation under future climate change scenarios, the organic material buried was derived from terrestrial plant matter not typically found within the environment. There is evidence from terrestrial leaf decay studies that the soil biotic community are specialised at decomposing litter derived from their local environment, with decomposition rates differing when litter is derived from elsewhere (even when taking into account litter quality; Edward, *et al.*, 2009). Additionally, the TBI index only provides a proxy of the decomposition of fresh litter with marine systems accumulating varying amounts of fresh litter and degraded litter (i.e. from macroalgae) which can affect decomposition rates (Marley *et al.*, 2019). These limitations mean that the results from this experiment should be taken with a degree of caution, with other methods including carbon tracer experiments used to future investigate decomposition rates in Scottish rhodolith beds.

5.4.3 Increased OC production by rhodolith bed sediment at elevated temperatures

Organic carbon production, as measured through daily O_2 fluxes, suggested that rhodolith bed sediment can produce OC. O_2 fluxes varied with temperature in the summer, with an average daily flux of -3.16±31.6 O_2 mmol m^{-2} d^{-1} at ambient temperatures and 26.2±28.4 O_2 mmol m^{-2} d^{-1} at elevated temperatures showing that the sediment switched from net heterotrophic to net autotrophic with elevated temperature. A positive net O_2 flux at elevated temperatures, and positive O_2 flux during light incubations, is likely due to an active microphytobenthos community on the surface of the rhodolith bed sediment (Hancke and Glud, 2004; Vieira *et al.*, 2013). This may contribute to CO_2 drawdown in the rhodolith bed community, with OC subsequently produced and stored within the bed. On the other hand, increased ecosystem productivity can result in the enhanced remineralisation of both labile and refractory carbon (Trevathan-Tackett *et al.*, 2018; Ravaglioli *et al.*, 2020; Yuan *et al.*,

2021; Chen *et al.,* 2022), the elevated OC production by the microphytobenthos under elevated temperatures may have negative consequences for rhodolith bed carbon storage. Variations in OC production were high and larger in the summer, similar to previous measurements in the field (Attard *et al.*, 2015). Whilst cores did contain a few brittle stars, their contribution to benthic oxygen demand is low (Attard *et al.,* 2016), thus the large variations observed may be due to the active and variable microphytobenthos community. Furthermore, daily flux measurements (3.46±48.9 O_2 mmol m^{-2} d^{-1} in the summer and -24.5±13.8 O_2 mmol m^{-2} d^{-1} in the winter) are higher than previous net ecosystem metabolism measurements from rhodolith bed sediment at Loch Sween (Attard *et al.,* 2015). This may be driven by experimental setup, with laboratory-based incubations often underestimating respiration rates compared to in situ measurement (Glud 2008), and longer periods of high light intensity driving higher levels of photosynthesis (Attard *et al.,* 2015). Whilst the results suggest that in a warmer world the capacity of rhodolith bed sediment to store OC may increase, the effects of temperature on microphytobenthos photosynthesis may be smaller in the real world, with the sediment covered by coralline algae and therefore shaded from the light.

Whilst O_2 production was affected by temperature, DIC production was affected by CO_2, with DIC increasing by 8mmol m^{-2} h^{-1} under elevated pCO_2 in the summer experiments. In this experiment, DIC and O_2 did not follow a 1:1 ratio as previously observed (Martin *et al.*, 2013); this is likely because of the effects of CO_2 concentration on anaerobic, rather than aerobic, metabolic pathways within the sediment and water column. This is not the first sediment study to find a mismatch between DIC data and O_2 data (Billerbeck *et al.,* 2007), with DIC also driven by methanogenesis and sulphate reduction (Wu *et al.,* 2016; Meister *et al.,* 2019). Elevated CO_2 has been found to decrease methane emissions (Lee *et al.,* 2017; resulting in a more positive DIC). The results from the DIC measurements suggest the converse to the labile carbon measurements with decreased methane production and therefore anaerobic activity under elevated temperatures. However, as DIC flux measurements were taken after 1-month at treatment conditions, and green tea was removed at 4-months at treatment conditions, the disparity in the results may be due to changes in the microbial community with prolonged exposure to pCO_2. Furthermore, the relationship is complex and often driven by additional variables not measured in this experiment (e.g., nitrate concentration; Lee *et al.,* 2017; Yuan *et al.,* 2021), therefore the disparities may be due to other variables not considered in this experiment. Regardless of the trend, as methane emitted by BC systems can offset OC sequestered (Al-Haj and Fulweiler, 2020; Rosentreter *et al.,* 2021), methane emissions should be quantified in future rhodolith bed research.

Inorganic carbon production, as measured through net $CaCO_3$ fluxes, was not influenced by elevated CO_2 or temperature, with the sediment showing net dissolution throughout all treatments. Rhodolith bed sediment contains large proportions of dead coralline algae which undergo calcium carbonate dissolution (Martin and Gattuso 2009; Brodie *et al.*, 2014). The % of calcium carbonate in the sediment was not measured, therefore the large variation seen in the $CaCO_3$ fluxes may be an artefact of the large variation of dead coralline algae in the sediment. As dissolution removes CO_2 from the water column (Gattuso *et al.*, 1995), this finding suggests that rhodolith bed sediment will continue to draw down CO_2 in a future world, with annual inorganic production suggesting the absorption of 11.0 mol of CO_2 m^{-2} yr^{-1}.

5.4.4 Conclusion

This chapter aimed to investigate how the capacity of rhodolith beds to store labile and refractory carbon varied with global warming and OA, with O_2, DIC and $CaCO_3$ fluxes used to characterise any climate-driven changes to OC and IC production by rhodolith sediment. By using the TBI index, this study found that:

a) Labile carbon was vulnerable to both warming and OA, with changes in microbial activity likely driving changes in labile mass loss.

b) Refractory carbon was not affected by climate change, with low decomposition rates suggesting that the sediment properties of rhodolith bed sediment create suitable conditions for OC preservation.

c) Net OC production by the sediment community increased with temperature, potentially due to more activity by the microphytobenthos. Whilst the results here suggest that the rhodolith bed sediment is a net store of OC, this may not translate to the "real world" with sediment shaded by coralline algae fragments in rhodolith beds. Disparities between the O2 and DIC data suggested that methane was produced by microbes within the sediment. As methane is a potent GHG, future methane production by rhodolith beds should be measured, with methane production potentially reducing the capacity of rhodolith beds to act as a carbon sink.

d) Net IC production was unaffected by temperature and pCO2, with differences in the mass of dead coralline algae within the sediment likely driving large variability in the IC production measurements. Rhodolith bed sediment showed net dissolution, which may in part offset the CO_2 released via the calcification of live algae within the bed.

Chapter 6 Discussion

6.1 Background

Throughout this research project, there have been increasing calls from the scientific community to respond to the climate crisis and reduce greenhouse gas (GHG) emissions. The Intergovernmental Panel on Climate Change (IPCC) reports have provided startling predictions of the impacts of climate change on ecological and social systems, calling for the reduction of GHG emissions (IPCC 2022). Several climate tipping points, in which large parts of the climate system change, have been identified within the 1.5 to <2°C limit set by the Paris Agreement in 2016 (Armstrong McKay *et al.,* 2022). Such tipping points will have unequivocal effects on the Earth's system functioning resulting in natural, ecological, social and economic impacts globally (Jarraud and Steiner 2012; IPCC 2022; Armstrong McKay *et al.,* 2022). Whilst initiatives such as COP and the Paris Agreement have tried to bring countries together and create a framework to avoid climate change, currently, a warming of 2.6°C is still projected under current international policy (Armstrong McKay *et al.,* 2022). A warming of this magnitude will cause global change resulting in ecosystem degradation, biodiversity loss, mass human movement, increased pandemics, and increased human mortality (Jarraud and Steiner 2012).

Blue carbon (BC) has become increasingly recognised internationally as a nature-based solution for climate mitigation (Ahmed and Glaser 2016). Recent research has highlighted the quantity of OC both stored and sequestered by BC systems sediments (Howard *et al.,* 2011; Smith *et al.,* 2015; Macreadie *et al.,* 2020). Furthermore, research has documented the damage that anthropogenic activities can do to BC systems (Macreadie *et al.,* 2013; 2015; Githaiga *et al.,* 2019; Epstein *et al.,* 2022), with the potential for disturbed OC to be released back into the atmosphere via remineralisation by bacteria within the water column (Macreadie *et al.*¸ 2019). Combined with other natural systems (i.e. peat bogs, temperate and tropical rainforests), BC systems can play a role in sequestering CO_2 (Griscom *et al.,* 2017). If such systems are protected and restored, they may contribute to keeping warming to below 2°C as agreed by the Paris Agreement (Macreadie *et al.,* 2021).

6.2 Thesis Aims

The overall aim of this thesis was to investigate Scottish rhodolith bed BC in a changing world. Specifically, the thesis aimed to 1) investigate how carbon storage is influenced by bed type and structure, 2) contribute to the current rhodolith bed BC inventory for Scotland, and 3) provide context for future Scottish rhodolith bed blue carbon storage.

To address these aims, I explored rhodolith bed BC through four research objectives:

5) understand the characteristics of rhodolith beds that allow them to act as BC repositories (Chapter 2);

6) investigate the spatial variability in rhodolith BC and contribute to the current BC inventory for Scotland (Chapter 3);

7) investigate rhodolith bed community metabolism, organic carbon (OC) and inorganic carbon (IC) production under future conditions (elevated temperature and ocean acidification; Chapter 4);

8) explore how the burial and storage of allochthonous carbon will change under elevated temperature and ocean acidification (Chapter 5).

6.3 Synthesis

6.3.1 Current rhodolith bed blue carbon storage

Previous to this thesis, only one study had investigated carbon storage in Scottish rhodolith beds with the rhodolith bed at Loch Sween found to act as a carbon repository for over 4000 years and 7.23 ± 1.30 Mg OC ha^{-1} found in the top 25cm of sediment (Mao *et al.,* 2020). Whilst the quantified SOC stock was in the lower range compared to other Scottish BC systems (Austin *et al.,* 2021; Potouroglou *et al.,* 2021), the research highlighted the potential of rhodolith beds to store allochthonous BC which may in part offset the CO_2 emitted during calcification (Fodrie *et al.,* 2017; Mao *et al.,* 2020). This was contrary to previous reviews that categorise calcifying systems as CO_2 sources (Howard *et al.,* 2017; Lovelock and Duarte 2019). As the variability in the SOC in other systems can vary 20-fold (e.g. the SOC stock of muddy sediment can range from 6 to 123 Mg OC ha^{-1} in the top 1m; Parker *et al.,* 2020), the spatial variability of rhodolith bed carbon storage warranted further research. Furthermore, since Mao *et al.,* (2020), research quantifying the reactivity of carbon within marine sediment has gained traction using the carbon reactivity index (CRI; Black *et al.,* 2022; Smeaton and Austin, 2022). Such techniques provided further opportunities to investigate the reactivity of carbon within rhodolith beds with links between reactivity, carbon source and quantity explored.

6.3.1.1 Carbon reactivity, source and quantity are inter-dependant

To my knowledge, this study was the first to combine methods that measure carbon quantity, reactivity and source to characterise OC within marine sediments. The results from Chapter 3 highlighted the inter-dependence of OC quantity, source, and quality. Furthermore, by combining the three methods, the results provided a full overview of carbon decomposition within the rhodolith beds with carbon quantity and reactivity changing downcore. This allowed for carbon burial and storage to be interpreted compared to the cores at Loch Sween (Mao *et al.,* 2020).

Similarly to Loch Sween (Mao *et al.,* 2020), OC concentrations from Upper Loch Torridon decreased with sediment depth before becoming relatively stable. Whilst Mao *et al.,* (2020) attributed this decrease to bacterial remineralisation and the decomposition of organic matter, the only evidence of this was the decrease in OC concentrations. By using the CRI index, I was able to confirm that the decrease in OC with depth was due to the preferable decomposition of labile carbon by microbes (Canfield 1994; Burdige 2007; Arndt *et al.,*

2013), with the CRI index increasing downcore. The CRI index also suggested that in all cores some process of encapsulation was taking place (Burdige 2005; Arndt *et al.*, 2013; Hemingway *et al.*, 2019). Whilst the CRI index at the core base with high (~0.8 in all cores), the CRI was not 1 and therefore labile carbon was present within the sediment. Where longer cores were obtained (Upper Loch Torridon and Sound of Barra), the increase in CRI appeared to begin to flatten near the core base, along with stabilisation in OC%. This may suggest that after a certain depth or time, the labile carbon within the sediment is protected from further decomposition and is 'locked away'. This provides evidence that rhodolith beds can store BC by locking away OC for over 1000 years and is in agreement with Mao and co-authors (2020).

Conversely to Smeaton and Austin (2022), OC reactivity was not associated with proximity to shore. Instead, reactivity was linked to carbon source, with systems that store a high amount of terrigenous carbon having a less reactive SOC stock. Furthermore, whilst Tingwall stored more reactive marine carbon within the surface sediment, this was rapidly remineralised by bacterial within the sediment with CRI increasing to 0.8 at 10cm of depth. The results are disagreement that coastal and inshore sediments with a lower CRI index are more vulnerable to disturbance as argued by Smeaton and Austin (2020) and Black and co-authors (2022). In both studies, down-core variability was not considered when assessing the vulnerability of marine sediments, with only the top 1cm of sediment analysed. As labile carbon was decomposed rapidly within the top 10cm in all 4 cores, coastal and inshore sediments may be less vulnerable to disturbance than previously thought. However, whilst Smeaton and Austin (2020) argued the CRI index is a measure of vulnerability, with refractory carbon being less vulnerable to remineralisation following resuspension, there is evidence that even refractory carbon is vulnerable to remineralisation following exposure to O_2 (Macreadie *et al.*, 2019b). Therefore, whilst the CRI may be used to quantify the vulnerability of sedimentary organic carbon to decomposition during burial, I do not think it should be used as a proxy for vulnerability following resuspension.

6.3.1.2 Scottish rhodolith beds mainly store allochthonous organic carbon

Within Chapter 3, the rhodolith beds were found to store organic carbon from a range of sources providing evidence that they can act as BC repositories. Generally, calcifying systems are considered net CO_2 emitters (Howard *et al.*, 2017; Lovelock and Duarte 2019; Macreadie *et al.*, 2019a), with the combined processes of calcification and respiration theoretically resulting in a net release of CO_2 in heterotrophic systems (Frankignoulle and

Canon 1994; Gattuso *et al.,* 1998; Howard *et al.,* 2017; Lovelock and Duarte 2019). However such processes fail to acknowledge the role of allochthonous carbon burial, with Chapter 3 finding that only 4.5-11% of the organic carbon in the SOC predicted to have come from the coralline algae themselves. This highlights the ability of rhodolith beds to store carbon from allochthonous sources which may offset any CO_2 emitted during calcification.

This finding also suggests previous calculations regarding the contribution of coralline algae to carbon burial (as quantified by van der Heijden and Kamenos (2015)) may be inaccurate. This is for two reasons. Firstly, van der Heijden and Kamenos (2015) did not consider the burial of allochthonous carbon which likely resulted in an underestimation of the contribution of rhodolith-forming coralline algae to organic carbon burial. Secondly, van der Heijden and Kamenos (2015) assumed that all OC produced by coralline algae had the ability to be buried. Whilst Chapter 3 demonstrated that a proportion of OC from coralline algae is buried within the sediment, it is unlikely that 100% of this is preserved (Canfield *et al.,*1997; Burdgie *et al.,* 2005, 2007). Not considering the degradation of organic carbon produced by coralline algae likely resulted in an overestimation of their contribution to organic carbon burial. This suggests that the current national carbon inventory of rhodolith bed blue carbon (Burrows *et al.,* 2014, 2017) should be revised as it is based on calculations by van der Heijden and Kamenos (2015) and does not consider rhodolith bed SOC. As the results in Chapter 3 highlighted the large spatial variability in SOC stocks I was unable to confidently provide a update to this inventory. Further research is needed, with sediment cores taken from rhodolith beds in a suite of environmental settings, to quantify the environmental drivers in SOC variability and estimate the national carbon inventory.

The results from Chapter 3 suggest that the OC production values as calculated in Chapter 4 cannot be used to quantify the contribution of rhodolith bed communities to carbon burial. Instead, the findings from Chapter 4 can be used as a proxy of ecosystem productivity, with the potential for a proportion of the organic carbon produced within the ecosystem to be buried within the sediment. I recommend that future studies rely on sediment cores, rather than estimates of OC production, to quantify the potential of systems to store organic carbon, with the use of sediment cores removing any assumptions regarding carbon source and decomposition.

6.3.1.3 Dead rhodolith beds still store OC

A major outcome of this thesis was finding that dead rhodolith beds continue to store OC. The rhodolith bed at the Sound of Eriskay died as a consequence of the causeway construction in 2000-2001 when reduced water flow facilitated sedimentation which limited light and smothered live coralline algae (Bunker *et al.,* 2015). Whilst the rhodolith bed was dead, the SOC stock was preserved, with evidence that OC had accumulated within the sediments in the bed since it had died. This provides the first evidence that even when dead, rhodolith beds may continue to store OC. In Scotland, dead rhodolith beds are not recognised as a protected feature within the MPA network (i.e. dead beds around Cumbrae). This means that activities that disturb the sediment, including bottom trawled gear, are not licenced. There is evidence that trawling can disturb 6-16cm of the surface sediment (Bradshaw *et al.*, 2021) which could result in the disturbance of buried organic carbon that has accumulated over hundreds of years (as seen at Upper Loch Torridon). As trawling can expose such sediments to oxygen this could result in the permanent loss of carbon from the SOC, with organic carbon remineralised and reintroduced into the atmosphere further exasperating climate change. Recognising the potential for dead rhodolith beds to store organic carbon could result in dead rhodolith beds being considered as a feature that warrants protection. Restrictions on certain activities (i.e. trawling and dredging) and gear types (i.e. bottom trawled gears) could limit the disturbance of ancient carbon stocks.

6.3.1.4 Variability in rhodolith beds SOC stocks

The SOC stock in the top 25cm of sediment ranged from 1.67 Mg OC ha^{-1} to 17.21 Mg OC ha^{-1} with variability in SOC in agreement with other BC systems (i.e. muddy sediments store 6-123 Mg OC ha^{-1} in the top 1m; Parker *et al.,* 2020). When compared to other systems, the range of SOC stored in rhodolith beds was to the lower range of other temperate BC systems such as *Zostera marina* meadows which are estimated to store 3.18 to 2652 Mg OC ha^{-1} over 50cm depths (Potouroglou *et al.,* 2021). On the other hand, the SOC stocks were higher than other systems such as high-latitude kelp forests (Burrows *et al.,* 2014). Whilst per unit area, rhodolith beds may not function as large BC repositories, given the large distribution of rhodolith beds in Scotland's terrestrial waters (Simon-Nutbrown *et al.,* 2020) they may still contribute to the national carbon inventory (Turrell 2020). As the accumulation of OC took place over centuries, they are unlikely to play a large role in the sequestration of OC and reduction of CO_2 emissions. Instead, there should be a focus on protecting what is already stored as any damage to the SOC could result in the release of CO_2 and could further exasperate the climate crisis.

Globally, rhodolith beds can be found in a variety of environments with a range of hydrodynamical regimes (Riosmena-Rodríguez *et al.,* 2017). The results from this thesis suggest that fjordic beds in similar environments this study, for example, those distributed in the North Atlantic (i.e. de Grave *et al.,* 2000; Teichert *et al.,* 2014; Jørgensbye and Halfar 2017; Schoenrock *et al.,* 2018), may store similar quantities of SOC. In the North Atlantic, beds situated at higher latitudes than those in this thesis may store more SOC per unit area, with low temperatures driving high export rates and low remineralisation rates thus preserving OC (Chapter 2; Smith *et al.,* 2015; Henson *et al.,* 2019).

6.3.2 Future blue carbon storage by rhodolith beds

6.3.2.1 The fate of rhodolith beds under future conditions

To date, the majority of research has focused on the effects of global warming and OA on individual coralline algae thali, with few (Legrand *et al.,* 2017; Burdett *et al.,* 2018) focussing on community-level effects. The results from this thesis contribute to current knowledge of how rhodolith bed communities will function in a future world. As discussed in Chapter 4, whilst no changes in autochthonous OC production were observed in response to OA and warming, observed epiphyte growth in the cores and reduced calcification rates suggested that rhodolith beds will be negatively impacted under future conditions. This is in agreement with other community-level studies (Legrand *et al.,* 2017; Burdett *et al.,* 2018), and species-level studies (i.e. Ragazzola *et al.,* 2012; Kamenos *et al.,* 2013; Noisette *et al.,* 2013), with evidence from CO_2 vents suggesting that in a future world, fleshy algae will outcompete calcareous algae (Hall-Spencer *et al.,* 2008; Porzio *et al.,* 2013). The sensitivity of rhodolith beds to climate change means that such systems are anticipated to decrease in distribution in the coming century. For example, species distribution modelling suggests that the distribution of live Scottish rhodolith beds may decrease by up to 84% under future climate projections (Simon-Nutbrown *et al.,* 2020).

The results from Chapter 4 may indicate how BC sequestration by Scottish rhodolith beds will change under future conditions. In the short term, an increase in OC production and $CaCO_3$ dissolution may benefit BC storage, with the potential of enhanced OC production resulting in more autochthonous OC stored, and the dissolution of coralline algae absorbing CO_2. However, in the long term, this will have a negative impact on BC storage. Whilst the growth of fleshy algae may be enhanced in the future, the carbon in macroalgae is considered primarily labile (Hill *et al.,* 2015). As labile carbon is degraded faster with climate change (as seen in Chapter 5), whether the enhanced OC production is subsequently buried in

sediments remains unknown. Whilst $CaCO_3$ dissolution may result in CO_2 being absorbed this will gradually result in surficial coralline algae breaking up. It is currently not known if dead beds will continue to store SOC under future conditions, although the results from Chapter 5 suggest that refractory carbon may be protected. There is evidence that kelp-dominated habitats have a smaller SOC stock than rhodolith beds (Burrows *et al.,* 2014), thus the shift from a rhodolith bed to a macroalgae-dominated reef may reduce the ability of beds to sequester allochthonous BC. As the future distribution of live and dead coralline algae is predicted to decrease (Brodie *et al.,* 2014; Simon-Nutbrown *et al.,* 2020), their capacity to sequester allochthonous carbon may be reduced.

6.3.2.2 Carbon storage under future conditions

To my knowledge, Chapter 5 was the first to quantify the decomposition of carbon in rhodolith beds under current and future climate conditions. Similarly to other aquatic environments, rhodolith bed sediment was characterised by slow decomposition rates meaning that a larger proportion of labile and refractory material was preserved compared to terrestrial environments (Keuskamp *et al.,* 2013; Millar *et al.,* 2019). Labile carbon decomposition was faster under future conditions suggesting that anticipated increases in primary production by macrophytes (Koch *et al.,* 2013; Brodie *et al.,* 2014) may not result in more carbon being buried in marine sediments. On the other hand, the decomposition of refractory carbon was unaltered by warming or OA. As precipitation and run-off are projected to increase under future conditions (Ekstrom *et al.,* 2005; IPCC 2022), the contribution of refractory carbon to BC storage may increase in rhodolith beds that store terrestrial carbon.

Whilst climate change may reduce the capacity of rhodolith beds to sequester allochthonous carbon, results from Chapter 5 suggests that, if not disturbed, the refractory carbon within the sediment may not be vulnerable to OA or warming. With regard to climate change, this is good news. Rhodolith beds can store carbon that has gradually been deposited over millennia, with estimates from 1m cores at Loch Sween (Scotland), suggesting that the carbon stored spans 4,000 years (Mao *et al.,* 2020). As deposits can be thicker, with deposits found that are 1.2m and 2m thick (de Grave *et al.,* 2000; Porter *et al.,* 2020), some rhodolith bed deposits are likely to be significantly older. The results from this thesis suggest that if undisturbed, the OC will remain locked away, with the majority of the carbon stored at depth refractory, with evidence that the smaller proportion of labile carbon present (~20%) may be physically protected (i.e. encapsulation) from bacterial degradation.

6.4 Future Research

Whilst this study increased knowledge regarding BC storage in Scottish rhodolith beds, several areas warrant further investigation. Whilst this thesis contributed to knowledge surrounding the spatial resolution of rhodolith bed BC, I was unable to update the Scottish rhodolith bed BC inventory. Recent work by Simon-Nutbrown and co-authors (2020) has found that the current predicted distribution of Scottish rhodolith beds is 7130km^2 in Scotland. However, the spatial distribution of exposed, sheltered and dead beds is currently unknown. As Chapter 3 found that the quantity of OC stored may vary 10-fold between exposed and sheltered bed types this means that the current Scottish rhodolith bed BC inventory cannot be updated. Additional work is needed to map the distribution of exposed, sheltered and dead beds, with the potential of wave exposure (Burrows 2008) used as a proxy of exposed and sheltered bed types. Furthermore, work is needed to determine the depth of rhodolith beds, with the cores in this study not reaching the bottom of the deposit. As there is evidence that the SOC is preserved after a certain depth, beds found that are several meters thick (i.e. de Grave *et al.,* 2000) may store a significantly larger amount of OC than found in this study. This may result in the national BC inventory of rhodolith beds being larger than currently predicted.

In this thesis, a major outcome was finding that dead beds still store allochthonous BC. In Chapter 3, the rhodolith bed at the Sound of Eriskay died due to the construction of a causeway limiting water movement. However, rhodolith beds may be damaged by other activities, including aquaculture development, the dumping of sewage, nutrient enrichment, trawling, and calcium carbonate mining (Barbera *et al.,* 2003; Grall and Hall-Spencer, 2003; Kamenos *et al.,* 2003; Peña and Bárbara 2008; Aguado-Giménez and Ruiz-Fernández 2012; Bernard *et al.,* 2019). The ability of dead beds to preserve the SOC stock is expected to depend on the level of disturbance the bed has encountered and warrants further investigation. For example, the SOC may be lost in beds that have been physically disturbed (for example, via trawling or calcium carbonate mining; Hall-Spencer and Moore 2000; Bernard *et al.,* 2019), as SOC can be vulnerable to remineralisation following exposure to O_2 (Macreadie *et al.,* 2019). On the other hand, the sediment of beds that have died as a consequence of aquaculture developments (mussel rafts, fish cages) and offshore dumping of sewage/sediment (Barbera *et al.,* 2003; Grall and Hall-Spencer 2003; Aguado-Giménez and Ruiz-Fernández 2012; Abella *et al.,* 2014), may not have been physically disturbed thus the SOC may be preserved. There is also the potential for disturbed beds to recover following physical disturbance (Barberá *et al.,* 2017). Whilst beds that have recovered may continue

to store OC, physical damage previously done to the bed may reduce the previous SOC stock. Thus, whilst this study provides evidence that dead rhodolith beds can continue to store carbon, more research is needed.

To my knowledge, the studies in chapters 4 and 5 were the first to use Perspex cores to collect samples of a rhodolith community. The use of Perspex cores allowed for multiple replicas to be run at the same time reducing any effects of pseudo-replication. Furthermore, samples could be collected with ease with Scuba resulting in lower costs compared to other techniques (i.e. Legrand *et al.*, (2017) where sample collection required a boat). However, a major limitation with the Perspex cores was the inability to flow fresh seawater through the mesocosm. Rhodolith beds typically form in areas with sufficient water movement which reduces smothering. The lack of water movement in these studies may have had a negative impact on the coralline algae within the cores as implied by apparent methane production by the coralline algae community in Chapter 4. In the future, altering the Perspex cores to allow for a flow-through system would be recommended.

Whilst chapter 4 study captured the short-term effects of elevated temperature and pCO_2 on rhodolith bed community metabolism, this chapter did not investigate any long-term effects. As climate change happens over decadal scales (IPCC 2022), future work is needed to determine if, and what, the long terms effects of elevated temperature and pCO_2 are. I recommend that long-term experiments are run over several years *in vitro* with such experiments providing a suitable alternative to *in situ* studies, with the ability of parameters to be controlled over a long period.

This thesis investigated many different aspects of carbon burial and storage in rhodolith beds, however, more research is needed on the effects of climate change on carbon degradation and preservation. In Chapter 5, as labile and refractory were buried in the anoxic zone, I was unable to determine how climate change affects the initial degradation of carbon once it lands in the rhodolith bed. As discussed in Chapter 2, remineralisation rates and burial efficiency play an important role in the ability of systems to store carbon. If remineralisation rates increase, resulting in a lower burial efficiency, systems may sequester less BC playing a smaller role as a NBS to climate change. I recommend that carbon tracer experiments (c.f. Ravaglioli *et al.*, 2019) are used to investigate carbon burial in a future world, with such experiments able to incorporate climate effects on detritivores who play an important role in carbon storage in BC ecosystems.

In this thesis, BC was defined as OC stored by marine systems. However, the assumption that the process of calcification releases CO_2 is often based on theoretical calculations regarding processes at an individual level. Emerging research (Mao 2019) has shown that the ratio of CO_2 released to calcium carbonate precipitated is species-specific, with the potential of phototrophs to recycle calcification-derived CO_2. Further research is needed to determine if CO_2 recycling occurs in other species, with the potential of IC production releasing less CO_2 than previously thought. These findings may result in the definitions of BC being updated to include IC, with the potential of biological IC representing a long-term store of marine carbon.

6.5 Conclusion

The results from this thesis provide further evidence of rhodolith beds as BC, with low decomposition rates and the ability for beds to store terrigenous carbon resulting in the beds being BC repositories. Under future conditions, rhodolith beds were found to be negatively impacted providing further evidence that the distribution of rhodolith beds will decrease in the coming century (Simon-Nutbrown *et al.,* 2020). This thesis provided evidence that once dead, rhodolith beds can continue to store carbon trapped within the SOC stock with both live and dead rhodolith beds expected to continue to store the SOC stock under future conditions. If the role of rhodolith beds as BC repositories are ignored, there is the danger that beds will be damaged. Not only would this result in the loss of an ecologically and commercially important ecosystem, but could result in ancient carbon stored in the SOC being partially remineralised and reintroduced into the atmosphere, further exacerbating the climate crisis.

Chapter 7 Reference list

á Norði, G., Glud, R.N., Simonsen, K., and Gaard, E., 2018. Deposition and benthic mineralization of organic carbon: A seasonal study from Faroe Islands. *J. Mar. Syst.* 177: 53–61.

Abella, E., Barberá, C., Borg, J.A., Hall-Spencer, J., 2014. Maerl grounds: Habitats of high biodiversity in European seas. BIOMAERL project.

Aguado-Giménez, F., and Ruiz-Fernández, J.M., 2012. Influence of an experimental fish farm on the spatio-temporal dynamic of a Mediterranean maërl algae community. *Mar. Environ. Res.* 74: 47–55.

Aguirre, J., Riding, R., and Braga, J.C., 2000. Diversity of coralline red algae: origination and extinction patterns from the early Cretaceous to the Pleistocene. *Palebiology* 26: 651–667.

Ahmed, N., and Glaser, M., 2016. Coastal aquaculture, mangrove deforestation and blue carbon emissions: Is REDD+ a solution? *Mar. Policy.* 66: 58–66.

Ainley, L.B., and Bishop, M.J., 2015. Relationships between estuarine modification and leaf litter decomposition vary with latitude. *Estuar. Coat. Shelf. Sci.* 164: 244–252.

Al-Haj, A.N., and Fulweiler, R.W., 2020. A synthesis of methane emissions from shallow vegetated coastal ecosystems. *Glob. Chang. Biol.* 26: 2988–3005.

Alongi, D.M., 2014. Carbon cycling and storage in mangrove forests. *Ann. Rev. Mar. Sci.* 6: 195–219.

Alongi, D.M., 2012. Carbon sequestration in mangrove forests. Carbon Manag. 3(3): 313–322.

Anderson, C.M., *et al.,* 2019. Natural climate solutions are not enough. *Science* 363: 6430.

Anderson, K., and Peters, G., 2016. The trouble with negative emissions. *Science* 354: 182-183.

Anthony, K.R.N., *et al.*, 2008. Ocean acidification causes bleaching and productivity loss in coral reef builders. *Proc. Natl. Acad. Sci.* 105: 17442–17446.

Appleby, P.G., 2001. Chronostratigraphic techniques in recent sediments. In: Tracking Environmental Change Using Lake Sediments. Vol. 1: Basin Analysis, Coring, and Chronological Techniques [Last, W.M. and Smol, J.P. (eds.)]. Kluwer Academic Publishers, Dordrecht. 171-203pp.

Appleby, P.G., Richardson, N., and Nolan, P.J., 1992. Self-absorption corrections for well-type germanium detectors. *Nucl. Inst.* and *Methods B*, 71: 228-233.

Appleby, P.G., *et al.*, 2986. ^{210}Pb dating by low background gamma counting. *Hydrobiologia*, 141: 21-27.

Armstrong McKay, D.I., *et al.*, 2022. Exceeding 1.5°C global warming could trigger multiple climate tipping points. *Science* 377: 1171.

Arndt, S., *et al.*, 2013. Quantifying the degradation of organic matter in marine sediments: A review and synthesis. *Earth Sci. Rev.* 123: 53-86.

Arnosti, C., Jorgenson, B.B., Sagemann, J., and Thamdrump, B., 1998. Temperature dependence of microbial degradation of organic matter in marine sediments: Polysaccharise hydrolysis, oxygen consumption and sulphate reduction. *Mar. Ecol. Prog. Ser.* 165: 59–70.

Asmala, E., *et al.*, 2018. Eutrophication leads to accumulation of recalcitrant autochthonous organic matter in coastal environments. *Global Biogeochem. Cycles*, 32(11): 1673-1687.

Attard, K.M., Hancke, K., Sejr, M.K., and Glud, R.N., 2016. Benthic primary production and mineralization in a High Arctic Fjord: In situ assessments by aquatic eddy covariance. *Mar. Ecol. Prog. Ser*. 554: 35–50.

Attard, K.M., *et al.*, 2015. Benthic oxygen exchange in a live coralline algal bed and an adjacent sandy habitat: an eddy covariance study. *Mar. Eco. Prog. Ser.* 535: 99-115.

Atwood, T.B., *et al.*, 2018. Predators shape sedimentary organic carbon storage in a coral reef ecosystem. *Front. Eco. Evo.* 6, 110.

Austin, W.E.N., *et al.,* 2021. Blue carbon stock in Scottish saltmarsh soils. *Scottish Marine and Freshwater Science,* 12(13): 37pp.

Baldocchi, D., and Penuelas, J. 2019. Natural carbon solutions are not large or fast enough. *Glob. Chan. Bio.* 00: 1.

Balmonte, J.P., *et al.,* 2020. Sharp contrasts between freshwater and marine microbial enzymatic capabilities, community composition, and DOM pools in a NE Greenland fjord. *Limnol. Oceanogr.* 65: 77–95.

Barange, M., *et al.,* 2014. Impacts of climate change on marine ecosystem production in societies dependent on fisheries. *Nat. Clim. Chang.* 4: 211–216.

Barbera, C., *et al.,* 2017. Maerl beds inside and outside a 25-year-old no-take area. *Mar. Ecol. Prog. Ser.* 572: 77-90.

Barbera, C., *et al.,* 2003. Conservation and management of northeast Atlantic and Mediterranean maerl beds. *Aquat. Conserv.* 13: 65–76.

Barbier, E.B., *et al.,* 2011. The value of estuarine and coastal ecosystem services. *Ecol. Monogr.* 81(2): 169–193.

Barnes, D.K., *et al.,* 2020. Blue carbon gains from glacial retreat along Antarctic fjords: What should we expect? *Glob. Change Biol.* 26: 2750-2755.

Barnes, D.K.A., 2017. Polar zoobenthos blue carbon storage increases with sea ice losses, because across-shelf growth gains from longer algal blooms outweigh ice scour mortality in the shallows. *Glob. Change Biol. 23*: 5083-5091

Baxter, J.M., *et al.,* 2011. Scotland's marine atlas: Information for the National Marine Plan. https://marine.gov.scot/data-source-types/scotlands-marine-atlas [Assessed: 23/11/2022]

Behera, P., *et al.,* 2019. Spatial and temporal heterogeneity in the structure and function of sediment bacterial communities of a tropical mangrove forest. *Environ. Sci. Pollut. Res.* 26: 3893–3908

Behrenfeld, M.J., *et al.,* 2006. Climate-driven trends in contemporary ocean productivity. *Nature* 444: 752-755.

Bergamaschi, B.A., *et al.*, 1997. The effect of grain size and surface area on organic matter, lignin and carbohydrate concentration, and molecular compositions in Peru Margin sediments. *Geochim. Cosmochim. Acta* 61: 1247–1260.

Bernard, G., *et al.,* 2019. Declining maerl vitality and habitat complexity across a dredging gradient: Insights from in situ sediment profile imagery (SPI). *Sci. Rep.* 9: 16463.

Bianchi, T.S., *et al.,* 2020. Fjords as aquatic critical zones (ACZs). *Earth-Sci Rev*. 203: 103145.

Bianchi, T.S., 2011. The role of terrestrially derived organic carbon in the coastal ocean: A changing paradigm and the priming effect. *Proc. Natl. Acad. Sci.* 108: 19473–19481.

Billerbeck, M., Røy, H., Bosselmann, K., and Huettel, M., 2007. Benthic photosynthesis in submerged Wadden Sea intertidal flats. *Estuar. Coast. Shelf Sci.* 71: 704–716.

Birkett, D.A, Maggs, C, and Dring, M.J., 1998. Maerl: An overview of dynamics and sensitivity characteristics for conservation management of marine SACs. *UK Marine SACs Project.*

Black, K.E., Smeaton, C., Turrell, W.R., and Austin, W.E.N., 2022. Assessing the potential vulnerability of sedimentary carbon stores to bottom trawling disturbance within the UK EEZ. *Front. Mar. Sci.* 9:892892.

Blake, C., Maggs, C., and Reimer, P., 2007. Use of radiocarbon dating to interpret past environments of maerl beds. In: *Ciencias Marinas*. Universidad Autonoma de Baja California, pp. 385–397

Bosence, D., and Wilson, J., 2003. Maerl growth, carbonate production rates and accumulation rates in the northeast Atlantic. *Aquat. Conserv. 13*: S21-S31.

Bouillon, S., *et al.,* 2008. Mangrove production and carbon sinks: A revision of global budget estimates. *Global Biogeochem. Cycles* 22: GB2013.

Bourgeois, S., Archambault, P., and Witte, U., 2017. Organic matter remineralization in marine sediments: A Pan-Arctic synthesis. *Global Biogeochem Cycles* 31: 190–213.

Brodie, J., *et al.*, 2014. The future of the northeast Atlantic benthic flora in a high CO_2 world. *Ecol. Evol.* 4 (13): 2787–2798.

Bronk Ramsey, 2021. OxCal Verdon 4.4. https://c14.arch.ox.ac.uk/oxcal.html [Accessed 20/07/2022]

Büdenbender, J., Riebesell, U., Form, A., 2011. Calcification of the Arctic coralline red algae *Lithothamnion glaciale* in response to elevated CO_2. *Mar. Ecol. Prog. Ser.* 441: 79–87.

Buesseler, K.O., *et al.*, 2007. Revisiting carbon flux through the ocean's twilight zone. *Science* 316: 567-570.

Bunker, F.StP.D., *et al.*, 2015. Site condition monitoring of maerl beds and seagrass beds in the Sound of Barra SAC 2015 – diving survey, Scottish Natural Heritage Research Report No. 924.

Burdett, H.L., *et al.*, 2018. Community-level sensitivity of a calcifying ecosystem to acute in situ CO_2 enrichment. *Mar. Ecol. Prog. Ser.* 587: 73–80.

Burdett, H.L., Kamenos, N.A., and Law, A., 2011. Using coralline algae to understand historic marine cloud cover. *Palaeogeogr. Palaeoclimatol. Palaeoecol.* 302: 65-70.

Burdige, D.J., 2007. Preservation of organic matter in marine sediments: Controls, mechanisms, and an imbalance in sediment organic carbon budgets? *Chem Rev* 107: 467–485.

Burdige, D.J., 2005. Burial of terrestrial organic matter in marine sediments: A re-assessment. *Glob. Bio. Cycl.* 19: GB4011.

Burrows, M.T., *et al.*, 2014. Assessment of blue carbon resources in Scotland's inshore marine protected area network. *Scottish Natural Heritage Commissioned Report No. 957.*

Burrows, M.T., *et al.,* 2014. Assessment of carbon budgets and potential blue carbon stores in Scotland's coastal and marine environment. *Scottish Natural Heritage Commissioned Report No. 761.*

Burrows M., 2008. Wave exposure indices from digital coastlines and the prediction of rocky shore community structure. *Mar. Eco. Prog. Ser.* 353: 1-12.

Camargo, J.A and Alonso, Á., 2006. Ecological and toxicological effects of inorganic nitrogen pollution in aquatic ecosystems: A global assessment. *Environ. Int.* 32: 831–849.

Campbell, D. and Marchbank, M. 2013. Herbivore impact assessment of the Torridon Forest SSSI. Scottish Natural Heritage Commissioned Report No. 575.

Canadell, J.G., *et al.,* 2007. Contributions to accelerating atmospheric CO_2 growth from economic activity, carbon intensity, and efficiency of natural sinks. *Proc. Natl. Acad. Sci.* 104 (47): 18866–18870.

Canfield, D.E., 1994. Factors influencing organic carbon preservation in marine sediments. *Chem. Geol.* 114, 315–329.

Canfield, D.E., *et al.,* 1993. Pathways of organic carbon oxidation in three continental margin sediments. *Mar. Geol.* 113: 27-40.

Chambers, L.G., *et al.,* 2018. How well do restored intertidal oyster reefs support key biogeochemical properties in a coastal lagoon? *Estuaries Coast.* 41: 784-799.

Chen, Z., *et al.,* 2022. Organic carbon remineralization rate in global marine sediments: A review. *Reg Stud Mar Sci.* 49: 102112.

Chen. J., *et al.,* 2020. The carbon stock and sequestration rate in tidal flats from coastal China. *Global. Biogeochem. Cycles* 34: e2020GB006772.

Chen, G., *et al.,*2017. Mangroves as a major source of soil carbon storage in adjacent seagrass meadows. *Sci Rep* 7: 42406.

Chmura, G.L., Anisfeld, S.C., Cahoon, D.R., and Lynch, J.C., 2003. Global carbon sequestration in tidal, saline wetland soils. *Global Biogeochem. Cycles* 17(4): 1111.

Church, J.A., *et al.,* 2013. Sea Level Change. In: Climate Change 2013: The Physical Science Basis. Contribution of Working Group I to the Fifth Assessment Report of the Intergovernmental Panel on Climate Change [Stocker, T.F., *et al*. (eds.)]. Cambridge University Press, Cambridge, UK and New York, NY, USA: 493–499pp.

Cisneros-Montemayor, A.M., *et al.,* 2019. Social equity and benefits as the nexus of a transformative Blue Economy: A sectoral review of implications. *Mar. Policy* 109: 103702.

Cornwall, C.E., Diaz-Pulido, G., Comeau, S., 2019. Impacts of ocean warming on coralline algae calcification: Meta-analysis, knowledge gaps and key recommendations for future research. *Front. Mar. Sci.* 6: 186.

Cortés, J., *et al.*, 2018. Habitat characteristics provide insights of carbon storage in seagrass meadows. *Mar. Pollut. Bull.* 134: 106–117.

Costa, M., Lovelock, C., Waltham, N., and Macreadie, P.I. 2020. Blue carbon opportunities in Queensland: how much and where? A report provided to the Land Restoration Fund, Queensland Government. Deakin University.

Coppari, M., Zanella, C., and Rossi, S. 2019. The importance of coastal gorgonians in the blue carbon budget. *Sci Rep 9*, 1-12.

Costanza, R., *et al.,* 1997. The value of the world's ecosystem services and natural capital. *Nature* 387, 253–260.

Costanza, R., *et al.,* 2008. The value of coastal wetlands for hurricane protection. *Ambio*. 37(4): 241-8.

Cui, X., Bianchi, T.S., Savage, C., and Smith, R.W., 2016. Organic carbon burial in fjords: Terrestrial versus marine inputs. *Earth Planet. Sci. Lett.* 451: 41–50.

Dahl, M., *et al.*, 2016. Sediment properties as important predictors of carbon storage in *Zostera marina* meadows: A comparison of four European areas. *PLoS One* 11(12): e0167493.

Dahl, M., *et al.,* 2018. Increased current flow enhances the risk of organic carbon loss from *Zostera marina* sediments: Insights from a flume experiment. *Limnol. Oceanogr.* 63: 2793–2805.

Dame, R.F., Zingmark, R.G., and Haskin, E. 1984. Oyster reefs as processors of estuarine materials. *J. Exp. Mar. Biol. Ecol.* 83: 239-247.

Dauwe, B., Middelburg, J.J., and Herman, P.M.J., 2001. Effect of oxygen on the degradability of organic matter in subtidal and intertidal sediments of the North Sea area. *Mar. Ecol. Prog. Ser.* 215: 13–22.

De Grave, S., *et al.,* 2000. A study of selected maërl beds in Irish waters and their potential for sustainable extraction. Marine Resource Series, Marine Institute.

de Goeij, J.M., *et al.,* 2013. Surviving in a marine desert: The sponge loop retains resources within coral reefs. *Science* 342: 108–110.

Diaz, R.J., and Rosenberg, R., 2008. Spreading dead zones and consequences for marine ecosystems. *Science* 321: 926–929.

Diaz, R.J., and Rosenberg, R., 1995. Marine benthic hypoxia: A review of its ecological effects and the behavioural responses of benthic macrofauna. *Oceanogr. Mar. Biol.* 33: 245–303.

Dickson, A. G., Sabine, C. L., and Christian, J. R. (eds.), 2007, Guide to best practices for ocean CO_2 measurements., 191 pp., PICES Special Publication 3.

Dickson A.G., 1990. Standard potential of the reaction: AgCl(s) + 1/2H_2(g) = Ag(s) + HCl(aq), and the standard acidity constant of the ion HSO_4^- in synthetic sea water from 273.15 to 318.15 K. *J. Chem. Thermodyn.* 22: 113-127.

Djukic, I., *et al.,* 2018. Early-stage litter decomposition across biomes. Sci Tot. Environ. 628–629: 1369–1394.

Donato, D.C., *et al.,* 2011. Mangroves are among the most carbon-rich forests in the tropics. *Nat. Geosci.* 4: 293–297.

Doney, S.C., Fabry, V.J., Feely, R.A., Kleypas, J.A., 2009. Ocean acidification: The other CO_2 problem. *Ann. Rev. Mar. Sci.* 1: 169–192.

Duarte, C.M., *et al.*, 2013a. The role of coastal plant communities for climate change mitigation and adaptation. *Nat. Clim. Chang.* 3: 961-969.

Duarte, C.M., Sintes, T., and Marba, N., 2013b. Assessing the CO_2 capture potential of seagrass restoration projects. *J. Appl. Ecol.* 50: 1341-1349.

Duarte, C.M., Kennedy, H., Marbà, N., and Hendriks, I., 2011. Assessing the capacity of seagrass meadows for carbon burial: Current limitations and future strategies. *Ocean Coast. Manag.* 51: 671–688.

Duarte, C.M., Middelburg, J.J., Caraco, N., 2005. Major role of marine vegetation on the oceanic carbon cycle. *Biogeosciences* 2: 1–8.

Dunbar *et al.*, 2016. AMS 14C dating at the Scottish Universities Environmental Research Centre (SUERC) Radiocarbon Dating Laboratory. *Radiocarbon* 58(1):9-23.

Edward, A., *et al.*, 2009. Home-field advantage accelerates leaf litter decomposition in forests. *Soil Biol. Biochem.*, 41(3): 606-610.

M., Ekström, H.J., Fowler, C.G., Kilsby, P.D., Jones. 2005. New estimates of future changes in extreme rainfall across the UK using regional climate model integrations. 2. Future estimates and use in impact studies. *Journal of Hydrology*, 300 (1–4): 234-251.

Epstein, G., *et al.*,2022. The impacts of mobile demersal fishing on carbon storage in seabed sediments. *Glob. Change. Biol.*, 28(9): 2875-2894.

European Commission (COM), 2016. The Habitats Directive - Environment - European Commission. EU Nat. Law. [WWW Document]. URL https://ec.europa.eu/environment/nature/natura2000/index_en.htm (accessed 10.23.22).

Fabricius, K.E., *et al.*, 2015. In situ changes of tropical crustose coralline algae along carbon dioxide gradients. *Sci. Rep.* 5: 9537.

Fabry, V.J., Seibel, B.A., Feely, R.A., Orr, J.C., 2008. Impacts of ocean acidification on marine fauna and ecosystem processes. ICES Mar. Sci. 65, 414–432.

Farriols, M.T., *et al.*, 2022. Recovery Signals of Rhodoliths Beds since Bottom Trawling Ban in the SCI Menorca Channel (Western Mediterranean). *Diversity* 14(20).

Feely, R.A., Doney, S.C., Cooley, S.R., 2014. Ocean acidification: present conditions and future changes in a high-CO_2 world. *Oceanography* 22: 36–47.

Feely, R.A., *et al.,* 2004. Oxygen utilization and organic carbon remineralization in the upper water column of the Pacific Ocean. *J. Oceanogr.* 60: 45-52.

Figuerola, B., *et al.*, 2021. A review and meta-analysis of potential impacts of ocean acidification on marine calcifiers from the Southern Ocean. *Front. Mar. Sci.* 8: 584445.

Fodrie, F.J., *et al.*, 2017. Oyster reefs as carbon sources and sinks. *Proc. Royal Soc. B.* 284: 20170891.

Foster, M.S., 2001. Rhodoliths: Between rocks and soft places. *J. Phycol.* 37: 659–667.

Fourqurean, J.W., *et al.,* 2012. Seagrass ecosystems as a globally significant carbon stock. *Nat. Geosci.* 5: 505–509.

Frankignoulle, M., and Canon, C., 1994. Marine calcification as a source of carbon dioxide: Positive feedback of increasing atmospheric CO_2. *Limnol. Oceanogr.* 39(2): 458–462.

Fragkopoulou, E., *et al.*, 2021. Bottom trawling threatens future climate refugia of rhodoliths globally. *Front. Mar. Sci*. 7: 5944537.

Friedlingstein, P., *et al.,* 2022. Global carbon budget 2021. *Earth Syst. Sci. Data* 14: 1917–2005.

Garrabou, J., and Ballesteros, E., 2000. Growth of *Mesophyllum alternans* and *Lithophyllum frondosum* (*corallinales, rhodophyta*) in the North-western Mediterranean. *Eur. J. Phycol.* 35, 1–10. https://doi.org/10.1080/09670260010001735571

Gattuso, J., Epitalon, J., Lavigne, H., and Orr, J., 2022. seacarb: Seawater carbonate chemistry. R package version 3.3.1, <https://CRAN.R-project.org/package=seacarb>

Gattuso, J.P., *et al.*, 2000. Calcification does not stimulate photosynthesis in the zooxanthellate scleractinian coral *Stylophora pistillata*. *Limnol. Oceanogr. 45*: 246-250.

Gattuso, J.P., Allemand, D., and Frankignoulle, M., 1999. Photosynthesis and calcification at cellular, organismal and community levels in coral reefs: A review on interactions and control by carbonate chemistry. Amer. Zool. 39: 160–183.

Gattuso, J.P., Frankignoulle, and M., Wollast, R., 1998. Carbon and carbonate metabolism in coastal aquatic ecosystems. *Annu. Rev. Ecol. Syst.* 29: 405–434.

Gattuso, J.P., Pichon, M., and Frankignoulle, M., 1995. Biological control of air-sea CO_2 fluxes: effect of photosynthetic and calcifying marine organisms and ecosystems. Mar. Ecol. Prog. Ser. 129: 307–312.

Gattuso, J.P., Pichon, M., Delesalle, B., and Frankignoulle, M., 1993. Community metabolism and air-sea CO_2 fluxes in a coral reef ecosystem (Moorea, French Polynesia). *Mar. Ecol. Prog. Ser.* 96, 259–267.

Githaiga, M., Frouws, A.M., Kairo, J.G., and Huxham, M. 2019. Seagrass removal leads to rapid changes in fauna and loss of carbon. *Front. Ecol. Evol.* 7:62.

Glud, R.N., *et al.*, 2016. Benthic carbon mineralization and nutrient turnover in a Scottish sea loch: an integrative in situ study. *Aquat. Geochem.* 22: 443-467.

Glud, R.N., 2008. Oxygen dynamics of marine sediments. *Mar. Biol. Res.* 4(4): 243–289.

Glud, R. N., Kühl, M., Wenzhöfer, F. and Rysgaard, S., 2002. Benthic diatoms of a high Arctic fjord (Young Sound, NE Greenland): importance for ecosystem primary production. *Mar. Ecol. Prog. Ser.* 238: 15-29.

Glud, R. N., *et al.*, 2000. Benthic carbon mineralization in a high-Arctic sound (Young Sound, NE Greenland). *Mar. Ecol. Prog. Ser.* 206: 59-71.

Goldstein, A., *et al.,* 2020. Protecting irrecoverable carbon in Earth's ecosystems. *Nat. Clim. Chang.* 10: 287–295.

Goreau, T., 1961. On the relation of calcification to primary productivity in reef building organisms (University of Miami Press).

Grall, J., and Hall-Spencer, J.M., 2003. Problems facing maerl conservation in Brittany. *Aquatic Conserv: Mar and Freshw. Ecosyst.* 13: S55-S64.

Griscom, B.W., *et al.,* 2017. Natural climate solutions. *Proc. Natl. Acad. Sci.* 114 (44): 11645–11650.

Griscom, B.W., *et al.,* 2019. We need both natural and energy solutions to stabilize our climate. *Glob. Chang. Biol.* 25: 1889-1890.

Hall, P.O.J., *et al.,* 2017. Influence of natural oxygenation of Baltic proper deep water on benthic recycling and removal of phosphorus, nitrogen, silicon and carbon. Front. Mar. Sci. *4*: 27.

Hall-Spencer, J.M., Kelly, J., and Maggs, C.A., 2010. Assessment of maerl beds in the OSPAR area and the development of a monitoring program, Ireland.

Hall-Spencer, J.M., *et al.,* 2008. Volcanic carbon dioxide vents show ecosystem effects of ocean acidification. *Nature* 454: 96-99.

Hall-Spencer, J.M., and Moore, P.G., 2000. Scallop dredging has profound, long-term impacts on maerl habitats. *ICES J. Mar. Sci.* 57(5): 1407–1415.

Hancke, K., and Glud, R.N., 2004. Temperature effects on respiration and photosynthesis in three diatom-dominated benthic communities. *Aquatic Microbial. Ecology* 37: 265–281.

Hansen, J.C.R., and Reidenbach, M.A., 2013. Seasonal growth and senescence of a *Zostera marina* seagrass meadow alters wave-dominated flow and sediment suspension within a coastal bay. *Estuaries Coasts* 36: 1099–1114

Harley, C.D.G., *et al.,* 2012. Effects of climate change on global seaweed communities. *J. Phycol.* 48: 1064-1078.

Harris, D.B., *et al.,* 2007. Biotope mapping of the Sound of Barra, Scotland. Scottish Natural Heritage Commissioned Report No.258 (ROAME No. F06PA04).

Harrison, W., and Cota, G. 1991. Primary production in polar waters: relation to nutrient availability. *Polar Res.* 10: 87-104.

Hastings, R.A., *et al.,* 2020. Climate change drives poleward increases and equatorward declines in marine species. *Curr. Biol.* 30: 1572-1577.

Hedges, J.I., Keil, R.G., and Benner, R., 1997. What happens to terrestrial organic matter in the ocean? *Org. Geochem.* 27(5/6): 195–212.

Hedges, J.I., and Keil, R.G., 1995. Sedimentary organic matter preservation: an assessment and speculative synthesis. *Mar. Chem.* 49: 81–115.

Hemingway, J.D. *et al.,* 2019. Mineral protection regulates long-term global preservation of natural organic carbon. *Nature* 570: 228–231.

Henson, S., Le Moigne, F., and Giering, S. 2019. Drivers of carbon export efficiency in the global ocean. *Global. Biogeochem. Cycles* 33: 891-903.

Higgins, C.B., Stephenson, K., Brown, B.L., 2011. Nutrient bioassimilation capacity of aquacultured oysters: Quantification of an ecosystem service. *J. Environ. Qual.* 40: 271–277.

Hill, R., *et al.,* 2015. Can macroalgae contribute to blue carbon? An Australian perspective. *Limnol. Oceanogr.* 60: 1689-1706.

Hoegh-Guldberg, O., and Bruno, J.F., 2010. The impact of climate change on the world's marine ecosystems. *Science* 328: 1523–1529.

Hopwood, M.J., *et al.,* 2019. Review article: How does glacier discharge affect marine biogeochemistry and primary production in the Arctic? *Cryosphere,* 14: 1347–1383.

Howard, J., *et al.,* 2017. Clarifying the role of coastal and marine systems in climate mitigation. *Front. Ecol. Environ.* 15(1): 42–50.

Hughes, T.P., *et al.,* 2017. Global warming and recurrent mass bleaching of corals. *Nature* 543: 373–377.

Hulthe, G., Hulth, S., and Hall, P.O.J. 1998. Effect of oxygen on the degradation rate of refractory and labile organic matter in continental margin sediments. *Geochim. Cosmochim. Acta* 62: 1319-1328.

Hunt, C., *et al.,* 2020. Quantifying marine sedimentary carbon: A new spatial analysis approach using seafloor acoustics, imagery, and ground-truthing data in Scotland. *Front. Mar. Sci. 7*: 588.

Infantes, E., *et al.,* 2012. Effect of a seagrass (*Posidonia oceanica*) meadow on wave propagation. *Mar. Ecol. Prog. Ser.* 456: 63–72.

Inglis, G.N., *et al.,* 2022. Enhanced terrestrial carbon export from East Antarctica during the early Eocene. *Paleoceanogr. Paleoclimatol.* 37(2): e2021PA004348.

IPCC 2022: Climate Change 2022: Impacts, adaptation and vulnerability. Contribution of working group II to the sixth assessment report of the Intergovernmental Panel on Climate Change [Pörtner, H.-O., *et al.* (eds.)]. Cambridge University Press. Cambridge University Press, Cambridge, UK and New York, NY, USA: 3056pp

IPCC, 2014. 2013 Supplement to the 2006 IPCC guidelines for national greenhouse gas inventories: Wetlands [Hiraishi, T., *et al.,* (eds)]. Published: IPCC, Switzerland.

Jankowska, E., Michel, L.N., Zaborska, A., and Włodarska-Kowalczuk, M., 2016. Sediment carbon sink in low-density temperate eelgrass meadows (Baltic Sea). *J. Geophys. Res. Biogeosci.* 121: 2918–2934.

Jarraud, M., and Steiner, A., 2012. Summary for policymakers, managing the risks of extreme events and disasters to advance climate change adaptation: Special report of the Intergovernmental Panel on Climate Change.

Jokiel, P.L., *et al.,* 2008. Ocean acidification and calcifying reef organisms: A mesocosm investigation. *Coral Reefs* 27: 473–483.

Jørgensbye, H.I.Ø., and Halfar, J., 2017. Overview of coralline red algal crusts and rhodolith beds (*Corallinales, Rhodophyta*) and their possible ecological importance in Greenland. *Polar Biol* 40: 517–531.

Kamenos, N.A., *et al.*, 2013. Coralline algal structure is more sensitive to rate, rather than the magnitude, of ocean acidification. *Glob. Chang. Biol.* 19: 3621–3628.

Kamenos, N.A., and Law, A., 2010. Temperature controls on coralline algal skeletal growth. *J. Phycol.* 46: 331–335.

Kamenos, N.A., Moore, P.G., Hall-Spencer, J.M., 2004a. Small-scale distribution of juvenile gadoids in shallow inshore waters; what role does maerl play? *ICES Mar. Sci.* 61: 422–429.

Kamenos, N.A., Moore, P.G., Hall-Spencer, J.M., 2004b. Nursery-area function of maerl grounds for juvenile queen scallops *Aequipecten opercularis* and other invertebrates. *Mar. Ecol. Prog. Ser.* 274: 203–205.

Kamenos, N.A., Moore, P., and Hall-Spencer, J., 2003. Substratum heterogeneity of dredged vs un-dredged maerl grounds. *J. Mar. Biolog.* 83: 411-413.

Keeling, R.F., Körtzinger, A., Gruber, N., 2010. Ocean deoxygenation in a warming world. *Ann. Rev. Mar. Sci.* 2: 199–229.

Kell, R.G., Montlucon, D.B., Prahlt, F.G., and Hedges, J.I., 1994. Sorptive preservation of labile organic matter in marine sediments. *Nature* 370: 549–552.

Kelleway, J.J., Trevathan-Tackett, S.M., Baldock, J., and Critchley, L.P., 2022. Plant litter composition and stable isotope signatures vary during decomposition in blue carbon ecosystems. *Biogeochemistry* 158: 147-165.

Kennedy, H., *et al.*, 2010. Seagrass sediments as a global carbon sink: Isotopic constraints. *Global Biogeochem. Cycles* 24: GB4026.

Kennedy, H., *et al.*, 2004. Organic carbon sources to SE Asian coastal sediments. *Estuar. Coast. Shelf. Sci.* 60: 59–68.

Keuskamp, J.A., *et al.,* 2013. Tea Bag Index: A novel approach to collect uniform decomposition data across ecosystems. *Methods Ecol. Evol.* 4: 1070–1075.

Kirwan, M.L., and Mudd, S.M., 2012. Response of salt-marsh carbon accumulation to climate change. *Nature* 489: 550–553.

Koch, M., Bowes, G., Ross, C., Zhang, X.H., 2013. Climate change and ocean acidification effects on seagrasses and marine macroalgae. *Glob. Chang. Biol*. 19: 103–132.

Koziorowska, K., Kuliński, K., and Pempkowiak, J., 2016. Sedimentary organic matter in two Spitsbergen fjords: Terrestrial and marine contributions based on carbon and nitrogen contents and stable isotopes composition. *Cont. Shelf. Res.* 113: 38–46.

Krause-Jensen, D., *et al.,* 2018. Sequestration of macroalgal carbon: The elephant in the blue carbon room. *Biol. Lett.* 14: 20180236.

Krause-Jensen, D., and Duarte, C.M. 2016. Substantial role of macroalgae in marine carbon sequestration. *Nat. Geosci. 9*: 737-742.

Krause-Jensen, D., and Duarte, C.M., 2014. Expansion of vegetated coastal ecosystems in the future. *Arctic. Front. Mar. Sci. 1*(77): 1–10.

Kristensen, E., *et al.,* 2012. What is bioturbation? The need for a precise definition for fauna in aquatic sciences. *Mar. Ecol. Prog. Ser.* 446: 285-302.

Kristensen, E., 1994. Decomposition of macroalgae, vascular plants and sediment detritus in seawater: Use of stepwise thermogravimetry. *Biogeochemistry* 26: 1–24.

Kristensen, E., 1990. Characterization of biogenic organic matter by stepwise thermogravimetry (STG). *Biogeochemistry* 9: 135–159.

Lafon, A., Silva, N., and Vargas, C.A., 2014. Contribution of allochthonous organic carbon across the Serrano River Basin and the adjacent fjord system in Southern Chilean Patagonia: Insights from the combined use of stable isotope and fatty acid biomarkers. *Prog. Oceanogr.* 129: 98–113.

Land Use Consultants 1998. Orkney landscape character assessment, *Nature Scot Review 100.*

Lavery, P.S., Mateo, M.Á., Serrano, and O., Rozaimi, M., 2013. Variability in the carbon storage of seagrass habitats and its implications for global estimates of blue carbon ecosystem service. *PLoS One* 8(9): e73748.

Lee, H.Z.L., *et al.,* 2020. Missing the full story: First estimates of carbon deposition rates for the European flat oyster, *Ostrea edulis*. *Aquat. Conserv.* 30: 2076-2086.

Lee, S.H., Megonigal, P.J., and Kang, H., 2017. How do elevated CO_2 and nitrogen addition affect functional microbial community involved in greenhouse gas flux in salt marsh system. *Microb. Ecol.* 74: 670–680.

Legrand, E., Martin, S., Leroux, C., and Riera, P., 2020. Using stable isotope analysis to determine the effects of ocean acidification and warming on trophic interactions in a maerl bed community. *Mar. Ecol.* 41(5): e12612.

Legrand, E. *et al.,* 2017. Species interactions can shift the response of a maerl community to ocean acidification and warming. *Biogeosciences* 14:5359-5376.

Lehmann, M.F., Bernasconi, S.M., Barbieri, A., and McKenzie, J.A., 2002. Preservation of organic matter and alteration of its carbon and nitrogen isotope composition during simulated and in situ early sedimentary diagenesis. *Geochim. Cosmochim. Acta* 66: 3573–3584.

Liu, J., *et al.*, 2010. Effect of ocean acidification on microbial diversity and on microbe-driven biogeochemistry and ecosystem functioning. *Aquat. Microb. Ecol.* 61: 291–305.

Lohse, L., *et al.,* 1995. Sediment-water fluxes of inorganic nitrogen compounds along the transport route of organic matter in the North Sea. *Ophelia* 41(1): 173–197.

Lovelock, C.E., and Duarte, C.M., 2019. Dimensions of blue carbon and emerging perspectives. *Biol. Lett.* 15: 20180781.

Lueker, T. J., Dickson, A. G., and Keeling, C. D., 2000. Ocean pCO_2 calculated from dissolved inorganic carbon, alkalinity, and equations for K1 and K2: Validation based on

laboratory measurements of CO_2 in gas and seawater at equilibrium. *Mar. Chem.* 70(1-3): 105-119.

Lunt, J., Reustle, J., and Smee, D.L. 2017. Wave energy and flow reduce the abundance and size of benthic species on oyster reefs. *Mar. Ecol. Prog. Ser.* 569: 25-36.

Luo, M., *et al.*, 2018. Benthic carbon mineralization in hadal trenches: insights from in situ determination of benthic oxygen consumption. *Geophys. Res. Lett.* 45: 2752-2760.

Macreadie, P.I., *et al.*, 2021. Blue carbon as a natural climate solution. *Nat. Rev. Earth Environ.*2: 826-839.

Macreadie, P.I., *et al.*, 2019a. The future of blue carbon science. *Nat. Commun.* 10: 3998.

Macreadie, P.I., *et al.*, 2019b. Vulnerability of seagrass blue carbon to microbial attack following exposure to warming and oxygen. *Science Tot. Environ*. 686: 264–275.

Macreadie, P.I., *et al.*, 2021. Blue carbon as a natural climate solution. *Nat. Rev. Earth Environ.*2: 826-839.

Macreadie, P.I., *et al.*, 2017. Addressing calcium carbonate cycling in blue carbon accounting. *Limnol. Oceanogr. Lett.* 2: 195–201.

Macreadie, P.I., *et al.*, 2015. Do ENSO and coastal development enhance coastal burial of terrestrial carbon? *PLOS ONE* 10: e0145136.

Macreadie, P.I., Hughes, A.R., Kimbro, D.L., 2013. Loss of ‘blue carbon’ from coastal salt marshes following habitat disturbance. *PLoS One* 8 (7): e69244.

Macreadie, P.I., *et al.*, 2012. Paleoreconstruction of estuarine sediments reveal human-induced weakening of coastal carbon sinks. *Glob. Chang. Biol.* 18: 891–901.

Malits, A., *et al.*, 2021. Viral-mediated microbe mortality modulated by ocean acidification and eutrophication: Consequences for the carbon fluxes through the microbial food web. *Front. Microbiol.* 12: 635821.

Manis, J.E., Garvis, S.K., Jachec, S.M., and Walters, L.J. 2015. Wave attenuation experiments over living shorelines over time: a wave tank study to assess recreational boating pressures. *J. Coast. Conserv*. 19: 1-11.

Mao, J., 2019. The role of red coralline algal habitats as blue carbon stores. PhD thesis, University of Glasgow, Scotland.

Mao, J., *et al.*, 2020. Carbon burial over the last four millennia is regulated by both climatic and land use change. *Glob. Chang. Biol.* 26: 2496–2504.

Marbà, N., Krause-Jensen, D., Masqué, P., Duarte, C.M., 2018. Expanding Greenland seagrass meadows contribute new sediment carbon sinks. *Sci Rep* 8: 14024.

Marley, A.C.R.G., Smeaton, C., and Austin, W.E.N., 2019. An assessment of the Tea Bag Index method as a proxy for organic matter decomposition in intertidal environments. *J. Geophys. Res. Biogeosci.* 124: 2991–3004

Martin, S., and Hall-Spencer, J.M., 2017. Effects of ocean warming and acidification on rhodolith/maërl beds. In: Rhodolith/Maërl Beds: A Global Perspective [Riosmena-Rodríguez, R., Nelson, W., and Aguirre, J (eds.)]. Coastal Research Library (volume 15). 55–85pp.

Martin, S., *et al.*, 2013. One-year experiment on the physiological response of the Mediterranean crustose coralline alga, *Lithophyllum cabiocha*e, to elevated pCO_2 and temperature. *Ecol. Evol.* 3(3): 676–693.

Martin, S., and Gattuso, J.P., 2009. Response of Mediterranean coralline algae to ocean acidification and elevated temperature. *Glob. Chang. Biol.* 15: 2089–2100.

Martin, S., Clavier, J., Chauvaud, L., and Thouzeau, G., 2007. Community metabolism in temperate maerl beds. I. Carbon and carbonate fluxes. *Mar. Eco. Prog. Ser.* 335: 19-29.

Martin, S., *et al*., 2005. Comparison of *Zostera marina* and maerl community metabolism. *Aquat. Bot.* 83*:* 161-174.

Martone, P.T., Alyono, M., and Stites, S., 2010. Bleaching of an intertidal coralline alga: Untangling the effects of light, temperature, and desiccation. *Mar. Ecol. Prog. Ser.* 416: 57–67.

Mazarrasa, I., *et al.,* 2018. Habitat characteristics provide insights of carbon storage in seagrass meadows. *Mar. Pollut. Bull.* 134: 106–117.

Marzocchi, U., Thamdrup, B., Stief, P., and Glud, R.N. 2018. Effect of settled diatom-aggregates on benthic nitrogen cycling. *Limnol. Oceanogr.* 63: 431-444.

McCoy, S.J., and Kamenos, N.A., 2015. Coralline algae (*Rhodophyta*) in a changing world: Integrating ecological, physiological, and geochemical responses to global change. *J. Phycol.* 51: 6–24.

McCoy, S.J., and Ragazzola, F., 2014. Skeletal trade-offs in coralline algae in response to ocean acidification. *Nat. Clim. Chang.* 4: 719–723.

McLaren, D. A, 2012. A comparative global assessment of potential negative emissions technologies. *Process Saf. Environ. Prot.* 90: 489-500.

McLeod, E., *et al.,* 2011. A blueprint for blue carbon: Toward an improved understanding of the role of vegetated coastal habitats in sequestering CO_2. *Front. Ecol. Environ.* 9 (10), 552–560.

Meinshausen, M., *et al.,* 2011. The RCP greenhouse gas concentrations and their extensions from 1765 to 2300. *Clim Change* 109: 213–241.

Meister, P., *et al.,* 2019. Factors controlling the carbon isotope composition of dissolved inorganic carbon and methane in marine porewater: An evaluation by reaction-transport modelling. *J. Mar. Syst.* 200: 103227.

Mercer, T.M., Bunker, F.StP.D., Howson, C.M., and Kamphausen, L., 2015. Sound of Barra macrobenthic infaunal survey and Eriskay Causeway sediment survey 2015 survey and Eriskay Causeway sediment, Scottish Natural Heritage Research Report No. 951.

Middelburg, J.J., 2019. Primary production: From inorganic to organic carbon. *In: Marine Carbon Biogeochemistry: A Primer for Earth System Scientists.* Springer International Publishing. pp. 9-35.

Middelburg, J., and Levin, L. 2009. Coastal hypoxia and sediment biogeochemistry. *Biogeosciences* 6: 1273–1293.

Middelburg, J.J., *et al.,* 1996. Organic matter mineralization in intertidal sediments along an estuarine gradient. *Mar. Ecol. Prog. Ser.* 132: 157–168.

Moberg, F., and Folke, C., 1999. Ecological goods and services of coral reef ecosystems. *Ecol. Econ*. 29: 215–233.

Mollica, N.R., *et al.,* 2018. Ocean acidification affects coral growth by reducing skeletal density. *Proc. Natl. Acad. Sci.* 115, 1754-1759.

Moritsch, M.M., *et al.,* 2019. Estimating blue carbon sequestration under coastal management scenarios. *Sci. Total Environ.* 777: 145962.

Mueller, P., *et al.,* 2020. Unrecognized controls on microbial functioning in blue carbon ecosystems: The role of mineral enzyme stabilization and allochthonous substrate supply. *Ecol. Evol.* 10: 998–1011.

Mueller, P., *et al.,* 2018. Global change effects on decomposition processes in tidal wetlands: implications from a global survey using standardized litter. *Biogeosciences* 15: 3189–3202.

Multer, H.G. 1988. Growth rate, ultrastructure and sediment contribution of *Halimeda incrassata* and *Halimeda monile,* Nonsuch and Falmouth Bays, Antigua, W.I. *Coral Reefs* 6: 179-186.

Nagelkerken, I., and Connell, S.D., 2015. Global alteration of ocean ecosystem functioning due to increasing human CO_2 emissions. *Proc. Natl. Acad. Sci.* 112: 13272–13277.

Naumann, M.S., *et al.,* 2012. Budget of coral-derived organic carbon in a fringing coral reef of the Gulf of Aqaba, Red Sea. *Journ. Mar. Syst.* 105: 20-29.

Nellemann, C., *et al.,* 2009. Blue carbon: a rapid response assessment. United Nations Environment Programme, GRID-Arendal, www.grida.no

Nilsson, M.M., *et al.,* 2010. Organic carbon recycling in Baltic Sea sediments – An integrated estimate on the system scale based on in situ measurements. *Mar. Chem. 209*: 81-93.

Noisette, F., Egilsdottir, H., Davoult, D., and Martin, S., 2013a. Physiological responses of three temperate coralline algae from contrasting habitats to near-future ocean acidification. *J. Exp. Mar. Biol. Ecol.* 448: 179–187.

Noisette, F., *et al.,* 2013b. Effects of elevated pCO_2 on the metabolism of a temperate rhodolith *Lithothamnion corallioides* grown under different temperatures. *J. Phycol.* 49: 746-757.

Norling, P., and Kautsky, N. 2008. Patches of the mussel *Mytilus* sp. are islands of high biodiversity in subtidal sediment habitats in the Baltic Sea. *Aquat. Biol.* 4: 75-87.

Olesen, B., Krause-Jensen, D., Marbà, N., and Christensen, P.B., 2015. Eelgrass *Zostera marina* in subarctic Greenland: Dense meadows with slow biomass turnover in cold waters. *Mar. Ecol. Prog. Ser.* 518: 107–121.

O'Meara, T., Gibbs, E., and Thrush, S.F., 2018. Rapid organic matter assay of organic matter degradation across depth gradients within marine sediments. *Methods Ecol. Evol.* 9: 245–253.

Oreska, M.P.J., *et al.,* 2018. Non-seagrass carbon contributions to seagrass sediment blue carbon. *Limnol. Oceanogr.* 63: S3–S18.

Pan, Y., *et al.,* 2011. A large and persistent carbon sink in the world's forests. *Science* 333: 988–993.

Parker, R., *et al.,* 2020. Carbon stocks and accumulation analysis for Secretary of State (SoS) region. *Cefas project report for Defra*. 40pp.

Peck, L.S., *et al.,* 2010. Negative feedback in the cold: ice retreat produces new carbon sinks in Antarctica. *Glob. Change Biol.* 16: 2614-2623.

Peña, V., and Bárbara, I., 2008. Maërl community in the north-western Iberian Peninsula: A review of floristic studies and long-term changes. *Aquat Conserv*. 18: 339-366.

Pérez, A., Libardoni, B.G., and Sanders, C.J., 2018. Factors influencing organic carbon accumulation in mangrove ecosystems. *Biol. Lett*. 14: 20180237.

Perry, C.T., *et al.,* 2015. Linking reef ecology to island building: Parrotfish identified as major producers of island-building sediment in the Maldives. *Geology* 43: 503-506. 10.

Peters, G.P., and Hausfather, Z., 2020. Emissions - the "business as usual" story is misleading. *Nature* 577: 618–620.

Pickett, S.T.A., 1989. Space-for-Time Substitution as an Alternative to Long-Term Studies. In: Long-Term Studies in Ecology: Approaches and Alternatives [Likens, G.E. (ed.)]. Springer-Verlag, NY.

Pidgeon, E., 2009. Carbon Sequestration by coastal marine habitats: important missing sinks. In: The management of natural coastal carbon sinks [D. Laffoley, and G. Grimsditch, (eds.)]. IUCN, pp. 53.

Piepenburg, D., *et al.*,1995. Partitioning of benthic community respiration in the Arctic (northwestern Barents Sea). *Mar. Ecol. Prog. Ser.* 118: 199-213.

Pires J.C.M., 2019. Negative emissions technologies: A complementary solution for climate change mitigation. *Sci. Total. Environ.* 672: 502-514.

Porter, J., *et al.,* 2020. Blue carbon audit of Scottish waters. Scottish Marine and Freshwater Science *11*: 0-96.

Porzio, L., Garrard, S.L., and Buia, M.C., 2013. The effect of ocean acidification on early algal colonization stages at natural CO_2 vents. *Mar. Biol.* 160: 2247-2259.

Porzio, L., Buia, M.C., and Hall-Spencer, J.M., 2011. Effects of ocean acidification on macroalgal communities. *J. Exp. Mar. Biol. Ecol.* 400: 278–287.

Potouroglou, M., *et al.,* 2021. The sediment carbon stocks of intertidal seagrass meadows in Scotland. *Estuar. Coast. Shelf. Sci.* 258: 107442.

Potouroglou, M., *et al.*, 2019. Measuring the role of seagrasses in regulating sediment surface elevation. *Sci. Reports.* 7: 11917.

Queirós, A.M., *et al.,* 2019. Connected macroalgal-sediment systems: Blue carbon and food webs in the deep coastal ocean. Ecol. Monogr. 89(3): e01366.

Qui-Minet, Z.N., Davoult, D., Grall, J., and Martin, S., 2022. The relative contribution of fleshy epiphytic macroalgae to the production of temperate maerl (rhodolith) beds. *Mar. Ecol. Prog. Ser*. 693: 69–82.

Qui-Minet, Z.N., *et al.*, 2019. Combined effects of global climate change and nutrient enrichment on the physiology of three temperate maerl species. *Ecol. Evol.* 9: 13787–13807.

Rabalais, N.N., Turner, R.E., Wiseman, W.J., 2002. Gulf of Mexico hypoxia, A.K.A. "the dead zone". *Annu. Rev. Ecol. Syst*. 33: 235–263.

Ragazzola, F., *et al.*, 2013. Phenotypic plasticity of coralline algae in a high CO_2 world. *Ecol. Evol.* 3: 3436–3446.

Ragazzola, F., *et al.*, 2012. Ocean acidification weakens the structural integrity of coralline algae. *Glob. Chang. Biol*. 18: 2804–2812.

Ravaglioli, C., *et al.,* 2020. Ocean acidification alters meiobenthic assemblage composition and organic matter degradation rates in seagrass sediments. *Limnol. Oceanogr*. 65: 37–50.

Ravaglioli, C., *et al.,* 2019. Ocean acidification and hypoxia alter organic carbon fluxes in marine soft sediments. *Glob. Change Biol.* 25, 4165-4178.

Reef, R., *et al.,* 2017. Using eDNA to determine the source of organic carbon in seagrass meadows. *Limnol. Oceanogr.* 62(3): 1254–1265.

Rees, S.A., Opdyke, B.N., Wilson, P.A., and Henstock, T.J. 2007. Significance of *Halimeda bioherms* to the global carbonate budget based on a geological sediment budget for the Northern Great Barrier Reef, Australia. *Coral Reefs* 26: 177-188.

Reimer, P.J., *et al.*, 2013. IntCal13 and Marine13 Radiocarbon Age Calibration Curves 0–50,000 Years cal BP. *Radiocarbon* 55: 1869–1887.

Rhein, M., *et al.* 2013. Observations: Ocean. In: *Climate Change 2013: The Physical Science Basis. Contribution of Working Group I to the Fifth Assessment Report of the Intergovernmental Panel on Climate Change* [Stocker, T.F., *et al.* (eds.)]. Cambridge University Press, Cambridge, UK and New York, NY, USA: 257-315.

Richards, J., 1998. Western Isles landscape character assessment. *Scottish Natural Heritage Assessment 92.*

Ridge, J.T., Rodriguez, A.B., and Fodrie, F.J. 2017. Salt marsh and fringing oyster reef transgression in a shallow temperate estuary: Implications for restoration, conservation and blue carbon. *Estuaries Coast.* 40: 1013-1027.

Riosmena-Rodríguez, R., Nelson, W., and Aguirre, J., (eds.) 2017. Rhodolith / Maërl Beds : A Global Perspective. Coastal Research Library (volume 15).

Rivkin, R.B., and Legendre, L. 2001. Biogenic carbon cycling in the upper ocean: effects of microbial respiration. *Science* 291: 2398-2400.

Rix, L., *et al.*,2017. Differential recycling of coral and algal dissolved organic matter via the sponge loop. *Funct. Ecol.* 31: 778-789.

Robador, A., Brüchert, V., and Jørgensen, B.B., 2009. The impact of temperature change on the activity and community composition of sulfate-reducing bacteria in arctic versus temperate marine sediments. *Environ. Microbiol.* 11: 1692–1703.

Robador, A., *et al.,* 2016. Activity and community structures of sulfate-reducing microorganisms in polar, temperate and tropical marine sediments. *ISME Journal* 10: 796–809.

Röhr, M.E., *et al.,* 2018. Blue carbon storage capacity of temperate eelgrass (*Zostera marina*) meadows. *Glob. Biogeochem. Cycles.* 32: 1457-1475.

Röhr, M.E., Boström, C., Canal-Vergés, P., and Holmer, M. 2016. Blue carbon stocks in Baltic Sea eelgrass (*Zostera marina)* meadows. *Biogeosciences* 13: 6139-6153.

Rosentreter, J.A., Al-Haj, A.N., Fulweiler, R.W., and Williamson, P., 2021. Methane and nitrous oxide emissions complicate coastal blue carbon assessments. *Global Biogeochem Cycles* 35: e2020GB006858.

Sabine, C.L., *et al.*, 2004. The Oceanic Sink for Anthropogenic CO_2. *Science* 305: 367–371.

Saderne, V., *et al.*,2019. Role of carbonate burial in Blue carbon budgets. *Nat. Commun*. 10, 1-9.

Sala, E., *et al.*, 2021. Protecting the global ocean for biodiversity, food and climate. *Nature* 592: 397–402.

Samper-Villarreal, J., *et al.*, 2016. Organic carbon in seagrass sediments is influenced by seagrass canopy complexity, turbidity, wave height, and water depth. *Limnol. Oceanogr*. 61: 938–952.

Sasmito, S.D., *et al.*, 2022. Organic carbon burial and sources in soils of coastal mudflat and mangrove ecosystems. CATENA *187*: 104414.

Sasmito, S.D., *et al.*, 2020. Mangrove blue carbon stocks and dynamics are controlled by hydrogeomorphic settings and land-use change. *Glob. Chang. Biol.* 26(5): 3028-3039.

Sasmito, S.D., *et al.*, 2019. Effect of land-use and land-cover change on mangrove blue carbon: A systematic review. *Glob. Chang. Biol. 00:*1–12.

Schoenrock, K.M., *et al.*, 2018. Biodiversity of kelp forests and coralline algae habitats in southwestern Greenland. *Diversity* 10 (117).

Schubert, N., *et al.*, 2020. Editorial: Coralline algae: Globally distributed ecosystem engineers. *Front. Mar. Sci.* 7: 352.

Scottish Natural Heritage, 1996. Landscape assessment of Argyll and the Firth of Clyde. *Scottish Natural Heritage Assessment 78.*

Seddon, N., *et al.*, 2021. Getting the message right on nature-based solutions to climate change. *Glob. Chang. Biol.* 27(8): 1518-1546.

Seelen, L.M.S., *et al.,* 2019. An affordable and reliable assessment of aquatic decomposition: Tailoring the Tea Bag Index to surface waters. *Water Res.* 151: 31–43.

Serpetti, N., Heath, M., Rose, M., and Witte, U., 2012. High resolution mapping of sediment organic matter from acoustic reflectance data. *Hydrobiologia* 680: 265–284.

Serrano, O., *et al.,* 2016. Key biogeochemical factors affecting soil carbon storage in *Posidonia meadows*. *Biogeosciences* 13: 4581–4594.

Sheehan, E. v., Bridger, D., and Attrill, M.J., 2015. The ecosystem service value of living versus dead biogenic reef. *Estuar. Coast. Shelf. Sci.* 154: 248–254.

Simpson, L.T., Cherry, J.A., Smith, R.S., and Feller, I.C., 2021. Mangrove encroachment alters decomposition rate in saltmarsh through changes in litter quality. *Ecosystems* 24: 840–854.

Simon-Nutbrown, C., *et al*., 2020. Species distribution modelling predicts significant declines in coralline algae populations under projected climate change with implications for conservation policy. *Front. Mar. Sci.* 7: 575825.

Skudder, P.A., Backus, D.H., Goodwin, D.H., and Johnson, M.E., 2006. Sequestration of carbonate shell material in coastal dunes on the Gulf of California (Baja California Sur, Mexico). *Jour. Coast. Resear. 22*, 611-624.

Shields, M.R., *et al.,* 2017. Carbon storage in the Mississippi River delta enhanced by environmental engineering. *Nat. Geosci.* 10: 846-851.

Smale, D.A., *et al.,* 2018. Appreciating interconnectivity between habitats is key to blue carbon management. *Front. Ecol. Environ*. 16: 71-73.

Smeaton, C., and Austin, W.E.N., 2022a. Quality not quantity: Prioritizing the management of sedimentary organic matter across continental shelf seas. *Geophys. Res. Lett.* 49: e2021GL097481.

Smeaton, C., and Austin, W.E.N., 2022b. Distribution of particulate and dissolved organic carbon in surface waters of northern Scottish fjords. *Estuar. Coast. Shelf Sci.* 274: 107952.

Smeaton, C., *et al.,* 2017. Scotland's forgotten carbon: A national assessment of mid-latitude fjord sedimentary carbon stocks. *Biogeosciences* 14: 5663–5674.

Smeaton, C., *et al.,* 2016. Substantial stores of sedimentary carbon held in mid-latitude fjords. *Biogeosciences* 13: 5771–5787.

Smith, R.W., *et al.,* 2015. High rates of organic carbon burial in fjord sediments globally. *Nature. Geosci.* 8: 450-453.

Smith, A.M., 2014. Growth and calcification of marine bryozoans in a changing ocean. *Biol. Bull*. 226: 203–210.

Smith, S.V. 2013. Parsing the oceanic calcium carbonate cycle: A net atmospheric carbon dioxide source or a sink? (Association for the Sciences of Limnology and Oceanography).

Smith, M.D., *et al*., 2010. Sustainability and global seafood. *Science* 327: 784-786.

Smoak, J.M., Breithaupt, J.L., Smith III, T.J., and Sanders, C.J. 2013. Sediment accretion and organic carbon burial relative to sea-level rise and storm events in two mangrove forests in Everglades National Park. *Catena* 104: 58-66.

Sordo, L., Santos, R., Barrote, I., and Silva, J., 2019. Temperature amplifies the effect of high CO_2 on the photosynthesis, respiration, and calcification of the coralline algae *Phymatolithon lusitanicum*. *Ecol. Evol.* 9: 11000–11009.

Sordo, L., Santos, R., Barrote, I., and Silva, J., 2018. High CO_2 decreases the long-term resilience of the free-living coralline algae *Phymatolithon lusitanicum*. *Ecol. Evol.* 8: 4781–4792.

Spalding, M.D., *et al.,* 2014. The role of ecosystems in coastal protection: Adapting to climate change and coastal hazards. *Ocean Coast. Manag.* 90: 50-57.

Ståhl, H., *et al.,* 2004. Respiration and sequestering of organic carbon in shelf sediments of the oligotrophic northern Aegean Sea. *Mar. Ecol. Prog. Ser.* 269: 33-48.

Stock, B., *et al.,* 2018. Analyzing mixing systems using a new generation of Bayesian tracer mixing models. *PeerJ* 6: e5096.

Stock, B., and Semmens, B., 2016. MixSIAR GUI User Manual. Version 3.1. https://doi.org/10.5281

Sunday, J.M., Bates, A.E., Dulvy, N.K., 2012. Thermal tolerance and the global redistribution of animals. *Nat. Clim. Chang.* 2: 686–690.

Sutton-Grier, A.E., Wowk, K., Bamford, H., 2015. Future of our coasts: The potential for natural and hybrid infrastructure to enhance the resilience of our coastal communities, economies and ecosystems. *Environ. Sci. Policy* 51, 137–148.

Tabuchi, K., Kojima, H., and Fukui, M., 2010. Seasonal Changes in Organic Matter Mineralization in a Sublittoral Sediment and Temperature-Driven Decoupling of Key Processes. *Microb. Ecol.* 60: 551–560.

Takeshita, Y., *et al.,* 2016. Assessment of net community production and calcification of a coral reef using a boundary layer approach. *J. Geophys. Res. Oceans* 121: 5655-5671.

Tanaka, Y., *et al.,* 2008. Production of dissolved and particulate organic matter by the reef-building corals Porites cylindrica and Acropora pulchra. *Bull. Mar. Sci. 82*: 237-245.

Tauran, A., Dubreuil, J., Guyonnet, B., and Grall, J., 2020. Impact of fishing gears and fishing intensities on maerl beds: An experimental approach. *J. Exp. Mar. Biol. Ecol.* 533(472):151472.

Teichert, S., *et al.,* 2014. Arctic rhodolith beds and their environmental controls (Spitsbergen, Norway). *Facies* 60: 15–37.

Thamdrup, B., Hansen, J.W., and Jørgensen, B.B., 1998. Temperature dependence of aerobic respiration in coastal sediment. *FEMS Microbiol. Ecol.* 25: 189–200.

Thomson, A.C.G., *et al.,* 2019. Bioturbator-stimulated loss of seagrass sediment carbon stocks. *Limnol. Oceanogr.* 64: 342–356.

Townsend, M., *et al.,* 2018. The challenge of implementing the marine ecosystem service concept. *Front. Mar. Sci. 5*: 359.

Tremblay, P., *et al.,* 2012. Autotrophic carbon budget in coral tissue: a new ^{13}C-based model of photosynthate translocation. *J. Exp. Biol.* 215: 1384-1393.

Trevathan-Tackett, S.M., *et al.,* 2021. Ecosystem type drives tea litter decomposition and associated prokaryotic microbiome communities in freshwater and coastal wetlands at a continental scale. Sci. Tot. Environ. 782: 146819.

Trevathan-Tackett, S.M., Brodersen, K.E., and Macreadie, P.I., 2020. Effects of elevated temperature on microbial breakdown of seagrass leaf and tea litter biomass. *Biogeochemistry* 151: 171–185.

Trevathan-Tackett, S.M., Thomson, A.C.G., Ralph, P.J., and Macreadie, P.I., 2018. Fresh carbon inputs to seagrass sediments induce variable microbial priming responses. *Science Tot. Environ.* 621: 663–669.

Turrell, W.R., 2020. A compendium of marine related carbon stores, sequestrations and emissions. *Scottish Marine and Freshwater Science* 11: 1–70.

Tyler-Walters, H., *et al.,* 2016. Descriptions of Scottish Priority Marine Features (PMFs), Scottish Natural Heritage Commissioned Report No. 406.

UK Soil Observatory, 2020. British Geological Survey. Available at: https://mapapps2.bgs.ac.uk/ukso/home.html?layer=JHTopsoilOrganicarbon (Accessed: November 28, 2022).

Valiela, I., *et al.,* 1997. Macroalgal blooms in shallow estuaries: Controls and ecophysiological and ecosystem consequences. *Limn. Oceanogr.* 42: 1105–1118.

van der Heijden, L.H., and Kamenos, N.A., 2015. Reviews and syntheses: Calculating the global contribution of coralline algae to total carbon burial. *Biogeosciences* 12: 6429–6441.

Verardo, D.J., Froelich, P.N. and McIntyre, A., 1990. Determination of organic carbon and nitrogen in marine sediments using the Carlo Erba NA-1500 Analyzer. *Deep Sea Res. Part I Oceanogr. Res. Pap.*, 37(1): 157-165.

Vichkovitten, T., and Holmer, M., 2004. Contribution of plant carbohydrates to sedimentary carbon mineralization. *Org. Geochem.* 35: 1053–1066.

Vieira, S., Ribeiro, L., Marques da Silva, J., and Cartaxana, P., 2013. Effects of short-term changes in sediment temperature on the photosynthesis of two intertidal microphytobenthos communities. *Estuar. Coast. Shelf. Sci.* 119: 112–118.

Waldbusser, G.G., *et al.,* 2013. A developmental and energetic basis linking larval oyster shell formation to acidification sensitivity. *Geophys. Res. Lett.* 40(10): 2171-2176.

Walsh, P.J., *et al.*, 1991. Carbonate deposits in marine fish intestines: A new source of biomineralization. *Limnol. Oceanogr. 36*, 1227-1232.

Ware, J.R., Smith, S.V., and Reaka-Kudla, M.L., 1992. Coral reefs: sources or sinks of atmospheric CO_2? *Coral Reefs 11*: 127-130.

Wild, C., Woyt, H., and Huettel, M., 2005. Influence of coral mucus on nutrient fluxes in carbonate sands. *Mar. Ecol. Prog. Ser. 287*: 87-98.

Wigley, T.M.L., and Raper, S.C.B., 1987. Thermal expansion of sea water associated with global warming. *Nature* 330: 127–131.

Williamson, P., and Gattuso, J.P. (2022). Carbon removal using coastal blue carbon ecosystems is uncertain and unreliable, with questionable climatic cost-effectiveness. Front. Clim. *4*: 853666.

Witt, V., *et al.,*2011. Effects of ocean acidification on microbial community composition of, and oxygen fluxes through, biofilms from the Great Barrier Reef. *Environ Microbiol* 13: 2976–2989.

Wolf, C., *et al.,* 2019. Eating plants and planting forests for the climate. *Glob. Chang. Biol.* 00:1.

Wood, H.L., Spicer, J.I., Lowe, D.M., and Widdicombe, S., 2010. Interaction of ocean acidification and temperature; the high cost of survival in the brittlestar *Ophiura ophiura*. *Mar. Biol.* 157: 2001–2013.

Wu, Z.J., *et al.,* 2016. Quantifying the sources of dissolved inorganic carbon within the sulfate-methane transition zone in nearshore sediments of Qi'ao Island, Pearl River Estuary, Southern China. *Sci. China. Earth.* Sci. 59: 1959–1970.

Xue, J., *et al.,* 2015. Temporal variation and stoichiometric ratios of organic matter remineralization in bottom waters of the northern Gulf of Mexico during late spring and summer. *J. Geophys. Res. Oceans.* 120: 8304–8326.

Yamano, H., Miyajima, T., and Koike, I. 2000. Importance of foraminifera for the formation and maintenance of a coral sand cay: Green Island, Australia. *Coral Reefs* 19: 51-58.

Yousefi Lalimi, F., *et al.,* 2018. The spatial variability of organic matter and decomposition processes at the marsh scale. *J. Geophys. Res. Biogeosci.* 123: 3713–3727.

Yuan, F., *et al.*, 2021. An integrative model for soil biogeochemistry and methane processes. II: warming and elevated CO_2 effects on peatland CH_4 emissions. *J. Geophys. Res. Biogeosci.* 126: 1–18.

Zhao, B., *et al.,* 2018. The remineralization of sedimentary organic carbon in different sedimentary regimes of the Yellow and East China Seas. *Chem. Geol.* 495: 104–117.

Appendices

Appendix 1 - Chapter 2 Supplementary Information

1.1 Search Terms

Primary search terms: “BC” OR “carbon cycl*” OR “global carbon cycl*” OR “carbon burial” OR sequestration OR “total carbon” OR “inorganic carbon” OR “organic carbon” OR “carbon sequestration” OR carbonate OR “calcium carbonate” OR “standing stock” OR “CaCO3 budget” OR “carbonate production” OR “carbon content” OR “carbonate accumulation” OR “carbonate content” OR “carbon storage” OR “carbon reservoir*” OR “BC sequestration OR “sediment accumulation”

Secondary search terms: Primary search terms were combined sequentially with the following secondary search terms.

1. “biogenic reef*” OR mussel* OR bivalv* OR “shellfish bed*” OR “shellfish” OR Conchifera OR Lamellibranchiata OR Pelecypoda OR Modiolus OR Limaria OR Mytilus OR Mollusc* OR Mytilidae OR oyster* OR Ostreoidea OR zoobenthos
2. “bryozoa* reef” OR bryozoa* OR Polyzoa OR “moss animals” OR Ectoprocta OR “bryozoa colon*” OR “bryozoa thicket*” OR thicket OR “bryozoa mound*”
3. coral* OR “coral reef*” OR “coral mound*”
4. maerl OR “coralline algae” OR rhodolith* or “maerl bed*” or “coralline algae bed*” OR “Red coralline algae” OR “free living coralline algae” OR “free-living coralline algae” OR “Maerl habitat*” OR “Calcified algae” OR “maerl deposit*” OR “coralline algae deposit*”
5. fjord*
6. mudflat* OR tidalflat* OR mud AND flat* OR tidal AND flat*
7. sediment*
8. "rocky seabed” OR “rocky habitat”
9. respiration OR product* OR photosynthesis OR calcif* OR dissolution OR Net OR metabolism
10. community OR ecosystem OR habitat
11. "eddy cov*" OR incubat* OR flume* OR "chamber"

1.2 Complete meta-analysis reference list

á Norði, G. *et al.,* 2018. Deposition and benthic mineralization of organic carbon: A seasonal study from Faroe Islands. *J. Mar. Syst.* 177: 53–61.

Ahmed, N., and Glaser, M., 2016. Coastal aquaculture, mangrove deforestation and blue carbon emissions: is REDD+ a solution? *Mar. Policy* 66: 58-66.

Albright, R. *et al.,* 2013. Dynamics of seawater carbonate chemistry, production, and calcification of a coral reef flat, Central Great Barrier Reef. *Biogeosciences* 10(5): 7641–7676.

Alongi, D. M. 2014. Carbon cycling and storage in mangrove forests. *Ann. Rev. Mar. Sci.* 6: 195-219.

Alongi, D., *et al.,* 2016. Indonesia's BC: a globally significant and vulnerable sink for seagrass and mangrove carbon. *Wetl. Ecol. Manag.* 24(1): 3-13.

Anderson, C. M., *et al.,* 2019. Natural climate solutions are not enough. *Science* 363(6430): 933-934.

Andersson, A.J. *et al.,* 2009. Net Loss of $CaCO_3$ from a subtropical calcifying community due to seawater acidification: Mesocosm-scale experimental evidence. *Biogeosciences* 6(8): 1811–1823.

Anton, K. K., Liebezeit, G., Rudolph, C. and Wirth, H., 1993. Origin, distribution and accumulation of organic carbon in the Skagerrak. *Mar. Geol.* 111: 287-297.

Archer, D. and Devol, A., 1992. Benthic oxygen fluxes on the Washington shelf and slope: A comparison of in situ microelectrode and chamber flux measurements. *Limn. Ocean.* 37(3): 614–629.

Arina, N. *et al.,* 2020. Coralline macroalgae contribution to ecological services of carbon storage in a disturbed seagrass meadow. *Mar. Environ. Res.* 162: 105398.

Arndt, S. *et al.,* 2013. Quantifying the degradation of organic matter in marine sediments: A review and synthesis. *Earth. Sci. Rev.* 123: 53–86.

Atkinson, M.J. and Grigg, R.W., 1984. Model of a coral reef ecosystem - II. Gross and net benthic primary production at French Frigate Shoals, Hawaii. *Coral Reefs* 3(1): 13–22.

Attard, K.M. *et al.,* 2014. Seasonal rates of benthic primary production in a Greenland fjord measured by aquatic eddy correlation. *Limn. Ocean.* 59(5): 1555–1569.

Attard, K.M. *et al.,* 2015. Benthic oxygen exchange in a live coralline algal bed and an adjacent sandy habitat: An eddy covariance study. *Mar. Ecol. Prog. Ser.* 535: 99–115.

Attard, K.M. *et al.,* 2019. Seasonal ecosystem metabolism across shallow benthic habitats measured by aquatic eddy covariance. *Limn. Ocean.* 4(3): 79–86.

Attard, K.M. *et al.,* 2020. Metabolism of a subtidal rocky mussel reef in a high-temperate setting: Pathways of organic C flow. *Mar. Ecol. Prog. Ser.* 645: 41–54.

Atwood, T. B., *et al.,* 2018. Predators shape sedimentary organic carbon storage in a coral reef ecosystem. *Front. Ecol. Evol.* 6: 110.

Barbier, E. B., *et al.,* 2011. The value of estuarine and coastal ecosystem services. *Ecol. Monogr.* 81(2): 169-193.

Barnes, D. K., 2017. Polar zoobenthos blue carbon storage increases with sea ice losses, because across-shelf growth gains from longer algal blooms outweigh ice scour mortality in the shallows. *Glob. Change Biol.* 23(12): 5083-5091.

Barnes, D. K., *et al.,* 2020. Blue carbon gains from glacial retreat along Antarctic fjords: What should we expect? *Glob. Change Biol.* 26(5): 2750-2755.

Barnes, D.K.A., 2015. Antarctic sea ice losses drive gains in benthic carbon drawdown. *Curr. Biol.* 25(18): R789–R790.

Baudin, F. *et al.,* 2017. Origin and distribution of the organic matter in the distal lobe of the Congo deep-sea fan – A Rock-Eval survey. *Deep Sea Res. Part II Top. Stud. Oceanogr.* 142(January): 75–90.

Behrenfeld, M. *et al.,* 2006. Climate-driven trends in contemporary ocean productivity. *Nature* 444(7120): 752-755.

Berelson, W.M. *et al.,* 1990. In situ measurements of calcium carbonate dissolution rates in deep-sea sediments. *Geochim. Cosmochim. Acta* 54(11): 3013–3020.

Berg, P. *et al.,* 2013. Eddy correlation measurements of oxygen fluxes in permeable sediments exposed to varying current flow and light. *Limn. Ocean.* 58(4): 1329–1343.

Betts, J.N. and Holland, H.D., 1991. The oxygen content of ocean bottom waters, the burial efficiency of organic carbon, and the regulation of atmospheric oxygen. *Glob. Planet. Change* 5(1–2): 5–18.

Bianchi, T. S., *et al.*, 2020. Fjords as aquatic critical zones (ACZs). *Earth Sci. Rev.* 203: 103145.

Billerbeck, M. *et al.,* 2007. Benthic photosynthesis in submerged Wadden Sea intertidal flats. *Estuar. Coast. Shelf Sci.* 71(3–4): 704–716.

Boldt, K. V., Nittrouer, C. A., and Ogston, A. S.. 2013. Seasonal transfer and net accumulation of fine sediment on a muddy tidal flat: Willapa Bay, Washington. *Cont. Shelf Res.* 60S: S157–S172

Bosence, D. and Wilson, J., 2003. Maerl growth, carbonate production rates and accumulation rates in the northeast Atlantic. *Aquat. Conserv.: Mar. Freshw. Ecosyst.* 13: 21-31.

Bouillon, S., *et al.,* 2008 Mangrove production and carbon sinks: a revision of global budget estimates. *Global Biogeochem. Cycles* 22(2).

Bourgeois, S., Archambault, P., and Witte, U. (2017). Organic matter remineralization in marine sediments: A Pan-Arctic synthesis. *Global Biogeochem. Cycles* 31(1): 190-213.

Brodie, J., *et al.*, 2014. The future of the northeast Atlantic benthic flora in a high CO_2 world. *Ecol. Evol.* 4(13): 2787-2798.

Buesseler, K., e*t al.,* 2007. Revisiting carbon flux through the ocean's twilight zone. *Science* 316(5824): 567-570.

Burdett, H. L., *et al.,* 2018. Community-level sensitivity of a calcifying ecosystem to acute in situ CO_2 enrichment. *Mar. Ecol. Prog. Ser.* 587: 73-80.

Burdige, D.J., 2005. Burial of terrestrial organic matter in marine sediments: A re-assessment. *Global Biogeochem. Cycles* 19(4): GB4011.

Burrows, M.T., *et al.,* 2017. Assessment of blue Resources in Scotland's Inshore Marine Protected Area Network. *Scottish Natural Heritage Commissioned Report No. 957.*

Burrows, M T *et al.,* 2014. Assessment of carbon budgets and potential blue carbon stores in Scotland's coastal and marine environment. *Scottish Natural Heritage Commissioned Report No. 761.*

Canfield, D. E., *et al.,* 1993. Pathways of organic carbon oxidation in three continental margin sediments. *Mar. Geol.* 113(1): 27-40.

Cappelli, E.L.G. *et al.,* 2019. Organic-carbon-rich sediments: Benthic foraminifera as bio-indicators of depositional environments. *Biogeosciences* 16(21): 4183–4199.

Carroll, J.L. *et al.,* 2008. Accumulation of organic carbon in western Barents Sea sediments. *Deep Sea Res. Part II Top. Stud. Oceanogr.* 55(20–21): 2361–2371.

Chambers, L. G., *et al.,* 2018. How well do restored intertidal oyster reefs support key biogeochemical properties in a coastal lagoon? *Estuaries Coasts*. 41(3): 784-799.

Chen, G., *et al.,* 2017 Mangroves as a major source of soil carbon storage in adjacent seagrass meadows. *Sci. Rep.* 7: 42406.

Chen, J., *et al.,* 2020. The carbon stock and sequestration rate in tidal flats from coastal China. *Global Biogeochem. Cycles* 34: e2020GB006772.

Chmura, G.L., Anisfeld, S.C., Cahoon, D.R., and Lynch, J.C., 2003. Global carbon sequestration in tidal, saline wetland soils. *Global Biogeochem. Cycles* 17(4): 1111.

Coppari, M., Zanella, C., and Rossi, S. 2019. The importance of coastal gorgonians in the blue carbon budget. *Sci. Rep.* 9(1): 1-12.

Costa, M., Lovelock, C., Waltham, N., and Macreadie, P.I., 2020. Blue Carbon Opportunities in Queensland: How much and where? A report provided to the Land Restoration Fund, Queensland Government.

Cui, X. *et al.,* 2016. Organic carbon burial in fjords: Terrestrial versus marine inputs. *Earth Planet. Sci. Lett.* 451: 41–50.

Cui, X. *et al.,* 2017. Carbon Dynamics Along a Temperate Fjord-Head Delta: Linkages With Carbon Burial in Fjords. *Global Biogeochem. Cycles* 122(12): 3419–3430.

Dame, R. F., Zingmark, R. G., and Haskin, E., 1984. Oyster reefs as processors of estuarine materials. *J. Exp. Mar. Biol. Ecol.* 83(3): 239-247.

de Froe, E. *et al.,* 2019. Benthic Oxygen and Nitrogen Exchange on a Cold-Water Coral Reef in the North-East Atlantic Ocean. *Front. Mar. Sci.* 6(665): 1-13.

Díaz-Asencio, M. *et al.,* 2019. Sediment accumulation patterns on the slopes and abyssal plain of the southern Gulf of Mexico. *Deep Sea Res. Part I Oceanogr. Res. Pap.* 146(January): 11–23.

Donato, D. C., *et al.,* 2011. Mangroves are among the most carbon-rich forests in the tropics. *Nat. Geosci.* 4(5): 293-297.

Duarte, C. M., Middelburg, J. J., and Caraco, N., 2005. Major role of marine vegetation on the oceanic carbon cycle. *Biogeosciences* 2(1): 1-8.

Duarte, C.M. and Krause-Jensen, D., 2018. Greenland Tidal Pools as Hot Spots for Ecosystem Metabolism and Calcification. *Estuaries Coasts.* 41(5): 1314–1321.

Duffield, C.J. *et al.,* 2017. Spatial and temporal organic carbon burial along a fjord to coast transect: A case study from Western Norway. *Holocene* 27(9): 1325–1339.

Duineveld, G.C.A. *et al.,* 1997. Benthic respiration and standing stock on two contrasting continental margins in the western Indian Ocean: The Yemen-Somali upwelling region and the margin off Kenya. *Deep Sea Res. Part II Top. Stud. Oceanogr.* 44(6–7): 1293–1317.

Eidam, E.F. *et al.,* 2019. Variability of Sediment Accumulation Rates in an Antarctic Fjord. *Geophys. Res. Lett.* 46(22): 13271–13280.

Epping, E. *et al.,* 2002. On the oxidation and burial of organic carbon in sediments of the Iberian Margin and Nazaré Canyon (NE Atlantic). *Prog. Oceanogr.* 52(2–4): 399–431.

European Atlas of the Seas, 2020. European Union, viewed 17/11/2020. https://ec.europa.eu/maritimeaffairs/atlas/maritime_atlas/#lang=EN;p=w;bkgd= 5;theme= 787:0.75;c= 3523740.209543485,6607710.844755266;z= 2

Falter, J.L. *et al.,* 2008. Continuous measurements of net production over a shallow reef community using a modified Eulerian approach. *J. Geophys. Res. Oceans* 113(7): 1–14.

Falter, J.L. *et al.,* 2011. Short-term coherency between gross primary production and community respiration in an algal-dominated reef flat. *Coral Reefs* 30(1): 53–58.

Feely, R.A., *et al.,* 2004. Oxygen utilization and organic carbon remineralization in the upper water column of the Pacific Ocean. *J. Oceanogr.* 60(1): 45-52.

Fodrie, F. J., *et al.,* 2017. Oyster reefs as carbon sources and sinks. *Proc. Royal Soc. B.* 284(1859): 20170891.

Forster, S. *et al.,* 1999. In situ study of bromide tracer and oxygen flux in coastal sediments. *Estuar. Coast. Shelf Sci.* 49(6): 813–827.

Fourqurean, J. W., *et al.,* 2012. Seagrass ecosystems as a globally significant carbon stock. *Nat. Geosci.* 5(7): 505-509.

Frankignoulle, M., Canon, C., and Gattuso, J. P. 1994. Marine calcification as a source of carbon dioxide: Positive feedback of increasing atmospheric CO_2. *Limn. Ocean.* 39(2): 458-462.

Freese, E., Köster, J., and Rullkötter, J., 2008. Origin and composition of organic matter in tidal flat sediments from the German Wadden Sea. *Org. Geochem.,* 39: 820–829.

Gattuso, J.P. *et al.,* 1993. Community metabolism and air-sea CO_2 fluxes in a coral reef ecosystem (Moorea, French Polynesia). *Mar. Ecol. Prog. Ser.* 96(3): 259–267.

Gattuso, J.P., *et al.*, 2000. Calcification does not stimulate photosynthesis in the zooxanthellate scleractinian coral *Stylophora pistillata*. *Limn. Ocean.* 45(1): 246-250.

Gattuso, J.P., Allemand, D., and Frankignoulle, M., 1999. Photosynthesis and calcification at cellular, organismal and community levels in coral reefs: a review on interactions and control by carbonate chemistry. *Am. Zool.* 39(1): 160-183.

Gattuso, J.P. *et al.*, 1998. Carbon and carbonate metabolism in coastal aquatic ecosystems. *Annu. Rev. Ecol. Evol. Syst.* 29: 405–434.

Gattuso, J.P. *et al.*, 1996. Carbon fluxes in coral reefs. I. Lagrangian measurement of community metabolism and resulting air-sea CO_2 disequilibrium. *Mar. Ecol. Prog. Ser.* 145(1–3): 109–121.

Giles, H. *et al.*, 2006. Sedimentation from mussel (*Perna canaliculus*) culture in the Firth of Thames, New Zealand: Impacts on sediment oxygen and nutrient fluxes. *Aquaculture* 261(1): 125–140.

Glud, R.N., *et al.*, 2016. Benthic carbon mineralization and nutrient turnover in a Scottish sea loch: an integrative in situ study. *Aquat. Geochem.*, 22(5-6): 443-467.

Glud, R.N., 2008. Oxygen dynamics of marine sediments. *Mar. Biol. Res*. 4(4): 243-289.

Glud, R.N., Kühl, M., Wenzhöfer, F., and Rysgaard, S., 2002. Benthic diatoms of a high Arctic fjord (Young Sound, NE Greenland): importance for ecosystem primary production. *Mar. Ecol. Prog. Ser.* 238: 15-29.

Glud, R.N., *et al.*, 2000. Benthic carbon mineralization in a high-Arctic sound (Young Sound, NE Greenland). *Mar. Ecol. Prog. Ser.* 206: 59-71.

Glud, R.N. *et al.*, 1994. Diffusive and total oxygen uptake of deep-sea sediments in the eastern South Atlantic Ocean: in situ and laboratory measurements. Deep-Sea Research Part I 41(11–12), pp. 1767–1788.

Golléty, C. *et al.*, 2008. Benthic metabolism on a sheltered rocky shore: Role of the canopy in the carbon budget. *J. Phycol.* 44(5): 1146–1153.

Goreau, T., 1961. On the relation of calcification to primary productivity in reef building organisms. *University of Miami Press.*

Griscom, B.W., *et al.,* 2017. Natural climate solutions. *Proc. Natl. Acad. Sci.* 114(44): 11645-11650.

Griscom, B.W., *et al.,* 2019. We need both natural and energy solutions to stabilize our climate. *Glob. Change Biol.* 25(6): 1889-1890.

Hall, P.O.J., *et al.,*2017. Influence of Natural Oxygenation of Baltic Proper Deep Water on Benthic Recycling and Removal of Phosphorus, Nitrogen, Silicon and Carbon. *Front. Mar. Sci.* 4(27).

Harley, C. D., *et al.,* 2012. Effects of climate change on global seaweed communities. *J. Phycol.* 48(5): 1064-1078.

Haro, S., *et al.,* 2020. Microbenthic Net Metabolism Along Intertidal Gradients (Cadiz Bay, SW Spain): Spatio-Temporal Patterns and Environmental Factors. *Front. Mar. Sci.* 7(February): 1-22.

Harrison, W., and Cota, G., 1991. Primary production in polar waters: relation to nutrient availability. *Polar Res*. 10(1): 87-104.

Hartnett, H.E. *et al.,* 1998. Influence of oxygen exposure time on organic carbon preservation in continental margin sediments. *Nature* 391: 572–574.

Henson, S., Le Moigne, F., and Giering, S., 2019. Drivers of carbon export efficiency in the global ocean. *Global Biogeochem. Cycles* 33(7): 891-903.

Hill, R., *et al.,* 2015. Can macroalgae contribute to blue carbon? An Australian perspective. *Limn. Ocean.* 60(5): 1689-1706.

Honjo, S., Manganini, S. J., Krishfield, R. A., and Francois, R., 2008. Particulate organic carbon fluxes to the ocean interior and factors controlling the biological pump: A synthesis of global sediment trap programs since 1983. *Prog. Oceanogr*. 76(3): 217-285.

Hopwood, M. J., *et al.,* 2019. Review Article: How does glacier discharge affect marine biogeochemistry and primary production in the Arctic? *Cryosphere*, 14: 1347–1383.

Howard, J., *et al.*, 2017. Clarifying the role of coastal and marine systems in climate mitigation. *Front. Ecol. Environ.* 15(1): 42-50.

Hsu, S.C. *et al.,* 2006. Quantitative links between fluvial sediment discharge, trapped terrigenous flux and sediment accumulation, and implications for temporal and spatial distributions of sediment fluxes. *Deep Sea Res. Part I Oceanogr. Res. Pap. 53*(2): 241–252.

Hulth, S. *et al.,* 1997. Mineralization and burial of organic carbon in sediments of the southern Weddell Sea (Antarctica). *Deep Sea Res. Part I Oceanogr. Res. Pap.* 44(6): 955–981.

Hulthe, G., Hulth, S., and Hall, P.O.J., 1998. Effect of oxygen on the degradation rate of refractory and labile organic matter in continental margin sediments. *Geochim. Cosmochim. Acta*, 62(8): 1319-1328.

Isla, E. *et al.,* 2002. Sediment accumulation rates and carbon burial in the bottom sediment in a high-productivity area: Gerlache Strait (Antarctica). *Deep Sea Res. Part II Top. Stud. Oceanogr.* 49(16): 3275–3287.

Jahnke, R.A. and Jahnke, D.B., 2004. Calcium carbonate dissolution in deep sea sediments: Reconciling microelectrode, pore water and benthic flux chamber results. *Geochim. Cosmochim. Acta* 68(1): 47–59

Kamenos, N.A., *et al.,* 2013. Coralline algal structure is more sensitive to rate, rather than the magnitude, of ocean acidification. *Glob. Change Biol.* 19(12): 3621-3628.

Kandasamy, S. and Nath, B.N., 2016. Perspectives on the terrestrial organic matter transport and burial along the land-deep sea continuum: Caveats in our understanding of biogeochemical processes and future needs. *Front. Mar. Sci.* 3(December): 1–18.

Kennedy, H., *et al.,* 2013. Coastal wetlands. In 2013 Supplement to the 2006 IPCC Guidelines for National Greenhouse Gas Inventories: Wetlands. IPCC, Switzerland: IPCC.

Kent, F.E.A. *et al.,* 2017. *In situ* biodeposition measurements on a *Modiolus modiolus* (horse mussel) reef provide insights into ecosystem services. *Estuar. Coast. Shelf Sci.* 184: 151–157.

Khripounoff, A. *et al.,* 2017. Respiration of bivalves from three different deep-sea areas: Cold seeps, hydrothermal vents and organic carbon-rich sediments. *Deep Sea Res. Part II Top. Stud. Oceanogr.* 142: 233–243.

Kiesel, J. *et al.,* 2020. Variability in Benthic Ecosystem Functioning in Arctic Shelf and Deep-Sea Sediments: Assessments by Benthic Oxygen Uptake Rates and Environmental Drivers. *Front. Mar. Sci.* 7(July): 1–17.

Kim, J. *et al.,* 2015. Evaluation of carbon flux in vegetative bay based on ecosystem production and CO_2 exchange driven by coastal autotrophs. *Algae* 30(2): 121–137.

Kirwan, M. L., and Mudd, S. M., 2012. Response of salt-marsh carbon accumulation to climate change. *Nature* 489(7417): 550-553.

Koziorowska, K. *et al.,* 2016. Sedimentary organic matter in two Spitsbergen fjords: Terrestrial and marine contributions based on carbon and nitrogen contents and stable isotopes composition. *Cont. Shelf Res.* 113: 38–46.

Koziorowska, K. *et al.,* 2018. Comparison of the burial rate estimation methods of organic and inorganic carbon and quantification of carbon burial in two high Arctic fjords. *Oceanologia* 60(3): 405–418.

Krause-Jensen, D., and Duarte, C. M., 2016. Substantial role of macroalgae in marine carbon sequestration. *Nat. Geosci.* 9(10): 737-742.

Krause-Jensen, D., *et al.,* 2018. Sequestration of macroalgal carbon: the elephant in the blue carbon room. *Biol. Lett.* 14(6): 20180236.

Kristensen, E., *et al.,* 2012. What is bioturbation? The need for a precise definition for fauna in aquatic sciences. *Mar. Ecol. Prog. Ser.* 446: 285-302.

Kuliński, K. *et al.,* 2014. Particulate organic matter sinks and sources in high Arctic fjord. *Jour. Mar. Syst.* 139: 27–37.

Kwiatkowski, L. *et al.,* 2016. Interannual stability of organic to inorganic carbon production on a coral atoll. *Geophys. Res. Lett.* 43(8): 3880–3888.

Lafon, A. *et al.,* 2014. Contribution of allochthonous organic carbon across the Serrano River Basin and the adjacent fjord system in Southern Chilean Patagonia: Insights from the combined use of stable isotope and fatty acid biomarkers. *Prog. Oceanogr.* 129: 98–113.

Lantz, C.A. *et al.,* 2019. The effect of warming and benthic community acclimation on coral reef carbonate sediment metabolism and dissolution. *Coral Reefs* 38(1): 149–163.

Lee, H.Z.L. *et al.,* 2020. Missing the full story: First estimates of carbon deposition rates for the European flat oyster, *Ostrea edulis*. *Aquat. Conserv.: Mar. Freshw. Ecosyst.* 30: 2076-2086.

Legrand, E., *et al.,* 2018. Impact of ocean acidification and warming on the productivity of a rock pool community. *Mar. Environ. Res.* 136(October): 78–88.

Legrand, E., *et al.,* 2018. Ecological characterization of intertidal rockpools: Seasonal and diurnal monitoring of physico-chemical parameters. *Reg. Stud. Mar. Sci.* 17: 1–10.

Lin, W. J., Wu, J., and Lin, H. J., 2020. Contribution of unvegetated tidal flats to coastal carbon flux. *Glob. Change Biol.* 26(6): 3443–3454.

Loh, P.S. *et al.,* 2008. Assessing the biodegradability of terrestrially-derived organic matter in Scottish sea loch sediments. *Hydrol. Earth Syst. Sci.* 12(3): 811–823.

Lovelock, C. E., and Duarte, C. M., 2019. Dimensions of blue carbon and emerging perspectives. *Biol. Lett*. 15(3): 20180781.

Lovelock, C. E., *et al.,* 2017. Assessing the risk of carbon dioxide emissions from blue carbon ecosystems. *Front. Ecol. Environ.* 15(5): 257-265.

Lunt, J., Reustle, J., and Smee, D. L., 2017. Wave energy and flow reduce the abundance and size of benthic species on oyster reefs. *Mar. Ecol. Prog. Ser.* 569: 25-36.

Luo, M., *et al.,* 2018. Benthic carbon mineralization in hadal trenches: insights from in situ determination of benthic oxygen consumption. *Geophys. Res. Lett.* 45(6): 2752-2760.

Macreadie, P.I., *et al.,* 2019. The future of blue carbon science. *Nat. Comm.* 10(1): 1-13.

Macreadie, P. I., *et al.,*2015. Do ENSO and coastal development enhance coastal burial of terrestrial carbon? PloS one, 10(12): e0145136.

Macreadie, P.I., Hughes, A.R., and Kimbro, D.L. 2013. Loss of 'blue carbon' from Coastal Salt Marshes Following Habitat Disturbance. PloS one, 8(7): e69244.

Macreadie, P.I., *et al.,* 2012. Paleoreconstruction of estuarine sediments reveal human-induced weakening of coastal carbon sinks. *Glob. Change Biol.* 18(3): 891-901.

Macreadie, P.I., *et al.,* 2017. Addressing calcium carbonate cycling in blue carbon accounting. *Limnol. Oceanogr. Lett.* 2: 195–201.

Madsen, A. T., Murray, A. S., Andersen, T. J., and Pejrup, M., 2010. Spatial and temporal variability of sediment accumulation rates on two tidal flats in Lister Dyb tidal basin, Wadden Sea, Denmark. *Earth Surf. Process. Landforms* 35: 1556–1572.

Maier, K.L. *et al.,* 2019. Sediment and organic carbon transport and deposition driven by internal tides along Monterey Canyon, offshore California. *Deep Sea Res. Part I Oceanogr. Res. Pap.* 153(August): 103108.

Manis, J.E., Garvis, S.K., Jachec, S.M., and Walters, L.J. 2015. Wave attenuation experiments over living shorelines over time: a wave tank study to assess recreational boating pressures. *J. Coast. Conserv.* 19: 1-11.

Mao, J., 2019. The role of red coralline algal habitats as blue carbon stores. PhD thesis, University of Glasgow, Scotland.

Mao, J., *et al.,* 2020. Carbon burial over the last four millennia is regulated by both climatic and land use change. *Glob. Chang. Biol.* 26: 2496–2504.

Martin, S., Clavier, J., Chauvaud, L., and Thouzeau, G., 2007. Community metabolism in temperate maerl beds. I. Carbon and carbonate fluxes. *Mar. Eco. Prog. Ser.* 335: 19-29.

Martin, S., *et al*., 2005. Comparison of *Zostera* marina and maerl community metabolism. *Aquat. Bot.* 83*:* 161-174.

Martin, W.R. and Sayles, F.L., 2006. Organic matter oxidation in deep-sea sediments: Distribution in the sediment column and implications for calcite dissolution. *Deep Sea Res. Part II Top. Stud. Oceanogr.* 53(5–7): 771–792.

Marzocchi, U., Thamdrup, B., Stief, P., and Glud, R.N. 2018. Effect of settled diatom-aggregates on benthic nitrogen cycling. *Limnol. Oceanogr.* 63: 431-444.

Masson, D.G. *et al.,* 2010. Efficient burial of carbon in a submarine canyon. *Geology* 38(9): 831–834.

McLeod, E., *et al.,* 2011. A blueprint for blue carbon: Toward an improved understanding of the role of vegetated coastal habitats in sequestering CO_2. *Front. Ecol. Environ.* 9 (10), 552–560.

McMinn, A. *et al.,* 2010. In situ net primary productivity and photosynthesis of Antarctic sea ice algal, phytoplankton and benthic algal communities. *Mar. Biol.* 157(6): 1345–1356.

Middelburg, J., and Levin, L. 2009. Coastal hypoxia and sediment biogeochemistry. *Biogeosciences* 6: 1273–1293.

Migné, A. *et al.,* 2005. Benthic primary production, respiration and remineralisation: In situ measurements in the soft-bottom *Abra alba* community of the western English Channel (North Brittany). *J. Sea Res.* 53(4): 223–229.

Mollica, N.R., *et al.,* 2018. Ocean acidification affects coral growth by reducing skeletal density. *Proc. Natl. Acad. Sci.* 115, 1754-1759.

Muduli, P.R. *et al.,* 2013. Distribution of dissolved inorganic carbon and net ecosystem production in a tropical brackish water lagoon, India. *Cont. Shelf Res.* 64: 75–87.

Multer, H.G. 1988. Growth rate, ultrastructure and sediment contribution of *Halimeda incrassata* and *Halimeda monile*, Nonsuch and Falmouth Bays, Antigua, W.I. *Coral Reefs* 6: 179-186.

Naumann, M.S., *et al.*, 2012. Budget of coral-derived organic carbon in a fringing coral reef of the Gulf of Aqaba, Red Sea. *Journ. Mar. Syst.* 105: 20-29.

Ní Longphuirt, S. *et al.*, 2007. Primary production and spatial distribution of subtidal microphytobenthos in a temperate coastal system, the Bay of Brest, France. *Estuar. Coast. Shelf Sci.* 74(3): 367–380.

Nilsson, M.M., *et al.*, 2010. Organic carbon recycling in Baltic Sea sediments – An integrated estimate on the system scale based on in situ measurements. *Mar. Chem. 209*: 81-93.

Nilsen, M. *et al.*, 2006. Macrobenthic biomass, productivity (P/B-) and production in a high-latitude ecosystem, North Norway. *Mar. Ecol. Prog. Ser.* 321: 67–77.

Norling, P., and Kautsky, N. 2008. Patches of the mussel Mytilus sp. are islands of high biodiversity in subtidal sediment habitats in the Baltic Sea. *Aquat. Biol.* 4: 75-87.

Nowicki, B. L. and Nixon, S.W., 1985. Benthic community metabolism in a coastal lagoon ecosystem. *Mar. Ecol. Prog. Ser.* 22:21-30

Peck, L.S., *et al.*, 2010. Negative feedback in the cold: ice retreat produces new carbon sinks in Antarctica. *Glob. Change Biol.* 16: 2614-2623.

Pendleton, L., *et al.*, 2012. Estimating Global "blue carbon" Emissions from Conversion and Degradation of Vegetated Coastal Ecosystems. *PloS one*, 7(9): e43542.

Perry, C.T., *et al.*, 2015. Linking reef ecology to island building: Parrotfish identified as major producers of island-building sediment in the Maldives. *Geology* 43: 503-506. 10.

Pfeifer, K. *et al.*, 2002. Modelling of surface calcite dissolution, including the respiration and reoxidation processes of marine sediments in the region of equatorial upwelling off Gabon. *Geochim. Cosmochim. Acta* 66(24): 4247–4259.

Pidgeon, E., 2009. Carbon Sequestration by coastal marine habitats: important missing sinks. In: The management of natural coastal carbon sinks [D. Laffoley, and G. Grimsditch, (eds.)]. IUCN, pp. 53.

Piepenburg, D., *et al.*,1995. Partitioning of benthic community respiration in the Arctic (northwestern Barents Sea). *Mar. Ecol. Prog. Ser.* 118: 199-213.

Porter, J., *et al.,* 2020. Blue carbon audit of Scottish waters. Scottish Marine and Freshwater Science *11*: 0-96.

Pramneechote, P. *et al.,* 2020. An assessment of the net ecosystem metabolism and respiration of a tropical coral reef. *Appl. Ecol. Environ. Res.* 18(1): 1863–1881.

Price, N.N. *et al.*, 2012. Diel Variability in Seawater pH Relates to Calcification and Benthic Community Structure on Coral Reefs. *PLoS ONE* 7(8): 1–9.

Queirós, A.M., *et al.,* 2019. Connected macroalgal-sediment systems: Blue carbon and food webs in the deep coastal ocean. Ecol. Monogr. 89(3): e01366.

Rabalais, N.N., Turner, R.E., Wiseman, W.J., 2002. Gulf of Mexico Hypoxia, A.K.A. "The Dead Zone". *Annu. Rev. Ecol. Syst.* 33: 235–263.

Rabouille, C. *et al.,* 2009. Organic matter budget in the Southeast Atlantic continental margin close to the Congo Canyon: In situ measurements of sediment oxygen consumption. *Deep Sea Res. Part II Top. Stud. Oceanogr.* 56(23): 2223–2238.

Ravaglioli, C., *et al.,* 2019. Ocean acidification and hypoxia alter organic carbon fluxes in marine soft sediments. *Glob. Change Biol.* 25, 4165-4178.

Rees, S.A., Opdyke, B.N., Wilson, P.A., and Henstock, T.J. 2007. Significance of *Halimeda bioherms* to the global carbonate budget based on a geological sediment budget for the Northern Great Barrier Reef, Australia. *Coral Reefs* 26: 177-188.

Reisdorph, S.C. and Mathis, J.T., 2015. Assessing net community production in a glaciated Alaskan fjord. *Biogeosciences*12(17): 5185–5198.

Ricart, A. M., *et al.,* 2020. High variability of blue carbon storage in seagrass meadows at the estuary scale. *Sci. Rep.* 10(1):1-12.

Ridge, J.T., Rodriguez, A.B., and Fodrie, F.J. 2017. Salt marsh and fringing oyster reef transgression in a shallow temperate estuary: Implications for restoration, conservation and blue carbon. *Estuaries Coast.* 40: 1013-1027.

Rivkin, R.B., and Legendre, L. 2001. Biogenic carbon cycling in the upper ocean: effects of microbial respiration. *Science* 291: 2398-2400.

Rix, L., *et al.*,2017. Differential recycling of coral and algal dissolved organic matter via the sponge loop. *Funct. Ecol.* 31: 778-789.

Rodil, I.F. *et al.*, 2019. Towards a sampling design for characterizing habitat-specific benthic biodiversity related to oxygen flux dynamics using Aquatic Eddy Covariance. *PLoS ONE* 14(2): 1–21.

Rodil, I.F. *et al.,* 2020. Estimating Respiration Rates and Secondary Production of Macrobenthic Communities Across Coastal Habitats with Contrasting Structural Biodiversity. *Ecosystems* 23(3): 630–647.

Rojas, N. and Silva, N., 2005. Early diagenesis and vertical distribution of organic carbon and total nitrogen in recent sediments from southern Chilean fjords (Boca del Guafo to Pulluche Channel). *Investig. Mar.* 33(2): 183–194.

Rovelli, L. *et al.,* 2019. Benthic primary production and respiration of shallow rocky habitats: a case study from South Bay (Doumer Island, Western Antarctic Peninsula). *Polar Biol.* 42(8): 1459–1474.

Roxy, M. K., *et al.,* 2016. A reduction in marine primary productivity driven by rapid warming over the tropical Indian Ocean. *Geophys. Res. Lett.*, 43(2): 826-833.

Sabine, C.L., *et al.*, 2004. The Oceanic Sink for Anthropogenic CO_2. *Science* 305: 367–371.

Saderne, V., *et al.*,2019. Role of carbonate burial in blue carbon budgets. *Nat. commun*. 10, 1-9.

Sanders, C. J., *et al.*, 2010. Organic carbon burial in a mangrove forest, margin and intertidal mud flat. *Est. Coast. Shelf Sci.*, 90: 168 - 172

Sasmito, S.D., *et al.*, 2022. Organic carbon burial and sources in soils of coastal mudflat and mangrove ecosystems. CATENA *187*: 104414.

Sauer, S. *et al.*, 2016. Sources and turnover of organic carbon and methane in fjord and shelf sediments off northern Norway. *Geochemistry, Geophys. Geosystems* 17: 1312–1338.

Schubert, C.J. and Calvert, S.E., 2001. Nitrogen and carbon isotopic composition of marine and terrestrial organic matter in Arctic Ocean sediments: implications for nutrient utilization and organic matter composition. *Deep Sea Res. Part I* 48: 789–810.

Sczuciński, W., Zajaczkowski, M., and Scholten, J., 2009. Sediment accumulation rates in sub-polar fjords-Impact of post-Little Ice Age glaciers retreat, Billefjorden, Svalbard. *Estuarine, Coast. Shelf Sci.* 85 (3): 345–356.

Sepúlveda, J. *et al.,* 2011. Sources and distribution of organic matter in northern Patagonia fjords, Chile (~44-47°S): A multi-tracer approach for carbon cycling assessment. *Cont. Shelf Res.* 31(3–4): 315–329.

Shamberger, K.E.F. *et al.,* 2011. Calcification and organic production on a Hawaiian coral reef. *Mar. Chem.* 127(1–4): 64–75.

Shields, M. R., *et al.*, 2017. Carbon storage in the Mississippi River delta enhanced by environmental engineering. *Nat. Geosci.*, 10(11): 846-851.

Silverberg, N. *et al.*, 2000. Remineralization of organic carbon in eastern Canadian continental margin sediments. *Deep Sea Res. Part II Top. Stud. Oceanogr*. 47(3–4), pp. 699–731.

Silverman, J. *et al.,* 2007. Community metabolism of a coral reef exposed to naturally varying dissolved inorganic nutrient loads. *Biogeochemistry* 84(1): 67–82.

Simon-Nutbrown, C., *et al*., 2020. Species Distribution Modelling Predicts Significant Declines in Coralline Algae Populations Under Projected Climate Change With Implications for Conservation Policy. *Front. Mar. Sci.* 7: 575825.

Skudder, P.A., Backus, D.H., Goodwin, D.H., and Johnson, M.E., 2006. Sequestration of carbonate shell material in coastal dunes on the Gulf of California (Baja California Sur, Mexico). *Jour. Coast. Resear. 22*, 611-624.

Smale, D.A., *et al.,* 2018. Appreciating interconnectivity between habitats is key to blue carbon management. *Front. Ecol. Environ*. 16: 71-73.

Smeaton, C., *et al.,* 2017. Scotland's forgotten carbon: A national assessment of mid-latitude fjord sedimentary carbon stocks. *Biogeosciences* 14: 5663–5674.

Smeaton, C., *et al.,* 2016. Substantial stores of sedimentary carbon held in mid-latitude fjords. *Biogeosciences* 13: 5771–5787.

Smith, R.W., *et al.,* 2015. High rates of organic carbon burial in fjord sediments globally. *Nature. Geosci.* 8: 450-453.

Smith, S.V. 2013. Parsing the Oceanic Calcium Carbonate Cycle: A Net Atmospheric Carbon Dioxide Source Or a Sink? (Association for the Sciences of Limnology and Oceanography).

Smoak, J.M., Breithaupt, J.L., Smith III, T.J., and Sanders, C.J. 2013. Sediment accretion and organic carbon burial relative to sea-level rise and storm events in two mangrove forests in Everglades National Park. *Catena* 104: 58-66.

Spilmont, N., Migné, A., Seuront, L., and Davoult, D., 2007. Short-term variability of intertidal benthic community production during emersion and the implication in annual budget calculation. *Mar. Ecol. Prog. Ser.*, 333: 95–101.

Spilmont, N., *et al.,* 2005. Temporal variability of intertidal benthic metabolism under emersed conditions in an exposed sandy beach (Wimereux, eastern English Channel, France). J. Sea Res. 53: 161-167

Ståhl, H. *et al.*, 2004. Factors influencing organic carbon recycling and burial in Skagerrak sediments. *J. Mar. Res.* 62: 867–907.

Stahl, H. *et al.*, 2004. Recycling and burial of organic carbon in sediments of the Porcupine Abyssal Plain, NE Atlantic. *Deep Sea Res. Part I* 51: 777–791.

Ståhl, H., *et al.,* 2004. Respiration and sequestering of organic carbon in shelf sediments of the oligotrophic northern Aegean Sea. *Mar. Ecol. Prog. Ser.* 269: 33-48.

Stetten, E. *et al.,* 2015. Organic matter characterization and distribution in sediments of the terminal lobes of the Congo deep-sea fan: Evidence for the direct influence of the Congo River. *Mar. Geol.* 369: 182–195.

St-Onge, G. and Hillaire-Marcel, C., 2001. Isotopic constraints of sedimentary inputs and organic carbon burial rates in the Saguenay Fjord, Quebec. *Mar. Geol.* 176(1–4): 1–22.

Szczuciński, W. *et al.,* 2009. Sediment accumulation rates in subpolar fjords - Impact of post-Little Ice Age glaciers retreat, Billefjorden, Svalbard. *Estuar. Coast. Shelf Sci.* 85(3): 345–356.

Takeshita, Y. *et al.,* 2016. Oceans coral reef using a boundary layer approach. *J. Geophys. Res. Oceans* 121: 5655–5671.

Takeshita, Y., *et al.,* 2016. Assessment of net community production and calcification of a coral reef using a boundary layer approach. *J. Geophys. Res. Oceans* 121: 5655-5671.

Tanaka, Y., *et al.,* 2008. Production of dissolved and particulate organic matter by the reef-building corals Porites cylindrica and Acropora pulchra. *Bull. Mar. Sci. 82*: 237-245.

Thomson, A. C., Trevathan-Tackett, S. M., Maher, D. T., Ralph, P. J., and Macreadie, P. I. (2019). Bioturbator-stimulated loss of seagrass sediment carbon stocks. *Limn. Ocean.*, 64(1), 342-356.

Thomson, J., *et al.,* 2006. Radiocarbon age offsets in different-sized carbonate components of deep-sea sediments. *Radiocarbon*, 37: 91-102.

Townsend, M., *et al.,* 2018. The challenge of implementing the marine ecosystem service concept. *Front. Mar. Sci. 5*: 359.

Tremblay, P., *et al.,* 2012. Autotrophic carbon budget in coral tissue: a new 13C-based model of photosynthate translocation. *J. Exp. Biol.* 215(8): 1384-1393.

Turk, D. *et al.,* 2015. Community metabolism in shallow coral reef and seagrass ecosystems, lower Florida Keys. *Mar. Ecol. Prog. Ser.* 538: 35–52.

van der Heijden, L.H., and Kamenos, N.A., 2015. Reviews and syntheses: Calculating the global contribution of coralline algae to total carbon burial. *Biogeosciences* 12: 6429–6441.

van Weering, T. C. E., Berger, G. W. and Kalf, J., 1987. Recent sediment accumulation in the Skagerrak, northeastern North Sea. *Neth. Inst. Sea Res.* 21: 177-189

Volaric, M.P. *et al.,* 2020. Drivers of Oyster Reef Ecosystem Metabolism Measured Across Multiple Timescales. *Estuaries Coasts.* 43: 2034–2045.

Waldbusser, G. G., Powell, E. N., and Mann, R., 2013. Ecosystem effects of shell aggregations and cycling in coastal waters: an example of Chesapeake Bay oyster reefs. *Ecology,* 94(4): 895-903.

Walsh, P. J., *et al.,* 1991. Carbonate deposits in marine fish intestines: A new source of biomineralization. *Limn. Ocean.,* 36(6): 1227-1232.

Ware, J.R., Smith, S.V., and Reaka-Kudla, M.L., 1992. Coral reefs: sources or sinks of atmospheric CO_2? *Coral Reefs 11*: 127-130.

Wernberg, T., *et al.,* 2016. Climate-driven regime shift of a temperate marine ecosystem. *Science,* 353(6295): 169-172.

Wild, C., Woyt, H., and Huettel, M., 2005. Influence of coral mucus on nutrient fluxes in carbonate sands. *Mar. Ecol. Prog. Ser. 287*: 87-98.

Winogradow, A., and Pempkowiak, J., 2014. Organic carbon burial rates in the Baltic Sea sediments. *Estuar. Coast. Shelf Sci.* 138: 27-36.

Włodarska-Kowalczuk, M. *et al.,* 2019. Organic Carbon Origin, Benthic Faunal Consumption, and Burial in Sediments of Northern Atlantic and Arctic Fjords (60–81°N*). J. Geophys. Res.: Biogeosciences* 124(12): 3737–3751.

Wolanski, E. *et al.,* 2005. Fine sediment budget on an inner-shelf coral-fringed island, Great Barrier Reef of Australia. *Estuar. Coast. Shelf Sci.* 65(1–2): 153–158.

Wolf, C., *et al.,* 2019. Eating plants and planting forests for the climate. *Glob. Chang. Biol.* 00:1.

Xia, S., *et al.,* 2021. Distribution, sources, and decomposition of soil organic matter along a salinity gradient in estuarine wetlands characterized by C:N ratio, $\delta^{13}C$-$\delta^{15}N$, and lignin biomarker. *Glob. Change Biol.,* 27: 417–434.

Yamano, H., Miyajima, T., and Koike, I. 2000. Importance of foraminifera for the formation and maintenance of a coral sand cay: Green Island, Australia. *Coral Reefs* 19: 51-58.

Yates, K.K. and Halley, R.B., 2003. Measuring coral reef community metabolism using new benthic chamber technology. *Coral Reefs* 22(3): 247–255.

Zaborska, A. *et al.,* 2008. Recent sediment accumulation rates for the Western margin of the Barents Sea. *Deep Sea Res. Part II Top. Stud. Oceanogr.* 55(20–21): 2352–2360.

Zaborska, A. *et al.,* 2018. Sedimentary organic matter sources, benthic consumption and burial in west Spitsbergen fjords – Signs of maturing of Arctic fjordic systems? *J. Mar. Syst.* 180: 112–123.

Zajączkowski, M. *et al.,* 2004. Recent changes in sediment accumulation rates in Adventfjorden, Svalbard. *Oceanologia* 46(2): 217–231.

Zuo, Z. *et al.,* 1997. Accumulation rates and sediment deposition in the northwestern Mediterranean. *Deep Sea Res. Part II Top. Stud. Oceanogr.* 44(3–4): 597–609.

Appendix 2 - Chapter 3 Supplementary Information

2.1 Sediment Core Dating Information

2.1.1 Upper Loch Torridon

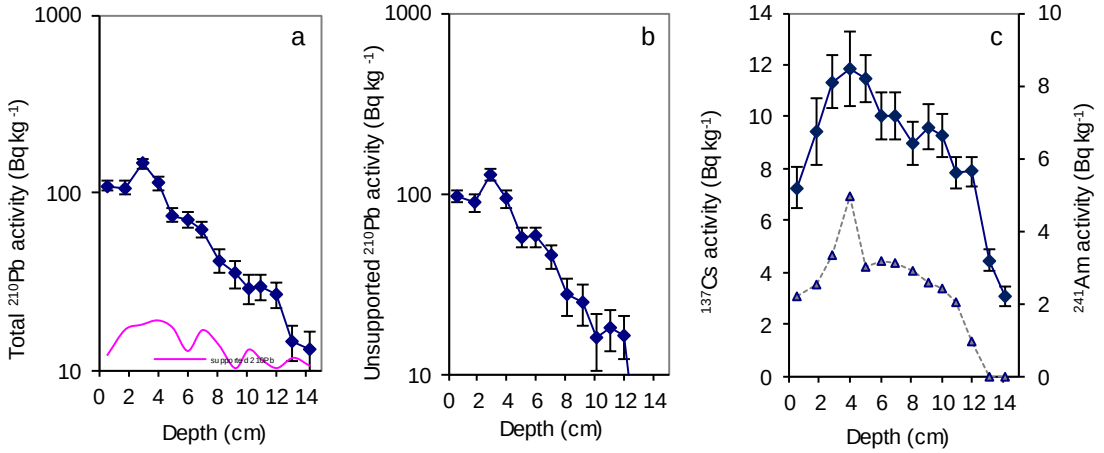

Figure 2.1: Fallout radionuclide concentrations from the core in Upper Loch **Torridon, Scotland, showing (a) total ^{210}Pb, (b) unsupported ^{210}Pb, and (c) ^{137}Cs and ^{241}Am concentrations versus depth.**

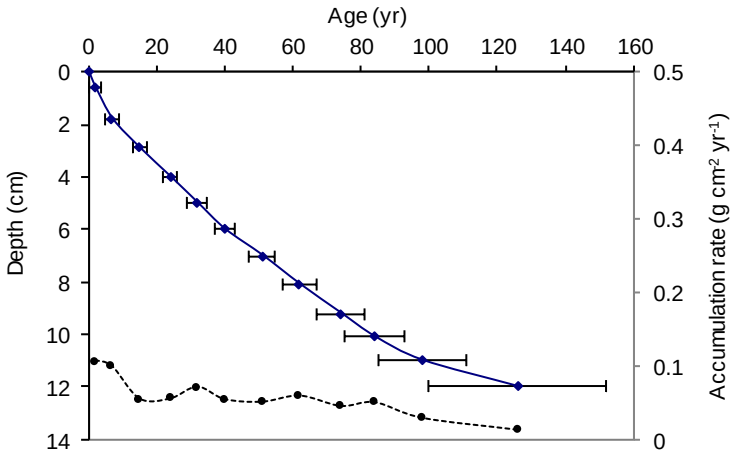

Figure 2.2: Radiometric chronology of the core in Upper Loch Torridon, Scotland, showing the CRS model ^{210}Pb dates and sedimentation rates. The solid line shows age while the dashed line indicates sedimentation rate.

2.1.2 Sound of Barra

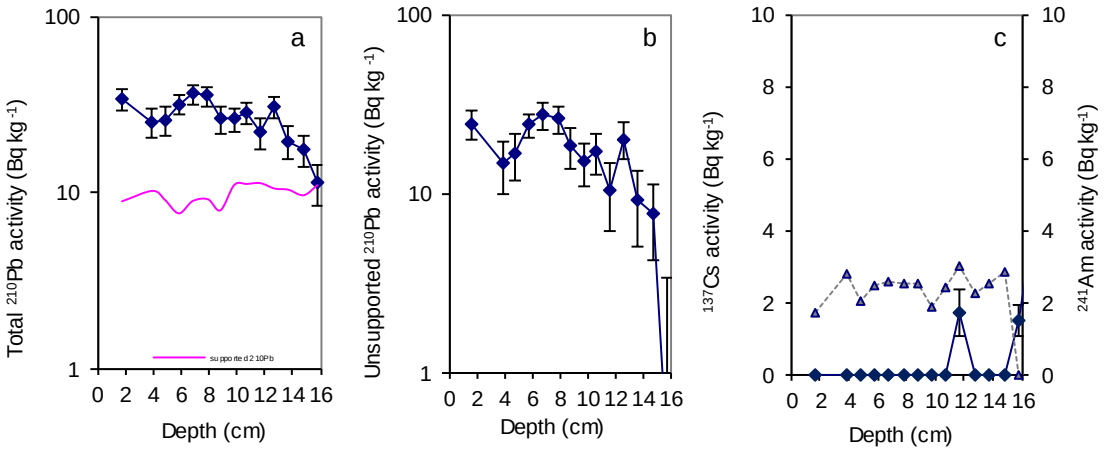

Figure 2.3: Fallout radionuclide concentrations from the core in the Sound of Barra, Scotland, showing (a) total ^{210}Pb, (b) unsupported ^{210}Pb, and (c) ^{137}Cs and ^{241}Am concentrations versus depth.

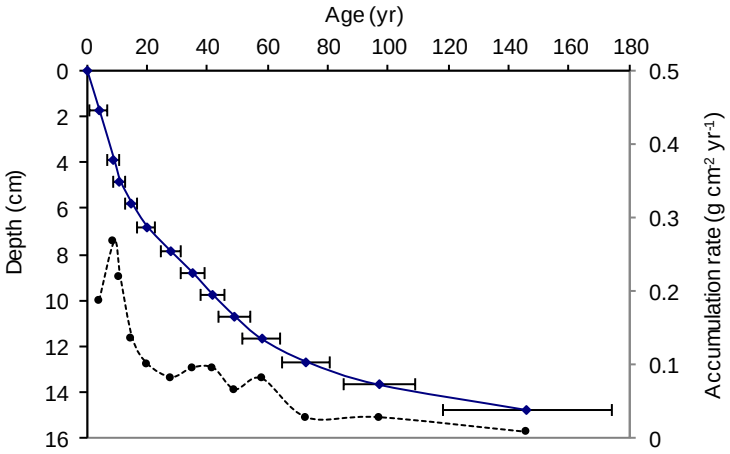

Figure 2.4: Radiometric chronology of the core in the Sound of Barra, Scotland, showing the CRS model ^{210}Pb dates and sedimentation rates. The solid line shows age while the dashed line indicates sedimentation rate.

2.1.3 Tingwall

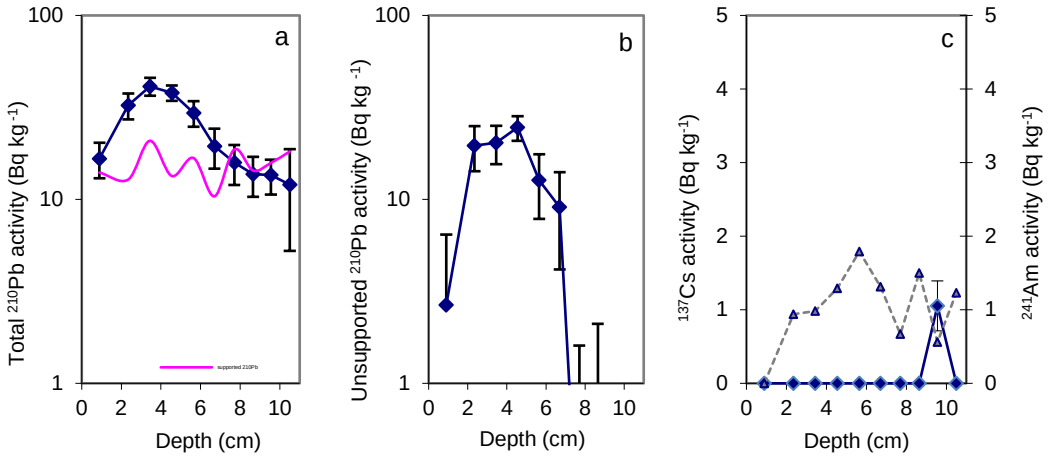

Figure 2.5: Fallout radionuclide concentrations in the core from Tingwall, showing (a) total ^{210}Pb, (b) unsupported ^{210}Pb, and (c) ^{137}Cs and ^{241}Am concentrations versus depth.

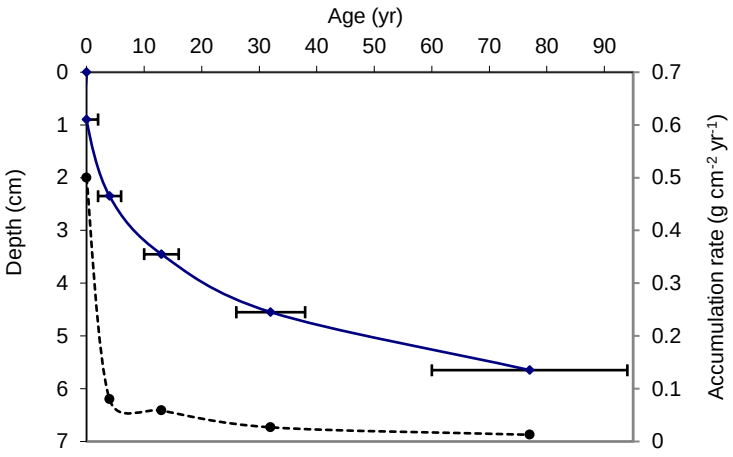

Figure 2.6: Radiometric chronology of the core from Tingwall, showing the CRS model ^{210}Pb dates and accumulation rates. The solid line shows age while the dashed line indicates accumulation rate.

2.1.4 Sound of Eriskay

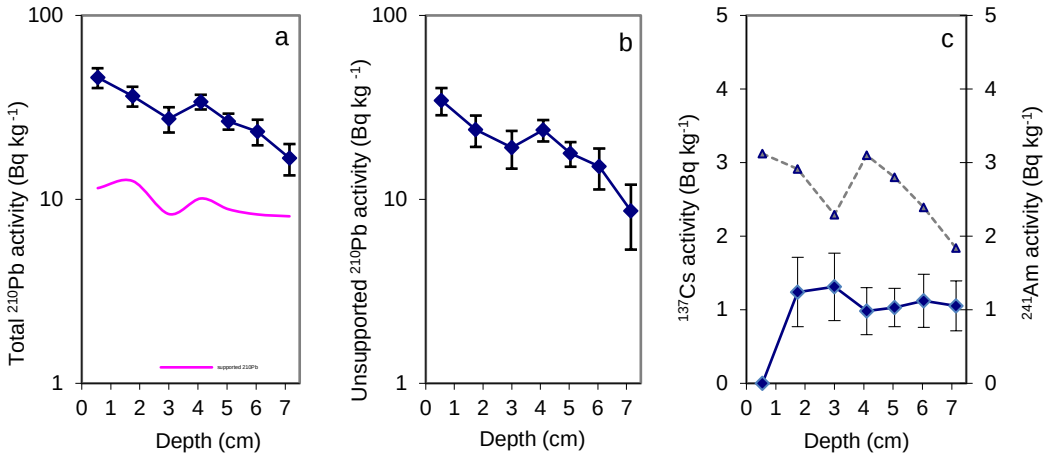

Figure 2.7: Fallout radionuclide concentrations in core from the Sound of Eriskay, showing (a) total ^{210}Pb, (b) unsupported ^{210}Pb, and (c) ^{137}Cs and ^{241}Am concentrations versus depth.

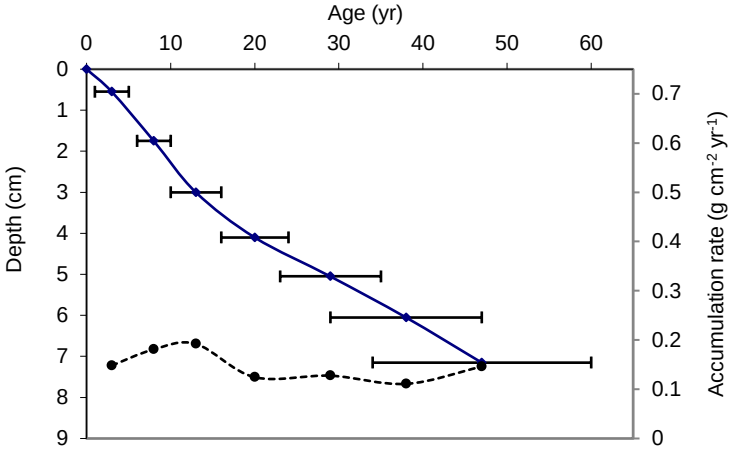

Figure 2.8: Radiometric chronology of the core from the Sound of Eriskay, showing the CRS model ^{210}Pb dates and accumulation rates. The solid line shows age while the dashed line indicates accumulation rate.

2.2 MixSIAR output

2.2.1 Marine and Terrestrial Contributions

Source	Upper Loch Torridon	Sound of Barra	Tingwall	Sound of Eriskay
Marine Fauna	66.2±7.5	72.2±7.0	67.7±9.6	70.0±10.5
Macroalgae	6.9±5.2	20.0±6.0	9.6±8.2	13.5±9.3
Coralline Algae	11.1±9	4.5±2.3	6.9±6.0	8.9±7.3
Seagrass	NA	NA	6.6±4.5	NA
Terrestrial Soil	9.8±6.7	1.1±1.0	5.6±4.4	2.6±2.1
Terrestrial Plants	6±4.7	1.3±1.1	3.6±3.0	2.8±2.1
Sheep Fecel Pellets	NA	1.0±0.9	NA	2.5±2.0

Figure 2.9: Showing the contributions of different sources to each site. Sources are marine fauna, macroalgae, coralline algae, seagrass, terrestrial soil, terrestrial plants, and sheep fecel pellets.

2.2.2 $\delta^{13}C$ and $\delta^{15}N$ with age – Upper Loch Torridon only

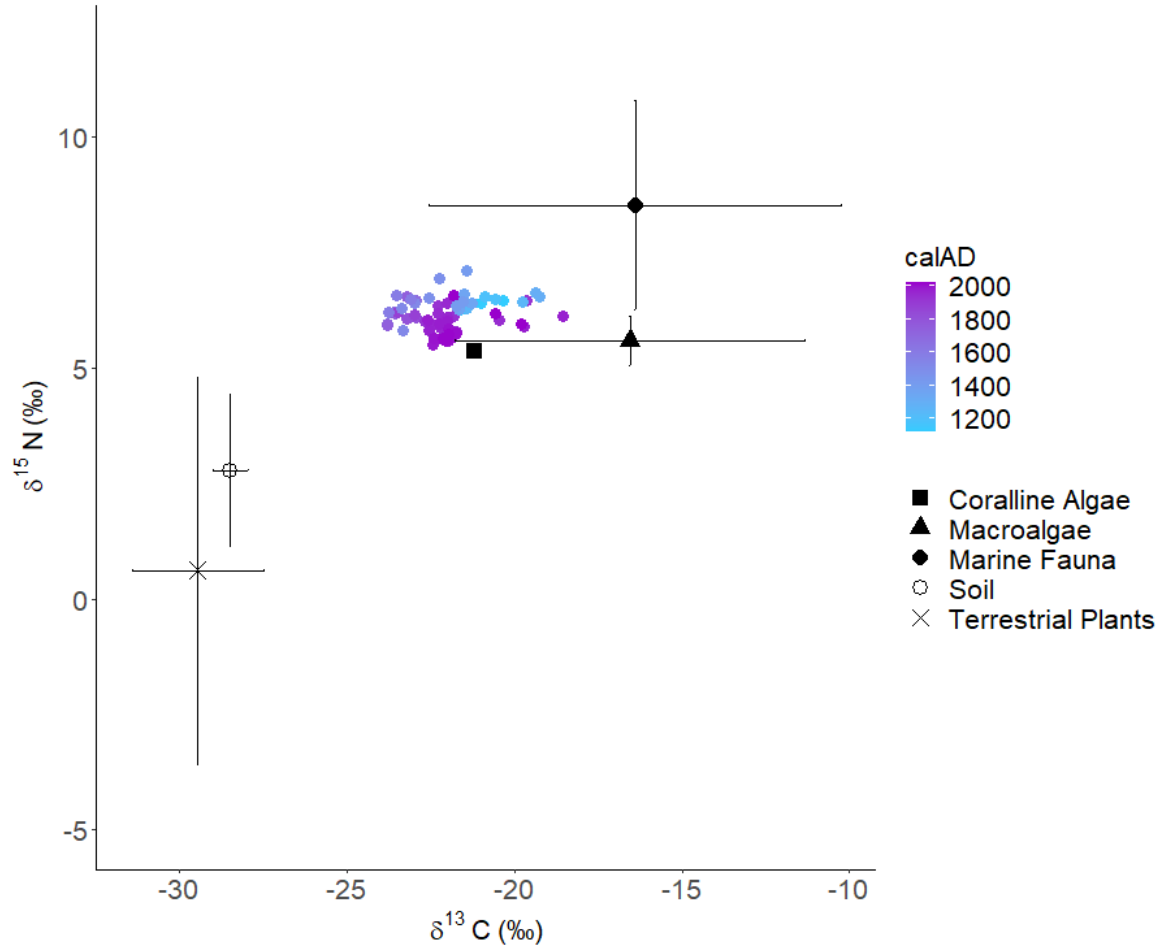

Figure 2.10: $\delta^{13}C$ against $\delta^{15}N$ (‰) for sediment organic material (including all fractions, points) and end-members (black points). Showing data from Upper Loch Torridon. Coloured points represent age (calAD).

2.2.3 $\delta^{13}C$ and $\delta^{15}N$ with depth

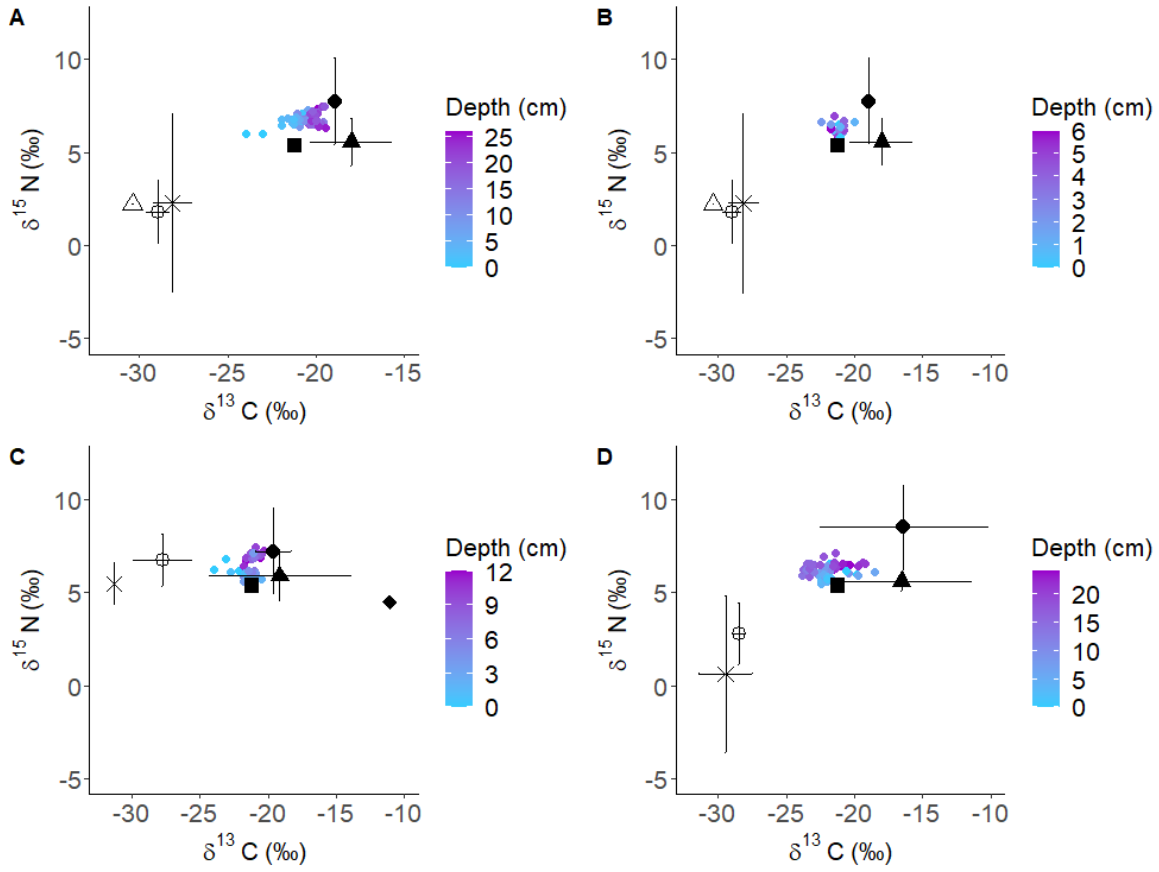

Figure 2.11: $\delta^{13}C$ against $\delta^{15}N$ (‰) for sediment organic material (including all fractions, points) and end-members (black points). Showing data from A) Sound of Barra, B) Sound of Eriskay, C) Tingwall and D) Upper Loch Torridon. Coloured points represent depth (cm).

2.2.4 $\delta^{13}C$ with age – Torridon Only

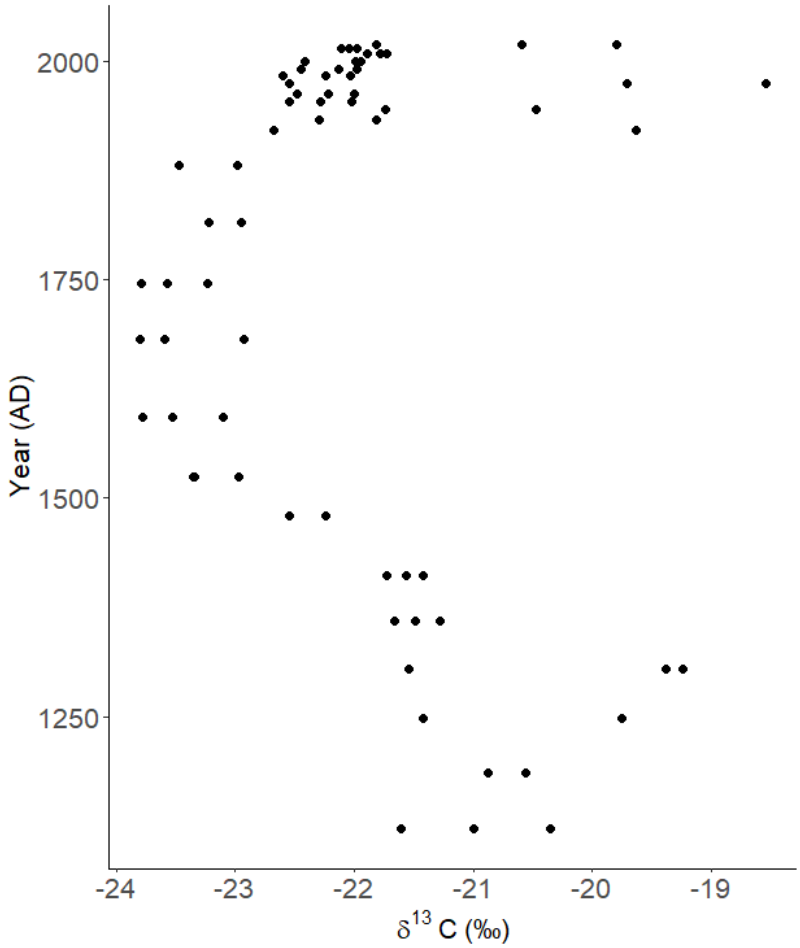

Figure 2.12: Year (AD) against $\delta^{13}C$ for sediment organic material (including all fractions) for Upper Loch Torridon.

2.2.5 $\delta^{13}C$ with depth

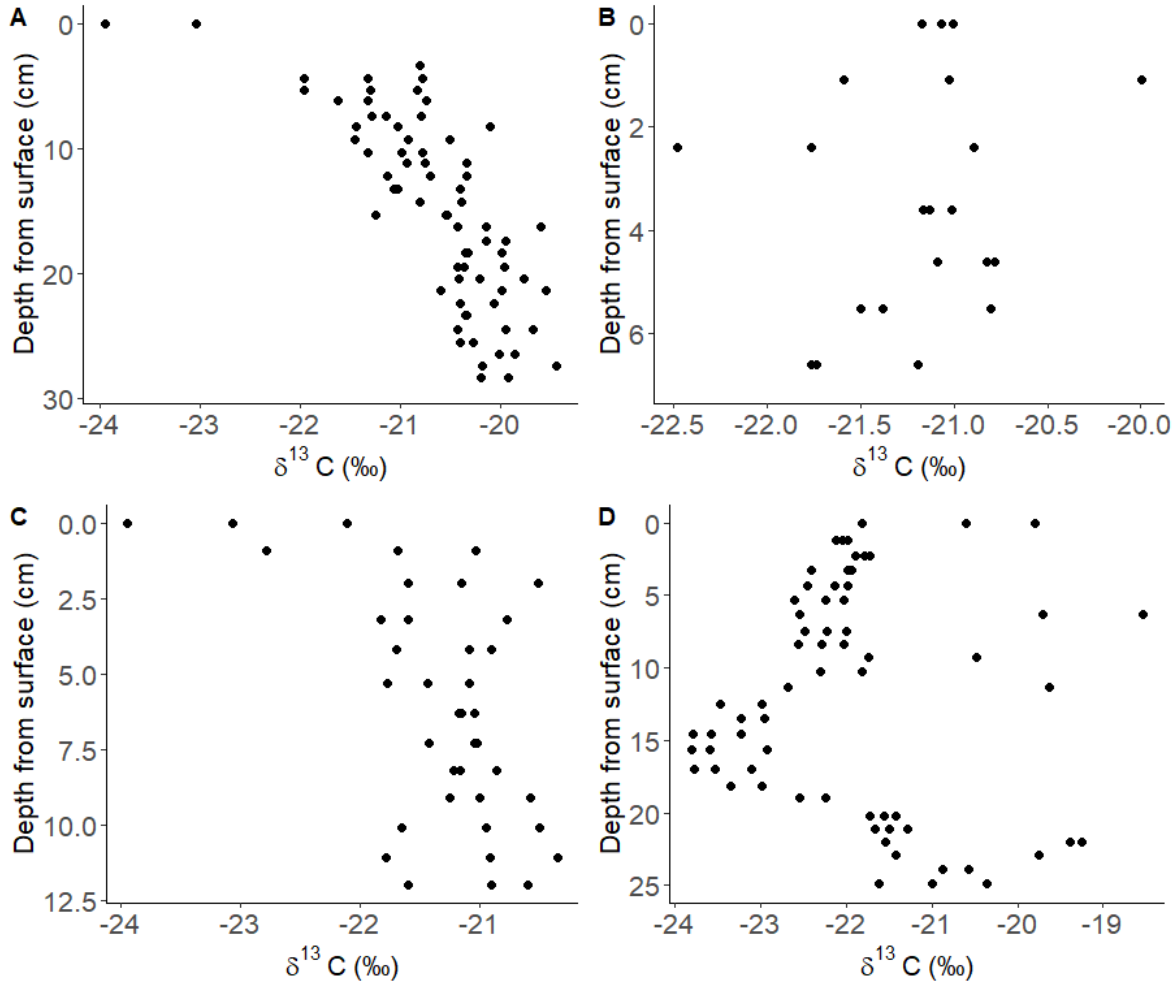

Figure 2.13: Depth (cm) against δ13C for sediment organic material (including all fractions). Showing data from A) Sound of Barra, B) Sound of Eriskay, C) Tingwall and D) Upper Loch Torridon. Coloured points represent depth (cm). For the Sound of Barra, sediment d13C values increased with depth (H(26) = 51.07, p<0.01). There was no significant association between depth and d13C for the other sites (p>0.05).

Appendix 3 - Chapter 4 Supplementary Information

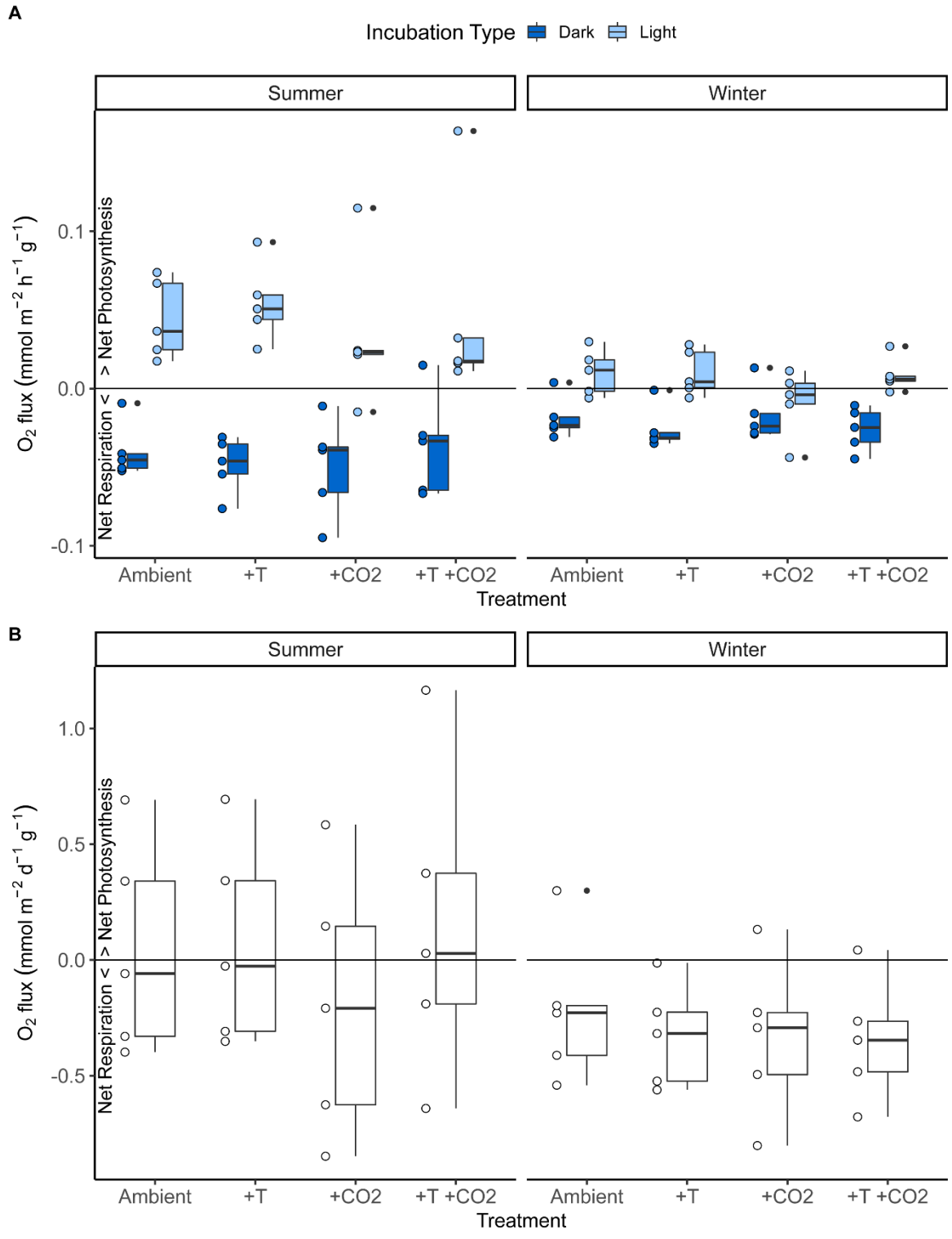

Figure 3.1: A) light (NDP) and dark (R) O_2 flux and B) net O_2 flux for both summer and winter experiments. Treatments are ambient conditions, elevated temperature (+T), elevated CO_2 (+CO2), and elevated temperature with elevated CO_2 (+T +CO2). Points to the left of the bar charts correspond to raw data. Boxplot bars represent median and interquartile ranges, and whiskers represent minimum and maximum values. Data has been scaled to per g of coralline algae.

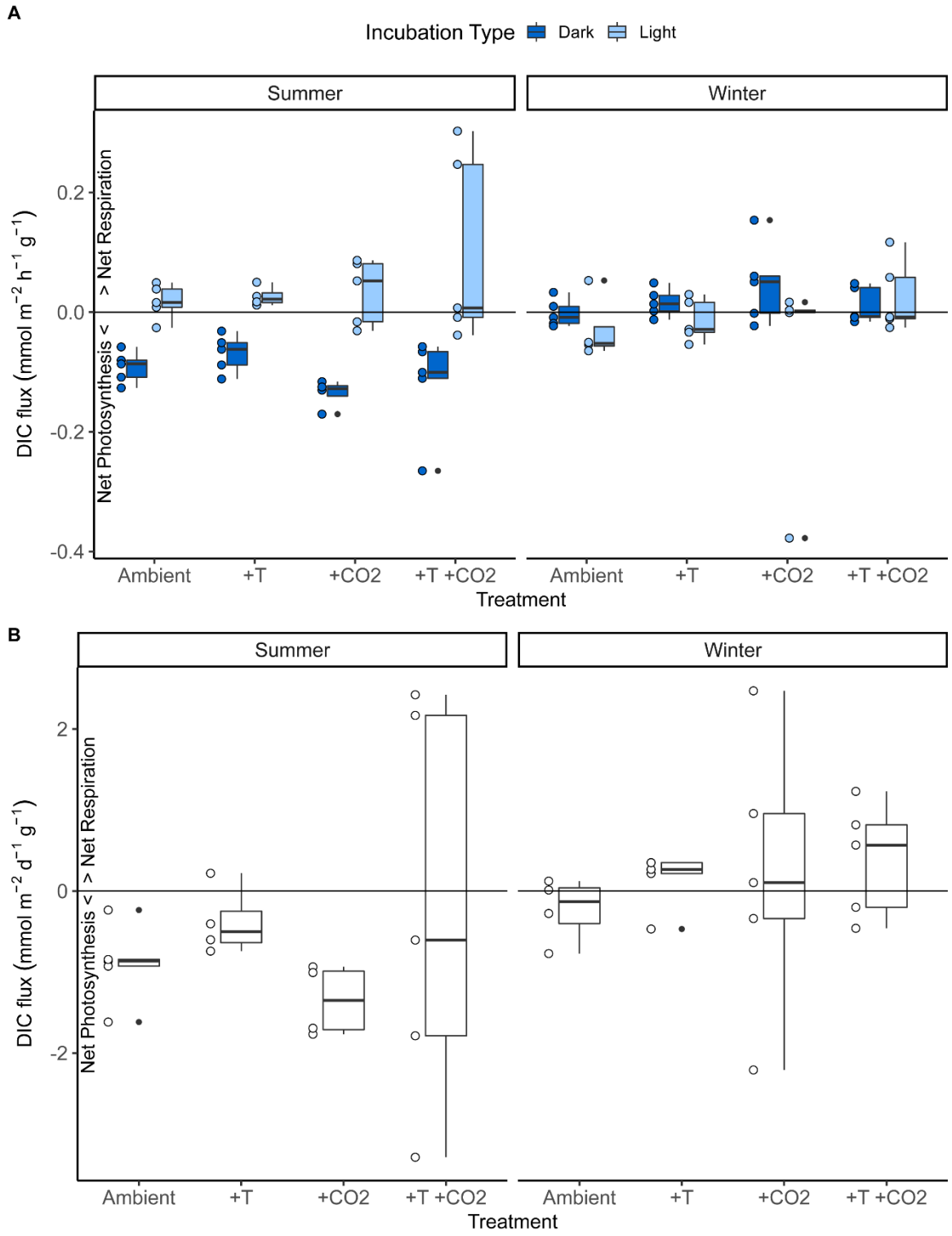

Figure 3.2 A) light and dark DIC flux and B) net DIC flux for both summer and winter experiments. Treatments are ambient conditions, elevated temperature (+T), elevated CO_2 (+CO2), and elevated temperature with elevated CO_2 (+T +CO2). Points to the left of the bar charts correspond to raw data. Boxplot bars represent median and interquartile ranges, and whiskers represent minimum and maximum values. Data has been scaled to per g of coralline algae.

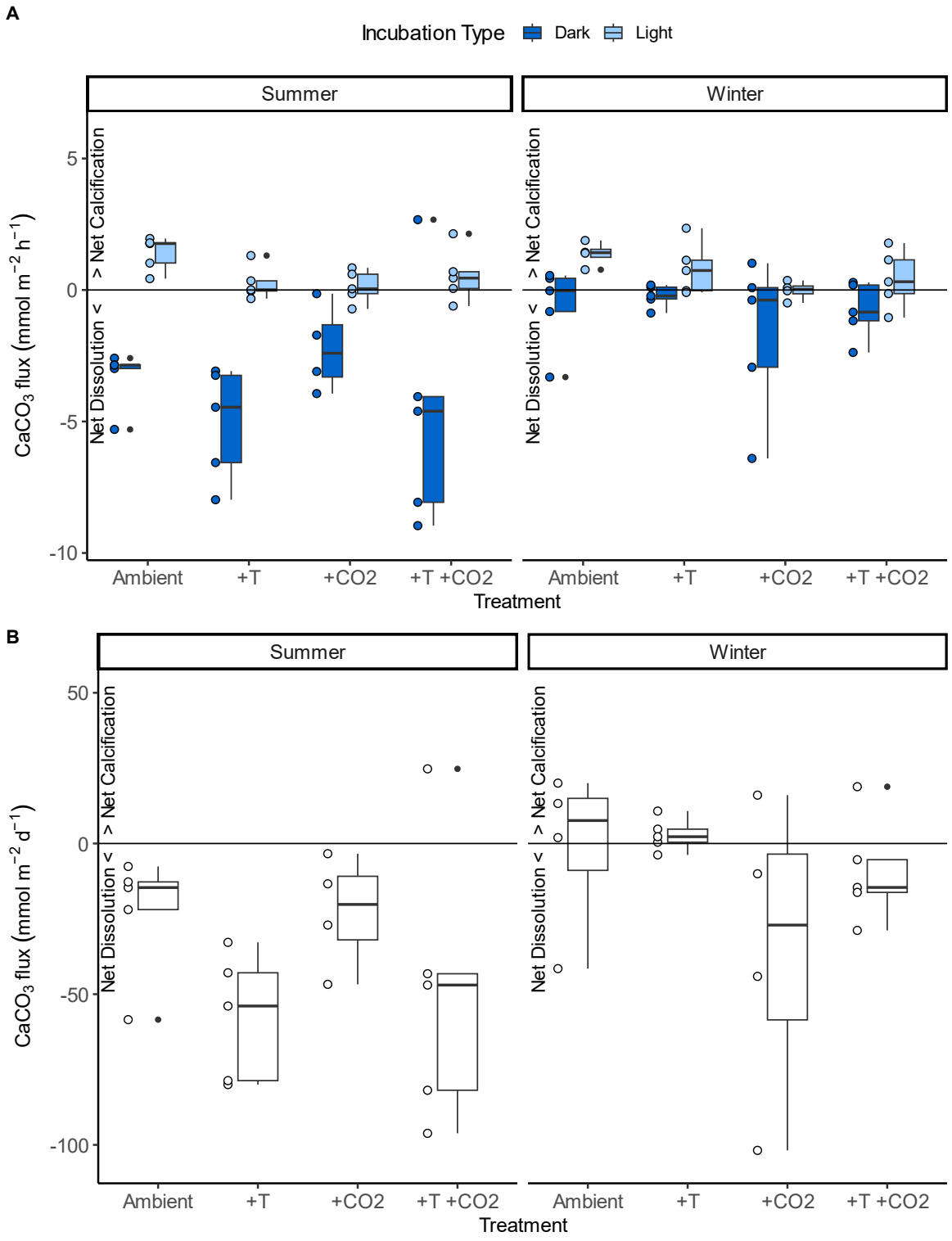

Figure 3.3 A) light and dark $CaCO_3$ flux and B) net $CaCO_3$ flux for both summer and winter experiments. Treatments are ambient conditions, elevated temperature (+T), elevated CO_2 (+CO2), and elevated temperature with elevated CO_2 (+T +CO2). Points to the left of the bar charts correspond to raw data. Boxplot bars represent median and interquartile ranges, and whiskers represent minimum and maximum values. Data has been scaled to per g of coralline algae.